

**Studies Towards the Total Synthesis of Grandilodine C**  
**and**  
**New Methods For Reversible Formation of Nitroxyl Radicals**

*A thesis submitted for the Degree of Master of Philosophy*

*by*

*Marta Klinska*



Research School of Chemistry  
The Australian National University  
Canberra, ACT, Australia

October 2016



**Declaration:**

I declare that, to the best of my knowledge, the material presented in this thesis represents the result of original work carried out by me, during the period 2012-2015 and has not been previously presented for the examination of any degree. Established methodologies have been acknowledged, wherever possible, by citation of the original publications from which they derive. This thesis is 34232 words in length.

Marta Klinska

October 2016

*Moim Rodzicom*



**Acknowledgements:**

I could not have accomplished this without the help and support of many great people. First and foremost, I would like to thank my family. Although they do not know what I do, they have always been extremely supportive and understanding. Words cannot express how grateful and fortunate I am to have them in my life.

This thesis would have never been written without the International Postgraduate Endeavour Scholarship I was awarded in 2012. I would like to thank the Endeavour Awards for having confidence in me. Special thanks go to my case manager, Trang Hoang, who was always there to listen and never gave up on encouraging and motivating me.

I would like to thank my principal supervisor, Martin Banwell, for taking me on as a graduate student. Your advice on synthetic aspects of my research work is much appreciated. I would like to extend these thanks to Michelle Coote, who co-supervised my second project. I am very thankful for the guidance and encouragement during my time at RSC and beyond. Lastly, I wish to sincerely thank Gottfried Otting for your time and support throughout the very final but the most crucial stages of my work.

I would like to thank all the members of the Banwell group, the Coote group and colleagues across the department, who made my time in the lab more enjoyable. I am greatly indebted to Leesa Smith and Ganna Gryn'ova for all their hard work and dedication that was instrumental in bringing the research on nitroxyl radicals to fruition. Thanks are also due to Tony Herlt, who very generously shared his expertise in LCMS and HPLC techniques and to RSC technical staff looking after NMR, MS and EA units.

I have been fortunate to mentor a number of exceptional undergraduate students and I would like to thank them for their hard work and enthusiasm for learning new things. It was a very rewarding experience.

Finally, I would like to thank all the truly amazing and inspirational people I was privileged to meet outside the world of chemistry and who have helped me keeping my life balanced. To those who have been closest to me during this time – thank you for all your support, and for making me a better, stronger person.

**Publications:**

**“Experimental demonstration of pH-dependent electrostatic catalysis of radical reactions”**

Klinska, M.; Smith, L. M.; Gryn'ova, G.; Banwell, M. G. and Coote, M.; *Chem. Sci.*, **2015**, *6*, 5623-5627.

**Abstract:**

This thesis contains two separate research projects within the broad topic of synthetic organic chemistry. The preparation of intermediates that could be used in total synthesis of a complex natural product and an experimental verification of a computational study are reported.



The first part of this thesis deals with the synthesis of organostannane carbamate reagents and their Stille cross coupling reactions with a triflate, which delivers an advanced precursor to a biologically active natural product indole alkaloid, grandilodine C. Intramolecular conjugate addition between an  $\alpha,\beta$ -unsaturated methyl ester and carbamate is studied and alternative approaches towards the target compound, such as iodolactonization and oxymercuration are investigated.

The second part of this thesis describes the synthesis of nitroxides and alkoxyamines containing carboxylic acid functional groups and the concept of pH switchable nitroxide mediated polymerization is explored. Several synthetic and analytical experiments are designed in an effort to verify the computational studies of stabilizing interactions in radical anions. Investigations into a hydrogen atom transfer reaction between profluorescent nitroxide and 4-carboxy TEMPO hydroxylamine reveal significant rate acceleration in low polarity solvent, which is in good agreement with computational predictions. More generally, these findings provide the first experimental proof of the theoretical concept that electrostatic stabilization of delocalized radicals remains particularly significant in low polarity environments.

**Key Words:**

Total synthesis, Natural Product, Grandilodine C, Stille Coupling, Conjugate Addition, Distonic Radical, Nitroxide Mediated Polymerization, pH Switchable Reagents, Profluorescent Nitroxide.

**Abbreviations:**

Å	Ångstrom ( $1 \times 10^{-10}$ m)
Ac	acetyl
AIBN	2,2'-azo- <i>bis</i> -isobutyronitrile
Alloc	allyloxycarbonyl
APT	attached proton test
<i>aq.</i> 	aqueous
Ar	aryl
BDE	bond dissociation energy
Bn	benzyl
Boc	<i>tertiary</i> -butoxycarbonyl
br	broad
Bu	butyl
°C	degrees Celcius
<i>ca.</i> 	<i>circa</i> (Latin: approximately)
cat.	catalyst or catalytic
conc.	concentrated
d	day(s)
δ	chemical shift (in nuclear magnetic resonance spectroscopy)
dba	dibenzylideneacetone
DBU	1,8-diazabicyclo[5.4.0]undec-7-ene
DCE	1,2-dichloroethane
DIBAL-H	diisobutylaluminium hydride
<i>dig</i>	digonal (sp hybridized)
DIPEA	<i>N,N</i> -diisopropylethylamine
DMAP	4-( <i>N,N</i> -dimethylamino)pyridine
DMF	<i>N,N</i> -dimethylformamide
DMSO	dimethyl sulfoxide
DNA	deoxyribonucleic acid
DPPA	diphenoxyphosphoryl azide (diphenyl phosphorazidate)

dppb	1,4- <i>bis</i> (diphenylphosphino)butane
dr	diastereoisomeric ratio
E	<i>entgegen</i> (German: opposite)
EA	elemental analysis
Ee	enantiomeric excess
e.g.	for example
EI	electron impact ionization (mass spectrometry)
EPR	electron paramagnetic resonance
Eq	equivalent
ESI	electron spray ionization (mass spectrometry)
Et	ethyl
<i>et al.</i>	<i>et alia</i> (Latin: and others)
<i>exo</i>	outside
g	gram(s)
GC	gas chromatography
h	hour(s)
HFIP	hexafluoroisopropanol
HMBC	heteronuclear multiple bond correlation
HMPA	hexamethylphosphoramide
HOMO	highest occupied molecular orbital
HPLC	high performance liquid chromatography
HR	high resolution (mass spectrometry)
HSQC	heteronuclear single quantum coherence
Hz	hertz
IC <sub>50</sub>	half maximal inhibitory concentration
<i>i</i> Pr	isopropyl
IR	infrared
IUPAC	The International Union of Pure and Applied Chemistry
<i>in vitro</i>	(Latin: in glass)
<i>J</i>	coupling constant (Hz)
KB cells	continuous cell line derived from human carcinoma

KHMDS	potassium <i>bis</i> (trimethylsilyl)amide
kJ	kilojoule(s)
L	litre(s)
$\lambda$	wavelength (nm)
LCMS	liquid chromatography mass spectrometry
LDA	lithium diisopropylamide
LHMDS	lithium <i>bis</i> (trimethylsilyl)amide
Log	logarithm
LR	low resolution (mass spectrometry)
LUMO	lowest unoccupied molecular orbital
m	multiplet
M	molar concentration (mol L <sup>-1</sup> )
<i>m</i> CPBA	<i>meta</i> -chloroperbenzoic acid
Me	methyl
MeOH	methanol
mg	milligram(s)
$\mu$ g	microgram(s)
MHz	megahertz
min	minute(s)
mL	milliliter(s)
$\mu$ L	microliter(s)
mmol	millimole(s)
mol	mole(s)
m.p.	melting point (°C)
MS	mass spectrometry
Ms	mesylate (salt or ester of methanesulfonic acid, CH <sub>3</sub> SO <sub>3</sub> H)
$\mu$ w	microwave irradiation
m/z	mass to charge ratio
n	number of monomeric units in an oligomer
<i>n</i>	unbranched alkyl chain
<i>N</i> -	indicates bonded to nitrogen atom (e.g. <i>N</i> -Boc)

---

NBS	<i>N</i> -bromosuccinimide
NHMDS	sodium <i>bis</i> (trimethylsilyl)amide
nm	nanometer(s) ( $1 \times 10^{-1}$ m)
NMO	<i>N</i> -methylmorpholine <i>N</i> -oxide
NMP	<i>N</i> -methyl 2-pyrrolidone (Part One of this Thesis)
NMP	nitroxide mediated polymerization (Part Two of this Thesis)
NMR	nuclear magnetic resonance
$\nu_{\max}$	absorbance maximum (infrared spectroscopy)
Ns	nosyl (2-nitrobenzenesulfonyl) group
ORTEP	Oak Ridge Thermal Ellipsoid Plot
PCC	pyridinium chlorochromate
PDI	polydispersity index
PFN	profluorescent nitroxide
PFN-H	hydroxylamine of profluorescent nitroxide
PG	protecting group
Ph	phenyl
pH	negative logarithm of the hydronium ion concentration
PMDETA	<i>N,N,N',N',N''</i> -pentamethyldiethylenetriamine
PS	proton sponge
q	quartet
RCM	ring closing metathesis
$R_f$	retardation factor (chromatography)
RNA	ribonucleic acid
RT or rt	room temperature
s	singlet
sat.	saturated
SEC	size exclusion chromatography
SOMO	singly occupied molecular orbital
T	temperature ( $^{\circ}\text{C}$ )
t	triplet
<i>t</i> or <i>tert</i>	tertiary

TBAF	tetra- <i>n</i> -butylammonium fluoride
TBDPS	<i>tertiary</i> -butyldiphenylsilyl
TBHP	<i>tertiary</i> -butyl hydroperoxide
TBS	<i>tertiary</i> -butyldimethylsilyl
TEA	triethylamine
TEMPO	2,2,6,6-tetramethyl-1-piperidinyloxy free radical
Teoc	2-trimethylsilylethyl carbamate
Tf	triflate (trifluoromethanesulfonate)
TFA	trifluoroacetic acid
TFP	2-furyl phosphine (ligand)
THF	tetrahydrofuran
TLC	thin layer chromatography
TMA	tetramethylammonium hydroxide
TMEDA	<i>N,N,N',N'</i> -tetramethylethylenediamine
TMS	trimethylsilyl
TPAP	tetrapropylammonium perruthenate
Ts	tosyl (4-toluenesulfonyl)
UV	ultraviolet
UV-vis	ultraviolet-visible (spectroscopy)
<i>vs</i>	<i>versus</i> (Latin: in opposition to; compared with)
<i>via</i>	(Latin: by way of; by (means of))
v/v	unit volume per unit volume
Wt Fr	weight fraction
w/v	unit weight per unit volume
<i>Z</i>	<i>zusammen</i> (German: together)
>	greater than
<	less than



## **Table of Contents:**

Declaration: .....	iii
Acknowledgements: .....	v
Publications: .....	vi
Abstract: .....	vii
Key Words: .....	vii
Abbreviations: .....	viii
Table of Contents: .....	xiii
Part One: Studies Towards the Total Synthesis of <i>Kopsia</i> Indole Alkaloid Grandilodine C.....	1
Chapter One: Introduction to Total Synthesis and Biologically Active <i>Kopsia</i> Indole Alkaloids.....	1
1.1 Reflection on the art and science of total synthesis.....	1
1.2 Background information about biochemical origin of natural products.....	1
1.3 Study of alkaloid natural products – historical perspective <sup>15,16</sup> .....	2
1.4 Indole alkaloids – rich source of unprecedented molecular architectures .....	3
1.5 Grandilodines A-C, biologically active indole alkaloids from <i>Kopsia grandifolia</i> .....	4
1.6 Total synthesis of (±)-lapidilectine B <sup>28</sup> .....	5
1.7 Total synthesis of (±)-lundurine A and (±)-lundurine B <sup>29,30</sup> .....	7
1.8 Synthetic efforts towards grandilodines and related <i>Kopsia</i> alkaloids .....	12
1.9 Retrosynthetic analysis of grandilodine C and the aim of the project .....	13
Chapter Two: Results and Discussion.....	15
2.1 Methyl carbamate series – synthesis and reactivity.....	15
2.1.1 The synthesis of organostannane and triflate compounds.....	15
2.1.2 Optimization of the Stille coupling reaction conditions.....	21
2.1.3 Investigation into the conjugate addition reaction.....	24
2.2. <i>Tert</i> -butyl carbamate series – synthesis and reactivity .....	26
2.2.1 Building block synthesis and Stille coupling reaction .....	27
2.2.2 <i>N</i> -Boc deprotection and intramolecular conjugate addition .....	28
2.3 Alternative strategies towards total synthesis of grandilodine C.....	31
2.4 Summary and conclusions .....	33
Chapter Three: Experimental Work Associated with Research Reported In Part One .....	35
3.1 General methods.....	35
References: .....	45
Part Two: New Methods For Reversible Formation Of Nitroxyl Radicals Under Mild Conditions.....	51

Chapter Four - Introduction .....	51
4.1 Computational chemistry origins of the project – unprecedented stabilizing interactions in distonic radicals.....	51
4.2 Effect of external conditions on radical stabilization and its consequences for possible practical applications.....	54
4.3 Theoretical background – pH switchable reagents for nitroxide mediated polymerization .....	56
4.4 Aims .....	58
Chapter Five – The Synthesis of TEMPO, SG1 and TIPNO Type Compounds and Related Polymerization Studies.....	59
5.1 The synthesis of 4-carboxy TEMPO alkyl alkoxyamines .....	59
5.2 The synthesis of 4-carboxy TEMPO aryl alkoxyamine and preliminary polymerization studies.....	61
5.3 The synthesis of SG1 type radicals and alkoxyamines.....	63
5.4 The synthesis of TIPNO-type radical .....	65
5.5 Alternative routes to 4-carboxy TIPNO – Grignard addition to aryl nitrones and imines	67
5.6 The synthesis of 4-carboxy TIPNO alkoxyamine and preliminary polymerization studies .....	67
5.7 Further polymerization studies – control experiments .....	69
5.7.1 Nitroxide Mediated Polymerizations of styrene with 4-carboxy-TEMPO and TEMPO and the choice of base.....	70
5.7.2 Effect of base on initiation .....	70
5.7.3 Control experiments at 60 °C .....	70
5.7.4 Control experiments at 80 °C .....	71
5.7.5 Control experiments at 100 °C .....	71
5.7.6 Acetylene switch – synthesis and polymerization.....	71
Chapter Six – Synthesis and Use of Analytical Tools for Detecting pH-induced Radical Formation .....	74
6.1 The synthesis of isoxazolidine type compounds <i>via</i> [2+3] cycloaddition.....	74
6.2 Bond dissociation in 4-carboxy TIPNO alkoxyamine monitored by <sup>1</sup> H NMR .....	77
6.3 Base titration experiments .....	78
6.4 Hydrogen atom exchange monitored by UV-vis spectroscopy .....	79
6.5 Using fluorescence to demonstrate pH induced radical switching.....	79
6.6 Summary and conclusions.....	86

Chapter Seven – Experimental Work Associated with Research Reported in Part Two .....	87
7.1 General methods .....	87
7.2 Preliminary Polymerization Studies - Experimental Details .....	106
7.2.1 General procedure for styrene polymerization with nitroxyl radical and initiator: .....	106
7.2.2 General procedure for styrene polymerization with alkoxyamine: .....	107
7.3 Fluorescence Hydrogen Exchange Experimental Details.....	107
7.3.1 Determination of equilibrium constant and rate constants in dichloromethane or acetonitrile for reaction between 4-CT-H and PFN. ....	107
7.3.2 Determination of equilibrium constant and rate constants in dichloromethane for reaction between TEMPOnaph-H and PFN. ....	108
References: .....	109
Appendix One: SEC Plots Supporting Polymerization Studies Reported In Chapter Five.....	113
A1.1 Chain extension of 4-carboxy-TIPNO-PSTY with styrene: .....	113
A1.2 Effect of base on initiation.....	114
A1.2.1 Polymerization of styrene with DBU: .....	114
A1.2.2 Polymerization of styrene with TEA and proton sponge: .....	114
A1.2.3 Test for cationic polymerization with ratio of benzoic acid to TEA and Proton Sponge:.....	115
A1.3 Control experiments at 60 °C .....	116
A1.4 Control experiments at 80 °C .....	116
A1.5 Control experiments at 100 °C .....	117
A1.6 Acetylene switch – styrene polymerization: .....	119
Appendix Two: Calibration Curves and Kinetic Analysis for the Hydrogen Atom Transfer Experiment Reported in Chapter Six.....	120
A2.1 Fluorescence Calibration Curves .....	120
A2.2 Second Order Kinetics in Equilibrium .....	122
A2.3 Second Order Kinetics Rate Constant .....	122
A2.4 Kinetic Model Fitting Plots .....	123
A2.5 PFN/4-CT-H system in dichloromethane at 10 °C .....	128
A2.6 PFN/4-CT-H system in acetonitrile .....	129
A2.7 PFN/TEMPOnaph-H system in dichloromethane .....	131
A2.8 Kinetic and Thermodynamic Data.....	133

Appendix Three: Single Crystal X-Ray Analysis Data for selected compounds reported in Parts One and Two.....	139
---	-----

## **Part One: Studies Towards the Total Synthesis of *Kopsia* Indole Alkaloid Grandilodine C.**

### **Chapter One: Introduction to Total Synthesis and Biologically Active *Kopsia* Indole Alkaloids**

This project describes the synthesis of intermediates that could be used to assemble the carbon framework of the biologically active indole alkaloid grandilodine C.

#### **1.1 Reflection on the art and science of total synthesis**

The ability to construct complex organic molecules from simple, readily available materials has inspired chemists across the globe to practice what is justly called both a creative art and a precise science of total synthesis.<sup>1</sup> Since its birth, marked by Wohler's preparation of urea in 1828, the field has evolved immensely contributing to many exciting discoveries in chemistry, biology and medicine.<sup>2,3</sup> For nearly 200 years synthetic chemists have been targeting natural and designed molecules with increasing structural complexity (vitamin B-12, steroids, alkaloids, prostaglandins etc.) and pushing the limits of chemical synthesis (palytoxin, erythropoietin, PG5).<sup>4,5</sup> The endeavours of replicating nature's molecules in the laboratories all over the world led to remarkable achievements, creating a landscape of molecular complexity and diversity.<sup>6</sup>

As the understanding of biology and chemistry became more advanced, the primary purpose for total synthesis changed.<sup>7</sup> Some total syntheses continue to aid biological verification or inspire the development of new chemical reagents and reactions.<sup>1-3</sup> Considering how powerful analytical tools for structural determination are available to us these days, the practicality of total synthesis and natural product synthesis in particular may and should be questioned.<sup>8,9</sup> It does not however prevent one from viewing this field as a way of showcasing the sophistication of modern synthetic organic chemistry.

#### **1.2 Background information about the biochemical origin of natural products**

Natural products can be simply described as organic compounds made by living organisms and divided into three broad categories.<sup>10</sup> First, the primary metabolites, such as nucleic acids, amino acids and sugars, which occur in all cells and play central roles in

their metabolism and reproduction. Secondly, the high molecular weight polymeric substances such as cellulose, lignins and polypeptides, which form cellular structures. And finally, the secondary metabolites, that are characteristic of a specific range of species and attract the most interest among chemists, due to their physiological effects on other organisms. Although not absolutely required for survival, they can act as competitive weapons against other species (toxins, venoms), social signaling molecules (pheromones) or nutrient transporting agents (siderophores).<sup>11</sup> Many secondary metabolites are cytotoxic and sometimes their biological activities may be used in managing disease symptoms.<sup>12</sup> For this reason various natural products, or rather their original plant sources have been widely used in traditional medicines.<sup>13</sup> With advances in science, these compounds could be isolated, characterized and even modified synthetically in order to study their pharmacological effects.<sup>12,13</sup>

There are several classes of secondary metabolites and depending on the type of biosynthetic pathway leading to them, one could distinguish the following categories: fatty acids and polyketides (acetate pathway); aromatic amino acids and phenylpropanoids (shikimate pathway); terpenoids and steroids (mevalonate pathway) and alkaloids (multiple pathways from amino acids).<sup>14</sup>

### **1.3 Study of alkaloid natural products – historical perspective<sup>15,16</sup>**

Alkaloid natural products have very diverse chemical structures and there are many different ways in which they can be synthesized.<sup>17</sup> Common processes involve Schiff base condensations and Mannich reactions and in general an alkaloid contains at least one nitrogen atom in an amine-type structure. This nitrogen can act as a base in acid-base reactions, just like the inorganic alkalis, hence the name alkaloid (“alkali-like”). Historically, alkaloids were classified by the common natural source, such as the families of plants. As the chemical structure and reactivity became well understood more recent classifications were based on structural or biosynthetic similarities.

Interest in alkaloids stems from the wide variety of physiological effects they produce in the human body. Alkaloid rich plants have been used since ancient times for therapeutic and recreational purposes but it was not until the 19<sup>th</sup> century that the scientific study of alkaloids began. Morphine was the first alkaloid to be isolated and crystallized in around 1804 and coniine was the first to be synthesized in 1886 by Albert Ladenburg.

Many well-known alkaloids were isolated around that period and several were synthesized. The invention of spectroscopic and chromatographic methods in the 20<sup>th</sup> century has greatly accelerated both isolation and synthesis, resulting in the rapid growth of this field. Many natural products and synthetic derivatives found use in conventional medicine as analgesics (morphine, oxycodone); antihypertensive (reserpine) and antimalarial agents (quinine) as well as mitotic inhibitors (vincristine, vinblastine).

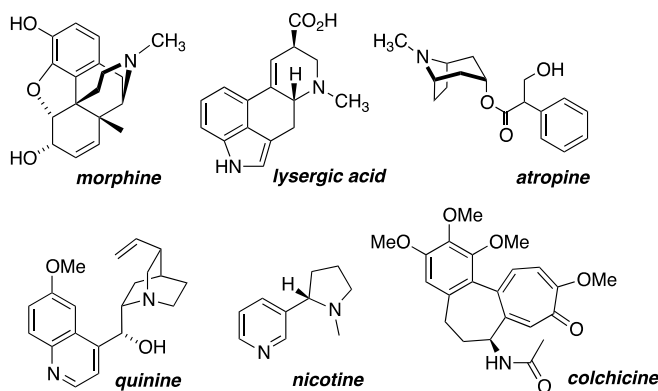


**Figure 1.1** Selected examples of alkaloids with interesting biochemical properties.

#### 1.4 Indole alkaloids – rich source of unprecedented molecular architectures

Indole alkaloids are one of the most studied indole-containing compounds and with over 4000 natural products known they represent a large class of alkaloids.<sup>18</sup> Biosynthetically, indole alkaloids are derived from the amino acid tryptophan and can be further categorized into non-isoprenoid alkaloids, such as simple derivatives of indole or  $\beta$ -carboline, isoprenoid alkaloids and bisindole alkaloids.<sup>19</sup> The last two classes are of particular interest to synthetic chemists, mainly due to their complex structures as well as unusual biological properties.<sup>20</sup>

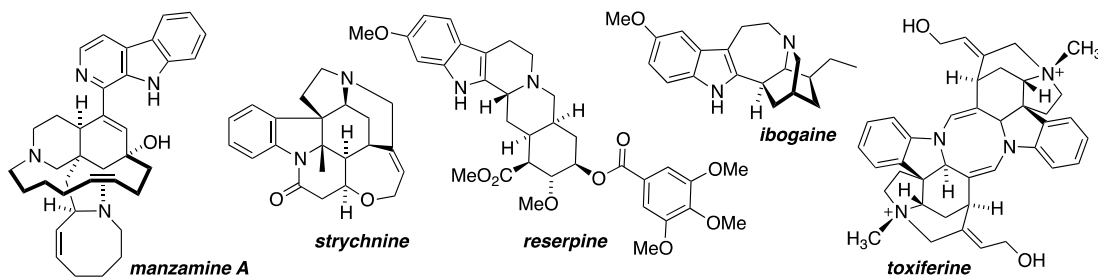


**Figure 1.2** Structural diversity of indole alkaloids.

The majority of monoterpenoid indole alkaloids are distributed among three families of dicotyledon plants: Apocynaceae (multiple genera), Rubiaceae (*Corynanthe*) and Loganiaceae (*Strychnos*).<sup>21</sup> The largest family, Apocynaceae, comprises some 1,500 species divided over about 424 genera.<sup>22</sup> Genus *Kopsia*, growing in South and Southeast Asia, is rich source of alkaloids with unique carbon frameworks and wide range of biological activities.<sup>23,24</sup>

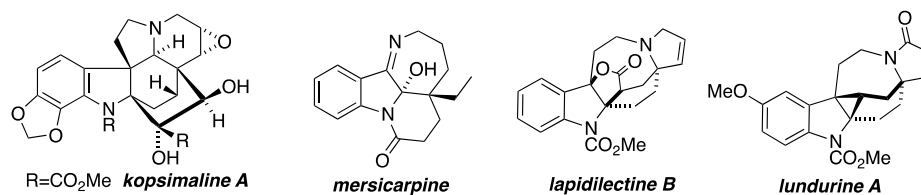


**Figure 1.3** Examples of biologically active indole alkaloids from *Kopsia* species.

### 1.5 Grandilodines A-C, biologically active indole alkaloids from *Kopsia grandifolia*

Grandilodines were isolated from the Malayan *Kopsia grandifolia* and first reported in 2011.<sup>25</sup> The structures were solved based on NMR and MS analyses and in the case of grandilodine A and B, confirmed by X-ray diffraction analysis.<sup>25</sup> Grandilodine A and C were found to restore vincristine activity in multidrug resistant KB cells (IC<sub>50</sub> 4.35 and 4.11  $\mu\text{g mL}^{-1}$  respectively, in the presence of 0.1  $\mu\text{g mL}^{-1}$  of vincristine) and show no toxicity against drug resistant cells in the absence of vincristine.<sup>25</sup> Although these *in vitro* preliminary results were interesting, the sparse availability of grandilodines prevented further testing from being undertaken. In this light, the total synthesis of grandilodines could facilitate detailed elucidation of their practical utility by providing appreciable quantities of the natural product. Aside from the potential applications, grandilodines possess a very unique carbon framework with a characteristic [4.2.2] bicyclic system found between the adjacent indoline core and pyrrolidine type ring. Although the biosynthetic details are unknown, grandilodines are structurally related to lapidilectine and lundurine classes of natural products, also found in *Kopsia* species.<sup>26,27</sup> With no total synthesis reported to date and the fascinating chemical structure, grandilodine C was selected as a target molecule for this project.



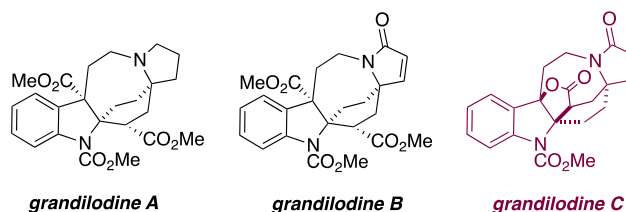
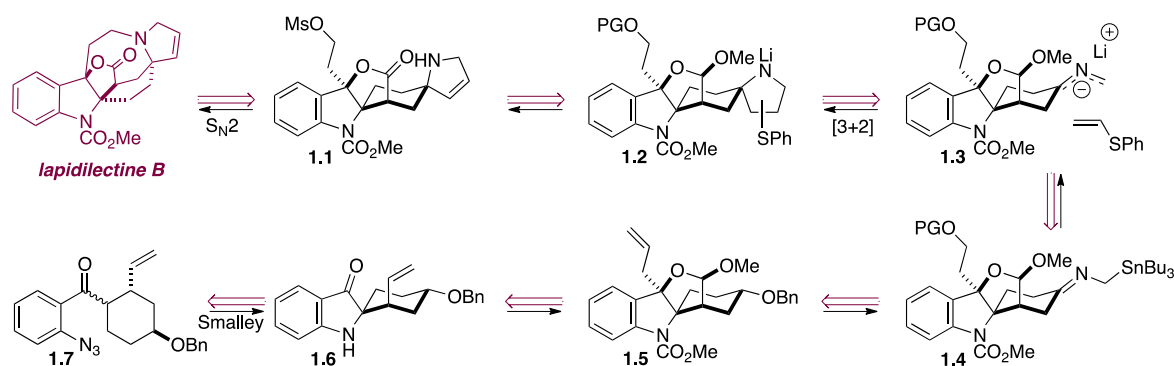


**Figure 1.4** Grandilodines A-C from *Kopsia grandifolia*.

Featuring a hexacyclic framework with four asymmetric carbon atoms and several different functional groups, grandilodine C poses several synthetic challenges. Inspection of this rather complex ring system reveals an indoline moiety fused with a five-membered lactone ring and an eight-membered ring, which are also connected *via* a single CH<sub>2</sub> group. Thus, the characteristic [4.2.2] bicyclic system becomes tricyclic, which stands out as possibly the most synthetically challenging fragment of grandilodine C. The adjacent tertiary centers of the indoline core and lactam ring on the opposite side of the molecule are very sterically demanding, which further complicates the synthesis. Some of these difficulties are best reflected by the fact that there are very few examples of synthesis of structurally similar intermediates reported in the scientific literature. The most relevant to this project is the total synthesis of *Kopsia lapidilecta* alkaloid, (±)-lapidilectine B, published by Pearson *et al* in 2004.<sup>28</sup> Interestingly, this was the first and up until very recently the only total synthesis reported for this type of natural product.<sup>29</sup> A decade later Nishida *et al* published total syntheses of lundurines A and B.<sup>30</sup>

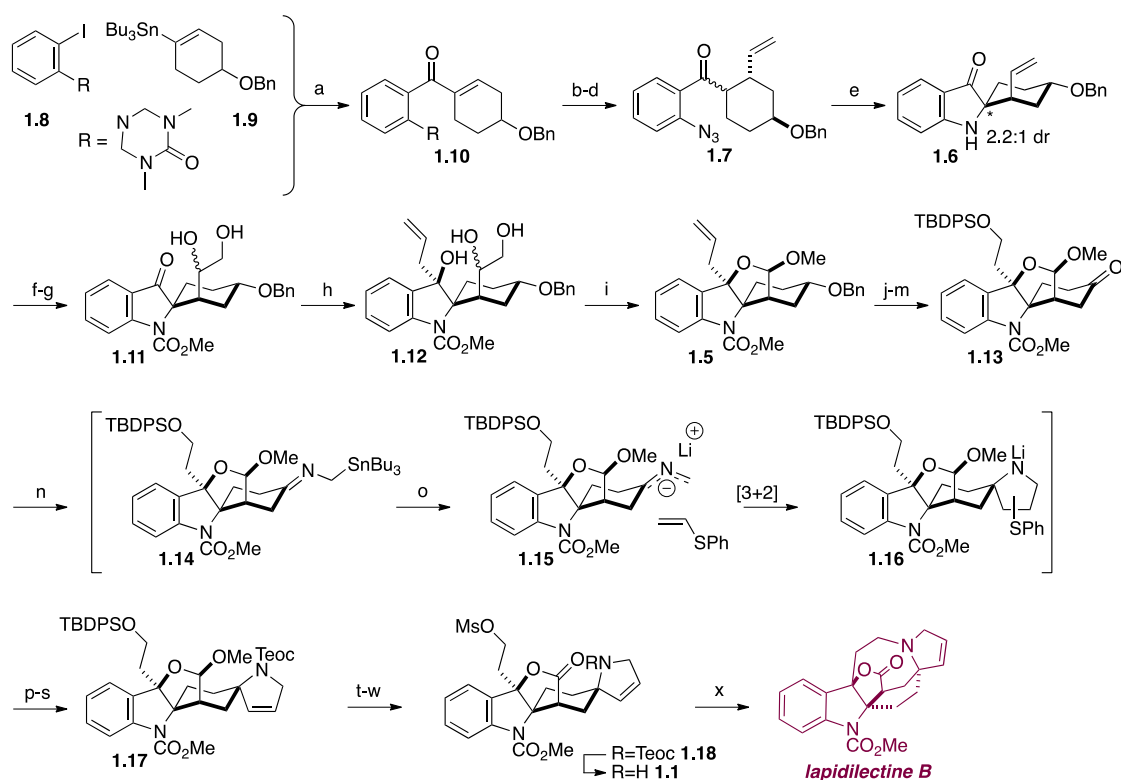
### 1.6 Total synthesis of (±)-lapidilectine B<sup>28</sup>

The synthesis of (±)-lapidilectine B was completed in 23 linear steps and in an overall 0.10% yield from 4-benzyloxycyclohexanone. As shown in **Scheme 1.1**, the key steps involved a Smalley cyclization to form the 1,2-dihydro-3*H*-indol-3-one core, which installed the problematic spiro carbon. The pyrrolidine ring was constructed using a [3+2] cycloaddition between 2-azaallyllithium reagent and phenyl vinyl sulfide and closure of the eight-membered ring was accomplished *via* intramolecular displacement of a mesylate leaving group.



**Scheme 1.1** Retrosynthetic analysis of (±)-lapidilectine B.

As depicted in **Scheme 1.2**, the synthesis started with preparation of protected 2-iodoaniline **1.8** and alkenyl stannane **1.9**, which were then subjected to carbonylative Stille coupling. Michael addition of vinylmagnesium bromide to **1.10**, removal of the nitrogen protecting group and subsequent conversion into an azide furnished precursor **1.7** for Smalley cyclization. Under optimized conditions, the Smalley reaction delivered a mixture of diastereomers in 2.2:1 ratio and 68% combined yield. The required major diastereoisomer **1.6** was then converted into a methyl acetal using dihydroxylation, addition of allylmagnesium bromide and oxidative cleavage of triol **1.12**. The methyl acetal **1.5** was then subjected to ozonolysis and debenzylation, followed by oxidation of the resulting alcohol to give a cycloaddition precursor, ketone **1.13**. Condensation of aminomethyltributylstannane with the ketone **1.13** afforded intermediate **1.14**, which upon treatment with phenylvinyl sulfide and *n*-butyllithium, underwent the [3+2] cycloaddition to produce a mixture of rotamers or diastereoisomers (combined 75% yield). Direct quenching with chloroformate and an oxidation of the sulfide, followed by thermolysis furnished a single product **1.17** in good overall yield. Next, the methyl acetal **1.17** was converted into lactone *via* PCC oxidation and the TBDPS protected alcohol was transformed into a mesylate **1.18**. The synthesis was completed by deprotection of the nitrogen and subsequent intramolecular  $S_N2$  reaction, facilitated by DIPEA and heating, to furnish the perhydroazocine ring, thus affording (±)-lapidilectine B.



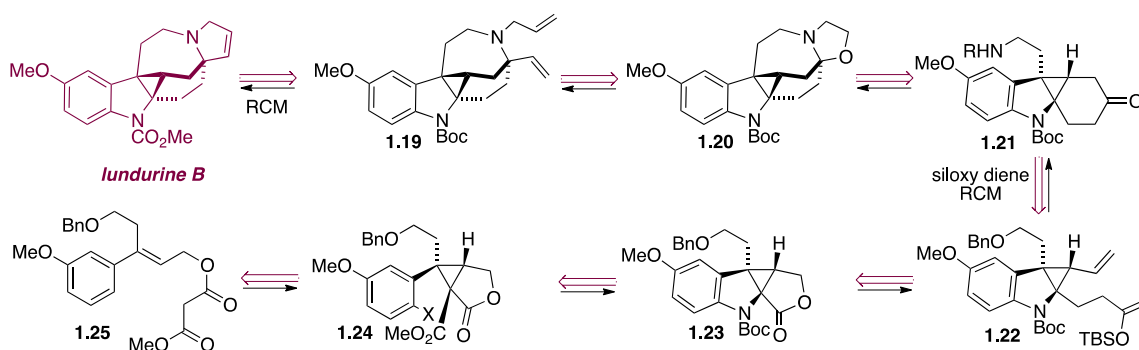
Reagents and conditions: (a)  $\text{Pd}_2(\text{dba})_3 \cdot \text{CHCl}_3$ ,  $\text{Ph}_3\text{As}$ ,  $\text{LiCl}$ ,  $\text{NMP}$ ,  $\text{CO}$  (70 psi),  $75^\circ\text{C}$ , 98%; (b)  $\text{vinylMgBr}$ ,  $\text{Li-2-thienylcyanocuprate}$ ,  $\text{BF}_3 \cdot \text{Et}_2\text{O}$ ,  $\text{THF}$ ,  $-78^\circ\text{C}$ , 82%; (c)  $\text{HCl}$  (conc),  $\text{MeOH}$ ,  $\text{RT}$ , 83%; (d)  $\text{HCl}$  (conc),  $\text{NaNO}_2$ ,  $\text{H}_2\text{O}$ ,  $0^\circ\text{C}$ , then *aq*  $\text{NaN}_3$ ,  $0^\circ\text{C}$ , not isolated; (e)  $\text{KOH}$ , *i* $\text{PrOH}$ ,  $0^\circ\text{C}$ , 68%; (f) *t* $\text{BuLi}$ ,  $\text{ClCO}_2\text{Me}$ ,  $-10^\circ\text{C}$ , 89%; (g)  $\text{OsO}_4$  (cat.),  $\text{NMO}$ ,  $\text{acetone}$ ,  $\text{RT}$ , 82%; (h)  $\text{allylMgBr}$ ,  $\text{THF}$ ,  $-40^\circ\text{C}$ , 90%; (i)  $\text{NaIO}_4$ ,  $\text{THF}$ ,  $\text{RT}$ , then  $\text{CSA}$ ,  $\text{MeOH}$ ,  $\text{RT}$ , 59%; (j)  $\text{O}_3$ , Sudan III,  $\text{CH}_2\text{Cl}_2$ - $\text{MeOH}$ ,  $-78^\circ\text{C}$ , then  $\text{NaBH}_4$ ,  $\text{MeOH}$ , 87%; (k)  $\text{TBDPSCl}$ ,  $\text{DIPEA}$ ,  $\text{CH}_2\text{Cl}_2$ , 91%; (l)  $\text{Pd}(\text{OH})_2\text{-C}$ ,  $\text{H}_2$  (1 atm),  $\text{AcOH}$  (cat.),  $\text{EtOH-THF}$ , 92%; (m)  $\text{TPAP}$ ,  $\text{NMO}$ , 4 Å molecular sieves,  $\text{CH}_2\text{Cl}_2$ , 95%; (n)  $\text{NH}_2\text{CH}_2\text{SnBu}_3$ ,  $\text{AlMe}_3$ ,  $\text{toluene}$ ,  $0^\circ\text{C}$ , not isolated; (o)  $\text{vinylSPh}$ ,  $n\text{BuLi}$ ,  $\text{THF}$ ,  $-78^\circ\text{C}$ , not isolated; (p) *aq*  $\text{NH}_4\text{Cl}$ , 75%; (q)  $\text{Teoc-Cl}$ ,  $\text{DIPEA}$ ,  $\text{CH}_2\text{Cl}_2$ , 91%; (r) *m*- $\text{CPBA}$  (1 eq),  $\text{NaHCO}_3$ ,  $\text{CH}_2\text{Cl}_2$ ,  $-30^\circ\text{C}$  to  $\text{RT}$ , 88%; (s)  $\text{Cl}_2\text{C=CCl}_2$ ,  $\text{pyridine}$ ,  $125^\circ\text{C}$ , 85%; (t)  $\text{BCl}_3$ ,  $\text{CH}_2\text{Cl}_2$ ,  $0^\circ\text{C}$ , 67%; (u)  $\text{PCC}$ ,  $\text{Celite}$ ,  $\text{CH}_2\text{Cl}_2$ , 91%; (v)  $\text{HF} \cdot \text{pyridine}$ ,  $\text{THF}$ , 88%; (w)  $\text{MsCl}$ ,  $\text{CH}_2\text{Cl}_2$ ,  $-10^\circ\text{C}$  to  $\text{RT}$ , 92%; (x)  $\text{DIPEA}$ ,  $\text{CH}_3\text{CN}$ ,  $60^\circ\text{C}$ , 76%.

**Scheme 1.2** A summary of the total synthesis of (±)-lapidilectine B.

### 1.7 Total synthesis of (±)-lundurine A and (±)-lundurine B<sup>29,30</sup>

In 2014 the Nishida group published the total synthesis of lundurines, hexacyclic *Kopsia* alkaloids with an unprecedented cyclopropane-fused indoline skeleton. The synthesis of (±)-lundurine B was completed in 29 steps, featuring a highly efficient and stereoselective synthesis of a cyclopropane-fused indoline, a siloxy-diene ring closing

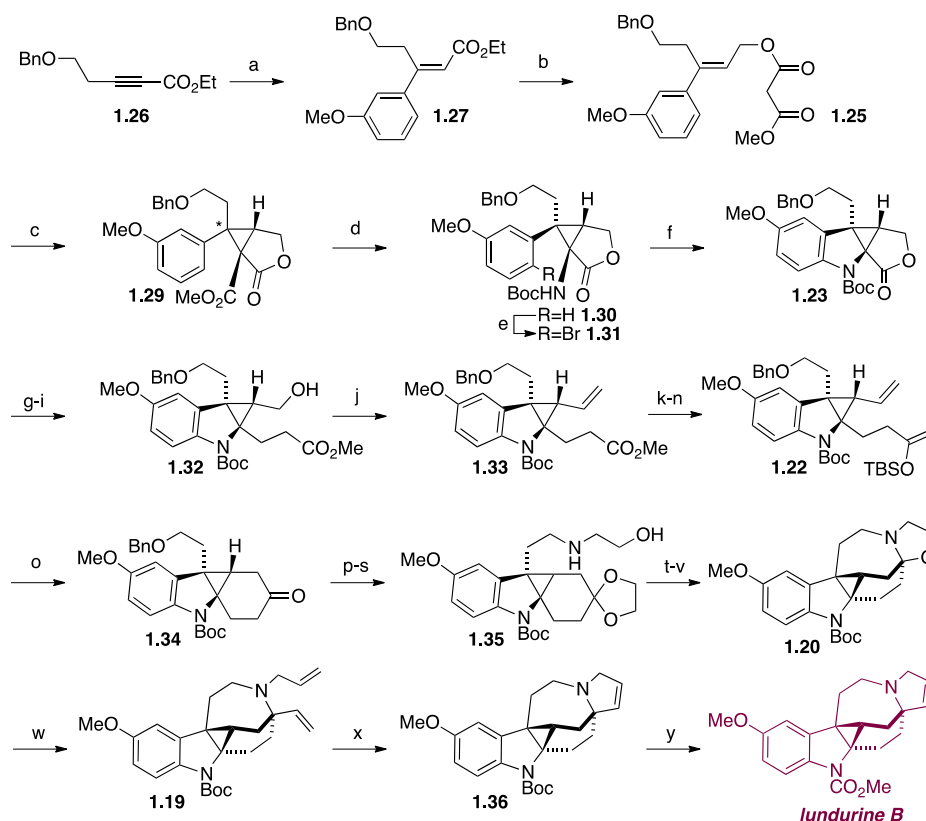
metathesis to construct the six-membered ring and intramolecular amino acetal formation to form an eight-membered ring (**Scheme 1.3**).<sup>29</sup>



**Scheme 1.3** Retrosynthetic analysis of (±)-lundurine B.

As depicted in **Scheme 1.3**, the alkyne **1.26** was converted into a cyclopropanation precursor **1.25** via palladium-catalyzed hydroarylation, followed by reduction with DIBAL-H and acylation. Iodine-mediated cyclopropanation delivered tricyclic lactone methyl ester **1.29**, which was then saponified and acidified to give the lactone carboxylic acid. Subsequent Curtius rearrangement delivered *N*-Boc protected amine **1.30** and selective bromination of the aromatic ring afforded bromide **1.31**. Copper-mediated cyclization completed construction of the cyclopropane-fused indoline core. Intermediate **1.23** was then transformed into **1.34** over a series of steps. First, the lactone **1.23** was reduced to a lactol, which was subjected to a Wittig reaction and selective olefin hydrogenation to give **1.32**. Oxidation of **1.32** to an aldehyde, which participated in another Wittig reaction installed the vinyl group in **1.33**. The methyl ester was then converted to a ketone, followed by silylation to deliver metathesis precursor **1.22**. Ring closing metathesis using Grubbs 2<sup>nd</sup> generation catalyst, and subsequent TBS deprotection furnished tetracyclic intermediate **1.34**. The formation of the fifth and the largest ring was achieved by protecting the cyclohexanone as a ketal and transforming the benzyl ether into a 2-hydroxyethylamino group **1.35**, which upon removal of the ketal group underwent transacetalization to give **1.20**. The cleavage of the acetal C-O bond and introduction of the vinyl group at the bridgehead, followed by conversion of the resulting hydroxyethynyl group into propenyl group and ring-closing metathesis formed the substituted dihydropyrrole ring of **1.36**. Finally, the *N*-Boc protecting group was converted into the

corresponding methyl carbamate *via* the silyl carbamate to complete the total synthesis of ( $\pm$ )-lundurine B.

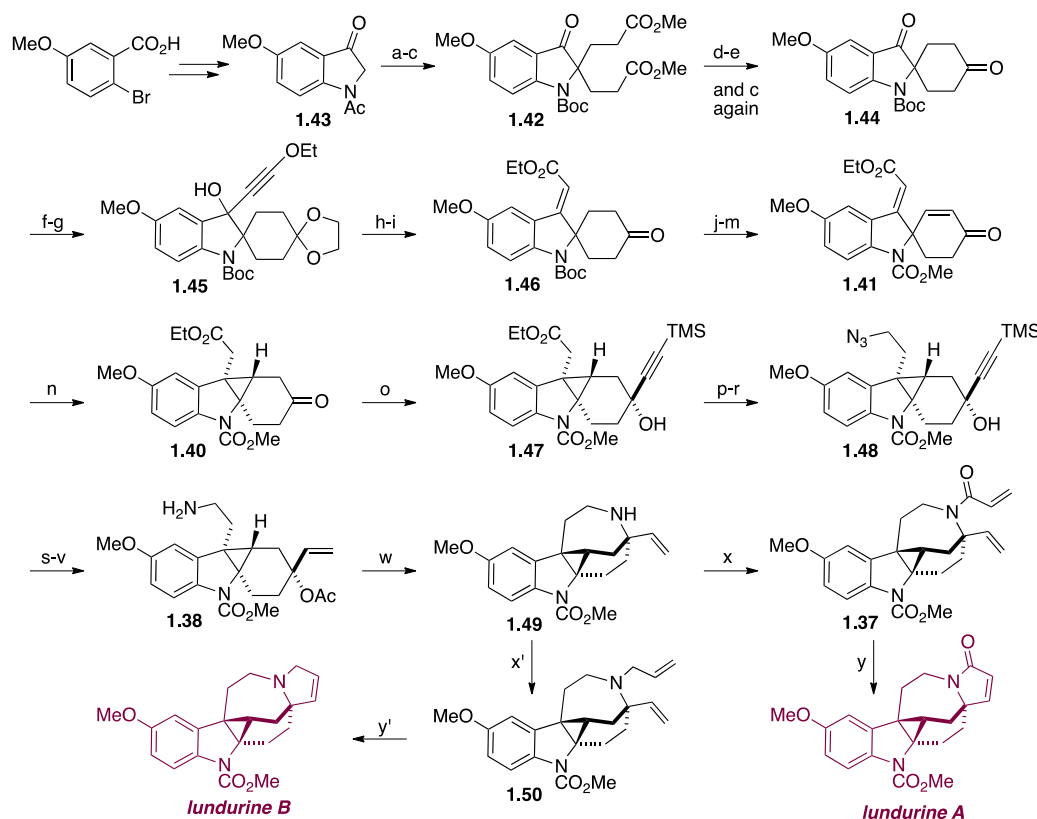


Reagents and conditions: (a) (3-OMe) $C_6H_4B(OH)_2$ ,  $Pd(OAc)_2$ , dppb, AcOH,  $CHCl_3$ , 50 °C, 81%; (b) DIBAL-H,  $CH_2Cl_2$ , -78 °C to -40 °C, then  $MeOCOCH_2COCl$ ,  $Et_3N$ , DMAP,  $CH_2Cl_2$ , RT, 87%; (c)  $I_2$ ,  $K_2CO_3$ ,  $BnNEt_3Cl$ , THF, 65 °C, 84%; (d) 10 M NaOH, 40 °C followed by 1M HCl-THF (1:1), 30 °C, then DPPA,  $Et_3N$ , *t*-BuOH, 4 Å molecular sieves, 80 °C, 90%; (e) NBS,  $CH_3CN$ , RT, not isolated; (f) CuI, TMEDA,  $Cs_2CO_3$ , DMSO, 100 °C, 88%; (g) DIBAL-H,  $CH_2Cl_2$ , -78 °C, 59%; (h)  $Ph_3PCHCO_2Me$ , PhMe, THF (9:1), 50 °C, 94%; (i)  $CoCl_2 \cdot 6H_2O$ ,  $NaBH_4$ , THF-MeOH (1:1), RT, 3 cycles, 94%; (j) TPAP, NMO, 4 Å molecular sieves,  $CH_2Cl_2$ , RT, then  $PPh_3=CH_2$ , THF, -78 °C to RT, 82%; (k) DIBAL-H,  $CH_2Cl_2$ , -78 °C, 82%; (l)  $ZrMe_4$ ,  $Et_2O$ , -78 °C, 89%; (m)  $(COCl)_2$ , DMSO,  $Et_3N$ ,  $CH_2Cl_2$ , -78 °C, 89%; (n) TBSCl, KHMDS, THF, -78 °C, 86%; (o) Grubbs II,  $CH_2Cl_2$ , RT, 2 cycles, then TBAF, AcOH, THF, RT, 92%; (p)  $TMSOCH_2CH_2OTMS$ , TMSOTf,  $CH_2Cl_2$ , -78 °C; (q)  $Pd(OH)_2-C$ ,  $H_2$ , EtOH, RT; (r)  $(COCl)_2$ , DMSO,  $Et_3N$ ,  $CH_2Cl_2$ , -78 °C, 83 % over 3 steps; (s) 2-aminoethanol, MeOH, RT, then  $NaBH_4$ , RT; (t) AcOH-THF- $H_2O$  (3:1:1), 40 °C, then  $CHCl_3$ , 4 Å molecular sieves, 81%; (u)  $vinylMgBr$ ,  $AlCl_3$ ,  $Et_2O-CH_2Cl_2$ , -78 °C, 86%; (v)  $(COCl)_2$ , DMSO,  $Et_3N$ ,  $CH_2Cl_2$ , -78 °C, 81%; (w)  $Ph_3PCH_3Br$ , *n*-BuLi, THF, RT, 63%; (x) Grubbs II,  $CH_2Cl_2$ , RT, 97%; (y) TBSOTf, TMEDA,  $CH_2Cl_2$ , RT, then MeI, TBAF, THF, 4 Å molecular sieves, 0 °C, 31%.

**Scheme 1.4** A summary of the total synthesis of ( $\pm$ )-lundurine B.

[illegible]

followed by ring closing metathesis completed the syntheses of (±)-lundurine A and (±)-lundurine B respectively.



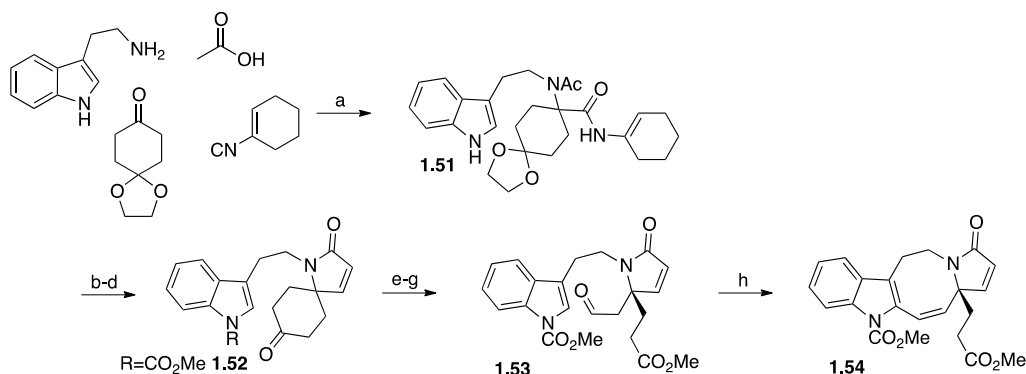
Reagents and conditions: (a) methyl acrylate, DBU, THF, RT; (b)  $K_2CO_3$ , MeOH, RT; (c)  $Boc_2O$ ,  $Et_3N$ , DMAP, THF, reflux, 33% over 8 steps; (d) LiHMDS, THF,  $-40\text{ }^\circ\text{C}$ ; (e) wet DMSO, NaCl,  $160\text{ }^\circ\text{C}$ , 72% over 3 steps; (f)  $(TMSOCH_2)_2$ , TMSOTf,  $CH_2Cl_2$ ,  $-78\text{ }^\circ\text{C}$ ; (g) ethoxyacetylene,  $nBuLi$ , THF,  $-78\text{ }^\circ\text{C}$  to RT; (h)  $Cu(OTf)_2$  (5 mol%),  $CH_2Cl_2$ -EtOH (4:1), RT; (i) TsOH, acetone,  $40\text{ }^\circ\text{C}$ ; (j) LiHMDS, THF,  $-78\text{ }^\circ\text{C}$ ; (k)  $Pd(OAc)_2$ , DMSO,  $O_2$ , RT, 66% over 6 steps; (l) trifluoroacetic acid, TMSOTf,  $CH_2Cl_2$ ,  $0\text{ }^\circ\text{C}$ ; (m)  $K_2CO_3$ ,  $ClCO_2Me$ , reflux, 77% over 2 steps; (n)  $SmI_2$ ,  $tBuOH$ , LiCl, THF,  $-78\text{ }^\circ\text{C}$ , 53%; (o)  $nBuLi$ , TMS acetylene,  $Et_2O$ ,  $-78\text{ }^\circ\text{C}$ , 86%; (p)  $LiBH_4$ , EtOH, THF, RT, 61%; (q) TsCl,  $Et_3N$ , DMAP,  $CH_2Cl_2$ , RT; (r)  $NaN_3$ , DMF,  $80\text{ }^\circ\text{C}$ ; (s)  $K_2CO_3$ , MeOH, RT; (t)  $Ac_2O$ , DMAP, pyridine,  $65\text{ }^\circ\text{C}$ , 79% over 4 steps; (u)  $SmI_2$ , THF,  $0\text{ }^\circ\text{C}$ ; (v) Lindlar cat, quinoline, EtOAc, RT, 73% over 2 steps; (w)  $Pd(PPh_3)_4$  (20 mol%),  $Et_3N$ , MeCN,  $65\text{ }^\circ\text{C}$ , 98%; (x)  $CH_2=CHCOCl$ ,  $Et_3N$ , DMAP (cat.),  $CH_2Cl_2$ ,  $0\text{ }^\circ\text{C}$ ; (y) Grubbs II (20 mol%),  $(CH_2Cl)_2$ ,  $50\text{ }^\circ\text{C}$ , 70% over 2 steps; (x') allyl bromide,  $K_2CO_3$ , MeCN,  $50\text{ }^\circ\text{C}$ ; (y') Grubbs II (20 mol%),  $CH_2Cl_2$ , RT, 85% over 2 steps.

**Scheme 1.6** A summary of total synthesis of (±)-lundurines A and B.

### 1.8 Synthetic efforts towards grandilodines and related *Kopsia* alkaloids

Several other groups have also published synthetic efforts towards lapidilectine, lundurine and grandilodine type alkaloids, all reaching an advanced tetracyclic intermediate with rings fused together but lacking the key spiro cyclohexane-indoline moiety.<sup>31-33</sup>

Sarpong's group reported studies towards lapidilectine type alkaloids using a four component Ugi coupling as a key step to install all the necessary carbons found in these natural products (**Scheme 1.7**).<sup>31</sup> The adduct **1.51** was subjected to acidic methanolysis followed by Dieckmann condensation, dehydration and protection of the indole nitrogen as the methyl carbamate to furnish spiro lactam **1.52**. The opening of the cyclohexanone ring was accomplished by silyl enol ether formation, dihydroxylation and oxidative cleavage. Several different protocols were investigated to convert intermediate **1.53** into a more advanced natural product precursor. For example, upon treatment with Amberlyst-15 resin, aldehyde **1.53** was converted into tetracyclic intermediate **1.54**.



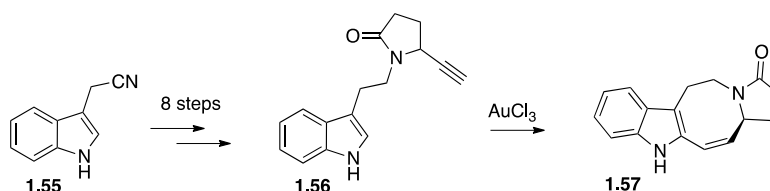
Reagents and conditions: (a) MeOH, 23 °C, 95%; (b) AcCl, MeOH, 0 °C to RT, 96%; (c) KO<sup>t</sup>Bu, THF, 0 °C, then NaBH<sub>4</sub>, *i*PrOH; (d) MeOCOC<sub>2</sub>H<sub>5</sub>, KO<sup>t</sup>Bu, THF, then HCl, 0 °C, 85% over 3 steps; (e) TBSOTf, Et<sub>3</sub>N, CH<sub>2</sub>Cl<sub>2</sub>, 0 °C to RT, 98%; (f) OsO<sub>4</sub>, TBHP, acetone-H<sub>2</sub>O (6:1); (g) Pb(OAc)<sub>4</sub>, MeOH, -40 °C, 65% over 2 steps; (h) Amberlyst-15, MeOH, RT 83%, then Amberlyst-15, DCE, 80 °C, 54%.

**Scheme 1.7** Studies towards Grandilodine C by the Sarpong group.

Echavarren's group explored the synthesis of the tetracyclic core of lundurines using gold-catalyzed cyclization.<sup>32</sup> The alkylindol precursor was prepared in 8 steps from indole derivative **1.55** (**Scheme 1.8**). Extensive screening revealed gold(III) chloride to be

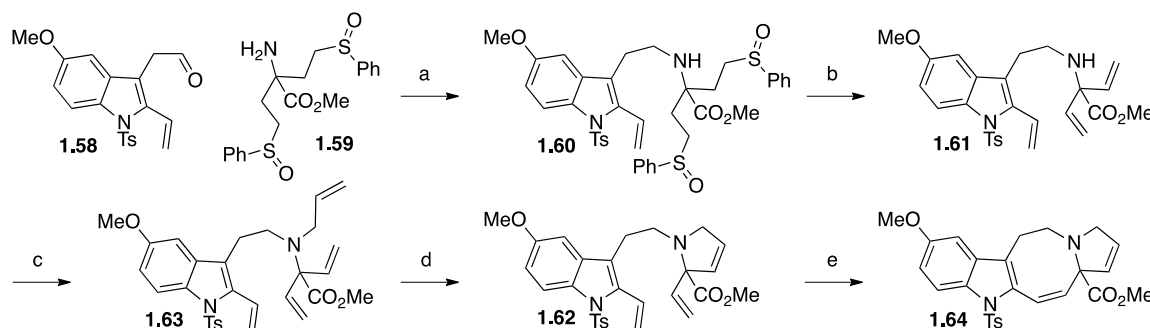


the most efficient catalyst for 8-*endo-dig* cyclization of alkynylindol **1.56** to azocino[5,4-*b*]-indole derivative **1.57**.



**Scheme 1.8** Construction of tetracyclic intermediate using gold catalysis.

Finally, the Martin's group investigated a double ring closing metathesis approach to the lundurines.<sup>33</sup> The RCM precursor was prepared *via* an oxidation-reductive amination reaction sequence between indole derivative **1.58** and amine **1.59** (**Scheme 1.9**). The resulting product **1.60** was then subjected to pyrolytic elimination to obtain triene **1.61**, which upon *N*-allylation delivered the key intermediate **1.63**. Grubbs 1<sup>st</sup> generation catalyst was found to give best results promoting the first RCM to form the five-membered ring as well as the second RCM to afford tetracycle **1.64**. Unfortunately, the second RCM reaction turned out to be irreproducible and the authors retracted the communication one year after publishing.<sup>34</sup>



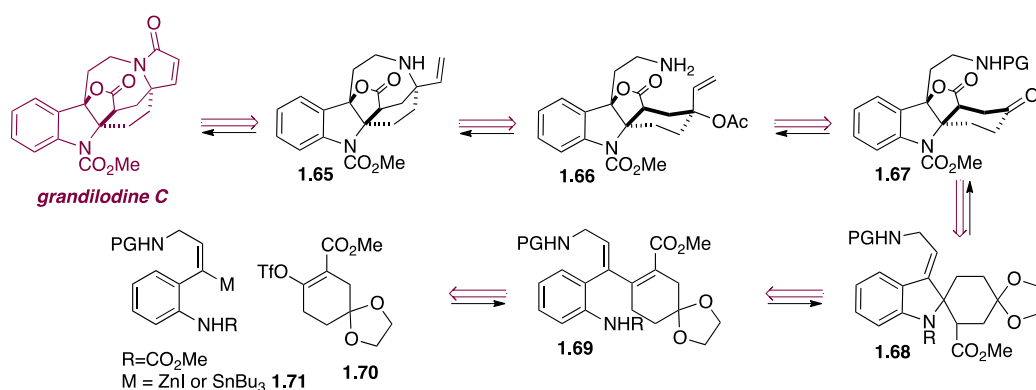
Reagents and conditions: (a)  $\text{NaBH}(\text{OAc})_3$ ,  $\text{CH}_2\text{Cl}_2$ , RT, 89%; (b) *p*-xylene,  $\mu\text{w}$ , 140 °C, 69%; (c) allyl bromide,  $\text{K}_2\text{CO}_3$ ,  $\text{CH}_3\text{CN}$ ,  $\mu\text{w}$ , 80 °C, 93%; (d) Grubbs I (10% mol),  $\text{CH}_2\text{Cl}_2$ ,  $\mu\text{w}$ , 50 °C, 2 cycles, 76%; (e) Grubbs I (20% mol),  $\text{CH}_2\text{Cl}_2$ ,  $\mu\text{w}$ , 50 °C, 2 cycles, 26%.

**Scheme 1.9** Double RCM approach by Martin's group.

### 1.9 Retrosynthetic analysis of grandilodine C and the aim of the project

Our initial retrosynthetic plan involved a Stille coupling, conjugate addition sequence, lactonization, nucleophilic displacement and ring closing metathesis reaction as

key steps (**Scheme 1.10**). The lactam ring could be assembled using *N*-acylation and an RCM protocol that has been recently proven to be successful in Nishida's total synthesis of ( $\pm$ )-lundurine A. Closure of the eight-membered ring could be accomplished by Nishida's intramolecular trapping of a palladium pi-allyl species. The vinyl group could be introduced using a Grignard reaction and the lactone ring could be assembled *via* lactonization or iodolactonization-dehalogenation of intermediate **1.68**. The spiroindoline compound **1.68** could arise from an intramolecular conjugate addition of adduct **1.69**, which could be obtained from palladium-catalyzed cross coupling between triflate **1.70** and organometallic carbamate **1.71**.



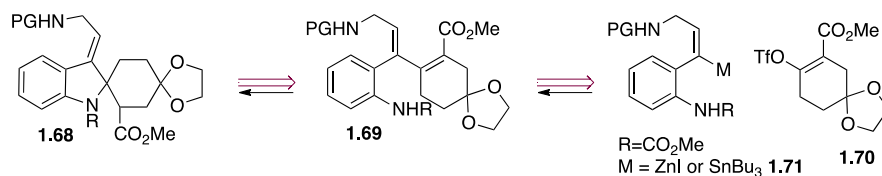
**Scheme 1.10** Retrosynthetic analysis of grandilodine C.

The project was designed to explore the potential of the conjugate addition reaction in constructing the indoline core of the grandilodine C natural product. If successful, the abovementioned approach could provide a facile synthetic route to grandilodine C and related *Kopsia* alkaloids, as well as being a novel method of synthesizing spiroindoline type compounds.

## Chapter Two: Results and Discussion

### 2.1 Methyl carbamate series – synthesis and reactivity

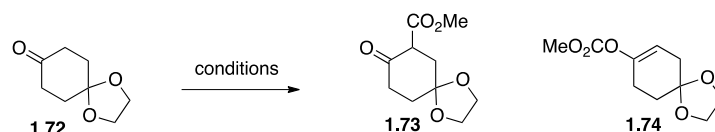
According to the retrosynthetic plan described in **Chapter One**, the key intermediate **1.68** could arise from an intramolecular conjugate addition within compound **1.69** (Scheme 1.11). In order to limit the number of linear steps in the total synthesis of grandilodine C, a convergent approach to the synthesis of **1.69** was required. Considering the electronic properties, the reactivity and commercial availability of the possible building blocks it was decided to prepare **1.69** via cross coupling reaction between organometallic compound **1.71** and triflate **1.70**.



**Scheme 1.11** Retrosynthetic analysis of the intermediate **1.68**.

#### 2.1.1 The synthesis of organostannane and triflate compounds

Triflate **1.70** was prepared in two steps from commercially available 1,4-cyclohexanedione monoethylene ketal. It is a known compound and the two-step preparation has been previously reported in the literature.<sup>35,36</sup> These published procedures usually involve conversion of ketal **1.72** into  $\beta$ -keto ester **1.73** using sodium hydride and dimethyl carbonate, followed by triflation to give the final product **1.70**. It was found however that under these conditions, the synthesis of a  $\beta$ -keto ester **1.73** was problematic due to *O*-substitution taking place exclusively, resulting in synthesis of the unwanted product **1.74**. This was the case whenever sodium hydride was used as a base in combination with dimethyl carbonate or methyl chloroformate in THF as solvent. Inspection of the  $^1\text{H}$  NMR spectrum of **1.74** revealed characteristic signal at around  $\delta$  5.4 ppm, typical of a methylylidene proton, which confirmed the formation of the *O*-substituted product.

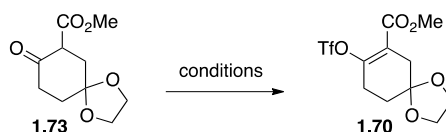


Entry	Conditions	Yield of <b>1.73</b>	Yield of <b>1.74</b>
1	NaH, (MeO) <sub>2</sub> CO, THF, 0 °C to RT, 12-24 h	0%	20-60%
2	NaH, MeO <sub>2</sub> CCl, THF, 0 °C to RT, 12-24 h	0%	30%
3	LDA, MeO <sub>2</sub> CCN, Et <sub>2</sub> O, -78 °C to 0 °C, 2 h	20-30%	0%
4	LDA, MeO <sub>2</sub> CCN, THF, -78 °C to 0 °C, 2 h	20-30%	0%
5	LDA, MeO <sub>2</sub> CCN, THF, -78 °C to 0 °C, 2 h, 30 mmol scale	46%	0%

**Table 1.1** The synthesis of  $\beta$ -keto ester **1.73**.

Switching to a different type of base and using methyl cyanoformate to introduce the methoxycarbonyl group, as described by Mander *et al*, was essential for the successful synthesis of **1.73**.<sup>37</sup> Following this method avoided formation of the undesired *O*-substituted product **1.74** and delivered the required  $\beta$ -keto ester **1.73** in moderate yield. Pleasingly, the yield was improved by scaling the reaction up, which allowed for preparation of sufficient quantities of compound **1.73**. Mander *et al* attribute selectivity for substitution at carbon to the use of diethyl ether instead of THF. Interestingly, during the synthesis of compound **1.73** using the Mander protocol neither yield nor selectivity was compromised when using THF.

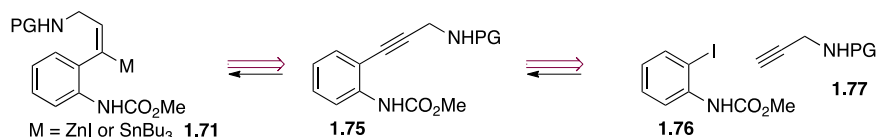
Unlike the synthesis of the  $\beta$ -keto ester, conversion of **1.73** into **1.70** proceeded smoothly (**Table 1.2**). Several conditions were tried and the vast majority delivered the product in excellent yield. Quantitative conversion was achieved when using *N*-phenylbis(trifluoromethanesulfonimide) as the triflating agent.<sup>35</sup>



Entry	Conditions	Yield of <b>1.70</b>
1	DIPEA, Tf <sub>2</sub> O, CH <sub>2</sub> Cl <sub>2</sub> , 0 °C to RT, 16 h	90%
3	LDA, Commins' Reagent, THF, -78 °C to 0 °C, 12 h	92%
4	LDA, Tf <sub>2</sub> NPh, THF, -78 °C to 0 °C, 12 h	90%
5	NaH, Tf <sub>2</sub> NPh, THF, 0 °C to RT, 16 h	quantitative

**Table 1.2** The synthesis of triflate **1.70**.

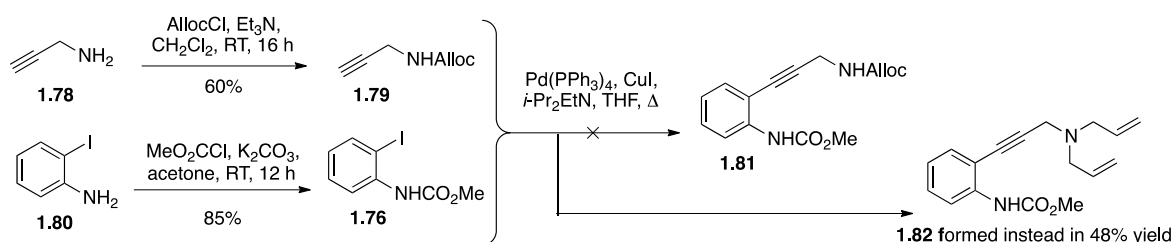
The second substrate required a suitable functional group **M** in order to participate in the cross coupling reaction with the triflate **1.70**. These groups typically contain metals or metalloids such as tin (Stille coupling), zinc (Negishi coupling), magnesium (Kumada coupling) or boron (Suzuki coupling).<sup>38</sup> Various protocols exist for the preparation of suitable organometallic cross coupling substrates, one of which is hydrometalation of the corresponding alkyne.<sup>39</sup> The main advantage of this method is that depending on the mode of addition, the reaction is often stereospecific.<sup>39</sup> Moreover, with carefully designed electronic properties of the substrate, high regioselectivity can be achieved.<sup>40</sup> The substrates for hydrometalation, the acetylenes, can be readily accessed *via* Sonogashira coupling<sup>41</sup> of rather simple, often commercially available building blocks. It was therefore planned that the cross coupling partner **1.71** could be obtained from the alkyne **1.75**, which should be easily accessible *via* cross coupling between methyl(2-iodophenyl) carbamate and *N*-protected propargylamine (**Scheme 1.12**).



**Scheme 1.12** Retrosynthetic analysis of the intermediate **1.71**.

The synthesis began with nitrogen protection of compounds **1.78** and **1.80** (**Scheme 1.13**). A methyl carbamate functional group is present in the grandilodine C natural product and therefore it could be incorporated right at the beginning of the synthesis, simultaneously serving as a protecting group for the aniline-like nitrogen

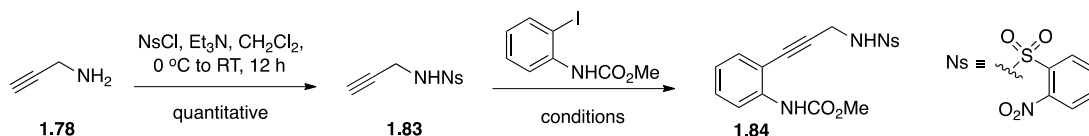
(compound **1.76**). The other nitrogen, delivered by compound **1.78**, was initially protected as an allyl carbamate.<sup>42,43</sup> This was dictated by the fact that it could be subsequently deprotected at late stages of the synthesis under mild conditions.<sup>44</sup> Unfortunately, the retrosynthetic plan did not account for the potential use of palladium (0) species in the preparation of compound **1.71**. The allyloxycarbonyl group was unsuitable for palladium-catalyzed reactions due to deprotection and alkylation taking place during Sonogashira coupling to deliver undesired product **1.82**.



**Scheme 1.13** Failed synthesis of an alkyne **1.81** and unexpected deprotection that delivered alkyne **1.82** instead.

Finding an alternative protecting group, which would be stable under all reaction conditions throughout the sequence and removable without destroying functional groups in already highly functionalized intermediate **1.66** was not a trivial task. The (2-nitrophenyl)sulfonyl group (Ns group) seemed to meet the abovementioned requirements and it was therefore used instead of the allyl carbamate.<sup>45</sup>

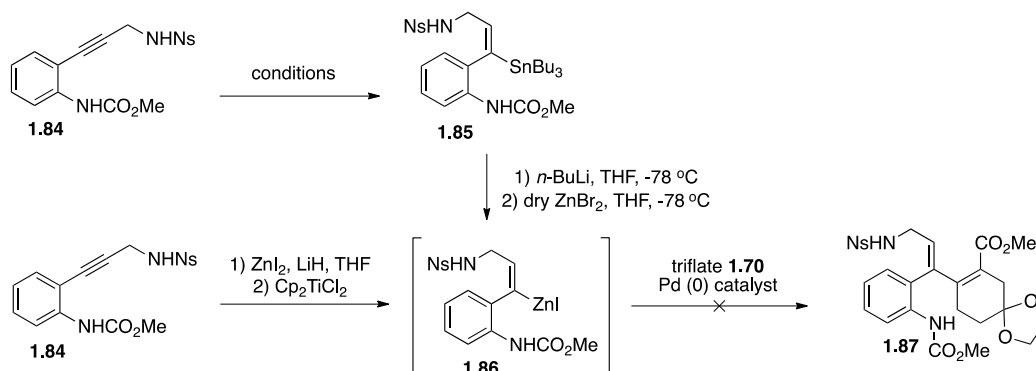
The commercially available propargylamine was protected with (2-nitrophenyl)sulfonyl chloride in quantitative yield.<sup>46</sup> The subsequent Sonogashira coupling with methyl(2-iodophenyl) carbamate delivered the acetylene compound **1.84** in moderate to high yields, depending on the reaction conditions and purification method. The best results were obtained with  $\text{PdCl}_2(\text{PPh}_3)_2$  catalyst, copper iodide, triethylamine and DMF as solvent (**Table 1.3**). Reaction was completed within 3 h if gently heated (up to 45 °C) and the crude product was usually pure enough to be used directly in the next step. Avoiding column chromatography was highly advantageous at this stage as the compound showed little stability on silica gel.



Entry	Conditions	Purification	Yield of <b>1.84</b>
1	$\text{Pd}(\text{PPh}_3)_4$ , CuI, DIPEA, THF, reflux, 12 h	chromatography	38%
3	$\text{Pd}(\text{PPh}_3)_4$ , CuI, DIPEA, THF, reflux, 12 h	recrystallization	54%
4	$\text{PdCl}_2(\text{PPh}_3)_2$ , CuI, TEA, DMF, $45\text{ }^\circ\text{C}$ , 5 h	recrystallization	75%
5	$\text{PdCl}_2(\text{PPh}_3)_2$ , CuI, TEA, DMF, $45\text{ }^\circ\text{C}$ , 3 h	none	>98%

**Table 1.3** The synthesis of alkyne **1.84**.

With the acetylene compound **1.84** in hand several hydrometalation protocols were tested (**Table 1.4**). Due to the regiochemistry required in **1.71**, compound **1.84** was unsuitable for hydroboration, which ruled out the use of highly reliable and extremely versatile Suzuki coupling.<sup>47</sup> There was however the possibility of using organozinc or organotin compounds instead, with the latter proving to be the most successful. In general, hydrostannylation procedures were more promising, primarily due to greater stability of the organostannanes over organozinc reagents.<sup>48</sup> The former could be isolated, purified and fully characterized, unlike the latter, which although reported to be more reactive are also known to be air and moisture sensitive, hence problematic to handle.<sup>49</sup> All attempts to prepare organozinc reagents *in situ* and then immediately subjecting them to coupling conditions failed to deliver the product **1.87**.<sup>50,51</sup> Experimenting with different hydrostannylation procedures was more rewarding and adapting a method from Alami and co-workers<sup>52</sup> enabled synthesis of the required stannane **1.85**.



Entry	Conditions	Yield of <b>1.85</b>
1	BuMgBr, 0.1 eq Cp <sub>2</sub> TiCl <sub>2</sub> , Bu <sub>3</sub> SnCl, Et <sub>2</sub> O, 0 °C to RT, 4 h	0%
2	Bu <sub>3</sub> SnH, 0.01 eq PdCl <sub>2</sub> (PPh <sub>3</sub> ) <sub>2</sub> , THF, 0 °C to RT, 8 h	43%
3	Bu <sub>3</sub> SnH, 0.01 eq Pd(PPh <sub>3</sub> ) <sub>4</sub> , THF, RT, 16 h	87%

**Table 1.4** The synthesis of organostannane **1.85**.

The best conditions were found when Pd(PPh<sub>3</sub>)<sub>4</sub> catalyst was used instead of PdCl<sub>2</sub>(PPh<sub>3</sub>)<sub>2</sub> and the reaction was run overnight (**Table 1.4, entry 3**). It was very pleasing to find that the reaction proceeded not only in very high yield but also with excellent regioselectivity to furnish the tributyltin substituent exclusively on the  $\alpha$  carbon. Neither TLC nor <sup>1</sup>H NMR analyses detected the other regioisomer. According to the Alami group the outcome of hydrostannylation reaction of substituted aryl alkynes was mostly influenced by the position of the substituent at the aromatic ring.<sup>52</sup> In particular, substituents in the *ortho* position significantly enhanced regioselectivity, leading to almost exclusive formation of the  $\alpha$  isomer.<sup>53</sup> Such preference could be attributed to the coordinative interaction between the palladium and the heteroatom, overcoming the steric effect and resulting in the bulky tributyltin group being added to what appears to be the more sterically hindered site.<sup>53</sup>

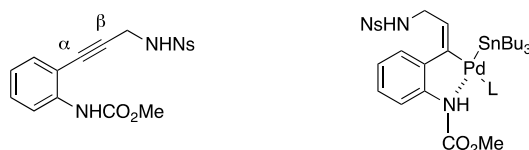


**Figure 1.5** *Ortho*-directing effect.

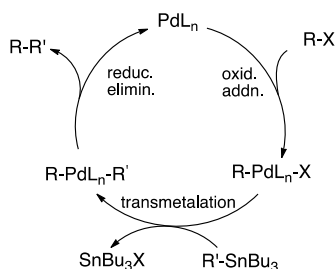


Compound **1.85** was fully characterized and  $^1\text{H}$  NMR analysis was used to confirm the correct regiochemistry. The methylylidene proton appeared at around  $\delta$  5.3 ppm as a triplet, which confirmed its position on the  $\beta$  carbon, right next to a  $\text{CH}_2$  group. The alkene geometry in **1.85** was assumed to be *Z* due to the fact that addition of tributyltin hydride to alkyne proceeds in *syn* fashion, where hydrogen and  $\text{SnBu}_3$  group are added to the same side of the triple bond.<sup>53</sup> Having successfully completed the synthesis of triflate **1.70** and organostannane **1.85**, the key cross coupling-conjugate addition sequence was attempted.

### 2.1.2 Optimization of the Stille coupling reaction conditions

Palladium-catalyzed reactions with organotin reagents were first explored by Colin Eaborn, Toshihiko Migita, and Masanori Kosugi in 1976 and 1977.<sup>54</sup> In 1978 John Stille and David Milstein developed a much milder and more broadly applicable procedure for the synthesis of ketones from acyl chlorides and organotin reagents.<sup>55</sup> The work continued in the 1980s and palladium-catalyzed coupling of unsaturated halides or sulfonates with organostannanes, now commonly referred to as the Stille coupling, began to gain popularity in organic synthesis.<sup>54,56</sup> Due to the availability of various organostannanes, their stability to air and moisture and broad scope, the reaction has been widely used in the synthesis of polymers as well as natural products.<sup>57,58</sup>

The general mechanism of the Stille coupling is well understood and just like other cross-coupling reactions involves an oxidative addition of palladium(0) into a carbon-halide or carbon-sulfonate bond, transmetalation with the organotin reagent and reductive elimination to yield the coupled product and regenerate the catalyst.<sup>38</sup> However, more detailed studies of the Stille coupling mechanism reveal that it is very complex with various reaction pathways possible.<sup>59</sup> Several studies reported that transmetalation is most likely to be the rate-determining step.<sup>60-62</sup> It has also been demonstrated that different ligands, additives and the nature of the solvent could all influence the overall performance of the catalytic cycle.<sup>59</sup>



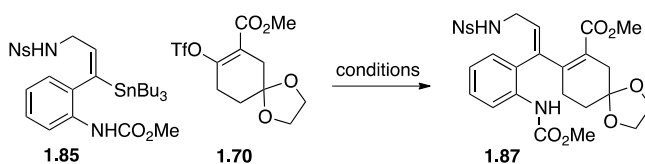
**Scheme 1.14** General mechanism of the Stille coupling.

Screening for optimal reaction conditions began with testing the simplest and most readily available set of reagents, namely compounds **1.70** and **1.85** and tetrakis(triphenylphosphine)palladium(0) catalyst in THF (**Table 1.5**). In his early work Stille reported addition of stoichiometric quantities of LiCl to be essential for coupling with triflates.<sup>56</sup> It was assumed that chloride ion could replace the triflate in the triflatopalladium(II) species, formed after oxidative addition of organic triflate.<sup>63</sup> The resulting chloropalladium(II) complex was supposed to undergo transmetalation step more readily, hence accelerate the overall catalytic cycle.<sup>63</sup> This requirement however turned out not to be general and exceptions were reported, where LiCl could either accelerate or retard coupling, depending on the polarity of solvent, type of triflate (aryl vs vinyl) and the ligand.<sup>63</sup> It soon became apparent (**Table 1.5, entry 12 and 13**) that in case of compound **1.87**, more sophisticated conditions would be required in order to achieve the coupling.

Another common additive that has been reported to enhance reaction rates is copper(I) iodide.<sup>64</sup> It has been theorized that in high polarity solvents, copper could transmetalate the organostannyl reagent before reacting with the palladium species in somewhat similar fashion to how acetylenes are introduced into the catalytic cycle of the Sonogashira coupling reaction.<sup>65</sup> Finally, adding a fluoride source, such as cesium fluoride, could further enhance reaction rate by acting on the triflate in a similar way to LiCl.<sup>66</sup> In addition, fluoride strongly binds to the tin byproducts, which often contaminate the final product, making them easier to remove by means of filtration.<sup>66</sup> Although using a combination of CuI and CsF in high polarity solvents has been reported to improve yields of the Stille coupling, it provided only a very modest improvement was observed for compound **1.87** (**Table 1.5, entry 11**).

At this stage it was necessary to explore other catalysts. This was achieved by using weakly coordinated tris(dibenzylideneacetone)dipalladium(0) as a source of palladium in combination with different ligands to form the catalyst *in situ*. Work published by Farina *et al*, who reported large rate accelerations with tri-2-furylphosphine (TFP) and triphenylarsine, was very encouraging and indeed great progress was made towards the synthesis of **1.87** after introducing these ligands (**Table 1.5, entries 8-10**).<sup>60</sup> In order to account for these observations the authors postulated that the rate-determining transmetalation step involves a  $\pi$  complex between the metal and the stannane double bond.<sup>60</sup> Thus the ligands that more readily dissociate from Pd(II) and facilitate formation of this  $\pi$  complex are the ones that enhance the coupling rates the most.<sup>60</sup> Major improvements in the yield were seen with AsPh<sub>3</sub> and to a lesser extent with TFP. Interestingly, PPh<sub>3</sub> ligand in DMF without additives mentioned earlier gave higher yields of **1.87** than when CuI and CsF were added to the reaction. It was later confirmed that copper and fluoride additives do not improve the reaction yield as better results were always obtained with the catalyst and ligand only (**Table 1.5, entries 6 and 7**). High polarity solvents were used throughout, giving slight improvement in yield over THF. Also the high boiling point of DMF allowed exploring the reaction over a greater temperature range. An alternative high polarity medium, *N*-methyl-2 pyrrolidone (NMP), was briefly explored, but DMF remained the solvent of choice, providing both excellent solubility and higher yields. Finally, the temperature and reaction time were optimized. It was discovered that the reaction would not work at room temperature and heating was required in order to initiate the catalytic cycle. According to TLC analysis, performing the reaction at 60 °C was required in order to begin to see the product being formed within the first couple of hours of reaction. It was also found that the reaction was completed in around 16 h. Increasing the temperature to 80 °C did not shorten the reaction time. In fact, the yield of **1.87** was compromised, as several byproducts were detected during TLC analysis of the reaction run at that temperature. Microwave irradiation was briefly explored in order to minimize byproduct formation observed at higher temperatures (**Table 1.5, entry 3**). The results were satisfactory due to the significantly shorter time required for completion, but the yield of **1.87** was slightly lower than the yield obtained from the conventionally heated reaction. In conclusion, the optimized conditions involved heating compound **1.85** and

**1.70**, Pd<sub>2</sub>(dba)<sub>3</sub> catalyst and AsPh<sub>3</sub> in DMF at 60 °C for 16 h to deliver adduct **1.87** in 77% yield.



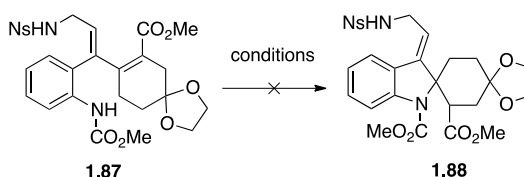
Entry	Conditions	Temperature	Time	Yield of <b>1.87</b>
1	Pd <sub>2</sub> (dba) <sub>3</sub> , AsPh <sub>3</sub> , DMF	20 °C	3 h	0%
2	Pd <sub>2</sub> (dba) <sub>3</sub> , AsPh <sub>3</sub> , DMF	45 °C	3 h	0%
3	Pd <sub>2</sub> (dba) <sub>3</sub> , AsPh <sub>3</sub> , DMF, $\mu$ w	100 °C	2 h	68%
<b>4</b>	<b>Pd<sub>2</sub>(dba)<sub>3</sub>, AsPh<sub>3</sub>, DMF</b>	<b>60 °C</b>	<b>16 h</b>	<b>77%</b>
5	Pd <sub>2</sub> (dba) <sub>3</sub> , AsPh <sub>3</sub> , NMP	60 °C	16 h	64%
6	Pd <sub>2</sub> (dba) <sub>3</sub> , AsPh <sub>3</sub> , CuI, DMF	60 °C	16 h	40%
7	Pd <sub>2</sub> (dba) <sub>3</sub> , AsPh <sub>3</sub> , CuI, CsF, DMF	60 °C	16 h	31%
8	Pd <sub>2</sub> (dba) <sub>3</sub> , AsPh <sub>3</sub> , DMF	80 °C	16 h	58%
9	Pd <sub>2</sub> (dba) <sub>3</sub> , P(furyl) <sub>3</sub> , DMF	80 °C	16 h	45%
10	Pd <sub>2</sub> (dba) <sub>3</sub> , PPh <sub>3</sub> , DMF	80 °C	16 h	40%
11	Pd(PPh <sub>3</sub> ) <sub>4</sub> , CuI, CsF, DMF	60 °C	20 h	12%
12	Pd(PPh <sub>3</sub> ) <sub>4</sub> , LiCl, THF	60 °C	20 h	0%
13	Pd(PPh <sub>3</sub> ) <sub>4</sub> , THF	60 °C	20 h	0%

**Table 1.5** Optimization of the Stille coupling reaction conditions.

### 2.1.3 Investigation into the conjugate addition reaction

It was initially expected that the product **1.87** would spontaneously cyclize to give compound **1.88**. Assembling intermediate **1.88** in this manner would not only reduce the total number of synthetic steps but would also construct the key spiro cyclohexane-indoline moiety found in grandilodine C. This was however not the case, as the adduct **1.87** was isolated from the Stille coupling reaction exclusively. Several methods

were tried to activate compound **1.87** towards intramolecular conjugate addition as described in the table below.<sup>67-70</sup>



Entry	Conditions	Time and temperature
1	KH, THF	3 days at RT
2	KOtBu, THF	3 days at RT
3	K <sub>2</sub> CO <sub>3</sub> , DMF	3 days at RT
4	CF <sub>3</sub> CO <sub>2</sub> H, CH <sub>2</sub> Cl <sub>2</sub>	3 days at RT
5	10% Cu(OTf) <sub>2</sub> , MeCN	7 h at RT then 15 h at reflux
6	LiClO <sub>4</sub> (5 M in Et <sub>2</sub> O)	24 h at RT then 24 h at reflux
7	AlCl <sub>3</sub> , THF	12 h at RT then 24 h at reflux
8	toluene	3 days, reflux
9	1,2-dichlorobenzene	3 days at 180 °C

**Table 1.6** Attempts to activate the Stille coupling product **1.87** towards conjugate addition.

It was possible that the methyl carbamate protected nitrogen was not nucleophilic enough to add to the  $\alpha,\beta$ -unsaturated system of **1.87**. Several basic conditions were tried in order to increase the nucleophilicity of the carbamate by deprotonating the nitrogen. With strong bases such as potassium hydroxide, partial decomposition was observed by TLC analysis. With milder bases, the starting material was recovered unchanged, even when increasing the reaction temperature.

Switching to acidic conditions did not bring any further improvements. Although Bland *et al* reported intramolecular addition of carbamate to cyclohexadien-1-one catalyzed by trifluoroacetic acid, applying these conditions to compound **1.87** was unsuccessful.<sup>67</sup> Since the conjugate addition involves the interaction between the HOMO and the LUMO, several Lewis acids were used to activate the  $\alpha,\beta$ -unsaturated system by lowering the energy of the LUMO, thus decreasing the energy difference between the two frontier molecular orbitals. Several reaction types, including Diels Alder, aldol

condensation and conjugate addition, have been reported to benefit from this form of activation.<sup>71-73</sup> Unfortunately this was not the case for compound **1.87**. Under all conditions tried either complex mixtures were formed (**Table 1.6, entry 5**) or starting material was recovered unchanged (**Table 1.6, entry 6 and 7**).

Finally, Stille coupling product **1.87** was subjected to thermal conditions. Prolonged heating in refluxing toluene did not induce the intramolecular cyclization. The compound started to decompose when heated at 180 °C.

At this stage it was clear that the forward reaction is not favored and the starting material **1.87** is fairly stable under a broad range of different conditions. The lack of reactivity could be due to poor nucleophilicity of the carbamate nitrogen as well as steric effects. In particular, steric hindrance could arise from the doubly substituted  $sp^2$  hybridized  $\beta$  carbon and some additional steric bulk of the protecting group.

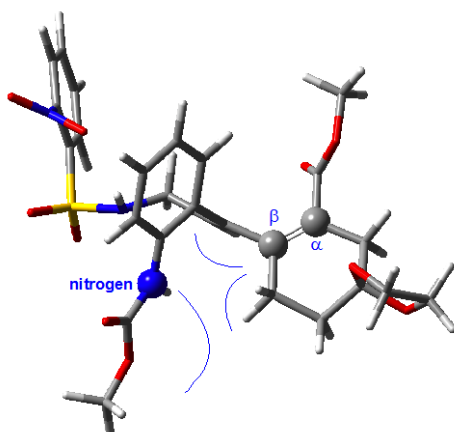


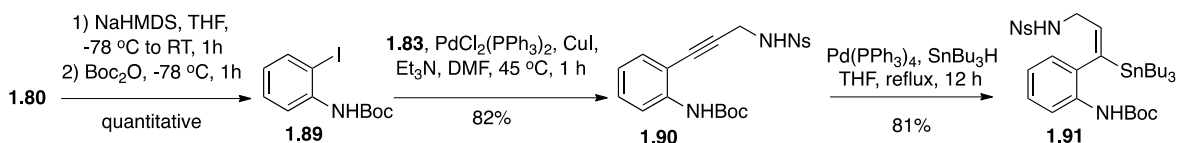
**Figure 1.6** Steric hindrance in compound **1.87**.<sup>74</sup>

## 2.2. *Tert*-butyl carbamate series – synthesis and reactivity

In order to further activate compound **1.87** towards conjugate addition, the methyl carbamate was replaced with a *tert*-butoxycarbonyl (Boc) group. Upon removal of the Boc group, some of the steric issues mentioned in the previous section would be removed and the resulting free amine would become a stronger nucleophile for the addition to the  $\alpha,\beta$ -unsaturated system of **1.87**.<sup>75</sup>

### 2.2.1 Building block synthesis and Stille coupling reaction

The synthesis of the Boc analogue of **1.87** started with preparation of organostannane **1.91** (Scheme 1.5). Thus commercially available 2-iodoaniline **1.80** was protected as the *tert*-butyl carbamate in quantitative yield using the standard procedures.<sup>76</sup> Then, similarly to methyl carbamate series, compound **1.90** was subjected to Sonogashira coupling, followed by highly regioselective hydrostannylation reaction to give compound **1.91** in high yield. Interestingly, the Sonogashira coupling proceeded very quickly and the reaction was complete within 1 h under the same conditions as for compound **1.84**. Hydrostannylation on the other hand required slightly harsher conditions and running the reaction in refluxing THF over 12 h was needed to obtain **1.91** with efficiency similar to compound **1.85**.



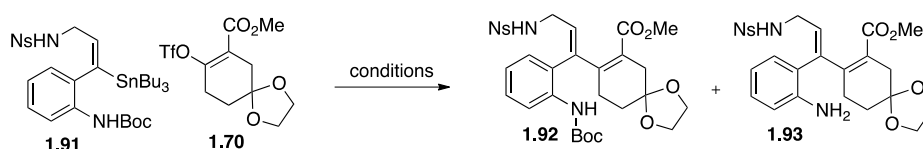
**Scheme 1.15** The synthesis of organostannane **1.91**.

Having successfully completed the synthesis of the Boc protected organostannane, the two building blocks **1.91** and **1.70** were subjected to the previously optimized conditions of the Stille coupling (Table 1.7). Unfortunately, the efficiency of the reaction was found to be significantly lower than for the methyl carbamate counterpart. Despite several modifications to the procedure and careful adjustments of the reaction time and temperature, the yield of the cross coupling was low in all cases (Table 1.7).

Heating the reaction mixture at 90 °C for 16 h (Table 1.7, entry 5) produced only modest quantities of the target compound **1.92**. A slight improvement was observed with microwave irradiation<sup>77</sup> (Table 1.7, entry 8), where the product was obtained in 39% yield. Adding another equivalent of organostannane further increased the yield to 46% (Table 1.7, entry 6). However, considering the effort required to prepare this reagent and the relatively small increase in efficiency, using a two-fold excess of **1.91** was rather wasteful.

Interestingly, during the microwave assisted experiments small amounts of a byproduct was formed, which was later identified to be a deprotected form of **1.92**.

Initially it appeared that at higher temperatures a greater proportion of compound **1.93** was formed, which potentially could be optimized to exclusively obtain the deprotected product. Unfortunately, at the same time the overall yield of an already inefficient reaction was decreased even further, thus requiring other methods to remove the Boc group to be investigated. It was also interesting to learn that despite high temperatures, compound **1.93** did not engage in intramolecular conjugate addition. Due to the small quantities of **1.93** obtained, collecting full characterization data was problematic. Mass spectrometric analyses were inconclusive, as the cyclized product would have the same mass as **1.93**. Finally, subjecting compound **1.93** to Boc protection conditions returned a product whose characterization data fully matched compound **1.92**, which confirmed the structure of **1.93**.



Entry	Conditions	Temp.	Time	Yield
1	Pd <sub>2</sub> (dba) <sub>3</sub> , P(furyl) <sub>3</sub> , DMF	90 °C	5 h	15% of <b>1.92</b>
2	Pd <sub>2</sub> (dba) <sub>3</sub> , P(furyl) <sub>3</sub> , DMF	80 °C	2 d	11% of <b>1.92</b>
3	Pd <sub>2</sub> (dba) <sub>3</sub> , AsPh <sub>3</sub> , DMF	90 °C	5 h	16% of <b>1.92</b>
4	Pd <sub>2</sub> (dba) <sub>3</sub> , AsPh <sub>3</sub> , DMF	80 °C	2 d	15% of <b>1.92</b>
5	Pd <sub>2</sub> (dba) <sub>3</sub> , AsPh <sub>3</sub> , DMF	90 °C	16 h	31-37% of <b>1.92</b>
6	Pd <sub>2</sub> (dba) <sub>3</sub> , AsPh <sub>3</sub> , DMF	90 °C	16 h	46% of <b>1.92</b> (2 .0 eq of <b>1.91</b> )
7	Pd <sub>2</sub> (dba) <sub>3</sub> , AsPh <sub>3</sub> , DMF , μw	-78 °C	0.5 h	no rxn
8	Pd <sub>2</sub> (dba) <sub>3</sub> , AsPh <sub>3</sub> , DMF , μw	90 °C	5 h	39% of <b>1.92</b> and 3% of <b>1.93</b>
9	Pd <sub>2</sub> (dba) <sub>3</sub> , AsPh <sub>3</sub> , DMF , μw	100 °C	2 h	27% of <b>1.92</b> and 9% of <b>1.93</b>
10	Pd <sub>2</sub> (dba) <sub>3</sub> , AsPh <sub>3</sub> , DMF , μw	110 °C	5 h	25% of <b>1.92</b> and 10% of <b>1.93</b>
11	Pd <sub>2</sub> (dba) <sub>3</sub> , AsPh <sub>3</sub> , DMF , μw	200 °C	2 h	decomposition

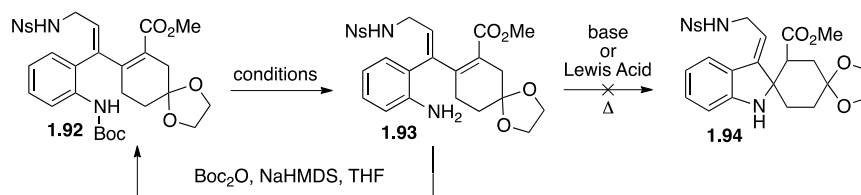
**Table 1.7** Optimization of the Stille coupling reaction conditions for the *N*-Boc series.

### 2.2.2 *N*-Boc deprotection and intramolecular conjugate addition

The choice of protecting group was dictated by the fact that unlike methyl carbamate, the Boc group could be readily removed under acidic conditions or at high

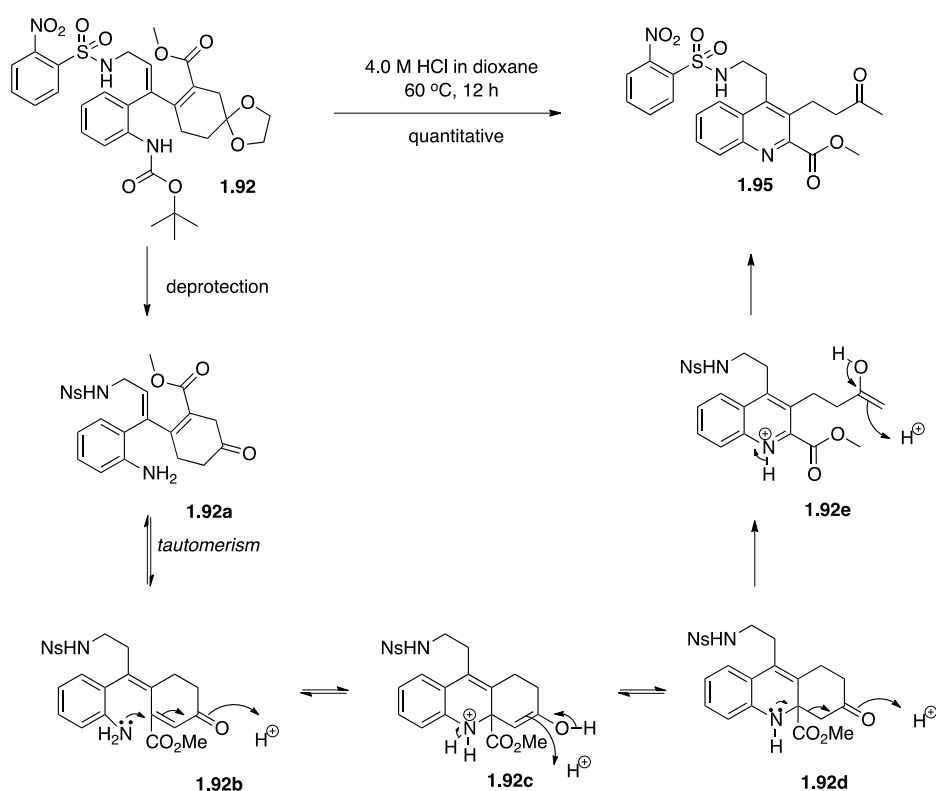


temperatures.<sup>43</sup> It was already seen during the Stille coupling that the group is unstable under harsh conditions but it remained intact when compound **1.92** was heated in refluxing toluene for several days (Table 1.8, entry 3). Changing the solvent and increasing the temperature resulted in gradual decomposition of the starting material with several by-products observed during TLC analysis. Using a more traditional approach and subjecting compound **1.92** to acidic conditions resulted either in decomposition or additional unwanted deprotection of the ketone (Table 1.8, entries 1 and 2).<sup>75</sup> Finally, heating **1.92** in hexafluoroisopropanol (HFIP) in a microwave reactor allowed for the partial conversion into the product **1.93**.<sup>78</sup> Despite reaching high temperatures in those reactions, the product **1.93** did not engage in conjugate addition to give compound **33**. Just like the methyl carbamate analogue **1.87**, amine **1.93** was subjected to a variety of bases, Lewis acids as well as thermal conditions. Unfortunately, all attempts to activate compound **1.93** towards conjugate addition failed to deliver compound **1.94**.



Entry	Conditions	Comments
1	TFA, CH <sub>2</sub> Cl <sub>2</sub> , RT, 12 h	complex mixture formed
2	4.0 M HCl in dioxane, 60 °C, 12 h	both Boc group and acetal removed
3	PhMe, reflux, 3 d	SM recovered unchanged
4	1,2-dichlorobenzene, 120 to 180 °C	Decomposition
6	HFIP, 150 °C, 1 h, $\mu$ w	50% conversion
7	HFIP, 100 °C, 3 h, $\mu$ w	
8	HFIP, 100 °C, 3 h, $\mu$ w	reaction incomplete plus many by-products
9	HFIP, 100 °C, 6 h, $\mu$ w	

**Table 1.8** N-Boc deprotection.



**Scheme 1.16** *N*-Boc deprotection with 4.0 HCl in dioxane.

An interesting result was obtained from the reaction of **1.92** with 4 M HCl in dioxane (**Scheme 1.16**).<sup>79</sup> Under these conditions both Boc and acetal protecting groups were removed and the isoquinoline compound **1.95** was formed in quantitative yield. A possible mechanism for this transformation has been presented in **Scheme 1.16**. After the initial deprotection compound **1.92a** could isomerize to form a highly conjugated intermediate **1.92b**. This intermediate could then undergo an intramolecular conjugate addition to  $\alpha,\beta$ -unsaturated ketone to give intermediate **1.92c**. A subsequent ring opening and formation of a stable aromatic isoquinoline could be a driving force in formation of compound **1.95**. The structure of **1.95** was confirmed by single crystal X-ray analysis. Subjecting the methyl carbamate compound **1.87** to the same reaction conditions was unsuccessful and resulted in recovery of partially decomposed starting material.

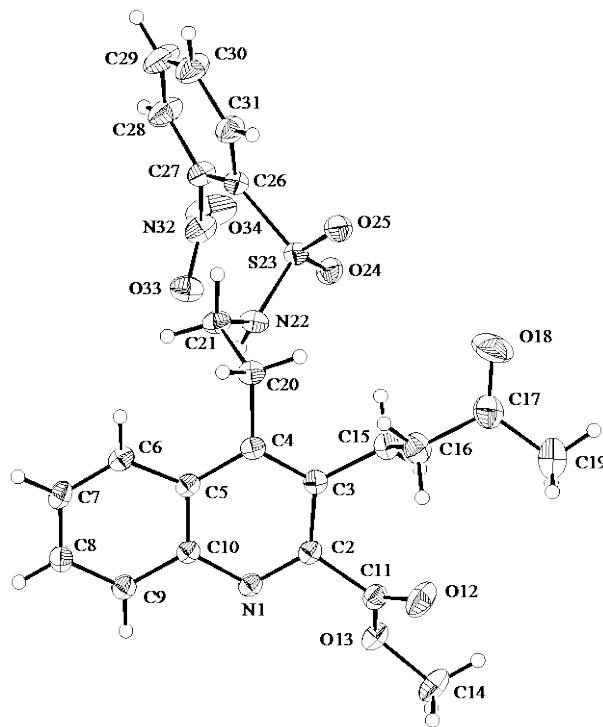


**Figure 1.7** An ORTEP of the isoquinoline compound **1.95**.

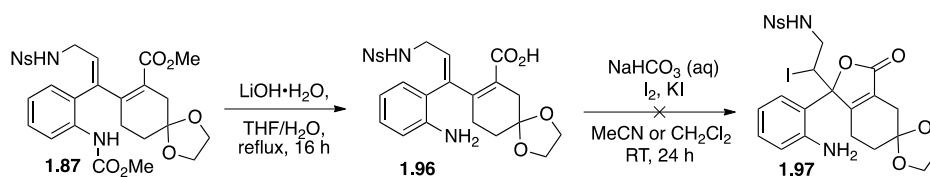
If correct, the mechanism described in **Scheme 1.16** could reveal an additional reason for lack of success with conjugate addition. Thus the intermediate **1.92b** would undergo this exact reaction and given the quantitative yield of this transformation one could assume that the nitrogen adds exclusively to the  $\alpha,\beta$ -unsaturated ketone instead of ester to form **1.92c**. Furthermore, the resulting cyclized product **1.92c** is unstable and readily aromatizes to eventually form **1.95**.

### 2.3 Alternative strategies towards the total synthesis of grandilodine C

Due to the lack of success with synthesizing intermediate **1.68** *via* conjugate addition several different approaches were briefly investigated. For example the order of synthetic steps (as outlined in the initial retrosynthetic plan) was changed and iodolactonization<sup>80</sup> was attempted right after the Stille coupling, hoping that the resulting lactone **1.97** would be a better candidate for the key conjugate addition step.

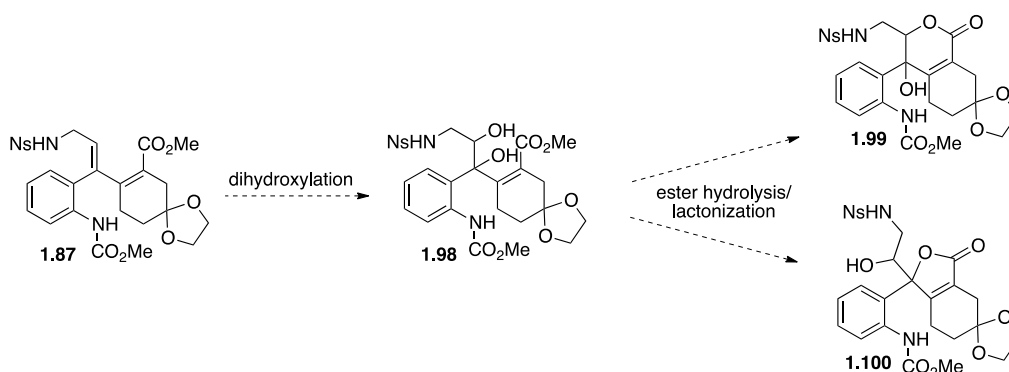
In order to carry out this transformation the methyl ester of **1.87** had to be hydrolyzed first. The best results were obtained when using lithium hydroxide monohydrate refluxing in a mixture of THF and water (**Scheme 1.17**). The purification of

**1.96** however turned out to be problematic and submitting crude reaction mixtures to iodolactonization reaction conditions were unsuccessful.



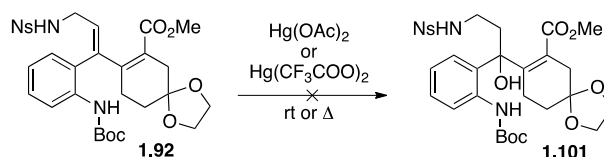
**Scheme 1.17** Ester hydrolysis and iodolactonization reaction.

Although iodolactonization is one of the most effective ways to prepare lactones and has been successfully used in the natural product setting, cyclic esters can also be synthesized from carboxylic acids and alcohols.<sup>80</sup> It was initially suggested to subject compound **1.87** to dihydroxylation conditions in order to introduce the hydroxyl group.<sup>81</sup> Although there are well-developed protocols that can provide good diastereoselectivity, the reaction itself generates some regioselectivity issues by introducing two hydroxyl groups across the double bond (**Scheme 1.18**). Investigation of molecular models suggested that a six-membered ring (**1.99**) would be more likely to form. Unfortunately, it is the more strained five-membered ring (**1.100**) that is required in the structure of grandilodine C.



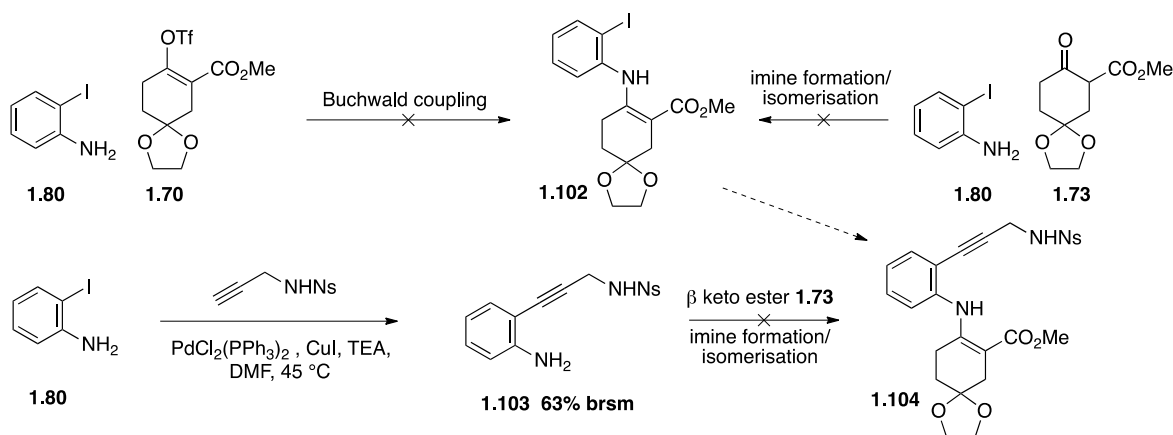
**Scheme 1.18** Dihydroxylation reaction and regioselectivity.

In order to install a single hydroxyl group and avoid the regioselectivity issues described above, several oxymercuration/demercuration protocols<sup>82-84</sup> were explored using compound **1.92** as the starting material (**Scheme 1.19**). The literature procedures often described rapid reactions, typically going to completion within several minutes. Unfortunately, under all conditions tried, no reaction was observed and compound **1.92** was recovered unchanged.



Scheme 1.19 Oxymercuration/demercuration attempts.

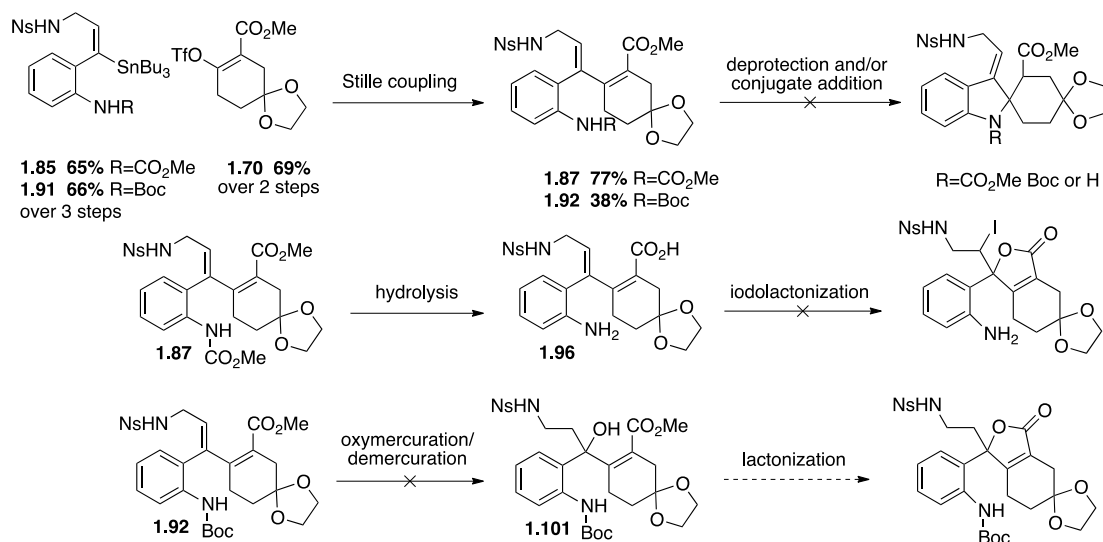
Several strategies that avoid Stille coupling were also investigated but they failed to deliver intermediates that would have the level of complexity similar to compounds **1.87** or **1.92**. These are summarized in Scheme 1.20.



Scheme 1.20 Alternative strategies.

## 2.4 Summary and conclusions

In order to carry out the key cross-coupling intramolecular conjugate addition reaction sequence two series of building blocks were synthesized. Compounds **1.85** and **1.91** were prepared from commercially available 2-iodoaniline in three steps with 65% and 66% overall yields, respectively. The reactions involved protection of the nitrogen, Sonogashira coupling and regioselective hydrostannylation. Compound **1.70** was prepared in two steps in 69% yield from 1,4-cyclohexanedione monoethylene ketal. With the organostannanes **1.85** and **1.91** and triflate **1.70** in hand, the Stille coupling was performed. Under optimized conditions cross coupling products **1.87** and **1.92** were delivered in 77% and 38% yields, respectively. Unfortunately, the conjugate addition product was not isolated and all attempts to activate **1.87** or **1.92** towards cyclization were unsuccessful.



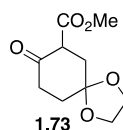
**Scheme 1.21** Summary of experimental work carried out in Part One.

Several alternative approaches were investigated. For example, changing the order of steps by introducing the lactone earlier *via* iodolactonization or oxymercuration methods as well as redesigning the synthesis to avoid the problematic conjugate addition altogether. Despite a lot of time and effort expended none of these strategies was promising, leading to the conclusion that the original retrosynthetic analysis requires major reconsideration and more careful planning in the future.

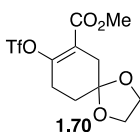
## **Chapter Three: Experimental Work Associated with Research Reported In Part One**

### **3.1 General methods**

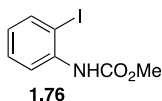
NMR spectra were recorded at 298 K using a Bruker AVANCE 400 spectrometer. The  $^1\text{H}$  NMR signal of residual chloroform ( $\delta$  7.26 ppm) or residual dimethyl sulfoxide ( $\delta$  2.50 ppm) was used as internal reference for  $^1\text{H}$  NMR spectra measured in these solvents. Coupling constants ( $J$ ) are quoted to the nearest 0.1 Hz. The  $^{13}\text{C}$  NMR signal of chloroform ( $\delta$  77.1 ppm) or dimethyl sulfoxide ( $\delta$  39.5 ppm) was used as internal reference for  $^{13}\text{C}$  NMR spectra measured in these solvents. Assignment of proton signals was assisted by HSQC experiments when necessary; assignment of carbon signals was assisted by APT experiments, HSQC and HMBC experiments were employed when necessary. IR spectra were recorded on a Perkin-Elmer Spectrum One spectrometer as neat films on NaCl plates for oils or as KBr disks for solid products. Mass spectra were recorded by the Mass Spectrometry Facility of the Research School of Chemistry, Australian National University, Canberra on a VG Autospec M series sector (EBE) MS for EI, VG Quattro II triple quadrupole MS for LR ESI and Bruker Apex3 4.7T FTICR-MS for HR ESI. Microanalyses were performed at the Microanalytical Laboratory, Research School of Chemistry, Australian National University, Canberra. Melting points were measured on Optimelt automated melting point apparatus and are uncorrected. Analytical TLC was performed with Merck (A.T. 5554) silica gel 60 F254 (0.2 mm) plates, precoated on aluminium sheets. Flash chromatography employed Merck Kiesegel 60 (230–400 mesh) silica gel. Reactions were conducted under positive pressure of dry argon or nitrogen in oven-dried glassware. Diethyl ether, toluene and THF were dried over sodium wire and distilled from sodium benzophenone ketyl. Dichloromethane was distilled from calcium hydride. Commercially available chemicals were used directly as purchased.



**Methyl 8-oxo-1,4-dioxaspiro[4.5]decane-7-carboxylate:** To a solution of DIPEA (5.10 mL, 36 mmol, 1.2 eq) in dry THF (35 mL), *n*-butyl lithium solution in hexane (22.5 mL, 36 mmol, 1.2 eq) was added slowly between -65 and -60 °C. The resulting solution was stirred for 30 min at -60 °C and then at 0 °C respectively. After cooling down to -60 °C a solution of 1,4-cyclohexanedione monoethylene acetal (4.685 g, 30 mmol, 1.0 eq) in dry THF (35 mL) was added dropwise. The resulting reaction mixture was allowed to slowly warm up to 0 °C and stirred at that temperature for 1 h. After cooling down to -60 °C, HMPA (5.22 mL, 30 mmol, 1.0 eq) was added in one portion followed by methyl cyanoformate (2.86 mL, 36 mmol, 1.2 eq) added dropwise over 10 min. The resulting reaction mixture was allowed to reach RT before being poured into ice-cold water (300 mL) and extracted with EtOAc. Organic layer was separated, washed with brine several times, dried with MgSO<sub>4</sub>, filtered and concentrated *in vacuo*. The residue was purified by flash column chromatography (10% to 40% EtOAc/hexane) to give the product as off-white solid (3.25 g, 69%). Characterization data were identical to those previously reported for this compound.<sup>35</sup>

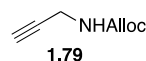


**Methyl 8-(((trifluoromethyl)sulfonyl)oxy)-1,4-dioxaspiro[4.5]dec-7-ene-7-carboxylate:** To a suspension of sodium hydride (448 mg, 11.20 mmol, 1.2 eq) in dry THF (15 mL), a solution of methyl 8-oxo-1,4-dioxaspiro[4.5]decane-7-carboxylate (2.00 g, 9.336 mmol, 1.0 eq) in dry THF (10 mL) was added at 0 °C. The resulting reaction mixture was stirred at 0 °C for 30 min. Phenyl triflimide (4.00 g, 11.20 mmol, 1.2 eq) was added in one portion and the resulting reaction mixture was stirred at RT for 12 h. Quenched with ice-cold water and extracted with EtOAc. Organic layer was separated, washed with brine, dried with MgSO<sub>4</sub>, filtered and concentrated *in vacuo*. The residue was purified by flash column chromatography (0% to 20% EtOAc/hexane) to give the product as off-white solid in quantitative yield. Characterization data were identical to those previously reported for this compound.<sup>35</sup>

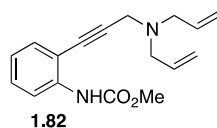




**Methyl (2-iodophenyl)carbamate:** To a solution of 2-iodoaniline (2.19 g, 10 mmol, 1.0 eq) in acetone (40 mL), potassium carbonate (8.26 g, 60 mmol, 6.0 eq) followed by methyl chloroformate (3.09 mL, 40 mmol, 4.0 eq) was added at 0 °C. Once addition was complete the cooling bath was removed and the resulting reaction mixture was stirred at RT for 2 days. All volatiles were removed under reduced pressure and the residue was partitioned between EtOAc and water. Organic layer was separated, washed with brine, dried with MgSO<sub>4</sub>, filtered and concentrated *in vacuo* to give the crude product as off-white solid (2.36 g, 85%). The crude product was used directly in the next step: <sup>1</sup>H NMR (400 MHz, CDCl<sub>3</sub>) δ 3.80 (s, 3H), 6.78-6.82 (m, 1H), 6.96 (br s, 1H), 7.32-7.36 (m, 1H), 7.76 (dd, *J* = 8.1, 1.5 Hz, 1H), 8.04 (d, *J* = 8.1 Hz, 1H).

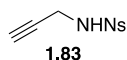


**Allyl prop-2-yn-1-ylcarbamate:** To a magnetically stirred solution of propargylamine (5.0 g, 90.8 mmol, 1.0 eq) in CH<sub>2</sub>Cl<sub>2</sub> (50 mL), triethylamine (25.2 mL, 182 mmol, 2.0 eq) was added and the resulting reaction mixture was cooled down to -5 °C. A solution of allyl chloroformate in CH<sub>2</sub>Cl<sub>2</sub> (20 mL) was added slowly at -5 to 0 °C. The reaction mixture was stirred at that temperature for 30 min and then at RT overnight. Organic layer was washed sequentially with 1M *aq.* HCl solution, sat. *aq.* NaHCO<sub>3</sub> solution, water and brine. Dried with MgSO<sub>4</sub>, filtered and concentrated *in vacuo* to give the crude product as pale yellow liquid (7.65 g, 61%). The crude product was used directly in the next step. The characterization data were identical to those previously reported for this compound.<sup>42</sup>

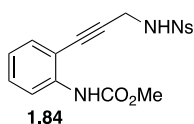


**Methyl (2-(3-(diallylamino)prop-1-yn-1-yl)phenyl)carbamate:** A reaction vessel was charged with methyl (2-iodophenyl)carbamate (100 mg, 0.361 mmol, 1.0 eq), allyl prop-2-yn-1-ylcarbamate (55 mg, 0.397 mmol, 1.1 eq), diisopropylethylamine (94 μL, 0.542 mmol, 1.5 eq), copper (I) iodide (7 mg, 0.036 mmol, 0.1 eq), tetrakis(triphenylphosphine)palladium(0) (21 mg, 0.018 mmol, 0.05 eq) and dry THF (3 mL). Purged with argon and stirred at reflux for 36 h. After cooling down to RT, the reaction mixture was filtered through Celite and washed with CH<sub>2</sub>Cl<sub>2</sub>. The solvent was

removed under reduced pressure and the residue was purified by flash column chromatography (20% EtOAc/hexane) to give 49 mg (48% yield) of the title compound:  $^1\text{H}$  NMR (400 MHz,  $\text{CDCl}_3$ )  $\delta$  3.22 (d,  $J$  = 6.8 Hz, 4H), 3.70 (s, 2H), 3.80 (s, 3H), 5.20-5.22 (m, 2H), 5.28-5.33 (m, 2H), 5.86-5.93 (m, 2H), 6.97-6.01 (m, 1H), 7.31-7.43 (m, 3H), 8.14 (d,  $J$  = 8.0 Hz, 1H);  $^{13}\text{C}$  NMR (101 MHz,  $\text{CDCl}_3$ )  $\delta$  42.2 ( $2\times\text{CH}_2$ ), 56.7 ( $2\times\text{CH}_2$ ), 80.7 (C), 91.3 (C), 111.4 (C), 117.5 ( $2\times\text{CH}$ ), 118.5 ( $2\times\text{CH}_2$ ), 122.4 (CH), 129.5 (CH), 131.9 (CH), 135.1 (CH), 139.1 (C), 153.6 (C); MS (EI+)  $m/z$  (%): 283 (100,  $[\text{M}]^+$ ).



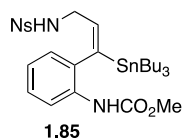
**2-nitro-*N*-(prop-2-yn-1-yl)benzenesulfonamide:** To a magnetically stirred solution of propargylamine (500 mg, 9.08 mmol, 1.05 eq) in  $\text{CH}_2\text{Cl}_2$  (10 mL), triethylamine (1.20 mL, 8.65 mmol, 1.0 eq) was added at RT under argon. A solution of 2-nitrobenzenesulfonyl chloride (1.916 g, 8.65 mmol, 1.0 eq) in  $\text{CH}_2\text{Cl}_2$  (10 mL) was added at 0 °C and the resulting reaction mixture was stirred at that temperature for 5 min, then at RT for 12 h. Quenched with sat. *aq.*  $\text{NH}_4\text{Cl}$  solution. Organic layer was separated, washed with water and brine, dried with  $\text{MgSO}_4$ , filtered and concentrated *in vacuo* to give the crude product as pale yellow solid (2.062 g, 99%). The crude product was used directly in the next step. The characterization data were identical to those previously reported for this compound.<sup>46</sup>



**Methyl (2-(3-(2-nitrophenylsulfonamido)prop-1-yn-1-yl)phenyl)carbamate:**

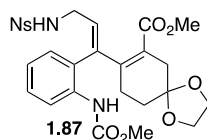
A reaction vessel was charged with methyl (2-iodophenyl)carbamate (1.25 g, 4.511 mmol, 0.9 eq), 2-nitro-*N*-(prop-2-yn-1-yl)benzenesulfonamide (1.20 g, 5.013 mmol, 1.0 eq), triethylamine (689  $\mu\text{L}$ , 4.962 mmol, 1.1 eq), copper (I) iodide (86 mg, 0.451 mmol, 0.1 eq), bis(triphenylphosphine)palladium(II) dichloride (157 mg, 0.226 mmol, 0.05 eq) and dry DMF (8 mL). Purged with argon and stirred at 45 °C for 2.5 h. After cooling down to RT, the reaction mixture was diluted with ether and washed sequentially with 0.5 M HCl solution, sat. *aq.*  $\text{NaHCO}_3$  solution, water and brine. Organic layer was separated, dried with  $\text{MgSO}_4$ , filtered and concentrated *in vacuo*. The crude product (1.72 g, 98%) was pure enough to be used directly in next step. For the purpose of characterization small

amount of the crude product was recrystallized from EtOAc and hexane to give off-white crystals:  $^1\text{H}$  NMR (400 MHz,  $\text{CDCl}_3$ )  $\delta$  3.79 (s, 3H), 4.33 (d,  $J$  = 6.4 Hz, 2H), 5.87 (t,  $J$  = 6.4 Hz, 1H), 6.86-6.91 (m, 2H), 6.98 (dd,  $J$  = 7.8 and 1.4 Hz, 1H), 7.29-7.30 (m, 1H), 7.52-7.60 (m, 2H), 7.80 (dd,  $J$  = 7.4 and 1.4 Hz, 1H), 8.02 (d,  $J$  = 8 Hz, 1H), 8.19 (dd,  $J$  = 7.2 and 2 Hz, 1H);  $^{13}\text{C}$  NMR (101 MHz,  $\text{CDCl}_3$ )  $\delta$  34.3 ( $\text{CH}_3$ ), 52.5 ( $\text{CH}_2$ ), 80.6 (C), 89.8 (C), 109.7 (C), 117.7 (CH), 122.4 (CH), 125.4 (CH), 130.1 (CH), 131.4 (CH), 131.8 (CH), 132.8 (CH), 133.6 (CH), 134.0 (C), 138.9 (C), 147.7 (C), 153.3 (C); IR (KBr disc)  $\nu_{\text{max}}$  3347 (broad), 3097, 2954, 1735, 1579, 1523, 1450, 1348, 1238, 1168, 1063, 732  $\text{cm}^{-1}$ ; MS (ESI+)  $m/z$  (%): 412 (100,  $[\text{M}+\text{Na}]^+$ ), 390 (20,  $[\text{M}+\text{H}]^+$ ); HRMS (ESI+)  $m/z$  calculated for  $\text{C}_{17}\text{H}_{15}\text{N}_3\text{O}_6\text{S}$   $[\text{M}+\text{H}]^+$ : 390.0760, found: 390.0760;  $[\text{M}+\text{Na}]^+$ : 412.0579, found: 412.0578,  $[\text{M}+\text{K}]^+$ : 428.0319, found: 428.0320; mp=84 °C.



**(E)-methyl (2-(3-(2-nitrophenylsulfonamido)-1-(tributylstannyl)prop-1-en-1-yl)phenyl)carbamate:** A reaction vessel was charged with methyl (2-(3-(2-nitrophenylsulfonamido)prop-1-yn-1-yl)phenyl)carbamate (115 mg, 0.289 mmol, 1.0 eq) and tetrakis(triphenylphosphine)palladium(0) (3 mg, 2.89  $\mu\text{mol}$ , 0.01 eq). Evacuated and refilled with argon three times. Dry THF (500  $\mu\text{L}$ ) was added, followed by a solution of tributyltin hydride (86 mg, 0.451 mmol, 1.5 eq) in dry THF (500  $\mu\text{L}$ ). The resulting reaction mixture was stirred under argon for 4 h at RT. The solvent was then removed *in vacuo* and the residue was purified by flash column chromatography (0% to 20% EtOAc/hexane) to give the product as pale yellow solid (171 mg, 87%):  $^1\text{H}$  NMR (400 MHz,  $\text{CDCl}_3$ )  $\delta$  0.81-0.86 (m, 15H), 1.20-1.27 (m, 6H), 1.33-1.39 (m, 6H), 3.52 (t,  $J$  = 6 Hz, 2H), 3.76 (s, 3H), 5.43 (t,  $J$  = 5.9 Hz, 1H), 5.97 (t,  $J$  = 6.3 Hz, 1H), 6.50 (s, 1H), 6.70 (dd,  $J$  = 7.6, 1.6 Hz, 1H), 6.91-6.95 (m, 1H), 7.10-7.14 (m, 1H), 7.62-7.71 (m, 2H), 7.83 (dd,  $J$  = 7.8, 1.4 Hz, 1H), 7.90 (d,  $J$  = 8.2 Hz, 1H), 7.95 (dd,  $J$  = 7.5, 1.7 Hz, 1H);  $^{13}\text{C}$  NMR (101 MHz,  $\text{CDCl}_3$ )  $\delta$  10.1 ( $3\times\text{CH}_3$ ), 27.3 ( $3\times\text{CH}_2$ ), 28.7 ( $3\times\text{CH}_2$ ), 42.9 ( $\text{CH}_2$ ), 52.3 ( $\text{CH}_3$ ), 119.1 (CH), 123.3 (CH), 125.4 (CH), 126.3 (CH), 126.8 (CH), 131.0 (CH), 132.3 (C), 132.6 (C), 132.8 (CH), 133.4 (C), 133.5 (CH), 138.6 (CH), 147.8 (C), 147.9 (C), 153.7 (C); IR (KBr disc)  $\nu_{\text{max}}$  3356 (broad), 2955, 2926, 2868, 2847,

1737, 1579, 1542, 1517, 1447, 1360, 1216, 1168, 1065, 740  $\text{cm}^{-1}$ ; MS (ESI+)  $m/z$  (%): 704 (100,  $[\text{M}+\text{Na}]^+$ ), 682 (70,  $[\text{M}+\text{H}]^+$ ); HRMS (ESI+)  $m/z$  calculated for  $\text{C}_{29}\text{H}_{43}\text{N}_3\text{O}_6\text{SSn}$  ( $^{120}\text{Sn}$ )  $[\text{M}+\text{H}]^+$ : 682.1973, found: 682.1975,  $[\text{M}+\text{Na}]^+$ : 704.1792, found: 704.1793,  $[\text{M}+\text{K}]^+$ : 720.1532, found: 720.1530; mp=107  $^{\circ}\text{C}$ .

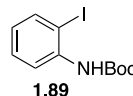


(Z)-methyl

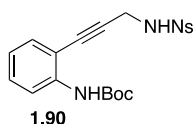
**8-(1-(2-((methoxycarbonyl)amino)phenyl)-3-(2-nitrophenylsulfonamido)prop-1-en-1-yl)-1,4-dioxaspiro[4.5]dec-7-ene-7-carboxylate:**

A reaction vessel was charged with methyl 8-(((trifluoromethyl)sulfonyl)oxy)-1,4-dioxaspiro[4.5]dec-7-ene-7-carboxylate (50 mg, 0.144 mmol, 0.9 eq), triphenylarsine (10 mg, 0.028 mmol, 0.2 eq) and tris(dibenzylideneacetone)dipalladium(0) (8 mg, 0.014 mmol, 0.1 eq of Pd). Evacuated and refilled with argon three times. Dry DMF (1 mL) was added and the resulting reaction mixture was stirred at RT for 30 min. A solution of (E)-methyl (2-(3-(2-nitrophenylsulfonamido)-1-(tributylstannyl)prop-1-en-1-yl)phenyl)carbamate (109 mg, 0.160 mmol, 1.0 eq) in dry DMF (1 mL) was added and the resulting reaction mixture was stirred at 60  $^{\circ}\text{C}$  for 16 h. After cooling down to RT, quenched with water and diluted with EtOAc. Organic layer was washed sequentially with water and brine; dried with  $\text{Na}_2\text{SO}_4$ ; filtered and concentrated *in vacuo*. The residue was purified by flash column chromatography (30% to 50% EtOAc/hexane) to give the product as off-white foam (65 mg, 77%):  $^1\text{H}$  NMR (400 MHz,  $\text{CDCl}_3$ )  $\delta$  1.61 (t,  $J$  = 6.5 Hz, 2H), 2.11 (t,  $J$  = 6.5 Hz, 2H), 2.56 (br s, 2H), 3.53 (t,  $J$  = 6.5 Hz, 2H), 3.71 (s, 3H), 3.79 (s, 3H), 3.90-3.99 (m, 4H), 5.29 (t,  $J$  = 5.7 Hz, 1H), 5.71 (t,  $J$  = 7.1 Hz, 1H), 6.90-6.92 (m, 2H), 7.22-7.26 (m, 1H), 7.60-7.70 (m, 2H), 7.82 (dd,  $J$  = 7.7, 1.4 Hz, 1H), 7.89 (dd,  $J$  = 7.7, 1.4 Hz, 1H), 8.00 (d,  $J$  = 8.3 Hz, 1H), 8.48 (s, 1H);  $^{13}\text{C}$  NMR (101 MHz,  $\text{CDCl}_3$ )  $\delta$  28.6 ( $\text{CH}_2$ ), 30.4 ( $\text{CH}_2$ ), 37.0 ( $\text{CH}_2$ ), 42.3 ( $\text{CH}_2$ ), 52.2 ( $\text{CH}_3$ ), 52.3 ( $\text{CH}_3$ ), 64.5 (2x $\text{CH}_2$ ), 106.6 (C), 120.3 (CH), 122.6 (CH), 125.4 (C), 125.5 (CH), 126.2 (C), 127.4 (CH), 129.2 (CH), 130.6 (CH), 130.9 (CH), 132.7 (CH), 132.9 (C), 133.5 (CH), 136.7 (C), 142.5 (C), 145.7 (C), 147.8 (C), 154.6 (C), 170.1 (C); IR ( $\text{CDCl}_3$  film)  $\nu_{\text{max}}$  3346 (broad), 3277, 2954, 2888, 1727, 1584, 1539, 1450, 1364, 1253, 1228, 1168, 1062, 731  $\text{cm}^{-1}$ ; MS (ESI+)  $m/z$  (%): 610 (100,  $[\text{M}+\text{Na}]^+$ ), 588 (30,  $[\text{M}+\text{H}]^+$ ); HRMS (ESI+)  $m/z$  calculated for

$C_{27}H_{29}N_3O_{10}S$   $[M+H]^+$ : 588.1652, found: 588.1652,  $[M+Na]^+$ : 610.1471, found: 610.1470.

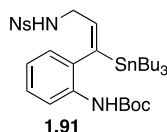


***Tert*-butyl (2-iodophenyl)carbamate:** To a magnetically stirred solution of 2-iodoaniline (2.19 g, 10 mmol, 1.0 eq) in dry THF (10 mL), 1.0 M solution of NaHMDS in THF (20 mL, 10 mmol, 1.0 eq) was added at -78 °C under argon. The resulting solution was warmed up to RT, stirred at that temperature for 30 min, before cooling back to -78 °C. A solution of di-*tert*-butyl dicarbonate (2.40 g, 11 mmol, 1.1 eq) in dry THF (10 mL) was added slowly over a period of 10 min and the resulting reaction mixture was stirred at -78 °C for 1 h. Quenched with sat. *aq.*  $NH_4Cl$  solution and extracted with EtOAc. Organic layer was separated, washed with brine, dried with  $MgSO_4$ , filtered and concentrated *in vacuo*. The crude product was obtained in quantitative yield and was used in the next step without further purification. Characterization data were identical to those previously reported for this compound.<sup>76</sup>

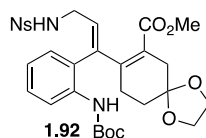


***Tert*-butyl (2-(3-(2-nitrophenylsulfonamido)prop-1-yn-1-yl)phenyl)carbamate:** A reaction vessel was charged with *tert*-butyl (2-iodophenyl)carbamate (351 mg, 1.1 mmol, 1.1 eq), 2-nitro-*N*-(prop-2-yn-1-yl)benzenesulfonamide (240 mg, 1.0 mmol, 1.0 eq), triethylamine (153  $\mu$ L, 1.1 mmol, 1.1 eq), copper (I) iodide (19 mg, 0.1 mmol, 0.1 eq), bis(triphenylphosphine)palladium(II) dichloride (35 mg, 0.05 mmol, 0.05 eq) and dry DMF (2 mL). Purged with argon and stirred at 45 °C for 1 h. After cooling down to RT, the reaction mixture was diluted with ether and washed sequentially with 0.5 M *aq.* HCl solution, sat. *aq.*  $NaHCO_3$  solution, water and brine. Organic layer was separated, dried with  $MgSO_4$ , filtered and concentrated *in vacuo*. The crude product was purified by flash column chromatography (0% to 30 % EtOAc/hexane) to give the target material as off-white crystalline solid (353.5 mg, 82%):  $^1H$  NMR (400 MHz,  $CDCl_3$ )  $\delta$  1.54 (s, 9H), 4.33 (d,  $J$  = 6.5 Hz, 2H), 5.86 (t,  $J$  = 6.5 Hz, 1H), 6.75 (s, 1H), 6.84 (td,  $J$  = 7.5, 1.1 Hz, 1H), 6.94 (dd,  $J$  = 7.7, 1.7 Hz, 1H), 7.23 – 7.27 (m, 2H), 7.49 – 7.57 (m, 2H), 7.76

(dd,  $J = 7.3, 2.0$  Hz, 1H), 8.03 (d,  $J = 8.4$  Hz, 1H), 8.18 (dd,  $J = 7.6, 1.6$  Hz, 1H),  $^{13}\text{C}$  NMR (101 MHz,  $\text{CDCl}_3$ )  $\delta$  28.2 ( $3 \times \text{CH}_2$ ), 81.0 (C), 81.3 (C), 89.52 (C), 109.4 (C), 117.6 (CH), 121.9 (CH), 125.3 (CH), 130.1 (CH), 131.4 (CH), 131.8 (CH), 132.7 (CH), 133.5 (CH), 134.1 (C), 139.5 (C), 152.1 (C), (one quaternary carbon signal obscured or overlapping); IR (KBr disc)  $\nu_{\text{max}}$  3399, 3354, 3095, 2979, 1726, 1580, 1539, 1516, 1447, 1365, 1242, 1166, 732  $\text{cm}^{-1}$ ; MS (ESI+)  $m/z$  (%): 454 (100,  $[\text{M}+\text{Na}]^+$ ); HRMS (ESI+)  $m/z$  calculated for  $\text{C}_{19}\text{H}_{21}\text{N}_3\text{O}_6\text{S}$   $[\text{M}+\text{Na}]^+$ : 451.1049, found: 451.1049; mp=108  $^{\circ}\text{C}$ .



**(E)-tert-butyl (2-(3-(2-nitrophenylsulfonamido)-1-(tributylstannyl)prop-1-en-1-yl)phenyl)carbamate:** A reaction vessel was charged with *tert*-butyl (2-(3-(2-nitrophenylsulfonamido)prop-1-en-1-yl)phenyl)carbamate (2.70 g, 6.200 mmol, 1.0 eq) and tetrakis(triphenylphosphine)palladium(0) (358 mg, 0.310 mmol, 0.01 eq). Evacuated and refilled with argon three times. Dry THF (10 mL) was added followed by a solution of tributyltin hydride (2.706 g, 9.300 mmol, 1.5 eq) in dry THF (5 mL). The resulting reaction mixture was stirred at reflux for 16 h. The solvent was removed *in vacuo* and the residue was purified by flash column chromatography (0% to 20% EtOAc/hexane) to give the product as pale yellow oil (3.65 g, 81%):  $^1\text{H}$  NMR (400 MHz,  $\text{CDCl}_3$ )  $\delta$  0.82-0.86 (m, 15H), 1.19-1.28 (m, 6H), 1.34-1.40 (m, 6H), 1.51 (s, 9H), 3.54 (t,  $J = 6.4$  Hz, 2H), 5.43 (t,  $J = 5.6$  Hz, 1H), 5.96 (t,  $J = 6.4$  Hz, 1H), 6.30 (s, 1H), 6.68 (dd,  $J = 7.8, 1.4$  Hz, 1H), 6.86-6.90 (m, 1H), 7.06-7.10 (m, 1H), 7.61-7.71 (m, 2H), 7.82 (dd,  $J = 8.0, 1.2$  Hz, 1H), 7.88 (d,  $J = 8.0$  Hz, 1H), 7.96 (dd,  $J = 7.4, 1.4$  Hz, 1H);  $^{13}\text{C}$  NMR (101 MHz,  $\text{CDCl}_3$ )  $\delta$  10.1 ( $3 \times \text{CH}_2$ ), 13.6 ( $3 \times \text{CH}_3$ ), 27.2 ( $3 \times \text{CH}_2$ ), 28.3 ( $3 \times \text{CH}_3$ ), 28.7 ( $3 \times \text{CH}_2$ ), 42.9 ( $\text{CH}_2$ ), 80.6 (C), 119.0 (CH), 122.8 (CH), 125.4 (CH), 126.2 (CH), 126.7 (CH), 131.0 (CH), 132.0 (C), 132.7 (CH), 133.1 (C), 133.4 (C), 133.5 (CH), 138.4 (CH), 147.9 (C), 148.0 (C), 153.4 (C); IR ( $\text{CDCl}_3$  film)  $\nu_{\text{max}}$  3412, 3356 (broad), 2956, 2927, 2868, 2851, 1729, 1579, 1542, 1511, 1444, 1365, 1164  $\text{cm}^{-1}$ ; MS (ESI+)  $m/z$  (%): 746 (100,  $[\text{M}+\text{Na}]^+$ ); HRMS (ESI+)  $m/z$  calculated for  $\text{C}_{32}\text{H}_{49}\text{N}_3\text{O}_6\text{SSn}$  ( $^{120}\text{Sn}$ )  $[\text{M}+\text{H}]^+$ : 724.2442, found: 724.2443,  $[\text{M}+\text{Na}]^+$ : 746.2262, found: 746.2262.

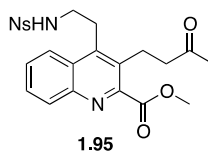


(Z)-methyl

8-(1-(2-((*tert*-butoxycarbonyl)amino)phenyl)-3-(2-

nitrophenylsulfonamido)prop-1-en-1-yl)-1,4-dioxaspiro[4.5]dec-7-ene-7-carboxylate:

A reaction vessel was charged with methyl 8-(((trifluoromethyl)sulfonyl)oxy)-1,4-dioxaspiro[4.5]dec-7-ene-7-carboxylate (100 mg, 0.289 mmol, 1.0 eq), triphenylarsine (18 mg, 0.058 mmol, 0.2 eq) and tris(dibenzylideneacetone)dipalladium(0) (26 mg, 0.029 mmol, 0.1 eq). Evacuated and refilled with argon three times. Dry DMF (2.5 mL) was added and the resulting reaction mixture was stirred at RT for 10 min. Then a solution of (E)-*tert*-butyl (2-(3-(2-nitrophenylsulfonamido)-1-(tributylstannyl)prop-1-en-1-yl)phenyl)carbamate (418 mg, 0.578 mmol, 2.0 eq) in dry DMF (2.5 mL) was added and the resulting reaction mixture was stirred at 90 °C for 16 h. After cooling down to RT, quenched with water and diluted with CH<sub>2</sub>Cl<sub>2</sub>. Organic layer was sequentially washed with water and brine; dried with Na<sub>2</sub>SO<sub>4</sub>; filtered and concentrated *in vacuo*. The residue was purified by flash column chromatography (30% to 50% EtOAc/hexane) to give the product as pale yellow oil (84 mg, 46%): <sup>1</sup>H NMR (400 MHz, CDCl<sub>3</sub>) δ 1.46 (s, 9H), 1.61 (t, *J* = 6.0 Hz, 2H), 2.11 (t, *J* = 6.0 Hz, 2H), 2.58 (br s, 2H), 3.58 (t, *J* = 6.4 Hz, 2H), 3.78 (s, 3H), 3.90-4.00 (m, 4H), 5.28 (t, *J* = 5.6 Hz, 1H), 5.69 (t, *J* = 7.0 Hz, 1H), 6.87-6.92 (m, 2H), 7.21-7.25 (m, 1H), 7.60-7.70 (m, 2H), 8.82 (d, *J* = 7.6 Hz, 1 H), 7.89-7.95 (m, 2H), 8.20 (s, 1H); <sup>13</sup>C NMR (101 MHz, CDCl<sub>3</sub>) δ 28.3 (3xCH<sub>3</sub>), 28.8 (CH<sub>2</sub>), 30.4 (CH<sub>2</sub>), 37.2 (CH<sub>2</sub>), 42.3 (CH<sub>2</sub>), 52.2 (CH<sub>3</sub>), 64.5 (2xCH<sub>2</sub>), 79.8 (C), 106.7 (C), 120.6 (CH), 122.3 (CH), 125.4 (CH), 125.5 (C), 125.8 (C), 127.0 (CH), 129.1 (CH), 130.6 (CH), 131.0 (CH), 132.7 (CH), 133.2 (C), 133.5 (CH), 137.1 (C), 142.7 (C), 146.6 (C), 147.9 (C), 153.3 (C), 169.6 (C); IR (CDCl<sub>3</sub> film) ν<sub>max</sub> 3356 (broad), 3273, 2976, 2888, 1710, 1583, 1539, 1448, 1366, 1248, 1163, 1051, 731 cm<sup>-1</sup>; MS (ESI+) *m/z* (%): 652 (100, [M+Na]<sup>+</sup>); HRMS (ESI+) *m/z* calculated for C<sub>30</sub>H<sub>35</sub>N<sub>3</sub>O<sub>10</sub>S [M+H]<sup>+</sup>: 630.2121, found: 630.2122, [M+Na]<sup>+</sup>: 652.1941, found: 652.1940.



**Methyl 4-(2-(2-nitrophenylsulfonamido)ethyl)-3-(3-oxobutyl)quinoline-2-carboxylate:** To a magnetically stirred solution of methyl 8-(1-(2-((*tert*-butoxycarbonyl)amino)phenyl)-3-(2-nitrophenylsulfonamido)prop-1-en-1-yl)-1,4-dioxaspiro[4.5]dec-7-ene-7-carboxylate (50 mg, 0.079 mmol, 1.0 eq) in anhydrous dioxane, 4.0 M HCl in dioxane (199 mL, 0.794 mmol, 10 eq) was added slowly at RT. Stirred at 60 °C for 16 h. The reaction mixture was cooled down to RT and concentrated *in vacuo*. The residue was dissolved in EtOAc. Organic layer was sequentially washed with saturated aqueous NaHCO<sub>3</sub> solution, water and brine; dried with MgSO<sub>4</sub>; filtered and concentrated *in vacuo*. The residue was purified by flash column chromatography (50% to 100% EtOAc/hexane) to give a mixture of products (20 mg, approximately 7:1 mixture according to <sup>1</sup>H NMR data). The structure of the major product was confirmed by a single crystal X-Ray analysis (Appendix Three, A3.1): <sup>1</sup>H NMR (400 MHz, CDCl<sub>3</sub>) δ 2.19 (s, 3H), 2.86 (t, *J* = 7.6 Hz, 2H), 3.15 (t, *J* = 7.6 Hz, 2H), 3.40-3.51 (m, 4H), 4.03 (s, 3H), 5.77-5.80 (m, 1H), 7.65-7.69 (m, 4H), 7.81-7.83 (m, 1H), 8.00-8.13 (m, 3H); IR (CDCl<sub>3</sub> film) ν<sub>max</sub> 3400-3200 (broad), 3095, 2953, 2892, 1730, 1541, 1455, 1439, 1412, 1360, 1164, 731 cm<sup>-1</sup>; MS (ESI+) *m/z* (%): 508 (100, [M+Na]<sup>+</sup>), 486 (30, [M+H]<sup>+</sup>); HRMS (ESI+) *m/z* calculated for C<sub>23</sub>H<sub>23</sub>N<sub>3</sub>O<sub>7</sub>S [M+Na]<sup>+</sup>: 508.1154, found: 508.1155.



**References:**

- (1) Nicolaou, K. C.; Vourloumis, D.; Winssinger, N.; Baran, P. S. *Angew. Chem. Int. Ed.* **2000**, 39, 44.
- (2) Marko, I. E. *Science* **2001**, 294, 1842.
- (3) Molinski, T. F. *Org. Lett.* **2014**, 16, 3849.
- (4) Kuttruff, C. A.; Eastgate, M. D.; Baran, P. S. *Nat. Prod. Rep.* **2014**, 31, 419.
- (5) Zhang, B.; Wepf, R.; Fischer, K.; Schmidt, M.; Besse, S.; Lindner, P.; King, B. T.; Sigel, R.; Schurtenberger, P.; Talmon, Y.; Ding, Y.; Kröger, M.; Halperin, A.; Schlüter, A. D. *Angew. Chem. Int. Ed.* **2011**, 50, 737.
- (6) Nicolaou, K. C.; Hale, C. R. H.; Nilewski, C.; Ioannidou, H. A. *Chem. Soc. Rev.* **2012**, 41, 5185.
- (7) Gaich, T.; Baran, P. S. *J. Org. Chem.* **2010**, 75, 4657.
- (8) Mulzer, J. *Nat. Prod. Rep.* **2014**, 31, 595.
- (9) Marko, I. E. *Actual. Chimique* **2003**, 4-5, 143.
- (10) Hanson, J. R. In *Natural Products: The Secondary Metabolites*; Hanson, J. R., Ed.; The Royal Society of Chemistry: 2003; Vol. 17, p 1.
- (11) Demain, A. L.; Fang, A. In *History of Modern Biotechnology I*; Fiechter, A., Ed.; Springer Berlin Heidelberg: 2000; Vol. 69, p 1.
- (12) Szychowski, J.; Truchon, J. F.; Bennani, Y. L. *J. Med. Chem.* **2014**, *Just Accepted Manuscript*.
- (13) Robson, B.; Baek, O. K. *The Engines of Hippocrates: From the Dawn of Medicine to Medical and Pharmaceutical Informatics*; John Wiley & Sons, 2009.
- (14) Bhat, S. V.; Nagasampagi, B. A.; Sivakumar, M. *Chemistry of Natural Products*; Springer, 2005.
- (15) Roberts, M. F.; Wink, M. *Alkaloids: Biochemistry, Ecology and Medicinal Applications*; Springer Science & Business Media, 1998.
- (16) Saxena, P. B. *Chemistry of Alkaloids*; Discovery Publishing House, 2007.
- (17) Facchini, P. J. *Annu. Rev. Plant Physiol. Plant. Mol. Biol.* **2001**, 52, 29.
- (18) Seigler, D. S. *Plant Secondary Metabolism*; Springer Science & Business Media, 1998.

- (19) Taylor, I. W. *Indole Alkaloids: An Introduction to the Enamine Chemistry of Natural Products*; Elsevier, 2013.
- (20) Saxton, E. J. *The Chemistry of Heterocyclic Compounds, Indoles: The Monoterpenoid Indole Alkaloids*; John Wiley & Sons, 2009.
- (21) Aniszewski, T. *Alkaloids - Secrets of Life:: Alkaloid Chemistry, Biological Significance, Applications and Ecological Role*; Elsevier, 2007.
- (22) The Angiosperm Phylogeny, *G. Bot. J. Linn. Soc.* **2009**, *161*, 105.
- (23) D.J., M. *Harvard Pap. Bot.* **2004**, *9*, 89.
- (24) Kam, T. S.; Lim, K. H. In *The Alkaloids: Chemistry and Biology*; Cordell, G. A., Ed.; Academic Press: The Netherlands: **2008**; Vol. 66, p 1.
- (25) Yap, W. S.; Gan, C. Y.; Low, Y. Y.; Choo, Y. M.; Etoh, T.; Hayashi, M.; Komiyama, K.; Kam, T. S. *J. Nat. Prod.* **2011**, *74*, 1309.
- (26) Awang, K.; Sevenet, T.; Hamid, A.; Hadi, A.; David, B.; Pais, M. *Tetrahedron Lett.* **1992**, *33*, 2493.
- (27) Kam, T. S.; Lim, K. H.; Yoganathan, K.; Hayashi, M.; Komiyama, K. *Tetrahedron* **2004**, *60*, 10739.
- (28) Pearson, W. H.; Lee, I. Y.; Mi, Y.; Stoy, P. *J. Org. Chem.* **2004**, *69*, 9109.
- (29) Hoshi, M.; Kaneko, O.; Nakajima, M.; Arai, S.; Nishida, A. *Org. Lett.* **2014**, *16*, 768.
- (30) Arai, S.; Nakajima, M.; Nishida, A. *Angew. Chem. Int. Ed.* **2014**, *53*, 5569.
- (31) Schultz, E. E.; Pujanauski, B. G.; Sarpong, R. *Org. Lett.* **2012**, *14*, 648.
- (32) Ferrer, C.; Escribano-Cuesta, A.; Echavarren, A. M. *Tetrahedron* **2009**, *65*, 9015.
- (33) Orr, S. T.; Tian, J.; Niggemann, M.; Martin, S. F. *Org. Lett.* **2011**, *13*, 5104.
- (34) Orr, S. T. M.; Tian, J.; Niggemann, M.; Martin, S. F. *Org. Lett.* **2012**, *14*, 4701.
- (35) Su, J.; Tang, H.; McKittrick, B. A. *Tetrahedron Lett.* **2011**, *52*, 3382.
- (36) Fischer, D.; Theodorakis, E. A. *Eur. J. Org. Chem.* **2007**, *2007*, 4193.
- (37) Crabtree, S. R.; Chu, W. L. A.; Mander, L. N. *Synlett* **1990**, *1990*, 169.
- (38) Molnar, A. *Palladium-Catalyzed Coupling Reactions: Practical Aspects and Future Developments*; John Wiley & Sons, 2013.

- 
- (39) Barry M. Trost, Z. T. *Synthesis* **2005**, 6 853.
- (40) Makabe, H.; Negishi, E.-i. In *Handbook of Organopalladium Chemistry for Organic Synthesis*; John Wiley & Sons, Inc.: 2003, p 2789.
- (41) Sonogashira, K. *J. Organomet. Chem.* **2002**, 653, 46.
- (42) Baumhof, P.; Griesang, N.; Bachle, M.; Richert, C. *J. Org. Chem.* **2006**, 71, 1060.
- (43) Kocienski, P. J. *Protecting Groups*; Thieme, 2005.
- (44) Franco, D.; Dunach, E. *Tetrahedron Lett.* **2000**, 41, 7333.
- (45) Nihei, K.-i.; Kato, M. J.; Yamane, T.; Palma, M. S.; Konno, K. *Synlett* **2001**, 7, 1167.
- (46) Deschamps, N. M.; Elitzin, V. I.; Liu, B.; Mitchell, M. B.; Sharp, M. J.; Tabet, E. A. *J. Org. Chem.* **2011**, 76, 712.
- (47) Brown, H. C.; Gupta, S. K. *J. Am. Chem. Soc.* **1972**, 94, 4370.
- (48) Neumann, W. P. *J. Organomet. Chem.* **1992**, 437, 23.
- (49) Knochel, P.; Millot, N.; Rodriguez, A. L.; Tucker, C. E. In *Organic Reactions*; John Wiley & Sons, Inc.: 2004, p 417.
- (50) Gao, Y.; Harada, K.; Hata, T.; Urabe, H.; Sato, F. *J. Org. Chem.* **1995**, 60, 290.
- (51) Pimm, A.; Kociński, P.; Street, S. D. A. *Synlett* **1992**, 11, 886.
- (52) Liron, F.; Gervais, M.; Peyrat, J.-F.; Alami, M.; Brion, J.-D. *Tetrahedron Lett.* **2003**, 44, 2789.
- (53) Liron, F.; Le Garrec, P.; Alami, M. *Synlett* **1999**, 1999, 246.
- (54) Kosugi, M.; Fugami, K. *J. Organomet. Chem.* **2002**, 653, 50.
- (55) Milstein, D.; Stille, J. K. *J. Am. Chem. Soc.* **1978**, 100, 3636.
- (56) Scott, W. J.; Stille, J. K. *J. Am. Chem. Soc.* **1986**, 108, 3033.
- (57) Heravi, M. M.; Hashemi, E.; Azimian, F. *Tetrahedron* **2014**, 70, 7.
- (58) Pattenden, G.; Sinclair, D. J. *J. Organomet. Chem.* **2002**, 653, 261.
- (59) Espinet, P.; Echavarren, A. M. *Angew. Chem. Int. Ed.* **2004**, 43, 4704.
- (60) Farina, V.; Krishnan, B. *J. Am. Chem. Soc.* **1991**, 113, 9585.
- (61) Farina, V.; Krishnan, B.; Marshall, D. R.; Roth, G. P. *J. Org. Chem.* **1993**, 58, 5434.

- (62) Casado, A. L.; Espinet, P. *J. Am. Chem. Soc.* **1998**, *120*, 8978.
- (63) Casado, A. L.; Espinet, P.; Gallego, A. M. *J. Am. Chem. Soc.* **2000**, *122*, 11771.
- (64) Liebeskind, L. S.; Fengl, R. W. *J. Org. Chem.* **1990**, *55*, 5359.
- (65) Farina, V. In *Pure App. Chem.* 1996; Vol. 68, p 73.
- (66) Mee, S. P. H.; Lee, V.; Baldwin, J. E. *Angew. Chem. Int. Ed.* **2004**, *43*, 1132.
- (67) Bland, D.; Chambournier, G.; Dragan, V.; Hart, D. J. *Tetrahedron* **1999**, *55*, 8953.
- (68) Palomo, C.; Oiarbide, M.; Halder, R.; Kelso, M.; Gomez-Bengoa, E.; Garcia, J. M. *J. Am. Chem. Soc.* **2004**, *126*, 9188.
- (69) Banwell, M. G.; Beck, D. A. S.; Smith, J. A. *Org. Biomol. Chem.* **2004**, *2*, 157.
- (70) Saidi, M. R.; Azizi, N.; Akbari, E.; Ebrahimi, F. *J. Mol. Cat. A: Chem.* **2008**, *292*, 44.
- (71) Houk, K. N.; Strozier, R. W. *J. Am. Chem. Soc.* **1973**, *95*, 4094.
- (72) Matsuo, J.-i.; Murakami, M. *Angew. Chem. Int. Ed.* **2013**, *52*, 9109.
- (73) Qian, B.; Shi, D.; Yang, L.; Huang, H. *Adv. Synth. Catal.* **2012**, *354*, 2146.
- (74) Lowest energy geometry calculated by Anya Gryn'ova.
- (75) Shimizu, K.; Takimoto, M.; Mori, M. *Org. Lett.* **2003**, *5*, 2323.
- (76) Guthrie, D. B.; Curran, D. P. *Org. Lett.* **2009**, *11*, 249.
- (77) Sasaki, A.; Tanaka, K.; Sato, Y.; Kuwahara, S.; Kiyota, H. *Tetrahedron Lett.* **2009**, *50*, 4637.
- (78) Choy, J.; Jaime-Figueroa, S.; Jiang, L.; Wagner, P. *Syn. Commun.* **2008**, *38*, 3840.
- (79) Mansurova, M.; Koay, M. S.; Gärtner, W. *Eur. J. Org. Chem.* **2008**, *2008*, 5401.
- (80) Oderinde, M. S.; Hunter, H. N.; Bremner, S. W.; Organ, M. G. *Eur. J. Org. Chem.* **2012**, *2012*, 175.
- (81) Kolb, H. C.; VanNieuwenhze, M. S.; Sharpless, K. B. *Chem. Rev.* **1994**, *94*, 2483.

- (82) Crouch, R. D.; Mitten, J. V.; Span, A. R.; Dai, H. G. *Tetrahedron Lett.* **1997**, 38, 791.
- (83) Barrero, A. F.; Sanchez, J. F.; Altarejos, J.; Perales, A.; Torres, R. *J. Chem. Soc. Perkin Trans. I* **1991**, 2513.
- (84) Brown, H. C.; Geoghegan, P. J.; Kurek, J. T. *J. Org. Chem.* **1981**, 46, 3810.



## **Part Two: New Methods For Reversible Formation Of Nitroxyl Radicals Under Mild Conditions.**

Research work reported in this Part of the thesis resulted in first author publication (Klinska *et al. Chem. Sci.*, 2015,6, 5623-5627). Portions of text and figures featured in the manuscript have been reprinted in part and used in **Chapter Six, Section 6.5** with permission from all authors.

### **Chapter Four - Introduction**

This project describes the synthesis of various nitroxyl radicals and alkoxyamines that could potentially be used to control nitroxide mediated polymerization under mild conditions and verifies experimentally the computational studies of stabilizing interactions in radical anions.

#### **4.1 Computational chemistry origins of the project – unprecedented stabilizing interactions in distonic radicals**

Recently the Coote group has reported significant stabilizing interactions between non-conjugated remote anions and radicals in SOMO-HOMO converted distonic radical anions.<sup>1,2</sup> Distonic radicals are a family of radical ions, in which spin and charge are spatially separated, in contrast to conventional radical ions, where the spin and charge reside on the same atom or conjugated fragment.<sup>3</sup> Although electronically unusual, distonic ions are not uncommon and a number of studies have been devoted to the reactivity characteristics of these stable gas-phase species, often revealing very pronounced differences in stability and reactivity between distonic radicals and their conventional, neutral radical or charged closed-shell counterparts.<sup>4-8</sup> Several studies have demonstrated that radical ions in which spin and charge are in close proximity (i.e. separated by one or two chemical bonds) can be stabilized or destabilized by polar effects, which implies that these effects could potentially have significant influence on bond dissociation energies and therefore reaction kinetics.<sup>9-12</sup> For example, theoretical studies have shown that deprotonation at the heteroatom in  $\cdot\text{CH}_2\text{XH}$  radicals ( $\text{X}=\text{NH}_2$ ,  $\text{OH}$ ,  $\text{PH}_2$ , and  $\text{SH}$ ) results in contraction (i.e. strengthening) of C-X bond due to the greater  $n(\text{Y}) \rightarrow p(\text{C}^\bullet)$

electron-donation present with the radical anion.<sup>11</sup> Furthermore, formic and acetic acid radicals  $\text{RCOO}^\bullet$  were predicted to have abnormally low  $\text{pK}_a$  values for the loss of C-H protons.<sup>12</sup> Similar effects at larger separations, up to 10 Å, are also known, provided that the radical and charge are directly  $\pi$ -conjugated.<sup>13-15</sup> In the absence of  $\pi$ -conjugation, through-space or through-bond polar effects are possible but insignificant at separations larger than 5 Å.<sup>16</sup> For instance, calculations showed that remote C-H bonds could be activated *via* intramolecular hydrogen-atom transfer involving an amine radical cation intermediate.<sup>17</sup> Another computational study demonstrated that polar and inductive field effects could deactivate backbone and side-chain positions towards hydrogen abstraction by chlorine atoms in peptides, contributing to their resistance against radical damage.<sup>18</sup> More recently, destabilizing effects of protonation of the nitroxide part in alkoxyamines were used to control pH-sensitive C-ON bond homolysis both computationally and experimentally.<sup>19</sup>

In the light of the abovementioned studies, stabilization of distonic radicals computationally discovered by Gryn'ova and Coote, stands out as an unprecedented example of a truly remote interaction between a negative charge and a radical without any type of orbital conjugation and at separations greater than 5 Å.<sup>1,2</sup> The authors reported that deprotonation of an acidic group such as carboxylate, alkoxide or sulfate results in significant stabilization of a remote radical by lowering the bond dissociation energy (BDE) of its bonds to carbon-centered radicals by approximately 20  $\text{kJ mol}^{-1}$  compared to the protonated form (**Figure 2.1**). In other words, species such as alkoxyamines bearing suitable acidic groups should be releasing carbon-centered radicals, generated by cleavage of the C-ON bond more readily when deprotonated.



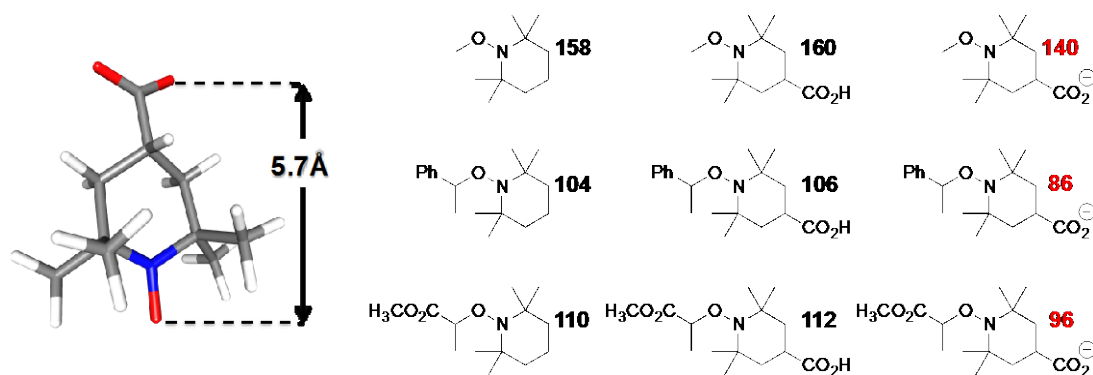


**Figure 2.1** Deprotonation of the remote carboxylic acid group makes the oxygen-carbon bond weaker by ca. 20 kJ mol<sup>-1</sup>. Bond dissociation free energies of C-ON bond in gas phase at 25 °C, kJ mol<sup>-1</sup>. Calculated by Ganna Gryn'ova (Coote group).

These theoretical results were verified experimentally by gas phase thermochemistry measurements obtained *via* mass spectrometry and so called BDE switches derived experimentally were in excellent agreement with the calculated values.<sup>1</sup> It was also shown that the stabilization decays with increasing distance between the charge and the radical and interestingly no bonding between the two entities is required in order to maintain the effect. The physical origin of the effect was initially linked to orbital conversion observed in all switched species, but it was unclear whether the unusual orbital configuration was the primary cause or just an effect associated with radical switching.<sup>1</sup>

The electronic configuration in atoms and molecules generally follows the Aufbau principle, according to which the orbitals are filled by a maximum of two electrons each in the order of increasing energy.<sup>20,21</sup> There are however examples of fully organic molecules that violate this principle,<sup>21</sup> including radical species,<sup>22-24</sup> where the singly occupied molecular orbital (SOMO) is not necessarily the highest occupied molecular orbital (HOMO). This is referred to as SOMO-HOMO energy level conversion and according to Coote *et al* it occurs in virtually any distonic radical anion that contains a sufficiently stabilized radical, non- $\pi$ -conjugated with a negative charge.<sup>1</sup> Moreover, calculations revealed that upon protonation of the anion, the regular orbital order is restored, suggesting that the orbital configuration could be switched by changing the pH.<sup>1</sup> Following their initial report of this discovery, the authors provided a more detailed explanation of the physical origin of the effect.<sup>2</sup> Irregular electronic configuration seems to be closely related

to additional radical stabilization, which was described as a “new type of polar effect-electronic stabilization of a delocalized radical *via* deprotonation of a remote acidic group forming an anion”.<sup>2</sup>

In general, the stabilization in distonic species is significant if the corresponding, relatively stable, neutral radical (aminoxyl, aminyl and peroxy radicals were initially reported as most promising) is paired with a relatively destabilized conjugate base of a weak acid such as carboxylate, phosphate or sulfate.<sup>1</sup> Furthermore, the effect is not only limited to synthetic molecules, and switches as large as 40 kJ mol<sup>-1</sup> were calculated for guanine containing nucleotide building blocks of DNA and RNA (**Figure 2.2**).<sup>1</sup>

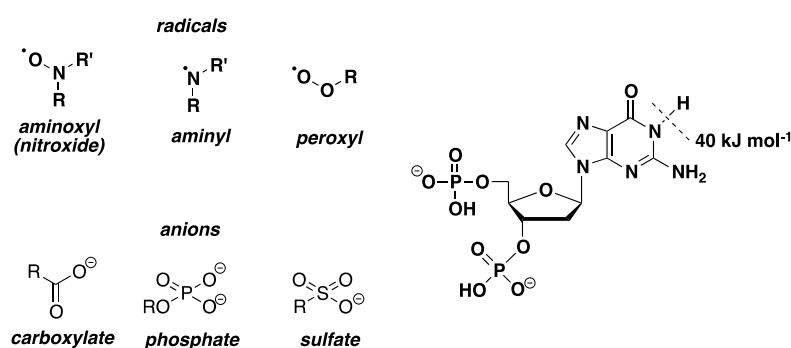


**Figure 2.2** Selected examples of compatible radicals and anions and gas-phase BDE-switch in guanine nucleotide.

#### 4.2 Effect of external conditions on radical stabilization and its consequences for possible practical applications

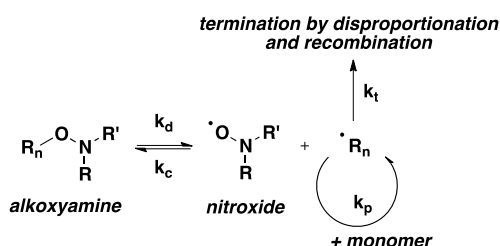
Lastly, the effect of external conditions on the switch was also evaluated (**Figure 2.3**).<sup>2</sup> It was found that switches calculated from the gas phase Gibbs free energies closely matched those calculated from electronic energies regardless of the temperature. In solution, which is a more realistic setting in terms of practical application of this effect, the BDE switches diminished in all cases. Fortunately, in low polarity solvents such as toluene, the switch was preserved and correlated linearly with the gas phase values. The more polar the solvent, the more stabilization was lost. In highly polar solvents such as DMSO or water, the switches dropped below 5 kJ mol<sup>-1</sup> and were no longer correlated to gas phase results.

**Figure 2.3** BDE-switches ( $\text{kJ mol}^{-1}$ ) for a set of distonic radical anions calculated from electronic energies and gas-phase free energies at 60 °C and 100 °C (A) and in various solvents at 25 °C (B–D) plotted against Gibbs free energy switches in the gas phase at 25 °C ( $\text{kJ mol}^{-1}$ ). Solvent dielectric constants are given in brackets. Graphic designed by Gryn'ova and Coote.<sup>2</sup>

Although this may limit potential applications of radical switching to nonpolar media only, there remains a number of fields in which this effect could be successfully incorporated. Most relevant to this project would be synthetic applications. These could involve generation of a radical protecting group, which could be introduced or removed by changing the pH of the reaction mixture or pH switchable reagents for nitroxide mediated polymerization (NMP). Switching was also demonstrated in biologically important molecules and therefore could have some potential in enzyme catalysis.

### 4.3 Theoretical background – pH switchable reagents for nitroxide mediated polymerization

Since its discovery and development,<sup>25,26</sup> nitroxide mediated radical polymerization (NMP) has become a versatile technique for the preparation of well-defined macromolecular architectures with precisely controlled molecular weights, compositions and functionalities.<sup>27</sup> The key feature of the nitroxide controlled polymerization process is establishment of a dynamic equilibrium between the propagating radicals  $\cdot R_n$  and the alkoxyamine dormant species (**Scheme 2.1**).<sup>27</sup> An investigation into the kinetics of NMP reveals that the success of the polymerization depends on the rate constant of the alkoxyamine C-ON bond homolysis,  $k_d$ ; the rate constant of the recombination of the nitroxide and the macroalkyl radical,  $k_c$ ; the propagation rate constant,  $k_p$ ; and the termination rate constant  $k_t$ .<sup>28</sup> These rate constants are monomer specific, therefore conditions need to be carefully optimized in order to perform NMP in a controlled manner.<sup>29</sup> Furthermore, thermal stability of the nitroxide at the temperature of the polymerization is also important. Highly stable nitroxides could stop the propagation step due to the nitroxide concentration build-up. Unstable nitroxides on the other hand, could lead to an uncontrolled polymerization due to premature decomposition of the nitroxide.

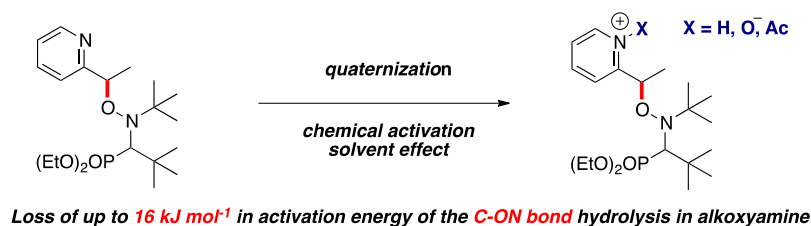


**Scheme 2.1** Simplified scheme for NMP. Adapted from Bagryanskaya *et al.*<sup>19</sup>

The main advantage of NMP is that due to a finely tuned equilibrium between the dormant and active species and the low concentration of active species throughout the process, termination events are minimized, allowing the polymer to grow.<sup>29</sup> Over the last two decades, the field has evolved immensely and many new NMP reagents have been developed during that time in order to achieve even better control and target new polymer structures.<sup>27</sup>

More recently the concept of pH switchable NMP has been introduced,<sup>19,30,31</sup> which is very relevant to this project, considering the discovery of a new class of stabilized nitroxide anions described in the previous section. Studies reported by the Marx and Matyjaszewski groups showed that either protonated or deprotonated forms of certain alkoxyamines could be of interest for pH switchable NMP.<sup>32,33</sup> In his theoretical study, Mazarin *et al* proposed that protonation of the nitroxide could decrease the rate of alkoxyamine homolysis dramatically<sup>30</sup> and later, Bagryanskaya *et al* showed experimentally that nitroxides with basic and acidic groups could be used to control polymerization.<sup>19</sup> According to the authors, the  $k_d$  values under basic conditions were up to 15-fold higher than in acidic solution, whereas the  $k_c$  values decreased in basic solution by a factor of only 2.<sup>19</sup> Using functionalized imidazoline alkoxyamines, those researchers successfully applied the concept of pH-switchable nitroxides to controlled polymerization of hydrophobic and hydrophilic monomers (styrene, acrylamide and styrene sulfonate) as well as block co-polymers in aqueous solution at temperatures below 100 °C.<sup>19</sup>

Another study by Bremond and Marque showed that homolysis of alkoxyamines could be chemically triggered by quaternization of the pyridinyl fragment by protonation, acylation or oxidation, resulting in a significant increase in the  $k_d$  rate constant and weakening of the C-ON bond of a similar order to that reported by the Coote group (Scheme 2.2).<sup>31</sup>



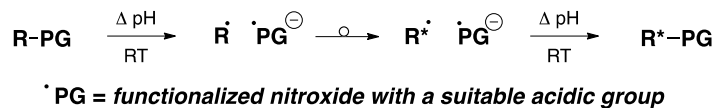
**Scheme 2.2** Chemically triggered C-ON bond homolysis of alkoxyamines. Adapted from Bremond and Marque.<sup>31</sup>

Although the field is in its infancy with very few experimental studies reported to date, this approach opens new and exciting opportunities for the synthetic design of novel NMP reagents. Stabilized nitroxide anions and the corresponding alkoxyamines containing acidic groups could potentially represent a new class of such reagents and serve as an excellent example of the practical application of computational studies in synthesis.

#### 4.4 Aims

The aim of this project was to design an experiment that will demonstrate pH switching of the nitroxyl radical anions in solution. The computational results were so far only confirmed by an experiment in the gas phase, where the theory predicted the switch would be the strongest. It was also expected that the stabilizing effect would decrease in solution to some extent, but remain consistent with the gas phase values in low polarity solvents such as toluene or benzene. Furthermore, the switch was decreased as the solvent became more polar, with no significant stabilization in water or DMSO. Very recently an experimental test of the Coote's theory in solution was published, using an EPR radical equilibration technique.<sup>34</sup> The study was focused on measuring the bond dissociation energies of O-H bond homolysis in the hydroxylamines derived from neutral and deprotonated forms of 4-carboxy TEMPO radical in acetonitrile and DMSO.<sup>34</sup> Unsurprisingly (see **Figure 2.3**), the researchers found that the stabilizing interactions in distonic radicals occurring in the gas phase are lost in high polarity solvents. Unfortunately, the study did not report any results for the same experiment in low polarity solvent. Therefore, a proof of principle experiment is urgently required to verify the calculations.

If the experimental results are favorable, there are various practical applications for stabilized radical anions in organic synthesis. As previously mentioned, one possibility could be the design of pH switchable NMP agents. In a broader scope, the distonic radicals could be viewed as radical protecting groups (**PG**), which could be removed and introduced in a controlled manner by simply changing the pH of the reaction medium (**Scheme 2.3**). This could provide an attractive alternative way of generating radical species under mild conditions that might be of interest to chemists working in the field of total synthesis.



**Scheme 2.3** The concept of using nitroxide anions as radical protecting groups.

## **Chapter Five – The Synthesis of TEMPO, SG1 and TIPNO Type Compounds and Related Polymerization Studies**

The project started with the computational design and synthesis of functionalized nitroxyl radicals, which should be suitable for testing the calculation results. Considering potential applications in polymer chemistry, the compounds in this study were derived from nitroxides that are commonly used as NMP reagents.<sup>27</sup> Carboxylic acid derivatives of TEMPO, SG1 and TIPNO radicals as well as a dealkylated SG1 derivative were chosen as representative compounds for investigating the stabilizing interactions in distonic radicals (**Figure 2.4**). Initial polymerization studies as well as specially designed synthetic experiments, supported by extensive analytical examination were undertaken in order to verify the computational predictions.

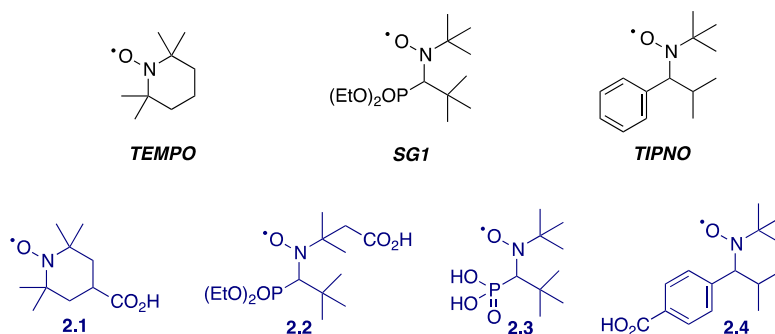
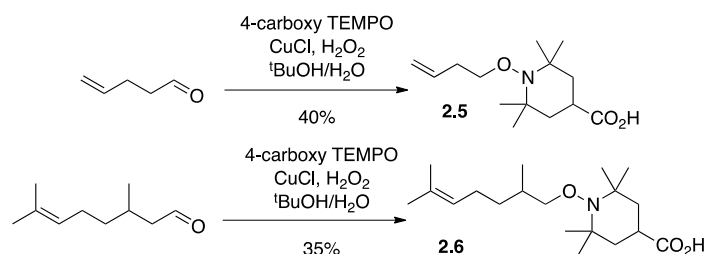


**Figure 2.4** Functionalized nitroxides as radical protecting groups that are commonly used as NMP reagents.

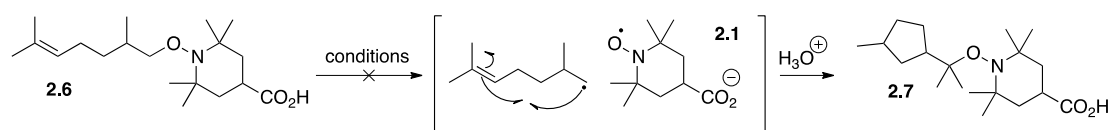
### **5.1 The synthesis of 4-carboxy TEMPO alkyl alkoxyamines**

In order to test the calculation results, an efficient preparation of alkoxyamines was required. The synthetic work in this project began with TEMPO derivatives, due to the fact that a great variety of this type of nitroxides, including 4-carboxy TEMPO, are commercially available. Finding suitable conditions for the synthesis of 4-carboxy TEMPO alkoxyamines was time consuming but adapting the method from Schoening and coworkers<sup>35</sup> was successful and delivered alkoxyamines **2.5** and **2.6** (**Scheme 2.4**). The yields were modest due to the product being unstable on silica gel.



**Scheme 2.4** The synthesis of alkyl 4-carboxy TEMPO alkoxyamines.

Unlike alkoxyamine **2.5**, which was prepared to test the general applicability of the synthetic method, alkoxyamine **2.6** was designed to provide an experimental proof of theoretical predictions. It was envisioned that upon deprotonation of the carboxylic acid, the resulting carboxylate would readily release an alkyl radical to form the stabilized, negatively charged nitroxide. The alkyl radical could then undergo *5-exo-trig* cyclization and upon protonation the nitroxide would trap the cyclized radical. The product **2.7** could be then fully characterized and the theory verified both qualitatively and quantitatively. The starting material **2.6** was subjected to a series of conditions (**Table 2.1**). Several different bases and solvents were tried as well as additives such as a crown ether, which could sequester the counter ion to help generate the free carboxylate. Unfortunately, it was found that even under forcing conditions, no cyclization was observed. This could be either due to the bond cleavage not taking place, or the radicals recombining immediately after cleavage to reform the starting material.



Entry	Conditions	Comments
1	EtOAc, DBU, RT then reflux	Starting material recovered unchanged
2	EtOAc, <i>i</i> Pr <sub>2</sub> NH, RT then reflux	
3	PhMe, KHMDS, RT then reflux	
4	PhMe, KHMDS, 18-crown-6, reflux	
5	Benzene, KH (50 eq) 18-crown-6, reflux	

**Table 2.1** Attempted radical cyclization of 4-carboxy TEMPO alkoxyamine **2.6**.



More recently, some additional calculations have suggested that the primary radical is a very poor leaving group, which could explain why the radical formation was disfavored under all conditions tried (**Figure 2.5**). According to these calculations, the forward reaction would be highly disfavored for both switched and unswitched 4-carboxy TEMPO alkoxyamine with a primary leaving group. With a benzyl leaving group on the other hand, at high temperatures the reaction would occur but benzene reflux is below the threshold above which no appreciable dissociation takes place. This is true since most NMPs require temperatures of around 120 °C.

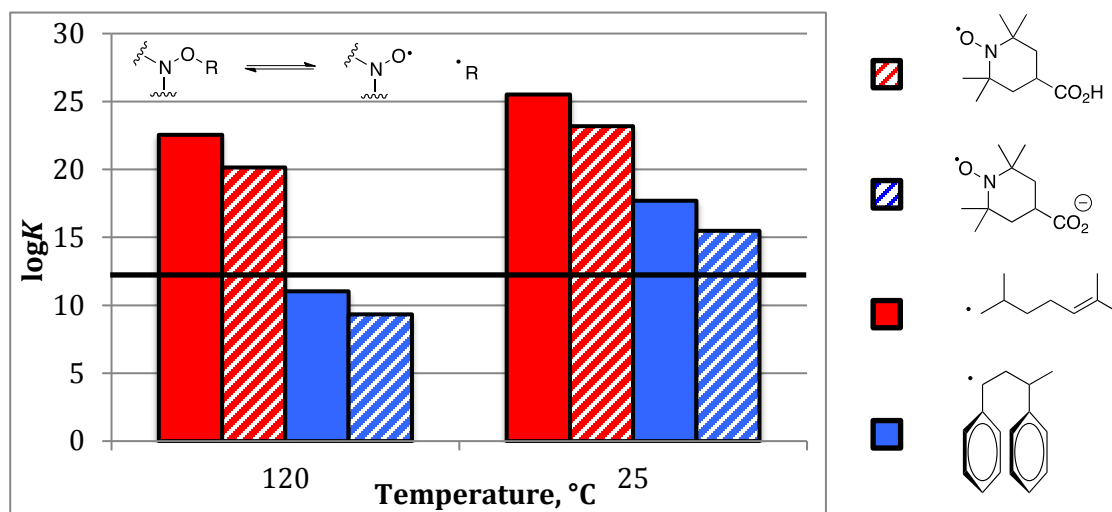
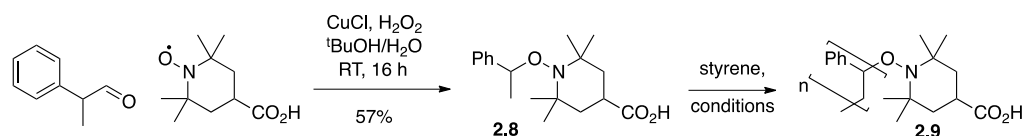


**Figure 2.5** The effect of the leaving group on reaction rate constant. Computational data and figure provided by Ganna Gryn'ova (Coote Group).

## 5.2 The synthesis of 4-carboxy TEMPO aryl alkoxyamine and preliminary polymerization studies

Considering how the nature of the leaving group affected the dissociation rate constant, the aryl alkoxyamine **2.8** was synthesized (see **Chapter Six**). Although it was unsuitable for the cyclization experiment, it could be used to investigate if pH switching would allow NMP to be performed at lower temperatures.

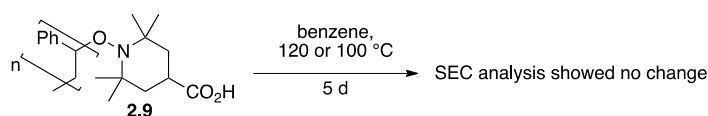


Entry	Conditions	Comments
1	125 °C, 12 h	High yield and good control $M_n=62000$ amu, PDI=1.1
2	100 °C, 12 h	Low yield of polymer and poor control
3	TEA (10 eq), 100 °C, 12 h	
4	100 °C, 5 days	
5	KH (1.2 eq), 100 °C, 5 days	
6	KH (1.2 eq), 18-crown-6, 100 °C, 5 days	

**Table 2.2** Styrene NMP with 4-carboxy TEMPO alkoxyamine **2.8**.

It was shown that the alkoxyamine **2.8** could control NMP at 125 °C, delivering a polymer ( $M_n=62000$  amu, PDI=1.1) in good yield and narrow mass distribution (**Table 2.2, entry 1**). Lowering the temperature to 100 °C resulted in low conversion and poor mass control under all conditions tried. Unfortunately, adding base and extending the reaction time to 5 days did not bring any further improvements. Furthermore, samples containing the potassium salt of 4-carboxy TEMPO alkoxyamine (with or without crown ether) produced polymers with lower molecular weights than a sample containing unswitched alkoxyamine and styrene only.

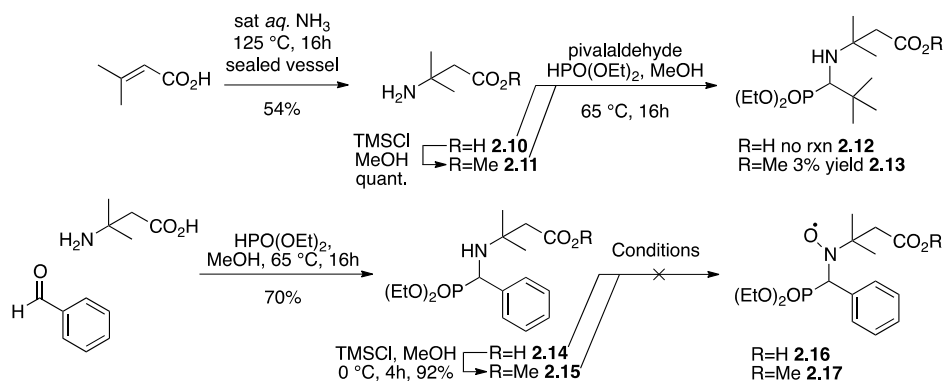
Finally, the samples of polystyrene **2.9** were heated with and without a base to see if chain extension would take place under “switched” conditions (**Scheme 2.5**). However, no change in the polymer mass was detected by SEC.



**Scheme 2.5** Chain extension experiments at 120 and 100 °C.

### 5.3 The synthesis of SG1 type radicals and alkoxyamines

The synthesis of SG1 derivatives began with a three component condensation between aldehyde, amine and phosphite compounds, also known as the Kabachnik-Fields or phospho-Mannich reaction.<sup>36</sup> This method typically involves a condensation between aldehyde and amine so that the resulting imine can then react with a dialkyl phosphite, which adds to the C=N unit of the intermediate. The aminophosphonate product can then be oxidized to the corresponding nitroxide using commercially available oxidants such as *m*CPBA or peroxides.<sup>37,38</sup> First, the synthesis of carboxy SG1 compound **2.2** was investigated (**Scheme 2.6**). The required amino acid starting material **2.10** was prepared by 1,4-addition of ammonia to 3,3-dimethylacrylic acid. Unfortunately, no condensation product was formed when compound **2.10** was reacted with pivalaldehyde and diethyl phosphite. Using the methyl ester analogue **2.11** instead allowed for isolation of very small amount of aminophosphonate **2.13**. It was not clear whether this poor yield was due to steric effects (which was unlikely considering the fact the SG1 radicals has been well studied) or instability on silica gel (only very little material was recovered after flash column chromatography). Furthermore, product **2.13** was not UV active and the majority of commonly used TLC stains were unsuitable for visualizing the spots. Replacing pivalaldehyde with benzaldehyde not only made the identification of intermediates less complicated but also significantly improved the yields. The condensation was now successful even with unprotected amino acid starting material, delivering aminophosphonate **2.14** in 70% yield. The product **2.14** could be then protected as the methyl ester in order to carry out oxidation step. Several different oxidants were tried, including various peracids,<sup>37,39</sup> peroxymonosulfate<sup>40</sup> and hydrogen peroxide.<sup>38</sup> All attempts to convert aminophosphonates **2.14** and **2.15** into the corresponding nitroxides **2.16** and **2.17** were unsuccessful (**Scheme 2.6** and **Table 2.3**).

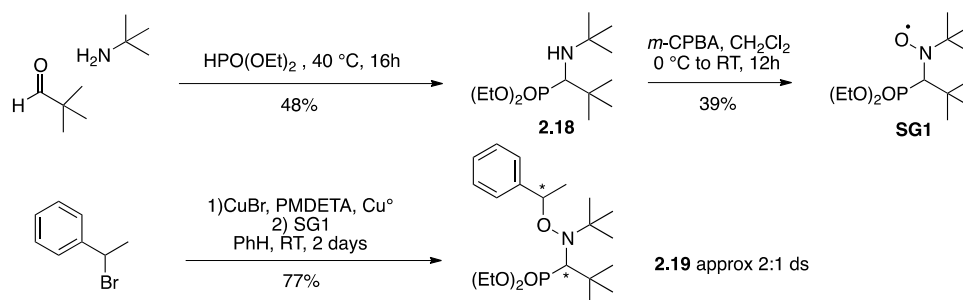


**Scheme 2.6** Attempts to synthesize carboxy SG1 derivatives

Entry	Conditions	Comments
1	Commercial <i>m</i> CPBA, CH <sub>2</sub> Cl <sub>2</sub> , 0 °C to RT	Starting material recovered unchanged or complex mixtures formed
2	Purified <i>m</i> CPBA, CH <sub>2</sub> Cl <sub>2</sub> , 0 °C to RT	
3	OXONE, Na <sub>2</sub> CO <sub>3</sub> , EtOH/H <sub>2</sub> O, 0 °C to RT	
4	H <sub>2</sub> O <sub>2</sub> , CH <sub>2</sub> Cl <sub>2</sub> , 0 °C to RT	
5	H <sub>2</sub> O <sub>2</sub> , Na <sub>2</sub> WO <sub>4</sub> , MeOH, 0 °C to RT	
6	CH <sub>3</sub> CO <sub>3</sub> H, KHCO <sub>3</sub> (aq), pH=5, 0 °C to RT	

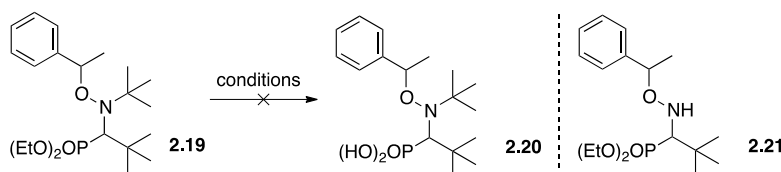
**Table 2.3** Oxidation of aminophosphonate **2.14** and **2.15** to nitroxides.

The lack of success in synthesizing carboxy SG1 led to investigation into an alternative SG1 derivative **2.3**. Instead of relying on the carboxylic acid group, it was expected that upon dealkylation of the original SG1 radical the resulting phosphonate could act as a switch. Furthermore, the double negative charge of the phosphonate could further enhance the switching effect. In order to test this hypothesis, the SG1 radical and aryl alkoxyamine **2.19** were synthesized, following the literature procedures (**Scheme 2.7**).<sup>41,42</sup> The alkoxyamine **2.19** was delivered as a mixture of diastereoisomers that could be separated by flash column chromatography, which made collecting the characterization data easier.



**Scheme 2.7** The synthesis of SG1 and SG1 alkoxyamine.

Next, the alkoxyamine **2.19** was subjected to a series of different reagents that were expected to promote dealkylation (**Table 2.4**). The majority of the literature procedures reported successful removal of the alkyl groups under acidic conditions.<sup>43-45</sup> It was found that whenever alkoxyamine **2.19** was treated with acid, whether aqueous or anhydrous, concentrated or dilute, the *tert*-butyl group on nitrogen was removed, producing unwanted product **2.21**. More unusual protocols involving use of TMSBr<sup>46</sup> or boron tribromide<sup>47</sup> delivered complex mixtures but none of the desired product **2.20** was detected by MS analysis.



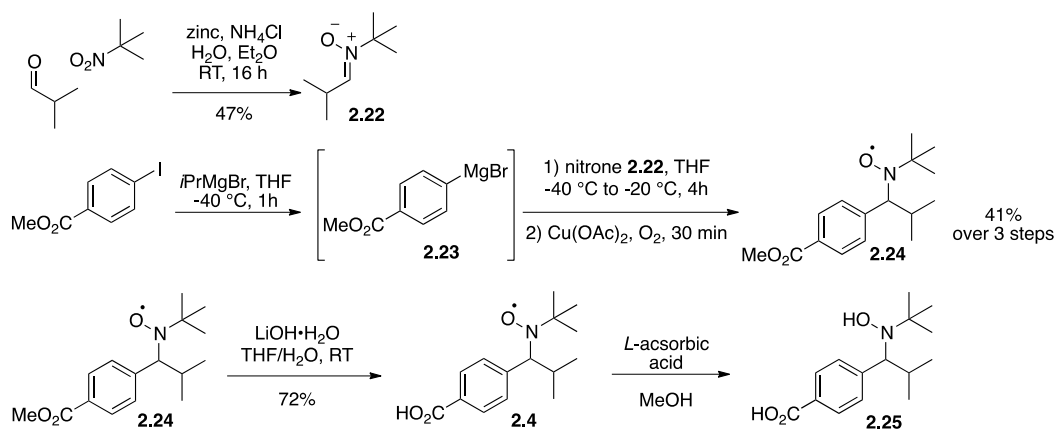
Entry	Conditions	Comments
1	HCl aqueous conc. 12 M, RT	<i>t</i> Bu group falls off
2	HCl aqueous dilute 1 M or 2 M, RT	
3	HCl 4 M in dioxane, RT	
4	TMSBr, then MeOH	complex mixtures
5	BBr <sub>3</sub> , then MeOH	

**Table 2.4** Attempts to remove ethyl groups from **2.19**.

#### 5.4 The synthesis of TIPNO-type radical

The last radical type to be tested was a TIPNO derivative **2.4** with the carboxylic acid group attached to the aromatic ring. The compound was previously reported in the literature and was successfully used to mediate polymerization in homogenous aqueous

solution at 95 °C.<sup>33</sup> It was very encouraging to see that polymerizations could proceed at this temperature in a high polarity solvent. According to the theoretical predictions, even lower temperatures should be achievable when the carboxylic acid was deprotonated and the switch operated in a low polarity solvent. The 4-carboxy TIPNO radical **2.4** was synthesized according to the procedure described by Matyjaszewski and coworkers (**Scheme 2.8**).<sup>33</sup> Nitrone **2.22** was prepared from isobutyraldehyde and 2-nitro-2-methylpropane following the known procedure.<sup>48</sup> The product **2.22** was found to be unstable (decomposing over time upon storage, even at low temperatures) and the purification was somewhat problematic due to several unidentified by-products present in the crude reaction mixture. Next, methyl 4-iodobenzoate was reacted with isopropyl magnesium bromide to form a Grignard reagent **2.23**, which was then added to the nitrone. The resulting hydroxylamine was subsequently oxidized using copper(II) acetate and air to give methyl ester **2.24**. Finally, base mediated hydrolysis afforded 4-carboxy TIPNO **2.4** in an overall moderate yield of 30% over 4 steps from methyl 4-iodobenzoate.



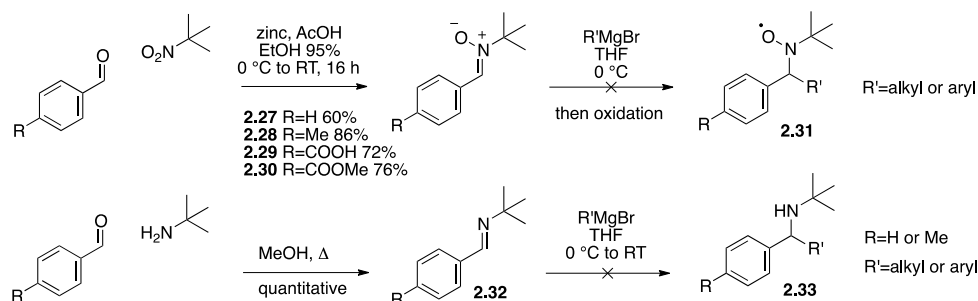
**Scheme 2.8** The synthesis of 4-carboxy TIPNO.

An interesting aspect of this synthesis was the preparation of the Grignard reagent **2.23**, which involved addition of isopropyl magnesium bromide to an ester, without affecting the carbonyl group. The reaction seemed to work at low temperatures with freshly titrated organomagnesium reagent, although the yields were variable, especially when running the reaction on larger scale. This could be due to the methyl ester reacting with the isopropylmagnesium bromide to some extent instead of undergoing metal-halide exchange. Radicals **2.24** and **2.4** were characterized using elemental analysis and mass

spectrometry. Additionally, a small amount of 4-carboxy TIPNO was reduced to the corresponding hydroxylamine **2.25**, and the  $^1\text{H}$  NMR analysis further confirmed the structure.

### 5.5 Alternative routes to 4-carboxy TIPNO – Grignard addition to aryl nitrones and imines

In order to achieve a more efficient synthesis of 4-carboxy TIPNO, a series of stable and easy to purify nitrones was synthesized from aromatic aldehydes and 2-methyl-2-nitropropane (**Scheme 2.9**).<sup>49</sup> Unlike nitrone **2.22**, all aryl nitrones were prepared in good yields and as a single isomer. There is strong evidence based on examination of the UV spectra, X-ray crystal structures and  $^1\text{H}$  NMR data that nitrones derived from aromatic aldehydes possess the *Z* configuration in which the aryl group and oxygen are on the same side of the double bond.<sup>50-52</sup> Unfortunately, all attempts to add Grignard reagents to these nitrones failed. This could be due to poor reactivity and steric hinderance of *N-tert* butyl *N*-benzyl nitrones in general<sup>53</sup> or due to Grignard reagent acting as a base and carrying out an E2 elimination reaction on the *tert*-butyl group, causing decomposition of the nitrone. Furthermore no reaction was observed when the corresponding imines were reacted with alkyl and aryl Grignards.

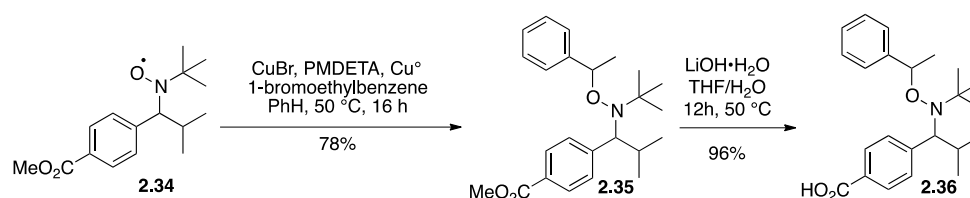


**Scheme 2.9** Addition of Grignard reagents to aryl nitrones and imines.

### 5.6 The synthesis of 4-carboxy TIPNO alkoxyamine and preliminary polymerization studies

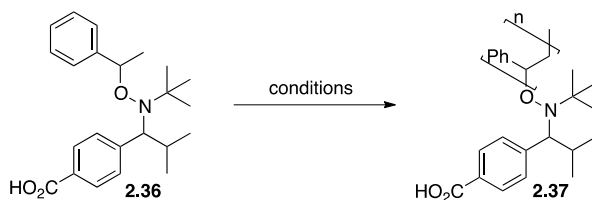
Having successfully completed the synthesis of 4-carboxy TIPNO, the next step was to attach a suitable leaving group. Direct synthesis of alkoxyamine **2.36** from radical **2.4** was unsuccessful, but using **2.34**, where the free carboxylic acid was protected as the methyl ester, furnished alkoxyamine **2.35** in good yield as an inseparable mixture of

diastereoisomers. Ester hydrolysis of **2.35** delivered the desired alkoxyamine **2.36** in excellent yield (**Scheme 2.10**).



**Scheme 2.10** The synthesis of 4-carboxy TIPNO alkoxyamines.<sup>33</sup>

Alkoxyamine **2.36** (used as a mixture of diastereoisomers) was then subjected to NMP conditions. It was expected that TIPNO derived compounds would perform better than 4-carboxy TEMPO ones. Unfortunately, NMP experiments with alkoxyamine **2.37** gave very similar results to 4-carboxy TEMPO alkoxyamine mediated polymerizations (**Table 2.5**). At 120 °C, the polymer was formed in good yield and with narrow mass distribution (PDI=1.2). Lowering the temperature to 100 °C resulted in very little polymer formation and poor control (PDI=1.4). Addition of a base at 100 °C resulted in a small amount of polymer with slightly higher molecular weight but with a significantly broadened mass distribution (PDI=3.1). At 80 °C only a few milligrams of polymer was recovered and interestingly, the addition of base at that temperature as well as at 60 °C halted polymerization completely, which was contrary to what the calculations predicted.

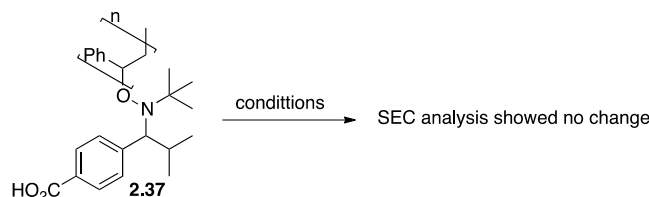


Entry	Conditions	Comments
1	styrene, 120 °C, 12 h	Good yield and control
2	styrene, 100 °C, 12 h	Poor control and broad mass distribution
3	styrene, DBU (10 eq), 100 °C, 12 h	
4	styrene, 80 °C, 12 h	No polymer formed
5	styrene, DBU (10 eq), 80 °C, 12 h	
6	styrene, DBU (10 eq), 60 °C, 12 h	



**Table 2.5** Styrene NMP with 4-carboxy TIPNO alkoxyamine **2.36**.

Just as with 4-carboxy TEMPO polystyrene **2.9**, chain extension experiments with 4-carboxy TIPNO polymer **2.37** were carried out with and without a base at 100 °C and 80 °C (**Table 2.6**). It was established that addition of base (DBU or proton sponge) had little effect on the resulting molecular weight distribution. A clear bimodal distribution was observed with the lower molecular peak due to the starting polymer and the higher molecular peak due to auto-polymerization of styrene monomer. There appeared to be very little change in the molecular weight of the starting polymer, which strongly suggests the expected chain extension did not take place (**Appendix One, Figures A1.1.1 and A1.1.2**).



### 5.7.1 Nitroxide Mediated Polymerizations of styrene with 4-carboxy-TEMPO and TEMPO and the choice of base

The polymerization of styrene mediated by 4-carboxy TEMPO and AIBN at 100 °C, with and without addition of DBU as a base, suggested that the presence of DBU could affect the molecular weight distribution of the polymerization. When DBU was present, the molecular weight of the polymer was reduced significantly (**Appendix One, Figure A1.2.1.1**). The same 4-carboxy TEMPO and AIBN system with triethylamine (TEA) or proton sponge (PS) instead of DBU also reduced the molecular weight of the final polymer but to a lesser extent. Therefore, either TEA or PS should be the base of choice for NMP experiments aimed at demonstrating the switch. When 4-carboxy TEMPO was replaced with TEMPO, neither TEA nor PS had a significant effect on the molecular weight (**Appendix One, Figure A1.2.2.1**). This showed that in the absence of the switch (i.e. carboxylate), the base itself does not interfere with the polymerization process. Increasing the amount of base (10 to 100 eq of either TEA or PS) caused a small reduction in the molecular weight of the final polymer (**Appendix One, Figure A1.2.2.2**). This was found to be insignificant as the change in molecular weight was not proportional to the amount of base added.

### 5.7.2 Effect of base on initiation

The addition of base (either TEA or PS) had no effect on the auto-polymerization of styrene at 100 °C. When AIBN was used as the initiator there was a slight reduction in the final molecular weight but this effect was small. Styrene auto-polymerization at 100 °C was also studied in the presence of benzoic acid and base to ascertain whether the combination of acid and base in the NMP systems was responsible for cationic polymerization. The presence of the base and benzoic acid was found to have no effect on the molecular weight of the final polymer (**Appendix One, Figure A1.2.3.1**).

### 5.7.3 Control experiments at 60 °C

To test for auto polymerization of styrene at 60 °C, samples of styrene with and without AIBN and also with and without 18-crown-6 were prepared and heated at 60 °C for 5 h. After this period, the samples that contained no AIBN yielded no polymer, confirming that there is essentially no self-initiation at 60 °C (**Appendix One,**

**Figure A1.3.1).** Samples with added AIBN yielded polymer but no effect of the 18-crown-6 on the final molecular weight was observed.

#### 5.7.4 Control experiments at 80 °C

Two sets of experiments were carried out, one in neat styrene and the other in a 1:1 v/v mixture of styrene and benzene (**Appendix One, Figure A1.4.1**). All samples were heated at 80 °C for 7 days. Control samples with styrene only as well as styrene and AIBN initiator yielded polymer in both sets, confirming that at 80 °C styrene self-initiation is significant. Samples containing 4-carboxy TEMPO (with or without base) did not yield any polymer in any of the reaction sets. Those containing the potassium salt of 4-carboxy TEMPO and 18-crown-6 did produce polymer but the sample in bulk styrene gave a bimodal molecular weight distribution. This was most likely due to the presence of two phases during the polymerization where the bottom of the sample solidified and the top was still a solution. The dilution of the monomer by the addition of benzene resulted in only one phase being present and therefore only a single molecular weight distribution was observed. However, it did appear that the potassium salt of 4-carboxy TEMPO in the presence of 18-crown-6 caused a reduction in the molecular weight of the polymer when compared to a sample containing just styrene and AIBN.

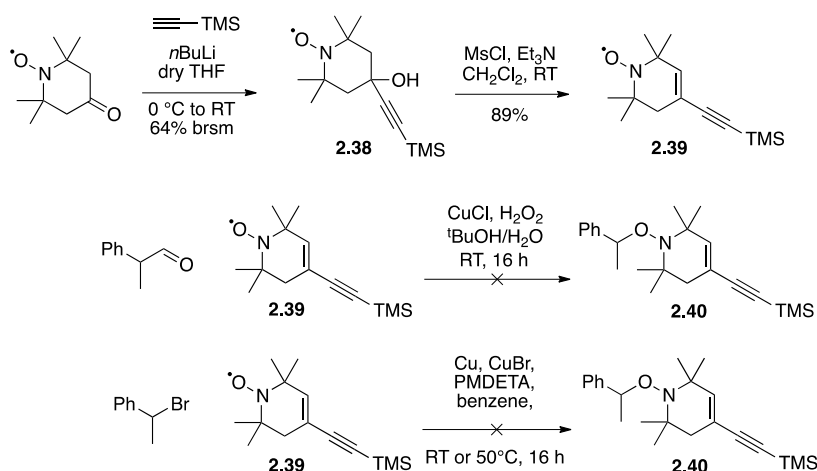
#### 5.7.5 Control experiments at 100 °C

A series of experiments was carried out at 100 °C for 5 days to study the effect of crown ether on styrene polymerization. The addition of 18-crown-6 to the styrene and AIBN system had little effect on the resulting polymer molecular weights (**Appendix One, Figure A1.5.2**). However, it appeared that in the auto polymerization of styrene, the addition of 18-crown-6 increased the molecular weight. Furthermore, the addition of the 18-crown-6 to the styrene polymerization systems containing the potassium salt of 4-carboxy TEMPO and AIBN or the potassium salt of benzoic acid appeared to have no effect on the molecular weight of the resulting polymer (**Appendix One, Figures A1.5.3, A1.5.4 and A1.5.5**).

#### 5.7.6 Acetylene switch – synthesis and polymerization

Due to several issues with the carboxylate switches, with the main one being the solubility in low polarity solvents, an alternative acetylene TEMPO type compound **2.39**

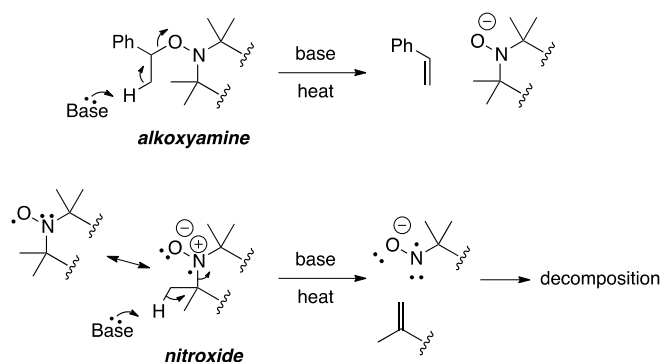
was designed to investigate its potential switching effect on polymerization. According to the computational model, the switch on the acetylide anion was of a similar magnitude to 4-carboxy TEMPO. The acetylide anion was expected to be more readily soluble in styrene and would also eliminate the need for base or crown ether additives. The anion could be generated *in situ* by treating silyl-protected acetylene **2.39** with TBAF. Additionally, the *n*-butyl groups of the ammonium cation could act in a similar fashion to crown ether, shielding the counter ion from the negative charge. The acetylene TEMPO compound **2.39** was synthesized from commercially available 4-oxo-TEMPO in two steps and an overall 57% yield using the addition of the organolithium reagent to the ketone, followed by dehydration of the resulting alcohol (**Scheme 2.11**). The product was characterized by MS and elemental analyses and the structure was further confirmed by single X-ray crystal analysis. Attempts to convert nitroxide **2.39** into alkoxyamine were unsuccessful most likely due to the triple bond reacting with the copper catalyst.



**Scheme 2.11** Synthesis of acetylene TEMPO compound **2.39**.

With nitroxide **2.39** in hand styrene polymerization was carried out (**Appendix One, Figure A1.6.1**). Samples containing nitroxide **2.39**, AIBN and styrene were heated at  $100\text{ }^{\circ}\text{C}$  or  $120\text{ }^{\circ}\text{C}$  for 24 h with or without TBAF added. At  $100\text{ }^{\circ}\text{C}$ , no polymer was formed for both samples. At  $120\text{ }^{\circ}\text{C}$ , the yield of polymer from the sample to which TBAF was added was half of that for samples with the unswitched nitroxide. Furthermore, the addition of TBAF resulted in a decreased molecular weight of the polymer.

Despite all the efforts to prove the calculation results with styrene polymerizations that were mediated by specially designed derivatives of commercially used nitroxides, no sign of the pH induced radical switching in solution was observed. During the review process of this a possible explanation for a failure of the polymerization experiments was suggested. Since the polymerization reaction involves both base and heat, it was proposed that decomposition could take place as a result of a base induced elimination reaction of either alkoxyamine or the nitroxide (**Scheme 2.12**).



**Scheme 2.12** Proposed mechanism of the base induced decomposition of alkoxyamine (top) and nitroxide (bottom) at elevated temperature.

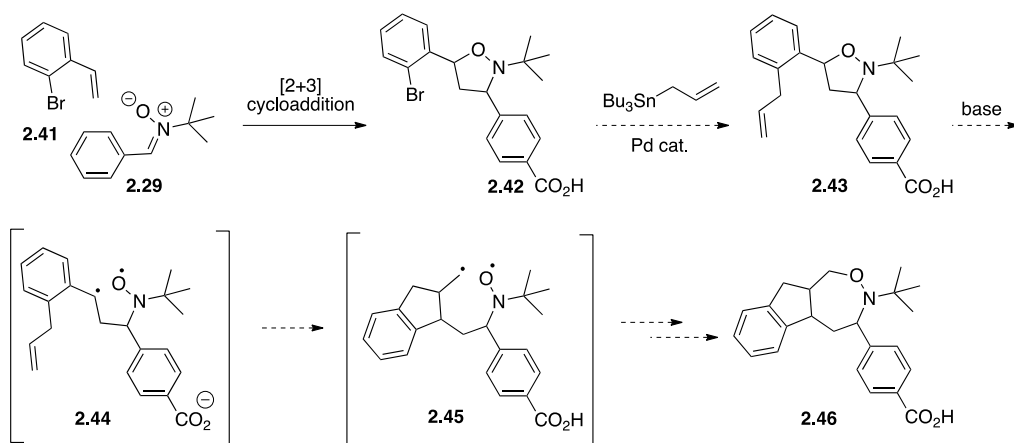
Unfortunately, thermal stability of TEMPO and TIPNO nitroxides, as well as their corresponding alkoxyamines, was not tested in the presence of the base to confirm the abovementioned hypothesis. Instead, the experimental work focused on designing a number of simpler synthetic experiments that could be closely monitored by analytical instrumentation.

## Chapter Six – Synthesis and Use of Analytical Tools for Detecting pH-induced Radical Formation

### 6.1 The synthesis of isoxazolidine type compounds *via* [2+3] cycloaddition

The synthesis of aryl *tert*-butyl nitrones, **2.27-2.30**, which turned out to be unsuitable for Grignard addition, led to the design of a potentially very efficient way of assembling protected radicals *via* a cycloaddition reaction. Nitrones are excellent candidates for [2+3] cycloadditions, also referred to as 1,3-dipolar cycloadditions, and reaction between nitrones and alkenes leading to isoxazolidines is one of the fundamental reactions in organic chemistry.<sup>54</sup>

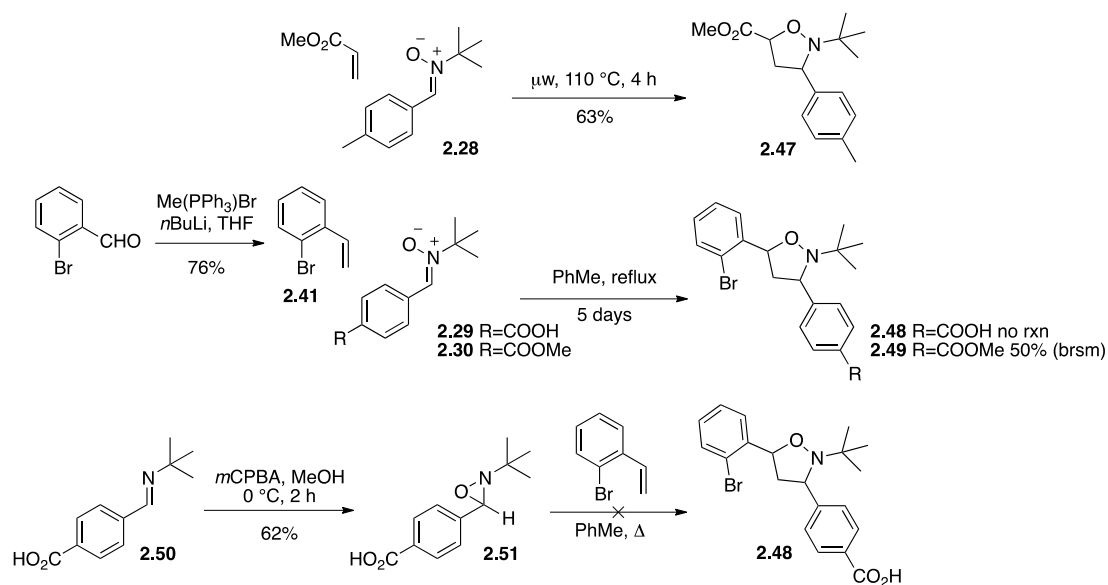
If successful, this strategy could be an elegant proof of principle experiment as it would have several advantages over the previous syntheses (**Scheme 2.13**). The major one being that both nitroxide protecting group and alkoxyamine leaving group are prepared in one step. The resulting isoxazolidine type compound **2.43** could be then further functionalized by introducing allyl group onto the aromatic ring of the leaving group. Upon base-induced C-O bond cleavage, diradical **2.44** could undergo cyclization, followed by trapping by the nitroxide in a similar manner as expected for 4-carboxy TEMPO alkyl alkoxyamine **2.8**. The rearranged product **2.46** would then serve as an evidence for successful pH-induced radical formation in solution.



**Scheme 2.13** Proof of principle experiment design using transformation of isoxazolidine.

The initial experiments with aryl *N*-*tert*-butyl nitrone **2.28** and methyl acrylate gave promising results and isoxazolidine **2.47** was formed in 63% yield as a mixture of diastereomers (**Scheme 2.14**). This was encouraging, given the fact that this particular class of nitrones is the least reactive.<sup>55</sup> Regiochemistry was established by analysis of the <sup>1</sup>H NMR spectrum, in particular splitting patterns of the four isoxazolidine protons. The two methylene protons appeared at  $\delta$  2.51 and  $\delta$  2.69 ppm each as a ddd, which could only be possible if they were in position 4 of the ring. The neighbouring protons next to nitrogen (position 3) and oxygen (position 5) appeared downfield at  $\delta$  4.23 ppm (dd) and  $\delta$  4.59 ppm (apparent t). Furthermore this regiochemistry was consistent with experimental results by Padwa and coworkers, who also reported cycloaddition between nitrones and electron deficient dipolarophiles to deliver 5-substituted isoxazolidines.<sup>56</sup> Relative and absolute configurations were not assigned as these were irrelevant to testing the calculation predictions. Adduct **2.47** was just a model compound, prepared to test the cycloaddition reaction. According to the design outlined in **Scheme 2.13**, a different set of substrates was required, where the nitrone had a switch functionality attached and the dipolarophile introduced a suitable aryl group. The alkene **2.41** was prepared from commercially available 2-bromo benzaldehyde *via* Wittig reaction in 76% yield<sup>57</sup> and the nitrone was synthesized from benzaldehyde as shown in **Scheme 2.6**. The cycloaddition failed to deliver any of the desired product **2.48** and both starting materials were recovered unchanged. Using more forcing conditions (pressure and temperatures > 120 °C) and prolonged reaction times (over one week) only resulted in partial decomposition of the nitrone as the *tert*-butyl group became unstable. Troisi and coworkers have reported successful use of aryl *N*-*tert*-butyl oxaziridines and alkenes in isoxazolidine synthesis.<sup>58</sup> According to the authors, the oxaziridine could participate in a cycloaddition directly or transform into a nitrone upon heating. Encouraged by this result, the oxaziridine **2.51** was prepared by *m*CPBA mediated oxidation of the corresponding imine **2.50**. Unfortunately, no cycloaddition product was detected and the starting material 2-bromostyrene **2.41** along with nitrone **2.29** were recovered from reaction mixture. Using the methyl ester protected nitrone **2.30** instead slightly improved the yield, but the reaction required 5 days in refluxing toluene to deliver the desired isoxazolidine product **2.49** in a very modest 21% yield or up to 50% yield if the recovered starting material was recycled twice. Lewis acids

such as copper(II) triflate and magnesium(II) chloride<sup>59</sup> as well as microwave irradiation<sup>60</sup> were used hoping to improve the yield, but these were ineffective.



**Scheme 2.14** Isoxazolidine synthesis *via* [2+3] cycloaddition.

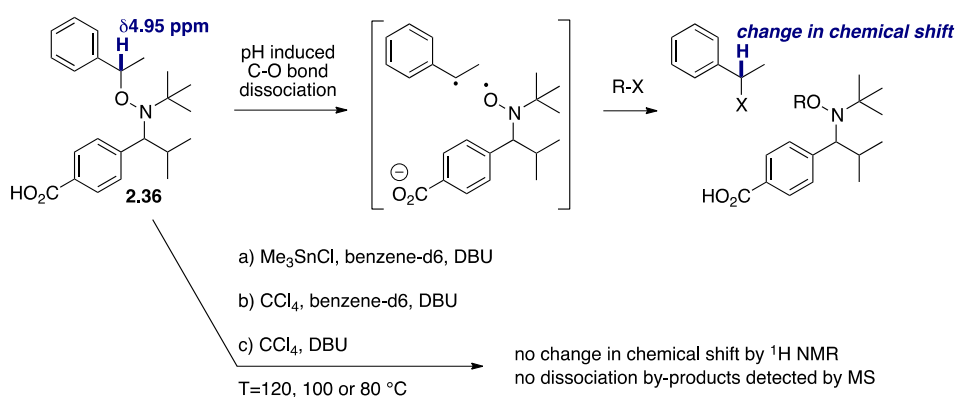
In parallel to the synthetic experiments our computational chemistry collaborators modeled deprotonation of the intermediate **2.43** (**Scheme 2.13**) and calculated a switch on the resulting carboxylate. According to these calculations, the switch in a low polarity solvent such as benzene was even lower than for 4-carboxy TEMPO alkoxyamine **2.8** (**Table 2.2**). Considering the time and effort invested in the synthesis of these isoxazolidines, it was very disappointing to discover that even at higher temperatures, no appreciable amount of radicals are calculated to be generated by these molecules. The main reason for such a small switch could be the entropy of the dissociation step. A reaction in which the alkoxyamine dissociates to give two radicals is more favored entropically than a reaction where cyclic alkoxyamine dissociates to form an acyclic biradical such as compound **2.44** (**Scheme 2.13**). Although experimentally it would have been an elegant demonstration of pH switching of the radicals, the calculations showed that the effect would be negligible and therefore not observable during the experiment. At this point, only a few milligrams of the intermediate **2.49** (**Scheme 2.14**) were available for further synthesis, and scaling up the reaction would have been even more time consuming. This, along with unfavorable theoretical predictions, resulted in termination of the isoxazolidine



synthesis project.

## 6.2 Bond dissociation in 4-carboxy TIPNO alkoxyamine monitored by $^1\text{H}$ NMR

Alkoxyamine **2.36** was heated with and without base in the presence of either carbon tetrachloride or trimethyltin chloride to observe halogen exchange products, which would be expected to form after the dissociation of the alkoxyamine. All samples were heated for 1 h in a microwave reactor at 120, 100 and 80 °C. No dissociation products were detected by  $^1\text{H}$  NMR nor by mass spectrometry.



**Scheme 2.15** Monitoring pH induced switching by  $^1\text{H}$  NMR.

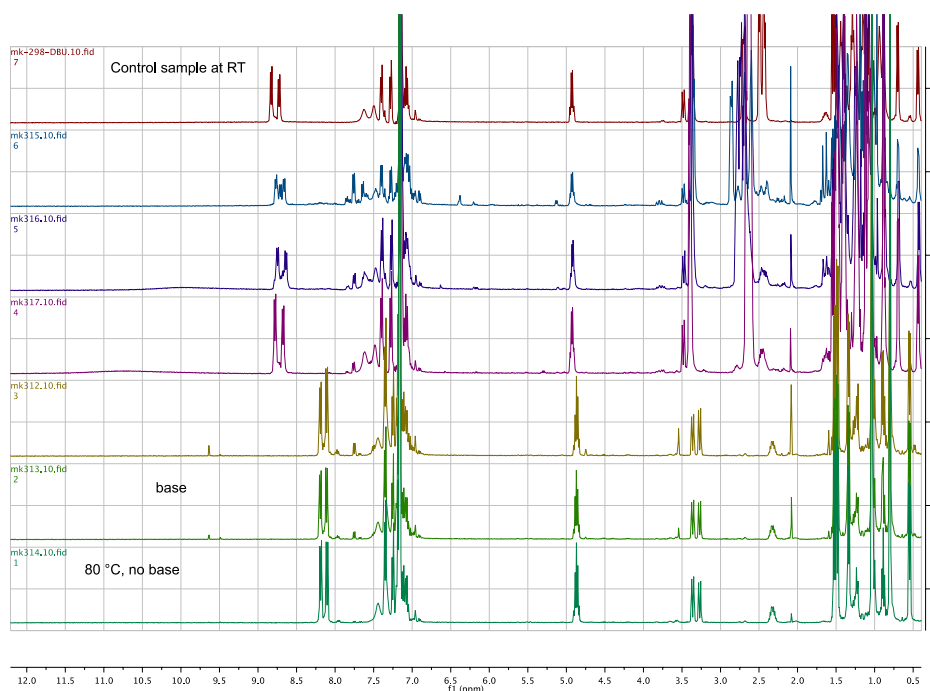


**Figure 2.6** Comparison of  $^1\text{H}$  NMR spectra after reaction in  $\text{C}_6\text{D}_6$  of samples containing alkoxyamine, carbon tetrachloride, with and without the base.

### 6.3 Base titration experiments

Potentiometric titration of 4-carboxy-TEMPO in acetonitrile with tetramethylammonium hydroxide (TMA) was investigated. It was found that this particular system resulted in “flat” titration curves with no discernable inflection points, even when Aliquat 336 was added in order to enhance the conductivity.

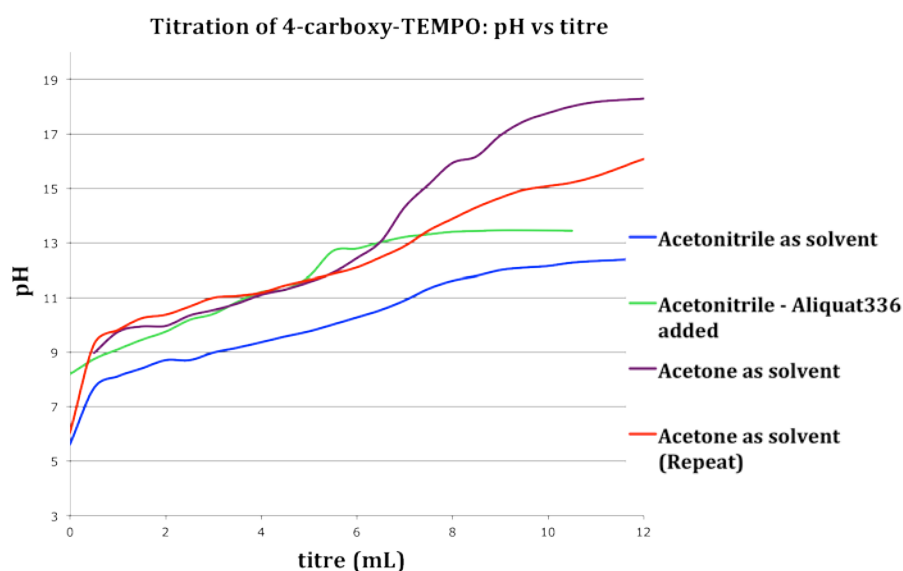
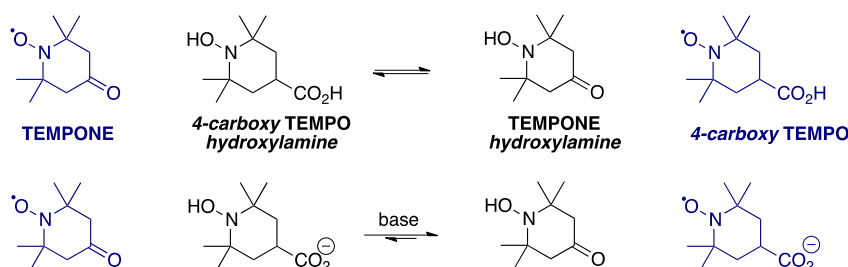


**Figure 2.7** Base titration experiments of 4-carboxy TEMPO.

Titration of carboxy TIPNO alkoxyamine **2.36** with TMA in acetonitrile or proton sponge in acetonitrile gave similar results, producing titration curves with no clear inflection point. Titrations in acetone gave improved titration curves but were not reproducible due to the quaternary ammonium salt precipitating from the acetone solution. There is some scope to improve these results by reducing the concentration of the base, sealing the titration vessel or choosing a more soluble base that was less likely to precipitate during titration. Monitoring the titration of 4-carboxy TEMPO with proton sponge by following the UV-vis absorption profile of proton sponge was explored but abandoned due to the absorption of proton sponge itself changing with time (possibility due to atmospheric moisture).

### 6.4 Hydrogen atom exchange monitored by UV-vis spectroscopy

Nitroxide species are UV active and TEMPO type radicals show characteristic absorption at around 400 nm, which could potentially be used to monitor changes in concentration of these radicals in solution. Furthermore, monitoring the final concentrations of reactants and products during proton exchange between a radical and hydroxylamine could be used to calculate the magnitude of the switch. Upon the addition of base an increase in reaction rate would be expected (**Scheme 2.16**).



**Scheme 2.16** Hydrogen exchange experiment between TEMPONE and 4-carboxy TEMPO hydroxylamine.

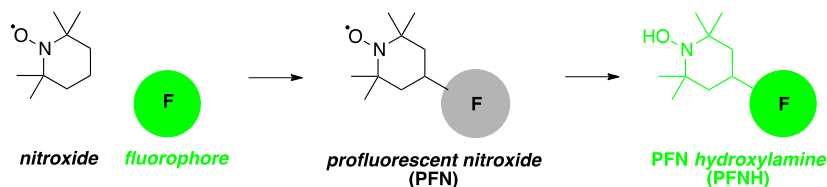
The reaction between TEMPONE and 4-carboxy TEMPO hydroxylamine was studied and concentrations of radicals were monitored *via* UV-vis spectrophotometry. Addition of DBU resulted in a larger reaction rate constant, *K*, but the method suffered from large experimental error introduced by trying to deconvolute two Gaussian spectra lines that lie very close to each other. Both TEMPONE and 4-carboxy TEMPO absorb at very similar wavelengths, and it was problematic to find an alternative nitroxide with a distinct absorption spectrum that would allow for more precise calculation of the reaction kinetics.

### 6.5 Using fluorescence to demonstrate pH induced radical switching

The hydrogen atom exchange experiment described in the previous section was by far the most promising from all the experiments carried out in this project. However, monitoring the reaction kinetics by UV-vis spectroscopy had several drawbacks, making the extraction of data problematic due to overlapping signals. The lesson learnt from the polymerization experiments was that the more variables introduced into the system, the more difficult it was to determine the effect of changing the pH had on the nitroxides or their alkoxyamines. Furthermore, no evidence of switching was observed by  $^1\text{H}$  NMR,

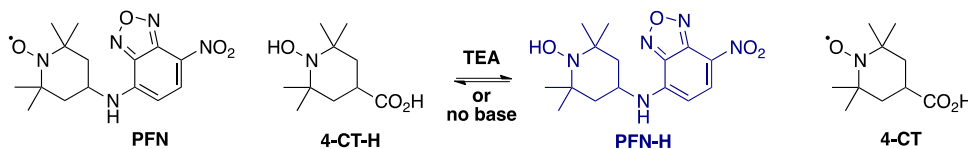
which suggested that perhaps the effect is very small in solution and a more sensitive analytical tool would be required in order to detect it. Putting all the pieces of information from previous, failed experiments together led to the design of a new experiment that would rely on monitoring hydrogen exchange reaction by fluorescence spectroscopy.

One of the recent applications of nitroxides is to attach them to fluorophores and use the resulting dual-functional molecules as fluorescent probes (**Scheme 2.17**).<sup>61,62</sup>



**Scheme 2.17** Cartoon representation of assembling profluorescent nitroxide and fluorescent hydroxylamine.<sup>62</sup>

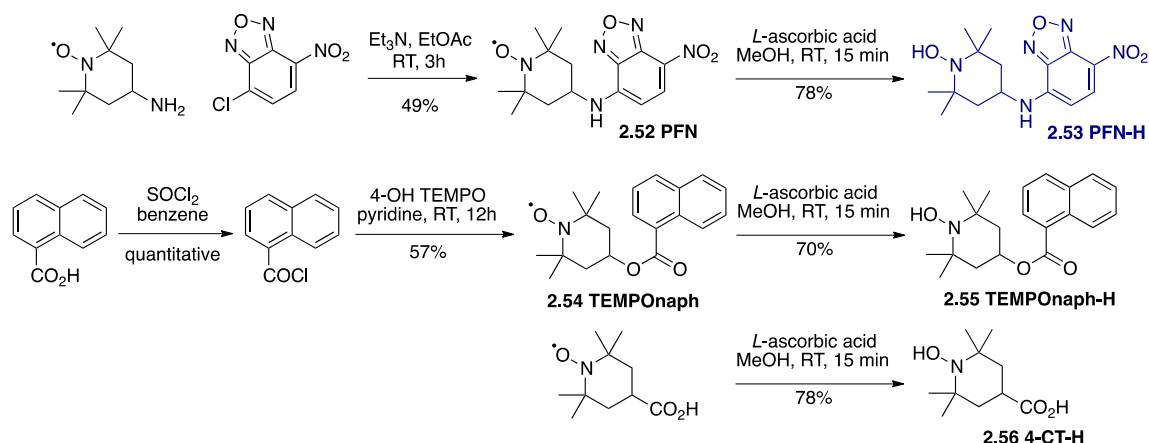
The most important feature of these molecules is that fluorescence is suppressed in PFNs themselves but returned upon removal of the radical.<sup>62</sup> Therefore, compounds such as hydroxylamines of alkoxyamines derived from PFNs are fluorescent. This unique behavior was the basis for our experiment, as upon hydrogen exchange the inactive PFN would pick up the proton and the amount of fluorescent hydroxylamine (PFN-H) product forming over time could be measured by fluorescence spectrometry. According to the calculations, upon addition of base in low polarity solvent, 4-carboxy TEMPO hydroxylamine (4-CT-H) should release the proton more readily and therefore the reaction would be expected to proceed faster and at higher rate, which should manifest in greater concentrations of PFN-H.



**Scheme 2.13** Hydrogen exchange experiment between PFN and 4-CT-H.

The synthesis of compounds required for the experiment was rather straightforward. Profluorescent nitroxide **2.52** was prepared *via* nucleophilic aromatic substitution of 4-chloro-7-nitrobenzofurazan with commercially available 4-amino TEMPO (**Scheme 2.19**).<sup>63</sup> The control compound **2.54** was prepared from 4-hydroxy

TEMPO and 1-naphthoic acid.<sup>64</sup> All hydroxylamines were prepared by reducing the corresponding nitroxides with ascorbic acid in methanol.



**Scheme 2.14** The synthesis of compounds required for fluorescence experiment.

**Figure 2.8** shows the concentration of the fluorescent hydrogen transfer product PFN-H as a function of time, in the presence of different amounts of the triethylamine (TEA) in dichloromethane and acetonitrile as well as control compound TEMPONaph-H in dichloromethane. Dichloromethane is a relatively low polarity solvent (dielectric constant  $\epsilon = 8.9$ ), while acetonitrile is relatively polar ( $\epsilon = 37.5$ ). The time dependent concentrations of PFN-H were determined from the measured fluorescence intensity in conjunction with separate calibration experiments. Calibration curves were constructed for each effective concentration of the base to ensure that the results were not an artifact of any pH effects on the fluorescence intensity of the PFN-H product (**Appendix Two, Figures from A2.1.1 to A2.1.4**). For each experiment, the final equilibrium concentrations of PFN-H were used to estimate the equilibrium constant, while the time dependent concentrations were fitted with a reversible second order kinetic model to determine the forward and reverse rate coefficients. The resulting kinetic and thermodynamic parameters are presented in **Table 2.7**. Full details of the experiments and kinetic analysis are described in the experimental section in **Chapter Seven** and in the **Appendix Two**.

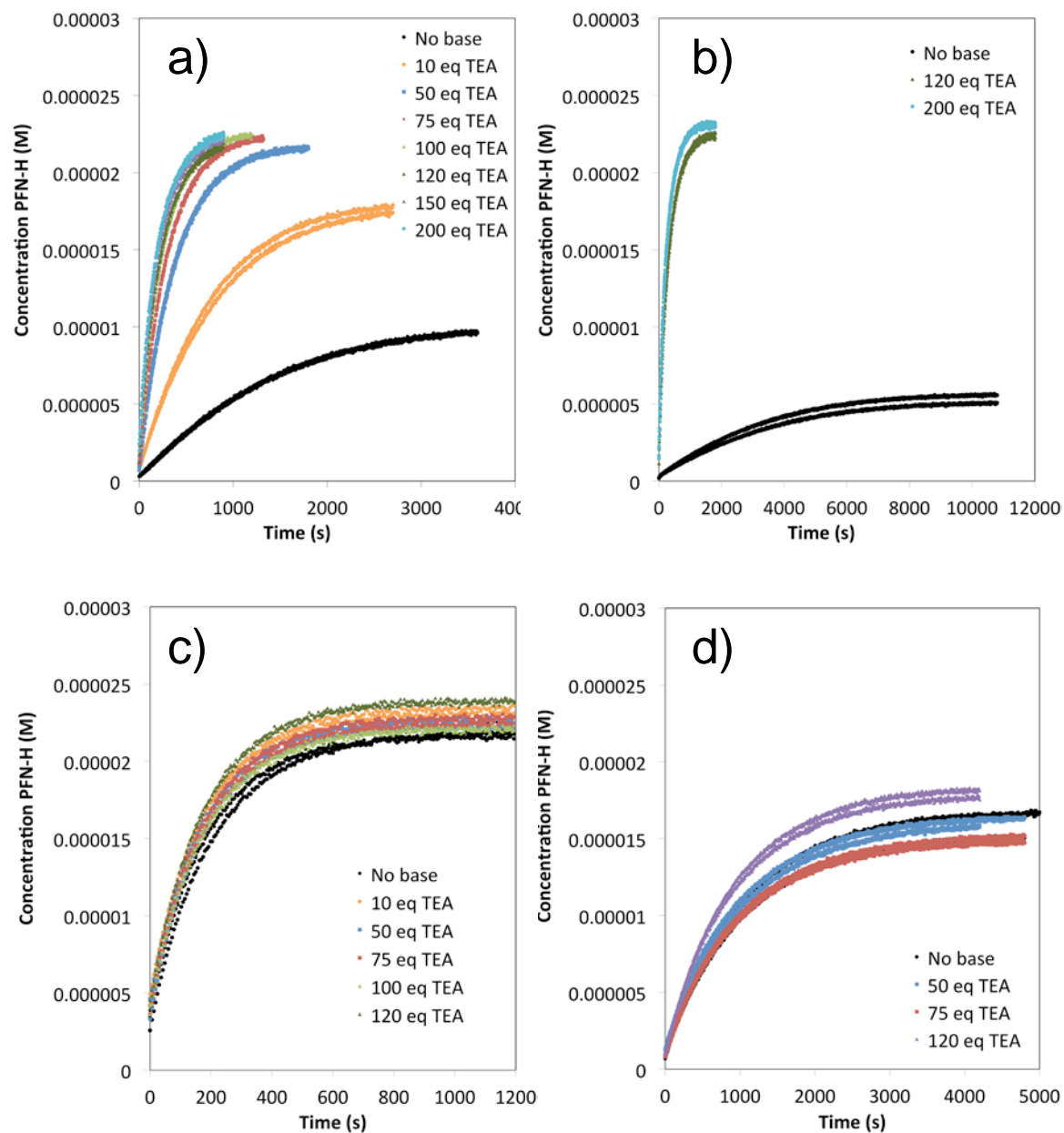


**Figure 2.8** Concentration of PFN-H vs time for the addition of triethylamine (TEA) at room temperature for a) PFN/4-CT-H system in dichloromethane at 25 °C, b) the same system at 10 °C, c) PFN/4-CT-H in acetonitrile at 25 °C and d) the PFN/ TEMPONaph-H control reaction in dichloromethane at 25 °C.

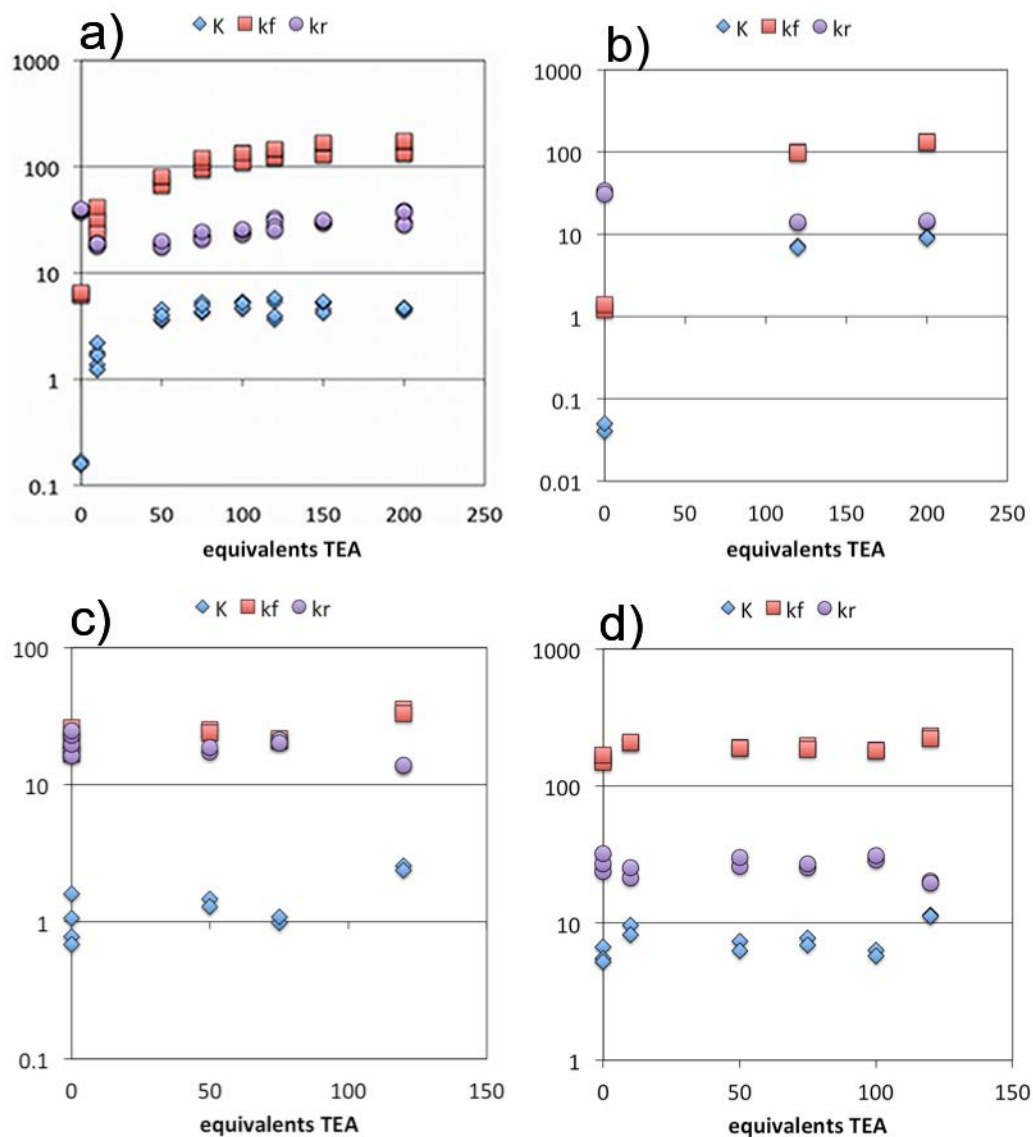


**Figure 2.9** Measured equilibrium constants ( $K$ ) and forward ( $k_f$ ) and reverse ( $k_r$ ) rate constants ( $\text{L mol}^{-1} \text{s}^{-1}$ ) as a function of the equivalents of triethylamine (TEA) base added for a) the PFN/4-CT-H reaction in dichloromethane at 25 °C, b) the same reaction at 10 °C, c) the same reaction in acetonitrile at 25 °C, and d) for the PFN/TEMPO<sub>naph</sub>-H control reaction in dichloromethane at 25 °C.

Conditions:	K			$k_f / \text{L mol}^{-1} \text{s}^{-1}$			$k_r / \text{L mol}^{-1} \text{s}^{-1}$		
	No base	120 eq	pH switch	No base	120 eq	pH switch	No base	120 eq	pH switch
(a) DCM 25 °C	0.17	4.7	28.5	6.4	133.9	21.0	39.2	29.1	0.7
(b) DCM 10 °C	0.05	14.4	319.1	1.3	201.6	155.1	32.3	28.0	0.9
(c) MeCN 25 °C	1.0	2.5	2.4	20.3	34.1	1.7	20.8	13.8	0.7
(d) control 25 °C	5.8	11.3	1.9	158.0	225.3	1.4	27.6	19.9	0.7

**Table 2.7** Average equilibrium constants (K) and forward ( $k_f$ ) and reverse ( $k_r$ ) rate constants ( $\text{L mol}^{-1} \text{s}^{-1}$ ) as a function of the equivalents of triethylamine (TEA) base added for (a) the PFN/4-CT-H reaction in dichloromethane (DCM) at 25 °C, (b) the same reaction at 10 °C, (c) the same reaction in acetonitrile (MeCN) at 25 °C, and (d) for the PFN/TEMPO<sub>naph</sub>-H control reaction in DCM at 25 °C. The pH switch is calculated as the ratio of corresponding values at 120 equivalents of base and with no base present.



Clearly, in the reaction of 4-CT-H with the PFN in dichloromethane, the addition of base increases both the rate at which equilibrium was achieved and the final equilibrium concentrations of PFN-H. These effects depend on the amount of base added up to approximately 120 equivalents, at which point the carboxylic acid was presumably fully deprotonated.

The pH switch can be quantified by comparing the average values of each parameter at 120 equivalents of base to the corresponding values under otherwise identical conditions in the absence of base (**Table 2.7**). For 4-CT-H reaction in dichloromethane at 25 °C, we find that the equilibrium constant shifts to the right by a factor of 28.5 upon full deprotonation of the remote carboxy group of 4-CT-H, corresponding to an increase in stability of the resulting distonic radical anion by approximately one order of magnitude. Interestingly, at 10 °C this pH switch increases by a further order of magnitude to 319.1. This temperature dependence, also noted in the recent work of Lucarni and co-workers<sup>34</sup> implies a significant opposing entropic contribution to the pH switch, which presumably arises in more specific solute-solvent interactions.

At both temperatures, the significant pH switch on the reaction thermodynamics is largely preserved in the reaction kinetics, implying that the transition state stabilization is similar in magnitude to that of the product radical. Whilst the unpaired electron density is distributed further from the negative charge in the transition state, this is presumably countered to a large extent by its greater polarizability. More generally, the greater polarizability of transition states, compared with stable species, implies that electrostatic catalysis of radical reactions could be significant even when the reactant and product radicals are not themselves especially delocalised provided there are appropriately placed charges in the vicinity of the reaction centre. Since the transition state and product radical are stabilized to similar extents, the pH switch on the reverse reaction is consequently relatively small at both temperatures.

In contrast, the addition of base had little or no effect on the kinetics and thermodynamics of the hydrogen transfer reaction between the TEMPO<sub>naph</sub>-H control compound and the PFN under the same conditions, confirming that the pH effects in 4-carboxy TEMPO hydroxylamine were associated with deprotonation of its carboxylic acid group rather than, for example, base catalysis of the hydrogen transfer reaction *via* a

sequential proton loss electron transfer (SPLET) mechanism.<sup>65</sup> Consistent with the recent experimental work of Lucarni *et al*, the pH switches in acetonitrile were also essentially negligible.<sup>34</sup> This further confirmed the electrostatic origin of the pH effects on the 4-carboxy TEMPO nitroxide radical stability, which were predicted to be quenched in polar environments.<sup>2</sup> Interestingly, in benzene (results not reported here due to lack of temperature control during measurements done in this solvent), the rate enhancement was rather modest compare to dichloromethane. These discrepancies are most likely due to poor solvation of the carboxylate in benzene as well as difficulties associated with computational modelling of solvent effects.

## 6.6 Summary and conclusions

Derivatives of TEMPO, SG1 and TIPNO were synthesized in order to investigate electronic stabilizing effects in distonic radicals. Aryl alkoxyamines of 4-carboxy TEMPO and 4-carboxy TIPNO were used to control polymerization of styrene in an attempt to demonstrate pH switching *via* NMP experiments. Additional polymerization experiments involving numerous control runs and an alternative acetylene TEMPO compound were studied in order to establish the role of the base and other additives as well as explore different type of switch. Despite a lot of time and effort invested in those experiments, it was not possible to utilize radical switching in polymerization.

Designing more operationally simple experiments that could be monitored both qualitatively and quantitatively using analytical instrumentation was more successful. The hydrogen atom transfer reaction between profluorescent nitroxides and carboxy nitroxide provided the first experimental verification of pH-dependent electrostatic stabilizing effect in radical anions in solution. The experiment demonstrated significant (up to 2 orders of magnitude) pH switching of radical stability in a low polarity organic solvent as well as electrostatic catalysis by a remote negatively charged functional group on the hydrogen transfer reaction between two locally equivalent nitroxide radicals.

More generally, these findings validated theoretical predictions that electrostatic stabilization of delocalized radicals remains practically significant in low polarity environments and, given the broad chemical scope of this effect, its persistence in low polarity solvents suggest that it is likely to be useful in synthetic applications, and may also be a contributor to enzyme catalysis.

## **Chapter Seven – Experimental Work Associated with Research Reported in Part Two**

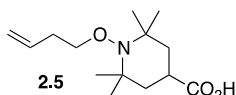
### **7.1 General methods**

NMR spectra were recorded at 298 K using a Bruker AVANCE 400 spectrometer. The  $^1\text{H}$  NMR signal of residual chloroform ( $\delta$  7.26 ppm) or residual dimethyl sulfoxide ( $\delta$  2.50 ppm) was used as internal reference for  $^1\text{H}$  NMR spectra measured in these solvents. Coupling constants ( $J$ ) are quoted to the nearest 0.1 Hz. The  $^{13}\text{C}$  NMR signal of chloroform ( $\delta$  77.1 ppm) or dimethyl sulfoxide ( $\delta$  39.5 ppm) was used as internal reference for  $^{13}\text{C}$  NMR spectra measured in these solvents. Assignment of proton signals was assisted by HSQC experiments when necessary; assignment of carbon signals was assisted by APT experiments, HSQC and HMBC experiments were employed when necessary. IR spectra were recorded on a Perkin-Elmer Spectrum One spectrometer as neat films on NaCl plates for oils or as KBr disks for solid products. Mass spectra were recorded by the Mass Spectrometry Facility of the Research School of Chemistry, Australian National University, Canberra on a VG Autospec M series sector (EBE) MS for EI, VG Quattro II triple quadrupole MS for LR ESI and Bruker Apex3 4.7T FTICR-MS for HR ESI. Microanalyses were performed at the Microanalytical Laboratory, Research School of Chemistry, Australian National University, Canberra. Melting points were measured on Optimelt automated melting point apparatus and are uncorrected. Analytical TLC was performed with Merck (A.T. 5554) silica gel 60 F254 (0.2 mm) plates, precoated on aluminium sheets. Flash chromatography employed Merck Kiesegel 60 (230–400 mesh) silica gel. Reactions were conducted under positive pressure of dry argon or nitrogen in oven-dried glassware. Diethyl ether, toluene and THF were dried over sodium wire and distilled from sodium benzophenone ketyl. Dichloromethane was distilled from calcium hydride.

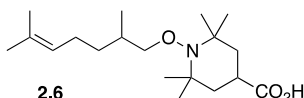
#### **General procedure 1: TEMPO-based Alkoxyamine Synthesis**

To a magnetically stirred solution of TEMPO type radical (1.0 eq) in *tert*-butanol, copper (I) chloride (3.5% mol) followed by an aldehyde (1.5 – 2.0 eq) was added at RT under nitrogen. Then 30% aqueous hydrogen peroxide (2.0 eq) was added dropwise and

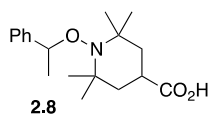
the resulting reaction mixture was stirred at 25 °C until the nitroxyl radical was no longer detectable by TLC analysis (3 h – 16 h). Quenched with 10% *aq.* ascorbic acid solution and extracted with ether. Organic layer was washed with water and brine, separated, dried with Na<sub>2</sub>SO<sub>4</sub>, filtered and concentrated *in vacuo*.



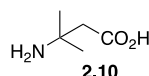
**1-(but-3-en-1-yloxy)-2,2,6,6-tetramethylpiperidine-4-carboxylic acid:** The compound was prepared according to the **General Procedure 1**. The residue was purified by flash column chromatography (15% EtOAc/hexane) to give the product as colourless oil (13 mg, 51%): <sup>1</sup>H NMR (400 MHz, CDCl<sub>3</sub>) δ 1.13 (s, 6H), 1.20 (s, 6H), 1.60-1.76 (m, 4H), 2.24-2.31 (m, 2H), 2.62-2.70 (m, 1H), 3.78 (q, *J* = 9.0 Hz, 2H) 5.00-5.10 (m, 2H) 5.78-5.90 (m, 1H); <sup>13</sup>C NMR (101 MHz, (CD<sub>3</sub>)<sub>2</sub>SO) δ 20.0 (2xCH<sub>3</sub>), 32.6 (2xCH<sub>3</sub>), 32.8 (CH<sub>2</sub>), 33.9 (CH), 41.5 (2xCH<sub>2</sub>), 58.9 (2xC), 75.6 (CH<sub>2</sub>), 116.3 (CH<sub>2</sub>), 135.6 (CH), 176.2 (C); IR (KBr disc)  $\nu_{\max}$  3600-2200 (broad), 3079, 2977, 2941, 1707 1453, 1361, 1170, 1037, 914 cm<sup>-1</sup>; MS (ESI+) *m/z* (%): 256 (100, [M+H]<sup>+</sup>); HRMS (ESI+) *m/z* calculated for C<sub>14</sub>H<sub>25</sub>NO<sub>3</sub> [M+H]<sup>+</sup>: 256.1913, found: 256.1913.



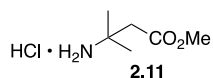
**1-((2,6-dimethylhept-5-en-1-yl)oxy)-2,2,6,6-tetramethylpiperidine-4-carboxylic acid:** The compound was prepared according to the **General Procedure 1**. The residue was purified by flash column chromatography (10% EtOAc/hexane) to give the product as colourless oil (23 mg, 35%): <sup>1</sup>H NMR (400 MHz, (CD<sub>3</sub>)<sub>2</sub>SO) δ 0.91 (d, *J* = 6.8 Hz, 3H), 1.03-1.18 (m, 2H), 1.07 (s, 6H), 1.12 (s, 6H), 1.36-1.47 (m, 3H), 1.56 (s, 3H), 1.64-1.67 (m, 5H) 1.93-1.99 (m, 2H), 2.50-2.57 (m, 1H), 3.48-3.60 (m, 2H) 5.06-5.09 (m, 1H); <sup>13</sup>C NMR (101 MHz, (CD<sub>3</sub>)<sub>2</sub>SO) δ 17.8 (CH<sub>3</sub>), 17.9 (CH<sub>3</sub>), 20.5 (2xCH<sub>3</sub>), 25.6 (CH<sub>2</sub>), 26.0 (CH<sub>3</sub>), 32.7 (CH), 33.0 (2xCH<sub>3</sub>), 34.0 (CH<sub>2</sub>), 34.3 (CH), 42.0 (2xCH<sub>2</sub>), 59.3 (2xC), 81.5 (CH<sub>2</sub>), 124.9 (CH), 131.1 (C), 176.6 (C); IR (KBr disc)  $\nu_{\max}$  3600-2600 (broad), 2968, 2926, 1707 1452, 1375, 1303, 1170, 1042 cm<sup>-1</sup>; MS (ESI+) *m/z* (%): 326 (80, [M+H]<sup>+</sup>), 348 (20, [M+Na]<sup>+</sup>); HRMS (ESI+) *m/z* calculated for C<sub>19</sub>H<sub>35</sub>NO<sub>3</sub> [M+H]<sup>+</sup>: 326.2695, found: 326.2694.



**2,2,6,6-tetramethyl-1-(1-phenylethoxy)piperidine-4-carboxylic acid:** The compound was prepared according to the **General Procedure 1**. The residue was purified by flash column chromatography (20% to 40% EtOAc/hexane) to give the product as white solid (227 mg, 57%):  $^1\text{H}$  NMR (400 MHz,  $(\text{CD}_3)_2\text{SO}$ )  $\delta$  0.60 (s, 3H), 0.99 (s, 3H), 1.14 (s, 3H), 1.28 (s, 3H), 1.33-1.74 (m, 7H), 2.50-2.58 (m, 1H), 4.72-4.77 (m, 1H), 7.23-7.33 (m, 5H), 12.16 (s, 1H);  $^{13}\text{C}$  NMR (101 MHz,  $(\text{CD}_3)_2\text{SO}$ )  $\delta$  20.3 (2xCH<sub>3</sub>), 23.1 (CH<sub>3</sub>), 33.6 (CH<sub>3</sub>), 33.8 (CH<sub>3</sub>), 33.9 (CH), 42.1 (CH<sub>2</sub>), 42.2 (CH<sub>2</sub>), 58.7 (C), 59.0 (C), 82.5 (CH), 126.4 (2xCH), 127.0 (CH), 128.1 (2xCH), 145.0 (C), 171.6 (C); IR (KBr disc)  $\nu_{\text{max}}$  3600-3200 (broad), 2991, 2971, 2925, 1704, 1459, 1312, 1236, 944, 703  $\text{cm}^{-1}$ ; MS (ESI+)  $m/z$  (%): 306 (100,  $[\text{M}+\text{H}]^+$ ), 328 (45,  $[\text{M}+\text{Na}]^+$ ); HRMS (ESI+)  $m/z$  calculated for  $\text{C}_{18}\text{H}_{27}\text{NO}_3$   $[\text{M}+\text{H}]^+$ : 306.2064, found: 306.2069; mp=157 °C.

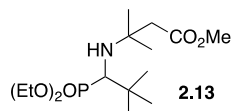


**3-amino-3-methylbutanoic acid:** An excess of sat. *aq.* ammonia solution (72 mL) and 3,3-dimethylacrylic acid (6.00 g, 60 mmol, 1.0 eq) were combined in a high-pressure vessel. The vessel was sealed and heated at 125 °C for 16 h. Cooled down to RT overnight. The pressure was released and the resulting pale yellow solution was concentrated *in vacuo*. The residue was recrystallized from ethanol to give a pure product as white solid (3.78 g, 54%):  $^1\text{H}$  NMR (400 MHz,  $\text{D}_2\text{O}$ )  $\delta$  1.20 (s, 6H), 2.28 (s, 2H);  $^{13}\text{C}$  NMR (101-MHz,  $\text{D}_2\text{O}$ )  $\delta$  25.0 (2xCH<sub>3</sub>), 45.2 (CH<sub>2</sub>), 52.1 (C), 178.1 (C); IR (KBr disc)  $\nu_{\text{max}}$  3800-2400 (broad), 3418, 2979, 2914, 2614, 2168, 1655, 1612, 1575, 1550, 1516, 1470, 1402, 1323, 1254, 728; MS (ESI+)  $m/z$  (%): 118 (80,  $[\text{M}+\text{H}]^+$ ), 140 (75,  $[\text{M}+\text{Na}]^+$ ); MS (ESI-)  $m/z$  (%): 116 (100,  $[\text{M}-\text{H}]^-$ ); HRMS (ESI+)  $m/z$  calculated for  $\text{C}_5\text{H}_{11}\text{NO}_2$   $[\text{M}+\text{H}]^+$ : 118.0868, found: 118.0868; HRMS (ESI-)  $m/z$  calculated for  $\text{C}_5\text{H}_{11}\text{NO}_2$   $[\text{M}-\text{H}]^-$ : 116.0712, found: 116.0712; mp=225 °C.



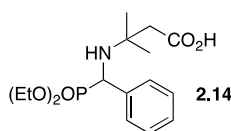
**Methyl 3-amino-3-methylbutanoate hydrochloride:** To a magnetically stirred solution of 3-amino-3-methylbutanoic acid (1.17 g, 10 mmol, 1.0 eq) in dry MeOH

(10 mL), trimethylsilyl chloride (2.56 mL, 20 mmol, 2.0 eq) was added at 0 °C. After stirring for 3 h the solvent was removed under reduced pressure to give the product as pale yellow viscous oil in quantitative yield. Characterization data were identical to those previously reported in the literature:  $^1\text{H}$  NMR (400 MHz,  $\text{D}_2\text{O}$ )  $\delta$  1.29 (s, 6H), 2.64 (s, 2H), 3.61 (s, 3H).<sup>66</sup>



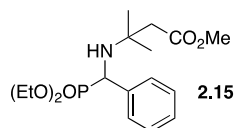
### Methyl 3-((1-(diethoxyphosphoryl)-2,2-dimethylpropyl)amino)-3-methylbutanoate

**Methyl 3-((1-(diethoxyphosphoryl)-2,2-dimethylpropyl)amino)-3-methylbutanoate:** A sample of methyl 3-amino-3-methylbutanoate hydrochloride (167 mg, 1 mmol, 1.0 eq) was mixed with MeOH (5mL). Triethylamine (349  $\mu\text{L}$ , 2.5 mmol, 2.5 eq) was added and the resulting reaction mixture was sonicated until all solids dissolved. Pivalaldehyde (126  $\mu\text{L}$ , 1.2 mmol, 1.2 eq) was added dropwise and the reaction mixture was stirred at 40 °C until imine formation was complete. After cooling down to RT, diethyl phosphite (193  $\mu\text{L}$ , 1.5 mmol, 1.5 eq) was added dropwise and the reaction mixture was stirred at 40 °C for 20 h. Cooled down to RT, diluted with  $\text{CH}_2\text{Cl}_2$  and washed sequentially with water and brine. Organic layer was separated, dried with  $\text{Na}_2\text{SO}_4$ , filtered and concentrated *in vacuo*. The residue was purified by flash column chromatography (20% to 50% EtOAc/hexane) to give trace amount of product as colourless oil (10 mg, 3%):  $^1\text{H}$  NMR (400 MHz,  $\text{CDCl}_3$ )  $\delta$  1.03 (s, 9H), 1.18 (s, 3H), 1.19 (s, 3H), 1.34 (t,  $J = 7.2$  Hz, 6H), 2.03 (br s, 1H), 2.40-5.56 (m, 2H), 2.78 (d,  $J = 17.2$  Hz, 1H), 3.65 (s, 3H), 4.06-4.13 (m, 4H);  $^{31}\text{P}$  NMR (40.5 MHz,  $\text{CDCl}_3$ )  $\delta$  2 IR (CDCl<sub>3</sub> film)  $\nu_{\text{max}}$  3382, 2979, 2954, 2909, 2872, 1735, 1236, 1053, 1026, 957  $\text{cm}^{-1}$ ; MS (ESI+)  $m/z$  (%): 360 (100,  $[\text{M}+\text{Na}]^+$ ); HRMS (ESI+)  $m/z$  calculated for  $\text{C}_{15}\text{H}_{32}\text{NO}_5\text{P}$   $[\text{M}+\text{H}]^+$ : 338.2096, found: 338.2098,  $[\text{M}+\text{Na}]^+$ : 360.1916, found: 360.1916.



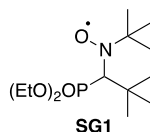
**3-(((diethoxyphosphoryl)(phenyl)methyl)amino)-3-methylbutanoic acid:** A reaction vessel was charged with 3-amino-3-methylbutanoic acid (234 mg, 2 mmol, 1 eq), benzaldehyde (204  $\mu\text{L}$ , 2 mmol, 1.0 eq), and diethyl phosphite (256  $\mu\text{L}$ , 2 mmol, 1.0 eq)

under nitrogen at RT. Dry MeOH (2 mL) was added and the resulting homogeneous mixture was stirred at 50 °C for 24 h. All volatiles were removed under reduced pressure and the residue was purified by flash column chromatography (5% isopropanol, 45% CH<sub>2</sub>Cl<sub>2</sub>, 50% hexane) to give the product as transparent solid (480 mg, 70%): <sup>1</sup>H NMR (400 MHz, CDCl<sub>3</sub>) δ 0.95 (s, 3H), 1.06 (t, *J* = 7.0 Hz, 3H), 1.20 (s, 3H), 1.33 (t, *J* = 7.2 Hz, 3H), 2.40 (s, 2H), 3.58-3.64 (m, 1H), 3.85-3.91 (m, 1H), 4.05-4.20 (m, 3H), 7.33-7.45 (m, 5H); <sup>13</sup>C NMR (101 MHz, CDCl<sub>3</sub>) δ 11.1 (dd, *J* = 20.8, 5.8 Hz, CH<sub>3</sub>), 12.2 (CH<sub>3</sub>), 28.4 (CH<sub>2</sub>), 46.8 (CH<sub>2</sub>), 54.2 (CH<sub>3</sub>), 54.4 (d, *J* = 15.6 Hz, C), 55.7 (CH<sub>3</sub>), 62.8 (d, *J* = 7.6 Hz, CH<sub>2</sub>), 63.6 (d, *J* = 7.2 Hz, CH<sub>2</sub>), 128.4 (2xCH), 128.5 (CH), 128.7 (2xCH), 136.5 (C), 172.8 (C); <sup>31</sup>P NMR (40.5 MHz, CDCl<sub>3</sub>) δ 1.72; IR (CDCl<sub>3</sub> film) ν<sub>max</sub> 3400-2800 (broad), 3245, 2979, 1721, 1454, 1385, 1236, 1053, 1026, 969, 701 cm<sup>-1</sup>; MS (ESI+) *m/z* (%): 366 (100, [M+Na]<sup>+</sup>), 344 (25, [M+H]<sup>+</sup>); HRMS (ESI) *m/z* calculated for C<sub>16</sub>H<sub>26</sub>NO<sub>5</sub>P [M+Na]<sup>+</sup>: 366.1446, found: 366.1446; mp=105 °C. X-ray analysis (Appendix Three, A3.2).

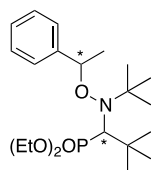


### Methyl 3-(((diethoxyphosphoryl)(phenyl)methyl)amino)-3-methylbutanoate:

To a magnetically stirred solution of 3-(((diethoxyphosphoryl)(phenyl)methyl)amino)-3-methylbutanoic acid (34.3 mg, 0.1 mmol, 1.0 eq) in dry MeOH (1 mL), trimethylsilyl chloride (26 µL, 0.2 mmol, 2.0 eq) was added at 0 °C and the resulting reaction mixture was stirred for 4 h. Concentrated *in vacuo* to give the product as colourless viscous oil (33 mg, 92%): <sup>1</sup>H NMR (400 MHz, CDCl<sub>3</sub>) δ 1.00 (s, 3H), 1.09 (t, *J* = 7.0 Hz, 3H), 1.13 (s, 3H), 1.27 (t, *J* = 7.2 Hz, 3H), 2.24-2.34 (br m, 3H), 3.59 (s, 3H), 3.69-3.73 (m, 1H), 3.87-3.93 (m, 1H), 4.06-4.17 (m, 3H), 7.21-7.31 (m, 3H), 7.42-7.43 (m, 2H); <sup>13</sup>C NMR (101 MHz, CDCl<sub>3</sub>) δ 16.3 (dd, *J* = 28.5, 5.9 Hz, CH), 27.6 (2xCH<sub>3</sub>), 46.3 (CH<sub>2</sub>), 51.2 (CH<sub>3</sub>), 53.6 (C), 54.7 (CH<sub>3</sub>), 56.2 (CH<sub>3</sub>), 62.6 (d, *J* = 6.8 Hz, CH<sub>2</sub>), 63.3 (d, *J* = 7.1 Hz, CH<sub>2</sub>), 127.5 (CH), 128.2 (2xCH), 128.3 (2xCH), 139.2 (C), 172.0 (C); IR (CDCl<sub>3</sub> film) ν<sub>max</sub> 3058, 3022, 2978, 2933, 1734, 1453, 1439, 1241, 1056, 1027 cm<sup>-1</sup>; MS (ESI+) *m/z* (%): 380 (100, [M+Na]<sup>+</sup>), 358 (20, [M+H]<sup>+</sup>); HRMS (ESI+) *m/z* calculated for C<sub>17</sub>H<sub>28</sub>NO<sub>5</sub>P [M+Na]<sup>+</sup>: 380.1603, found: 380.1604.



**SG1:** A 2-neck reaction vessel was charged with isobutyraldehyde (1.08 mL, 10 mmol, 1.0 eq) and *tert*-butylamine (1.05 mL, 10 mmol, 1.0 eq) under nitrogen. Molecular sieves were added and the reaction mixture was stirred at 35 °C until imine formation was complete (approx. 2 h). After cooling down to RT, diethyl phosphite (2.57 mL, 20 mmol, 2.0 eq) was added dropwise and the resulting reaction mixture was stirred at 35 °C for 20 h. After cooling down to RT, diluted with ether and acidified to pH=3 with 1 M *aq.* HCl solution. Organic layer was separated. Aqueous layer was basified to pH=8 with sat. *aq.* NaHCO<sub>3</sub> solution and extracted with ether. Organic extracts were washed with brine, dried with anhydrous Na<sub>2</sub>SO<sub>4</sub>, filtered and concentrated *in vacuo*. The crude product (1.33 g, 1.0 eq) was dissolved CH<sub>2</sub>Cl<sub>2</sub> (5 mL). A solution of *m*CPBA (1.29 g, 5.24 mmol, 1.1 eq) in CH<sub>2</sub>Cl<sub>2</sub> (10 mL) was added dropwise at 0 °C and the resulting reaction mixture was stirred for 12 h gradually warming up to RT. Quenched with sat. *aq.* NaHCO<sub>3</sub> solution. Organic layer was washed with brine, dried with Na<sub>2</sub>SO<sub>4</sub>, filtered and concentrated *in vacuo*. The residue was purified by flash column chromatography (80% pentane, 10% THF, 10% CH<sub>2</sub>Cl<sub>2</sub>) to give orange oil (546 mg, 39%): MS (ESI+) *m/z* (%): 295 (100, [M+H]<sup>+</sup>); HRMS (ESI+) *m/z* calculated for C<sub>13</sub>H<sub>29</sub>NO<sub>4</sub>P<sup>•</sup> [M]: 294.1833, found: 294.1834; Elemental analysis: C<sub>13</sub>H<sub>29</sub>NO<sub>4</sub>P<sup>•</sup> calculated: C, 53.05; H, 9.93; N, 4.76; found: C, 52.96; H, 10.10; N, 4.85.



**2.19** approx 2:1 mixture

### Diethyl

### (1-(*tert*-butyl(1-phenylethoxy)amino)-2,2-

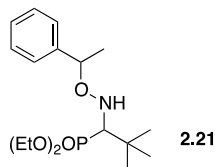
**dimethylpropyl)phosphonate:** A suspension of copper bronze (240 mg, 3.74 mmol, 1.1 eq), copper (II) bromide (270 mg, 1.87 mmol, 0.55 eq) in dry benzene (10 mL) was subjected to three freeze-pump-thaw cycles. N,N,N',N',N''-pentamethyldiethylenetriamine (400 μL, 1.87 mmol, 0.55eq) was added dropwise and the resulting reaction mixture was stirred for 30 min under nitrogen. A solution of **SG1** radical (1.00 g, 3.40 mmol, 1.0 eq) and 1-bromoethylbenzene (500 μL, 3.74 mmol, 1.1 eq) in dry benzene (10 mL) was added



over 10 min *via* syringe pump. Stirred at room temperature for two days. The reaction mixture was filtered through Celite and diluted with ether. Organic layer was washed sequentially with water and brine, dried with Na<sub>2</sub>SO<sub>4</sub>, filtered and concentrated *in vacuo*. The residue was purified by flash column chromatography (10% to 20% EtOAc/hexane) to give two diastereoisomers as colorless oil (1.06 g, 77% yield in approximately 2:1 ratio **A:B**): IR (CDCl<sub>3</sub> film)  $\nu_{\max}$  3034, 2977, 1469, 1481, 1456, 1393, 1364, 1244 cm<sup>-1</sup>; MS (ESI+) *m/z* (%): 422 (100, [M+Na]<sup>+</sup>), 400 (70, [M+H]<sup>+</sup>); HRMS (ESI+) *m/z* calculated for C<sub>21</sub>H<sub>38</sub>NO<sub>4</sub>P [M+Na]<sup>+</sup>: 422.2436, found: 422.2436.

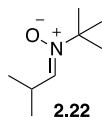
**A**: <sup>1</sup>H NMR (400 MHz, CDCl<sub>3</sub>)  $\delta$  0.81 (t, *J* = 7.0 Hz, 3H), 1.14 (s, 18H), 1.16 (t, *J* = 7.0 Hz, 3H), 1.48 (d, *J* = 7.0 Hz, 3H), 3.12-3.36 (m, 2H), 3.33 (d, *J* = 24 Hz, 1H), 3.73-3.95 (m, 2H), 5.17 (q, *J* = 6.6 Hz, 1H), 7.11-7.22 (m, 3H), 7.37-7.39 (m, 2H); <sup>13</sup>C NMR (101 MHz, CDCl<sub>3</sub>)  $\delta$  [ ] [CH] [ ], 21.2 (CH), 28.2 (3xCH<sub>3</sub>), 30.6 (3xCH<sub>3</sub>), 35.3 (C), 58.6 (CH<sub>2</sub>), 61.2 (C), 61.5 (CH<sub>2</sub>), 70.1 (d, *J* = 139 Hz, CH), 78.3 (CH), 127.3 (CH), 127.8 (2xCH), 127.9 (2xCH), 143.3 (C); <sup>31</sup>P NMR (40.5 MHz, CDCl<sub>3</sub>)  $\delta$  [ ] [ ] [ ] [ ]

**B**: <sup>1</sup>H NMR (400 MHz, CDCl<sub>3</sub>)  $\delta$  0.86 (s, 9H), 1.16 (s, 9H), 1.31-1.37 (m, 6H), 1.62 (d, *J* = 6.9 Hz, 3H), 3.36 (d, *J* = 26 Hz, 1H), 3.94-4.24 (m, 2H), 4.33-4.43 (m, 2H), 5.01 (q, *J* = 6.7 Hz, 1H), 7.20-7.31 (m, 5H); <sup>13</sup>C NMR (101 MHz, CDCl<sub>3</sub>)  $\delta$  1 [ ] [ ] [CH<sub>3</sub>], 28.5 (3xCH<sub>3</sub>), 30.1 (3xCH<sub>3</sub>), 35.6 (C), 58.8 (CH<sub>2</sub>), 61.1 (C), 61.6 (CH<sub>2</sub>), 69.8 (d, *J* = 139 Hz, CH), 85.3 (CH), 127.0 (CH), 127.1 (2xCH), 128.0 (2xCH), 145.5 (C); <sup>31</sup>P NMR (40.5 MHz, CDCl<sub>3</sub>)  $\delta$  [ ] [ ] [ ] [ ]

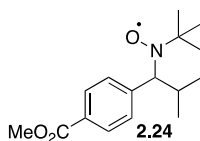


**Diethyl (2,2-dimethyl-1-((1-phenylethoxy)amino)propyl)phosphonate:** To a magnetically stirred solution of diethyl (1-(*tert*-butyl(1-phenylethoxy)amino)-2,2-dimethylpropyl)phosphonate (50 mg, 0.125 mmol, 1.0 eq) in anhydrous dioxane (1 mL), 4.0 M HCl in dioxane (310  $\mu$ L) was added dropwise at 0 °C. Stirred for 1 h at that temperature. Concentrated *in vacuo* and purified by flash column chromatography (20% EtOAc/hexane) to give the title product as colourless oil (24 mg, 56%): <sup>1</sup>H NMR

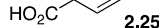
(400 MHz,  $\text{CDCl}_3$ )  $\delta$  1.02 (s, 9H), 1.19-1.26 (m, 6H), 1.32 (d,  $J = 6.6$  Hz, 3H), 2.94 (d,  $J = 18$  Hz, 1H), 3.98-4.07 (m, 4H), 4.70 (q,  $J = 6.6$  Hz, 1H), 5.21 (br s, 1H), 7.17-7.29 (m, 5H);  $^{31}\text{P}$  NMR (40.5 MHz,  $\text{CDCl}_3$ )  $\delta$  64.9; MS (ESI+)  $m/z$  (%): 366 (100,  $[\text{M}+\text{Na}]^+$ ), 343 (25,  $[\text{M}+\text{H}]^+$ ); HRMS (ESI+)  $m/z$  calculated for  $\text{C}_{17}\text{H}_{30}\text{NO}_4\text{P}$   $[\text{M}+\text{H}]$ : 344.1991, found: 344.1991



**(E)-2-methyl-N-(2-methylpropylidene)propan-2-amine oxide:** A 2-neck reaction vessel was charged with isobutyraldehyde (454  $\mu\text{L}$ , 5 mmol, 1.0 eq), 2-methyl-2-nitropropane (567 mg, 5.5 mmol, 1.1 eq), ammonium chloride (294 mg, 7.5 mmol, 1.5 eq), ether (2 ml) and water (2 mL). Cooled down to 0  $^\circ\text{C}$ . Activated zinc powder (1 g) was added in portions over 1 h. Stirred for 18 h, gradually warming up to RT. Filtered through Celite. The residue was washed with MeOH three times. Solvents were removed *in vacuo* and the residue was taken up into  $\text{CH}_2\text{Cl}_2$ . Organic layer was washed sequentially with water and brine, dried with  $\text{Na}_2\text{SO}_4$ , filtered and concentrated *in vacuo*. The crude product was purified by flash column chromatography (50% to 100% EtOAc/hexane) to give the title compound (339 mg, 47%) as colorless oil. Characterization data were identical to those previously reported for this compound.<sup>48</sup>



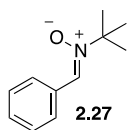
**4-COOMe TIPNO:** To a magnetically stirred solution of methyl 4-iodobenzoate (275 mg, 1.047 mmol, 1.5 eq) in dry THF (0.5 mL) a solution of isopropylmagnesium bromide in 2-methyltetrahydrofuran (361  $\mu\text{L}$ , 1.047 mmol, 1.5 eq) was added dropwise at -40  $^\circ\text{C}$  under nitrogen. Stirred for 1 h at -40  $^\circ\text{C}$ . A solution of (E)-2-methyl-N-(2-methylpropylidene)propan-2-amine oxide (100 mg, 0.698 mmol, 1.0 eq) in dry THF (1 mL) was added over 10 min *via* syringe pump while maintaining the internal temperature between -40  $^\circ\text{C}$  and -38  $^\circ\text{C}$ . Stirred for 4 h gradually warming up to -20  $^\circ\text{C}$ . The excess Grignard reagent was decomposed by addition of sat. *aq.*  $\text{NH}_4\text{Cl}$  solution followed by water until all solids dissolved. Organic layer was separated and aqueous layer



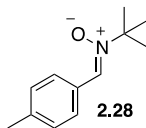
in MeOH. White solid was obtained:  $^1\text{H}$  NMR (400 MHz,  $(\text{CD}_3)_2\text{SO}$ )  $\delta$  0.47 (d,  $J$  = 6.7 Hz, 3H), 0.82 (s, 9H), 1.10 (d,  $J$  = 6.3 Hz, 3H), 1.10 (d,  $J$  = 6.3 Hz, 3H), 2.11-2.20 (m, 1H), 3.70-3.73 (m, 1H), 4.70 (s, 1H), 7.36 (s, 1H), 7.54 (d,  $J$  = 7.9 Hz, 2H), 7.80 (d,  $J$  = 7.9 Hz, 2H). MS (ESI+)  $m/z$  (%): 266 (100,  $[\text{M}+\text{H}]^+$ ); HRMS (ESI+)  $m/z$  calculated for  $\text{C}_{15}\text{H}_{24}\text{NO}_3$   $[\text{M}+\text{H}]^+$ : 266.1756, found: 266.1756.

### General procedure 2: Aryl Nitron Synthesis

A solution of 2-methyl-2-nitropropane (2 eq) in 95% ethanol was cooled down to 0 °C. Aldehyde (1 eq), followed by activated zinc powder (3 eq) was added to the reaction vessel while maintaining the internal temperature below 5 °C. Acetic acid (6 eq) was then added dropwise over a period of 10 min at 5 °C. The resulting reaction mixture was stirred at that temperature for 3 h, then at RT for 16 h. After filtering through a pad of Celite, the solvent was removed *in vacuo*.

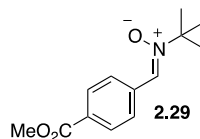


**(Z)-N-benzylidene-2-methylpropan-2-amine oxide:** The compound was prepared according to the **General Procedure 2**. The residue was dissolved in EtOAc and water was added. Organic layer was separated, washed with brine several times, dried with  $\text{MgSO}_4$ , filtered and concentrated *in vacuo* to give the product as off white needles (107 mg, 60%). Characterization data were identical to those previously reported for this compound (CAS 3376-24-7).

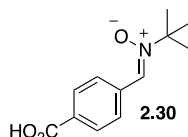


**(Z)-2-methyl-N-(4-methylbenzylidene)propan-2-amine oxide:** The compound was prepared according to the **General Procedure 2**. The residue was dissolved in EtOAc and water was added. Organic layer was separated, washed with brine several times, dried with  $\text{MgSO}_4$ , filtered and concentrated *in vacuo*. The crude product was purified by flash column chromatography (40% EtOAc/hexane) to give the title compound as off white solid (825 mg, 86%):  $^1\text{H}$  NMR (400 MHz,  $\text{CDCl}_3$ )  $\delta$  1.57 (s, 9H), 2.34 (s, 3H), 7.18 (d,  $J$  = 8 Hz, 2H), 7.47 (s, 1H), 8.16 (d,  $J$  = 8 Hz, 2H);  $^{13}\text{C}$  NMR (101 MHz,  $\text{CDCl}_3$ )

$\delta$  28.1 (3xCH<sub>3</sub>), 70.3 (C), 128.2 (C), 128.7 (2xCH), 128.9 (2xCH), 129.7 (C), 140.3 (CH); IR (CDCl<sub>3</sub> film)  $\nu_{\max}$  2975, 2923, 1411, 1361, 1195, 1179, 1120, 830 cm<sup>-1</sup>; MS (ESI+) m/z (%): 214 (100, [M+Na]<sup>+</sup>), 192 (45, [M+H]<sup>+</sup>); HRMS (ESI+) m/z calculated for C<sub>12</sub>H<sub>17</sub>NO [M+H]<sup>+</sup>: 192.1388, found: 192.1388; mp=72 °C.

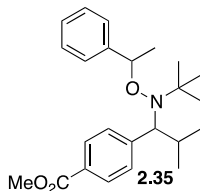


**(Z)-N-(4-(methoxycarbonyl)benzylidene)-2-methylpropan-2-amine oxide:** The compound was prepared according to the **General Procedure 2**. The residue was dissolved in EtOAc and water was added. Organic layer was separated, washed with brine several times, dried with MgSO<sub>4</sub>, filtered and concentrated *in vacuo*. The crude product was purified by flash column chromatography (20% to 50% EtOAc/hexane) to give the title compound as off white solid (273 mg, 76%): <sup>1</sup>H NMR (400 MHz, CDCl<sub>3</sub>)  $\delta$  1.61 (s, 9H), 3.90 (s, 3H), 7.61 (s, 1H), 8.05 (d, *J* = 8.4 Hz, 2H), 8.32 (d, *J* = 8.4 Hz, 2H); <sup>13</sup>C NMR (101 MHz, CDCl<sub>3</sub>)  $\delta$  28.3 (3xCH<sub>3</sub>), 71.6 (C), 128.3 (2xCH), 128.9 (CH), 129.6 (2xCH), 130.7 (C), 134.9 (C), 166.4 (C); IR (CDCl<sub>3</sub> film)  $\nu_{\max}$  3095, 2977, 2950, 2843, 1711, 1280, 1129, 1110, 865 cm<sup>-1</sup>; MS (ESI+) m/z (%): 236 (100, [M+H]<sup>+</sup>), 258 (45, [M+Na]<sup>+</sup>); HRMS (ESI+) m/z calculated for C<sub>13</sub>H<sub>17</sub>NO<sub>3</sub> [M+H]<sup>+</sup>: 236.1287, found: 236.1287; mp=110 °C.

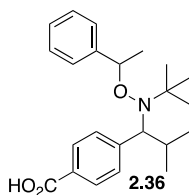


**(Z)-N-(4-carboxybenzylidene)-2-methylpropan-2-amine oxide:** The compound was prepared according to the **General Procedure 2**. The residue was partitioned between EtOAc and water. Organic layer was separated. Aqueous layer was acidified with 2 M aq. HCl (pH=3). Precipitate was collected by filtration and dried *in vacuo* overnight to give the product as white needles (1.05 g, 72%): <sup>1</sup>H NMR (400 MHz, (CD<sub>3</sub>)<sub>2</sub>SO)  $\delta$  1.52 (s, 9H), 7.94-7.98 (m, 3H), 8.44 (d, *J* = 12 Hz, 2H), 13.03 (br s, 1H); <sup>13</sup>C NMR (101 MHz, (CD<sub>3</sub>)<sub>2</sub>SO)  $\delta$  27.9 (3xCH<sub>3</sub>), 128.1 (2xCH), 128.3 (CH), 129.2 (2xCH), 130.9 (C), 135.3 (C), 166.8 (C); IR (KBr disc)  $\nu_{\max}$  3600-2200 (broad), 3420, 2980, 1696, 1413,

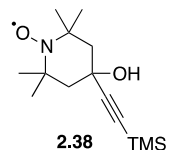
1258, 1083  $\text{cm}^{-1}$ ; MS (ESI+)  $m/z$  (%): 222 (100,  $[\text{M}+\text{H}]^+$ ), 244 (40,  $[\text{M}+\text{Na}]^+$ ); HRMS (ESI+)  $m/z$  calculated for  $\text{C}_{12}\text{H}_{15}\text{NO}_3$   $[\text{M}+\text{H}]^+$ : 222.1130, found: 222.1130; mp=208  $^{\circ}\text{C}$ .



**Methyl 4-(1-(*tert*-butyl(1-phenylethoxy)amino)-2-methylpropyl)benzoate:** A suspension of copper bronze (24 mg, 0.374 mmol, 1.1 eq), copper (II) bromide (27 mg, 0.187 mmol, 0.55 eq) in dry benzene (1 mL) was subjected to three freeze-pump-thaw cycles. N,N,N',N',N''-pentamethyldiethylenetriamine (40  $\mu\text{L}$ , 0.187 mmol, 0.55eq) was added dropwise and the resulting reaction mixture was stirred for 30 min under nitrogen. A solution of **4-COOMe TIPNO** (95 mg, 0.340 mmol, 1.0 eq) and 1-bromoethylbenzene (50  $\mu\text{L}$ , 0.374 mmol, 1.1 eq) in dry benzene (1 mL) was added over 10 min *via* syringe pump. Stirred at 50  $^{\circ}\text{C}$  for 12 h. The reaction mixture was filtered through Celite and the residue was washed with ether. The resulting filtrate was washed sequentially with water and brine. Organic layer was separated, dried with sodium sulfate, filtered and concentrated *in vacuo*. The residue was purified by flash column chromatography (1% to 5% EtOAc/hexane) to give a mixture of diastereoisomers (white solid, 101 mg, 78% yield in approximately 1:1 ratio):  $^1\text{H}$  NMR (400 MHz,  $\text{CDCl}_3$ )  $\delta$  0.17 (d,  $J = 6.6$  Hz, 3H), 0.50 (d,  $J = 6.6$  Hz, 3H), 0.75 (s, 9H), 0.91 (d,  $J = 6.2$  Hz, 3H), 1.01 (s, 9H), 1.29 (d,  $J = 6.4$  Hz, 3H), 1.31-1.38 (m, 1H), 1.52 (d,  $J = 6.6$  Hz, 3H), 1.61 (d,  $J = 6.6$  Hz, 3H), 2.27-2.36 (m, 1H), 3.34 (d,  $J = 10.7$  Hz, 1H), 3.46 (d,  $J = 10.5$  Hz, 1H), 3.85 (s, 3H), 3.89 (s, 3H), 4.85-4.91 (m, 2H), 7.17-7.58 (m, 10H), 7.82 (d,  $J = 8.7$  Hz, 4H), 7.93 (d,  $J = 8.8$  Hz, 4H), IR (KBr disc)  $\nu_{\text{max}}$  3030, 2973, 1724, 1244  $\text{cm}^{-1}$ ; MS (ESI+)  $m/z$  (%): 406 (100,  $[\text{M}+\text{Na}]^+$ ); HRMS (ESI+)  $m/z$  calculated for  $\text{C}_{24}\text{H}_{33}\text{NO}_3$   $[\text{M}+\text{H}]^+$ : 384.2539, found: 384.2539.

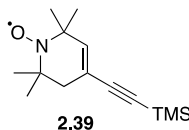


**4-(1-(*tert*-butyl(1-phenylethoxy)amino)-2-methylpropyl)benzoic acid:** To a magnetically stirred solution of 4-COOMe TIPNO alkoxyamine (73 mg, 0.190 mmol, 1.0 eq) in THF (3 mL) and water (1 mL), LiOH•H<sub>2</sub>O (80 mg, 1.90 mmol, 10 eq) was added in one portion and the resulting reaction mixture was stirred at 60 °C for 2 days. After cooling down to 0 °C acidified with 1 M *aq.* HCl solution (pH=2.0). Diluted with EtOAc (6 mL). Organic layer was separated and aqueous layer was extracted with ethyl acetate. Organic extracts were washed with brine, dried with Na<sub>2</sub>SO<sub>4</sub>, filtered and concentrated *in vacuo*. The residue was purified by flash column chromatography (20% to 100% EtOAc/hexane) to give an inseparable mixture of diastereoisomers as white solid (65 mg, 93%): <sup>1</sup>H NMR (400 MHz, CDCl<sub>3</sub>) δ 0.21 (d, *J* = 6.6 Hz, 3H), 0.55 (d, *J* = 6.5 Hz, 3H), 0.79 (s, 9H), 0.94 (d, *J* = 6.1 Hz, 3H), 1.06 (s, 9H), 1.32 (d, *J* = 6.3 Hz, 3H), 1.36-1.42 (m, 1H), 1.56 (d, *J* = 6.6 Hz, 3H), 1.65 (d, *J* = 6.6 Hz, 3H), 2.35-2.40 (m, 1H), 3.39 (d, *J* = 10.4 Hz, 1H), 3.53 (d, *J* = 10.7 Hz, 1H), 4.90-4.97 (m, 2H), 7.21-7.61 (m, 10H), 7.92 (d, *J* = 8.1 Hz, 4H), 8.03 (d, *J* = 8.0 Hz, 4H); IR (KBr disc)  $\nu_{\max}$  3200-2600 (broad), 2974, 2869, 1688, 1286 cm<sup>-1</sup>; MS (ESI) *m/z* (%): 370 (100, [M+H]<sup>+</sup>), 392 (30, [M+Na]<sup>+</sup>); HRMS (ESI) *m/z* calculated for C<sub>23</sub>H<sub>31</sub>NO<sub>3</sub> [M+H]<sup>+</sup>: 370.2382, found: 370.2384.

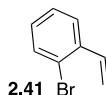


**1-oxyl-2,2,6,6-tetramethyl-4-((trimethylsilyl)ethynyl)piperidine-4-ol:** To a magnetically stirred solution of trimethylsilylacetylene (331 mg, 3.370 mmol, 1.2 eq) in dry THF (2.5 mL), *n*-butyllithium solution (0.75M in hexane), (4.5 mL, 3.370 mmol, 1.2 eq) was slowly added at 0 °C. Stirred for 30 min at 0 °C. Then a solution of 4-OXO TEMPO (478 mg, 2.808 mmol, 1.0 eq) in dry THF (2.5 mL) was added dropwise at 0 °C. Stirred for 16 h gradually warming up to RT. Quenched with cold sat. *aq.* NH<sub>4</sub>Cl solution and diluted with EtOAc. Organic layer was sequentially washed with water and brine, dried with Na<sub>2</sub>SO<sub>4</sub> and concentrated *in vacuo*. The residue was purified by flash column chromatography (10% EtOAc/hexane) to give the product as bright yellow powder (347 mg, 46%): IR (KBr disc)  $\nu_{\max}$  3600-3200 (broad), 2970, 2169, 1342, 1250, 1202, 863, 842 cm<sup>-1</sup>; MS (ESI+) *m/z* (%): 291 (100, [M+Na]<sup>+</sup>); HRMS (ESI+) *m/z* calculated for C<sub>14</sub>H<sub>26</sub>NO<sub>2</sub>Si<sup>+</sup> [M+H]<sup>+</sup>: 269.1811 found: 269.1813; [M+K]<sup>+</sup>: 307.1370 found: 307.1371;

Elemental analysis:  $C_{14}H_{26}NO_2Si$  calculated: C, 62.64; H, 9.76; N, 5.22; found: C, 62.84; H, 9.86; N, 5.20, mp=79 °C.



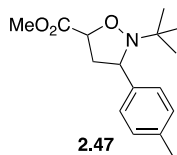
**1-oxyl-2,2,6,6-tetramethyl-4-((trimethylsilyl)ethynyl)-5,6-dihydropyridine:** To a magnetically stirred solution of acetylene **2.38** (347 mg, 1.294 mmol, 1.0 eq) in dry  $CH_2Cl_2$  (3 mL), mesyl chloride (200  $\mu$ L, 2.588 mmol, 2.0 eq) followed by triethylamine (717  $\mu$ L, 5.176 mmol, 4.0 eq) were added slowly at 0 °C. Stirred for 3 h gradually warming up to RT. Quenched with cold sat. *aq.*  $NH_4Cl$  solution and diluted with  $CH_2Cl_2$ . Organic layer was sequentially washed with water and brine, dried with  $Na_2SO_4$  and concentrated *in vacuo*. The residue was purified by flash column chromatography (5% EtOAc/hexane) to give the product as bright orange powder (288 mg, 89%): IR (KBr disc)  $\nu_{max}$ , 2969, 2150, 1247, 844  $cm^{-1}$ ; MS (ESI+)  $m/z$  (%): 273 (80,  $[M+Na]^+$ ); HRMS (ESI+)  $m/z$  calculated for  $C_{14}H_{24}NOSi$   $[M+H]^+$ : 251.1705 found: 251.1706;  $[M+Na]^+$ : 273.1525 found: 273.1526; Elemental analysis:  $C_{14}H_{26}NO_2Si$  calculated: C, 67.14; H, 9.66; N, 5.59; found: C, 67.38; H, 9.51; N, 5.72, mp=104 °C. X-ray analysis (Appendix Three, A3.3).



**2-bromostyrene:** To a magnetically stirred mixture of methyltriphenylphosphonium bromide (4.11 g, 11.5 mmol, 1.15 eq) and dry THF (40 mL) *n*-butyl lithium (1.6M in hexane, 11.2 mL, 1.12 eq) was added dropwise at 0 °C. After stirring for 15 min yellow solution was formed. Then a solution of 2-bromobenzaldehyde (1.17 mL, 10 mmol, 1.0 eq) in dry THF (20 mL) was added dropwise at 0 °C. The resulting reaction mixture was stirred for 4 h, gradually warming up to RT. Quenched with cold sat. *aq.*  $NH_4Cl$  solution and diluted with EtOAc. Organic layer was sequentially washed with water and brine, dried with  $Na_2SO_4$  and concentrated *in vacuo*. The residue was purified by flash column chromatography (hexane) to give the product as colourless viscous oil



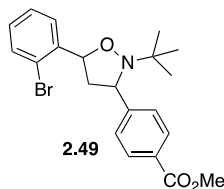
(1.45 g, 76%). The characterization data were identical to those previously reported for this compound.<sup>57</sup>



**Methyl 2-(tert-butyl)-3-(p-tolyl)isoxazolidine-5-carboxylate:** A reaction vessel was charged with (Z)-2-methyl-N-(4-methylbenzylidene)propan-2-amine oxide (50 mg, 0.261 mmol, 1.0 eq) and excess methyl acrylate (1mL). Purged with nitrogen and placed in the microwave reactor (200 psi, 300 W, 3 h, 110 °C). After cooling down to RT the reaction mixture was filtered through silica gel (20% EtOAc/hexane) and purified by reverse phase prep. HPLC (50% ACN, 49.9% H<sub>2</sub>O, 0.1 FA) to give two diastereomers in 3:1 ratio as colourless oils: MS (ESI+) m/z (%): 300 (100, [M+Na]<sup>+</sup>); HRMS (ESI+) m/z calculated for C<sub>16</sub>H<sub>24</sub>NO<sub>3</sub> [M+H]<sup>+</sup>: 278.1756, found: 278.1756.

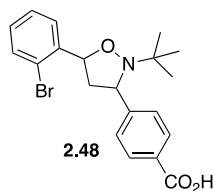
Major (33 mg, 46%): <sup>1</sup>H NMR (400 MHz, CDCl<sub>3</sub>) δ 1.07(s, 9H), 2.32(s, 3H), 2.51 (ddd, *J* = 12.4, 8.1 and 7.1 Hz, 1H), 2.69 (ddd, *J* = 12.4, 7.8 and 6.2 Hz, 1H), 3.76 (s, 3H), 4.23 (app t, *J* = 7.5 Hz, 1H), 4.59 (dd, *J* = 8.1, 6.2 Hz, 1H), 7.12 (d, *J* = 7.8 Hz, 2H), 7.32 (d, *J* = 7.8 Hz, 2H); <sup>13</sup>C NMR (101 MHz, CDCl<sub>3</sub>) δ 26.5 (CH<sub>3</sub>), 45.3 (CH<sub>2</sub>), 52.3 (CH), 59.3 (C), 62.1 (CH), 74.3 (CH<sub>3</sub>), 127.2 (2xCH), 129.3 (2xCH), 137.0 (C), 139.8 (C), 171.0 (C);

Minor (12 mg, 17%): <sup>1</sup>H NMR (400 MHz, CDCl<sub>3</sub>) δ 1.04(s, 9H), 2.31(s, 3H), 2.52 (ddd, *J* = 12.4, 8.0 and 6.7 Hz, 1H), 2.88 (dt, *J* = 12.4 and 7.8 Hz, 1H), 3.78 (s, 3H), 4.17 (app t, *J* = 8.0 Hz, 1H), 4.58 (dd, *J* = 7.7, 6.7 Hz, 1H), 7.09 (dd, *J* = 8.1 and 0.7 Hz, 2H), 7.29 (d, *J* = 8.1 Hz, 2H); <sup>13</sup>C NMR (101 MHz, CDCl<sub>3</sub>) δ 26.2 (CH<sub>3</sub>), 45.4 (CH<sub>2</sub>), 52.2 (CH), 59.4 (C), 62.7 (CH), 75.1 (CH<sub>3</sub>), 127.1 (2xCH), 129.1 (2xCH), 136.7 (C), 139.8 (C), 172.2 (C).

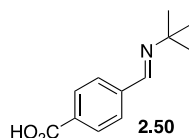


**Methyl 4-(5-(2-bromophenyl)-2-(tert-butyl)isoxazolidin-3-yl)benzoate:** To a magnetically stirred solution of (Z)-N-(4-(methoxycarbonyl)benzylidene)-2-methylpropan-

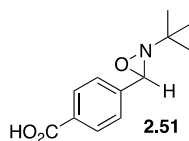
2-amine oxide (200 mg, 0.850 mmol, 1.0 eq) in toluene (5 mL), 1-bromo-2-vinylbenzene (234 mg, 1.28 mmol, 1.5 eq) was added under nitrogen at RT. Stirred at reflux for 5 days. After cooling down to RT, the reaction mixture was concentrated *in vacuo* and the residue was purified by flash column chromatography (0% to 30% EtOAc/hexane) to give the title compound as a mixture of diastereomers (179 mg, 75% brsm). Major diastereoisomer (>98% of the mixture):  $^1\text{H}$  NMR (400 MHz,  $\text{CDCl}_3$ )  $\delta$  1.12(s, 9H), 2.10-2.18 (m, 1H), 3.23-3.30 (m, 1H), 3.89 (s, 3H), 4.42-4.46 (m, 1H), 5.37-5.40 (m, 1H), 7.10-7.14 (m, 1H), 7.33-7.37 (m, 1H), 7.47-7.49 (m, 3H), 7.82-7.85 (m, 1H), 7.92-7.94 (m, 2H);  $^{13}\text{C}$  NMR (101 MHz,  $\text{CDCl}_3$ )  $\delta$  26.2 (CH<sub>3</sub>), 29.7 (CH<sub>3</sub>), 52.0 (CH), 60.0 (C), 63.9 (CH), 78 (CH<sub>3</sub>), 121.7 (C), 127.1 (2xCH), 127.4 (CH), 127.6 (CH), 128.7 (CH), 128.9 (C), 129.8 (2xCH), 132.4 (CH), 141.1 (C), 149.1 (C), 166.9 (C); IR ( $\text{CDCl}_3$  film)  $\nu_{\text{max}}$  2972, 2945, 1723, 1610, 1435, 1277, 1113, 1020, 754  $\text{cm}^{-1}$ ; MS (ESI+)  $m/z$  (%): 419 (100,  $[\text{M}+\text{H}]^+$ ), 441 (90,  $[\text{M}+\text{Na}]^+$ ), 362 (80,  $[\text{M}+\text{H}-t\text{Bu}]^+$ ); HRMS (ESI+)  $m/z$  calculated for  $\text{C}_{21}\text{H}_{24}\text{BrNO}_3$   $[\text{M}+\text{Na}]^+$ : 440.0837 and 442.0817, found: 440.0826 and 442.0822.



**4-(5-(2-bromophenyl)-2-(tert-butyl)isoxazolidin-3-yl)benzoic acid:** To a magnetically stirred solution of methyl 4-(5-(2-bromophenyl)-2-(tert-butyl)isoxazolidin-3-yl)benzoate (9 mg, 0.022 mmol, 1.0 eq) in THF (300  $\mu\text{L}$ ) and water (100  $\mu\text{L}$ ), lithium hydroxide monohydrate (2 mg, 0.043 mmol, 3.0 eq) was added. The resulting reaction mixture was heated at 50  $^{\circ}\text{C}$  for 16 h. After cooling down to RT diluted with EtOAc and acidified with 1 M *aq.* HCl to pH=3. Organic layer was separated, washed with brine, dried with  $\text{Na}_2\text{SO}_4$ , filtered and concentrated *in vacuo* to give the crude product:  $^1\text{H}$  NMR (400 MHz,  $\text{CDCl}_3$ )  $\delta$  1.13(s, 9H), 2.12-2.19 (m, 1H), 3.24-3.31 (m, 1H), 4.44-4.48 (m, 1H), 5.38-5.42 (m, 1H), 7.10-7.14 (m, 1H), 7.33-7.37 (m, 1H), 7.47-7.53 (m, 3H), 7.83-7.86 (m, 1H), 7.99-8.01 (m, 2H); MS (ESI+)  $m/z$  (%): 402 and 404 (70,  $[\text{M}+\text{H}]^+$ ); HRMS (ESI+)  $m/z$  calculated for  $\text{C}_{20}\text{H}_{22}\text{BrNO}_3$   $[\text{M}+\text{H}]^+$ : 402.0705 and 404.0684, found: 402.0700 and 404.0682.



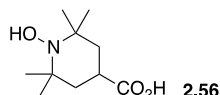
**(E)-4-((tert-butylimino)methyl)benzoic acid:** To a mixture of 4-carboxybenzaldehyde (1.5 g, 10 mmol, 1.0 eq) and methanol (10 mL), triethylamine (1.281 mL, 10 mmol, 1.0 eq) followed by *tert*-butylamine (2.545 mL, 15 mmol, 1.5 eq) was added. The resulting reaction mixture was stirred at reflux overnight and concentrated *in vacuo*, after cooling down to RT. The residue was washed several times with CH<sub>2</sub>Cl<sub>2</sub> and the crude product was dried *in vacuo*. The title compound was obtained in quantitative yield: <sup>1</sup>H NMR (400 MHz, CD<sub>3</sub>OD) δ 1.32 (s, 9H), 7.76 (d, *J* = 8.2 Hz, 2H), 7.99 (d, *J* = 8.2 Hz, 2H), 8.41 (s, 1H); <sup>13</sup>C NMR (101 MHz, (CD<sub>3</sub>)<sub>2</sub>SO) δ 28.4 (3xCH<sub>3</sub>), 127.2 (2xCH), 129.1 (2xCH), 138.0 (C), 139.8 (C), 157.0 (CH), 173.8 (C); MS (ESI+) *m/z* (%): 206 (100, [M+H]<sup>+</sup>), 228 (20, [M+Na]<sup>+</sup>); HRMS (ESI+) *m/z* calculated for C<sub>12</sub>H<sub>15</sub>NO<sub>2</sub> [M+H]<sup>+</sup>: 206.1181, found: 206.1185.



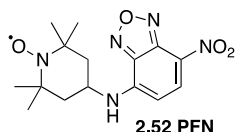
**4-(2-(tert-butyl)-1,2-oxaziridin-3-yl)benzoic acid:** To a magnetically stirred solution of (E)-4-((tert-butylimino)methyl)benzoic acid (205 mg, 1.0 mmol, 1.0 eq) in MeOH (1 mL) a solution of *m*CPBA (246 mg, 1.0 mmol, 1.0 eq) in CH<sub>2</sub>Cl<sub>2</sub> (5 mL) was added at 0 °C. The resulting reaction mixture was stirred at that temperature for 2 h. Concentrated *in vacuo* and purified by reverse phase HPLC (45% MeOH, 54.9% H<sub>2</sub>O and 0.1% formic acid; C-18 column; retention time 23 min) to give the title compound as white solid (137 mg, 62%): <sup>1</sup>H NMR (400 MHz, (CD<sub>3</sub>)<sub>2</sub>SO) δ 1.10 (s, 9H), 5.05 (s, 1H), 7.42 (d, *J* = 8.4 Hz, 2H), 7.96 (d, *J* = 8.4 Hz, 2H), 13.05 (br s, 1H); <sup>13</sup>C NMR (101 MHz, (CD<sub>3</sub>)<sub>2</sub>SO) δ 24.9 (3xCH<sub>3</sub>), 72.2 (CH), 127.8 (2xCH), 129.3 (2xCH), 138.0 (C), 140.5 (C), 170.0 (C); IR (KBr disc) ν<sub>max</sub> 3600-2600 (broad), 3429, 2977, 2667, 2550, 1687, 1615, 1581, 1429, 1292 cm<sup>-1</sup>; MS (ESI+) *m/z* (%): 244 (50, [M+Na]<sup>+</sup>), 222 (30, [M+H]<sup>+</sup>); HRMS (ESI+) *m/z* calculated for C<sub>12</sub>H<sub>15</sub>NO<sub>3</sub> [M+Na]<sup>+</sup>: 244.0950, found: 244.0950; HRMS (ESI-) *m/z* calculated for C<sub>12</sub>H<sub>15</sub>NO<sub>3</sub> [M-H]<sup>-</sup>: 220.0974, found: 220.0974; mp=144 °C.

### General procedure 3: Hydroxylamine Synthesis

To a magnetically stirred solution of nitroso radical (1.0 eq) in dry MeOH (1 mL) *L*-ascorbic acid (1.05 eq) was added in one portion. The resulting reaction mixture was stirred for 15-30 min at room temperature (or for shorter times if discolouration occurred immediately after addition of the reducing agent). The solvent was removed *in vacuo* and the residue was taken up in CH<sub>2</sub>Cl<sub>2</sub>. Organic layer was washed with water and brine, dried with Na<sub>2</sub>SO<sub>4</sub>, filtered and concentrated *in vacuo* to give the title hydroxylamine.

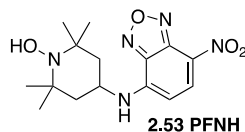


**1-hydroxy-2,2,6,6-tetramethylpiperidine-4-carboxylic acid:** The compound was prepared according to the **General Procedure 3** to give the title hydroxylamine as off-white solid in 78% yield: <sup>1</sup>H NMR (400 MHz, (CD<sub>3</sub>)<sub>2</sub>SO) δ 1.02 (s, 6H), 1.06 (s, 6H), 1.37-1.45 (m, 2H), 1.69-1.72 (m, 2H), 2.50-2.57 (m, 1H), 3.27 (br s, 1H), 7.18 (s, 1H); <sup>13</sup>C NMR (101 MHz, (CD<sub>3</sub>)<sub>2</sub>SO) δ 19.2 (4xCH<sub>3</sub>), 32.4 (CH<sub>2</sub>), 34.0 (CH<sub>2</sub>), 41.6 (CH), 57.3 (2xC), 176.4 (C); IR (KBr disc) ν<sub>max</sub> 3600-2400 (broad), 3435, 2985, 2951, 1404 cm<sup>-1</sup>; MS (ESI+) m/z (%): 202 (100, [M+H]<sup>+</sup>); HRMS (ESI+) m/z calculated for C<sub>10</sub>H<sub>19</sub>NO<sub>3</sub> [M+H]<sup>+</sup>:202.1443, found: 202.1443; mp=195 °C.



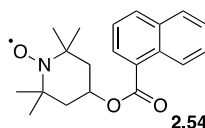
**1-oxyl-2,2,6,6-tetramethyl-4-((7-nitrobenzo[c][1,2,5]oxadiazol-4-yl)amino)piperidine:** To a magnetically stirred solution of 4-Chloro-7-nitrobenzofurazan (200 mg, 1 mmol, 1.0 eq) in dry EtOAc (2 mL), triethylamine (139 μL, 1 mmol, 1.0 eq) followed by 4-amino TEMPO radical (171 mg, 1 mmol, 1.0 eq) were added dropwise at RT. The resulting reaction mixture was stirred for 3 h under nitrogen. Diluted with EtOAc. Organic layer was sequentially washed with water and brine, dried with Na<sub>2</sub>SO<sub>4</sub> and concentrated *in vacuo*. The residue was purified by flash column chromatography (10% EtOAc/hexane) to give the product as bright orange powder (164 mg, 49%): IR (KBr disc) ν<sub>max</sub> 3214, 3063, 2978, 1578, 1530, 1492, 1317, 1282, 1261, 1237, 1185, 1027 cm<sup>-1</sup>; MS (ESI+) m/z (%): 357 (100, [M+Na]<sup>+</sup>), MS (ESI-) m/z (%): 334 (100, [M-H]<sup>-</sup>); HRMS (ESI) m/z calculated for C<sub>15</sub>H<sub>20</sub>N<sub>5</sub>O<sub>4</sub><sup>•</sup> [M+Na]<sup>+</sup>: 357.1413 found: 357.1413; Elemental

analysis:  $C_{15}H_{20}N_5O_4^{\bullet}$  calculated: C, 52.88; H, 6.03; N, 20.95; found: C, 53.92; H, 6.19; N, 20.94, mp=227 °C.



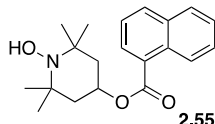
**2,2,6,6-tetramethyl-4-((7-nitrobenzo[c][1,2,5]oxadiazol-4-yl)amino)piperidin-1-**

**ol:** The compound was prepared according to the **General Procedure 3** to give the title hydroxylamine as red powder in 78% yield:  $^1H$  NMR (400 MHz,  $(CD_3)_2SO$ )  $\delta$  1.10 (s, 6H), 1.17 (s, 6H), 1.68-1.87 (m, 4H), 4.06 (br s, 1H), 6.45 (s, 1H), 7.23 (s, 1H), 8.48 (br s, 1H), 9.26 (br s, 1H);  $^{13}C$  NMR (101 MHz,  $(CD_3)_2SO$ )  $\delta$  19.5 (2x $CH_3$ ), 32.5 (2x $CH_3$ ), 43.3 (2x $CH_2$ ), 45.4 (CH), 57.8 (2xC), 99.2 (CH), 120.6 (C), 138.0 (CH), 144.1 (C), 144.4 (C), (one quaternary carbon signal obscured or overlapping); IR (KBr disc)  $\nu_{max}$  3500-3300 (broad), 3346, 2977, 2930, 1620, 1568, 1499, 1320, 1286, 1269  $cm^{-1}$ ; MS (ESI+) m/z (%): 336 (100,  $[M+H]^+$ ), 358 (80,  $[M+Na]^+$ ), MS (ESI-) m/z (%): 333 (100,  $[M-2H]^{2-}$ ); HRMS (ESI+) m/z calculated for  $C_{15}H_{21}N_5O_4^{\bullet}$   $[M+H]^+$ : 336.1672 found: 336.1671,  $[M+Na]^+$ : 357.1413 found: 357.1414; Elemental analysis:  $C_{15}H_{21}N_5O_4^{\bullet}$  calculated: C, 53.72; H, 6.31; N, 20.88; found: C, 53.48; H, 6.66; N, 20.29, mp=218-222 °C.



**1-oxyl-2,2,6,6-tetramethylpiperidin-4-yl 1-naphthoate:** To a magnetically stirred solution of 1-naphthoic acid (172 mg, 1 mmol, 1.0 eq) in benzene (0.2 mL), thionyl chloride (78  $\mu$ L, 1.1 mmol, 1.1 eq) and DMF (37  $\mu$ L, 0.03 mmol, 0.03 eq) were added dropwise at 0 °C. Stirred at RT overnight. The solvents were removed and the residue was dried *in vacuo* before dissolving in dry pyridine (1 mL). A solution of 4-OH-TEMPO (172 mg, 1 mmol, 1.0 eq) in dry pyridine (1 mL) was added dropwise at 0 °C and the resulting reaction mixture was stirred at RT for 16 h. Diluted with EtOAc and quenched with water. Organic layer was sequentially washed with 1 M *aq.* HCl, water and brine. Dried with  $Na_2SO_4$  and concentrated *in vacuo*. The residue was purified by flash column chromatography (10% EtOAc/hexane) to give orange solid (187 mg, 57%): IR (KBr disc)

$\nu_{\max}$  3004, 2979, 2968, 1709, 1133, 779  $\text{cm}^{-1}$ ; HRMS (ESI)  $m/z$  calculated for  $\text{C}_{20}\text{H}_{24}\text{NO}_3^+$   $[\text{M}+\text{Na}]^+$ : 349.1654 found: 349.1654; Elemental analysis:  $\text{C}_{20}\text{H}_{24}\text{NO}_3^+$  calculated: C, 73.59; H, 7.41; N, 4.29; found: C, 73.57; H, 7.54; N, 4.19.



**1-hydroxy-2,2,6,6-tetramethylpiperidin-4-yl 1-naphthoate:** The compound was prepared according to the **General Procedure 3** to give the title hydroxylamine as off-white solid in 70% yield:  $^1\text{H}$  NMR (400 MHz,  $\text{CDCl}_3$ )  $\delta$  1.33 (s, 6H), 1.35 (s, 6H), 1.81-1.87 (m, 2H), 2.17 – 2.20 (m, 2H), 4.16 (br s, 1H), 5.43-5.49 (m, 1H), 7.51-7.67 (m, 3H), 7.91 (d,  $J = 7.7$  Hz, 1H), 8.04 (d,  $J = 7.7$  Hz, 1H), 8.19 (d,  $J = 7.3$  Hz, 1H), 8.95 (d,  $J = 8.9$  Hz, 1H);  $^{13}\text{C}$  NMR (101 MHz,  $\text{CDCl}_3$ )  $\delta$  19.8 (2x $\text{CH}_3$ ), 31.3 (2x $\text{CH}_3$ ), 43.3(2x $\text{CH}_2$ ), 58.9 (2xC), 66.7 (CH), 123.8 (CH), 125.0 (CH), 125.5 (CH), 126.7(C), 127.0 (CH), 127.8 (CH), 129.4 (CH), 130.6 (C), 132.6 (CH), 133.1 (C), 166.4 (C); IR (KBr disc)  $\nu_{\max}$  3600-3200 (broad), 2975, 2940, 1711, 1239, 1135, 782  $\text{cm}^{-1}$ ; MS (ESI+)  $m/z$  (%): 228 (100,  $[\text{M}+\text{H}]^+$ ), 250 (12,  $[\text{M}+\text{Na}]^+$ ); HRMS (ESI+)  $m/z$  calculated for  $\text{C}_{20}\text{H}_{25}\text{NO}_3$   $[\text{M}+\text{H}]^+$ : 328.1914, found: 328.1913.

## 7.2 Preliminary Polymerization Studies - Experimental Details

Styrene 98%; 1,1-azobis (cyclohexanecarbonitrile) 98% (VAZO<sup>®</sup>88) and benzene (CHROMASOLV<sup>®</sup> Plus,  $\geq 99.9\%$ ) were supplied by Sigma-Aldrich. THF used for SEC analysis was GC/GPC grade stabilized with BHT, supplied by Honeywell Burdick & Jackson. Styrene was distilled under vacuum or filtered through basic alumina (Brockmann) to remove inhibitor and stored in the freezer. VAZO<sup>®</sup>88 and solvents were used as received. All experiments were conducted under positive pressure of dry argon or nitrogen in oven-dried glassware. Free-radical polymerizations of styrene were carried out across a broad range of temperatures in bulk and in the presence of benzene.

### 7.2.1 General procedure for styrene polymerization with nitroxyl radical and initiator:

A reaction vessel was charged with styrene (250 eq), nitroxide (1 eq) and initiator (0.006 eq); sealed and subjected to three freeze-thaw-pump cycles. The resulting reaction

mixture was heated at given temperature for a given amount of time. Various bases were used in excess; for samples containing potassium salt one molar equivalent of crown ether was added.

### **7.2.2 General procedure for styrene polymerization with alkoxyamine:**

A reaction vessel was charged with styrene (250 eq) and alkoxyamine (1 eq) and subjected to three freeze-thaw-pump cycles. The resulting reaction mixture was heated at given temperature for a given amount of time. Various bases were used in excess; for samples containing potassium salt one molar equivalent of crown ether was added to selected samples.

The monomer conversion for styrene was determined by gravimetric methods after drying the polymer samples under vacuum at 40 °C. The molecular weight distributions of the samples were determined using high performance gel liquid chromatography Viscotek GPC Max system fitted with a Viscotek TDA 305 triple detector array consisting of a differential viscometer; right-angle laser-light scattering; low-angle laser-light scattering; and refractive index detectors. The column set consisted of a Viscotek TGuard Organic Guard Column (10 × 4.6 mm) and a Viscotek LT5000L Mixed Medium Organic Column (300 × 7.8 mm). The system was fitted with an online solvent degasser system and eluent (THF) flow rate was set to 1 mL min<sup>-1</sup> and columns were held at 30 °C. Calibration was carried out using PolyCAL™ polystyrene standards with  $M_w = 98,251$  and  $M_n = 96,722$  and  $M_w = 231,820$  and  $M_n = 102,977$  using OmniSEC software version 4.6.1.354.

## **7.3 Fluorescence Hydrogen Exchange Experimental Details**

### **7.3.1 Determination of equilibrium constant and rate constants in dichloromethane or acetonitrile for reaction between 4-CT-H and PFN.**

Solutions of 4-CT-H (6.0 μmol) and profluorescent nitroxide (PFN) (6.0 μmol) were made up in 100 mL of solvent. PFN solution (2 mL) was added to quartz fluorescence cuvettes and then 4-CT-H solution (2 mL) was added to this solution. The cuvette was then placed in a Cary Eclipse fluorescence spectrometer and the emission fluorescence intensity was measured at 520 nm with the excitation wavelength set to 350 nm. Measurements were made periodically over a period of up to 2 h. For the samples in which triethylamine was added, this was added after the mixing of the two solutions and

prior to the measurement of the fluorescence emission. The number of equivalents of base is given relative to the concentration of 4-CT-H in solution. All concentrations were determined from a calibration curve of PFN-H emission intensity in dichloromethane, benzene or acetonitrile against concentration and separate calibration curves were made for each concentration of base in the presence of 4-CT-H to account for the effect of triethylamine on the fluorescence of PFN-H. The final concentration of PFN-H from each sample was used to determine the equilibrium rate constant and the kinetic data was fitted to a reversible second order kinetic model. All samples were corrected for the dilution effect of the addition of TEA.

### **7.3.2 Determination of equilibrium constant and rate constants in dichloromethane for reaction between TEMPOnaph-H and PFN.**

Solutions of TEMPOnaph-H (6.0  $\mu\text{mol}$ ) and profluorescent nitroxide (PFN) (6.0  $\mu\text{mol}$ ) were made up in 100 mL of dichloromethane. PFN solution (2 mL) was added to quartz fluorescence cuvettes and then 4-CT-H solution (2 mL) was added to this solution. The cuvette was then placed in a Cary Eclipse fluorescence spectrometer. The sample excitation wavelength was set at 350 nm. The emission fluorescence intensity was measured at 520 nm and samples were taken periodically over a period of up to 2 h. For the samples in which triethylamine was added, this was added after the mixing of the two solutions and prior to the measurement of the fluorescence emission. The number of equivalents of base is given relative to the concentration of 4-CT-H in solution. All concentrations were determined from a calibration curve of PFN-H emission intensity in dichloromethane against concentration and separate calibration curves were made for each concentration of base in the presence of TEMPOnaph-H to account for the effect of triethylamine (TEA) on the fluorescence of PFN-H. The final concentration of PFN-H from each sample was used to determine the equilibrium rate constant of the second order equilibrium and the kinetic data was fitted to a reversible second order kinetic model with equilibrium (**see Appendix Two**). All samples were corrected for the dilution effect of the addition of TEA.



**References:**

- (1) Gryn'ova, G.; Marshall, D. L.; Blanksby, S. J.; Coote, M. L. *Nat. Chem.* **2013**, *5*, 474.
- (2) Gryn'ova, G.; Coote, M. L. *J. Am. Chem. Soc.* **2013**, *135*, 15392.
- (3) Stirk, K. M.; Kiminkinen, L. K. M.; Kenttamaa, H. I. *Chem. Rev.* **1992**, *92*, 1649.
- (4) Kenttamaa, H. I. *Org. Mass Spectrom.* **1994**, *29*, 1.
- (5) Bouchoux, G.; Berruyer, F.; Hiberty, P. C.; Wu, W. *Chem. - Eur. J.* **2007**, *13*, 2912.
- (6) Williams, P. E.; Jankiewicz, B. J.; Yang, L.; Kenttamaa, H. I. *Chem. Rev.* **2013**, *113*, 6949.
- (7) Stringle, D. L. B.; Magri, D. C.; Workentin, M. S. *Chem. - Eur. J.* **2010**, *16*, 178.
- (8) Tanko, J. M.; Phillips, J. P. *J. Am. Chem. Soc.* **1999**, *121*, 6078.
- (9) Mayer, P. M.; Radom, L. *J. Phys. Chem. A* **1998**, *102*, 4918.
- (10) Mayer, P. M.; Glukhovtsev, M. N.; Gauld, J. W.; Radom, L. *J. Am. Chem. Soc.* **1997**, *119*, 12889.
- (11) Morris, M.; Chan, B.; Radom, L. *J. Phys. Chem. A* **2012**, *116*, 12381.
- (12) Yu, D.; Rauk, A.; Armstrong, D. A. *J. Chem. Soc. Perkin Trans. 2* **1994**, 2207.
- (13) Ho, J.; Coote, M. L.; Easton, C. J. *Aust. J. Chem.* **2011**, *64*, 403.
- (14) Tian, Z.; Chan, B.; Sullivan, M. B.; Radom, L.; Kass, S. R. *Proc. Natl. Acad. Sci.* **2008**, *105*, 7647.
- (15) Foti, M. C.; Amorati, R.; Pedulli, G. F.; Daquino, C.; Pratt, D. A.; Ingold, K. U. *J. Org. Chem.* **2010**, *75*, 4434.
- (16) Adcock, W.; Trout, N. A. *Magn. Reson. Chem.* **1998**, *36*, 181.
- (17) Richardson, R. D.; Carpenter, B. K. *J. Am. Chem. Soc.* **2008**, *130*, 3169.
- (18) O'Reilly, R. J.; Chan, B.; Taylor, M. S.; Ivanic, S.; Bacskay, G. B.; Easton, C. J.; Radom, L. *J. Am. Chem. Soc.* **2011**, *133*, 16553.

- (19) Edeleva, M. V.; Kirilyuk, I. A.; Zhurko, I. F.; Parkhomenko, D. A.; Tsentalovich, Y. P.; Bagryanskaya, E. G. *J. Org. Chem.* **2011**, *76*, 5558.
- (20) In *International Union of Pure and Applied Chemistry. Compendium of Chemical Terminology, 2nd ed; XML on-line corrected version*: <http://goldbook.iupac.org>; McNaught, A. D., Wilkinson, A., Eds.; Blackwell Scientific Publications, Oxford (1997).
- (21) Slipchenko, L. V.; Munsch, T. E.; Wenthold, P. G.; Krylov, A. I. *Angew. Chem. Int. Ed.* **2004**, *43*, 742.
- (22) Sugawara, T.; Komatsu, H.; Suzuki, K. *Chem. Soc. Rev.* **2011**, *40*, 3105.
- (23) Kusamoto, T.; Kume, S.; Nishihara, H. *J. Am. Chem. Soc.* **2008**, *130*, 13844.
- (24) Kobayashi, Y.; Yoshioka, M.; Saigo, K.; Hashizume, D.; Ogura, T. *J. Am. Chem. Soc.* **2009**, *131*, 9995.
- (25) Solomon, D. H.; Rizzardo, E.; Cacioli, P. In *US Patent 4581429* 1985.
- (26) Georges, M. K.; Veregin, R. P. N.; Kazmaier, P. M.; Hamer, G. K. *Macromolecules* **1993**, *26*, 2987.
- (27) Nicolas, J.; Guillaneuf, Y.; Lefay, C.; Bertin, D.; Gigmes, D.; Charleux, B. *Prog. Polym. Sci.* **2013**, *38*, 63.
- (28) Souaille, M.; Fischer, H. *Macromolecules* **2001**, *34*, 2830.
- (29) Bertin, D.; Gigmes, D.; Marque, S. R. A.; Tordo, P. *Chem. Soc. Rev.* **2011**, *40*, 2189.
- (30) Mazarin, M.; Girod, M.; Viel, S.; Phan, T. N. T.; Marque, S. R. A.; Humbel, S.; Charles, L. *Macromolecules* **2009**, *42*, 1849.
- (31) Audran, G.; Bosco, L.; Bremond, P.; Marque, S. R. A.; Roubaud, V.; Siri, D. *J. Org. Chem.* **2013**, *78*, 9914.
- (32) Marx, L.; Hemery, P. *Polymer* **2009**, *50*, 2752.
- (33) Nicolay, R.; Marx, L.; Hemery, P.; Matyjaszewski, K. *Macromolecules* **2007**, *40*, 6067.
- (34) Franchi, P.; Mezzina, E.; Lucarini, M. *J. Am. Chem. Soc.* **2014**, *136*, 1250.
- (35) Schoening, K.-U.; Fischer, W.; Hauck, S.; Dichtl, A.; Kuepfert, M. *J. Org. Chem.* **2009**, *74*, 1567.
- (36) Keglevich, G.; Balint, E. *Molecules* **2012**, *17*, 12821.

- (37) Abraham, S.; Choi, J. H.; Ha, C.-S.; Kim, I. *J. Polym. Sci. A Polym. Chem.* **2007**, *45*, 5559.
- (38) Yamasaki, T.; Mito, F.; Ito, Y.; Pandian, S.; Kinoshita, Y.; Nakano, K.; Murugesan, R.; Sakai, K.; Utsumi, H.; Yamada, K.-i. *J. Org. Chem.* **2010**, *76*, 435.
- (39) Gillet, J.-P.; Guerret, O.; Tordo, P. In *US 6,624,322 B1* 2003.
- (40) Fields, J. D.; Kropp, P. J. *J. Org. Chem.* **2000**, *65*, 5937.
- (41) Acerbis, S.; Bertin, D.; Boutevin, B.; Gigmes, D.; Lacroix-Desmazes, P.; Le Mercier, C.; Lutz, J.-F.; Marque, S. R. A.; Siri, D.; Tordo, P. *Helv. Chim. Acta* **2006**, *89*, 2119.
- (42) Grimaldi, S.; Finet, J.-P.; Le Moigne, F.; Zeghdaoui, A.; Tordo, P.; Benoit, D.; Fontanille, M.; Gnanou, Y. *Macromolecules* **2000**, *33*, 1141.
- (43) Soroka, M.; Zygmunt, J. *Synthesis* **1988**, *5*, 370.
- (44) David, T.; Kotek, J.; Kubíček, V.; Tosner, Z.; Hermann, P.; Lukes, I. *Heteroat. Chem.* **2013**, *24*, 413.
- (45) Howlader, R.; Walawalkar, M. G.; Murugavel, R. *Inorg. Chim. Acta.* **2013**, *405*, 147.
- (46) Dilmán, A. D.; Tishkov, A. A.; Lyapkalo, I. M.; Ioffe, S. L.; Strelenko, Y. A.; Tartakovsky, V. A. *Synthesis* **1988**, *2*, 181.
- (47) Gauvry, N.; Mortier, J. *Synthesis* **2001**, *4*, 553.
- (48) Benoit, D.; Chaplinski, V.; Braslau, R.; Hawker, C. J. *J. Am. Chem. Soc.* **1999**, *121*, 3904.
- (49) Huie, R.; Cherry, W. R. *J. Org. Chem.* **1985**, *50*, 1531.
- (50) Thesing, J.; Sirrenberg, W. *Chem. Ber.* **1958**, *91*, 1978.
- (51) Folting, K.; Lipscomb, W. N.; Jerslev, B. *Acta Chem. Scand.* **1963**, *17*, 2138.
- (52) Gree, R.; Tonnard, F.; Carrie, R. *Tetrahedron* **1976**, *32*, 675 and 678.
- (53) Hamer, J.; Macaluso, A. *Chem. Rev.* **1964**, *64*, 473.
- (54) Gothelf, K. V.; Jorgensen, K. A. *Chem. Rev.* **1998**, *98*, 863.
- (55) Badoiu, A.; Kundig, E. P. *Org. Biomol. Chem.* **2012**, *10*, 114.
- (56) Padwa, A.; Fisera, L.; Koehler, K. F.; Rodriguez, A.; Wong, G. S. K. *J. Org. Chem.* **1984**, *49*, 276.

- (57) Grigg, R. D.; Van Hoveln, R.; Schomaker, J. M. *J. Am. Chem. Soc.* **2012**, *134*, 16131.
- (58) Fabio, M.; Ronzini, L.; Troisi, L. *Tetrahedron* **2007**, *63*, 12896.
- (59) Gothelf, K. V.; Hazell, R. G.; Jorgensen, K. A. *J. Org. Chem.* **1996**, *61*, 346.
- (60) Andrade, M. M.; Barros, M. T.; Pinto, R. C. *Tetrahedron* **2008**, *64*, 10521.
- (61) Blinco, J. P.; Keddie, D. J.; Wade, T.; Barker, P. J.; George, G. A.; Bottle, S. E. *Polym. Degrad. Stab.* **2008**, *93*, 1613.
- (62) Blinco, J. P.; Fairfull-Smith, K. E.; Morrow, B. J.; Bottle, S. E. *Aust. J. Chem.* **2011**, *64*, 373.
- (63) Bogнар, B.; Osz, E.; Hideg, K.; Kalai, T. *J. Heterocyclic Chem.* **2006**, *43*, 81.
- (64) Jones, M. J.; Moad, G.; Rizzardo, E.; Solomon, D. H. *J. Org. Chem.* **1989**, *54*, 1607.
- (65) Litwinienko, G.; Ingold, K. U. *Acc. Chem. Res.* **2007**, *40*, 222.
- (66) Xia, Y.; Mendenhall, K. G.; Barsanti, P. A.; Walter, A. O.; Duhl, D.; Renhowe, P. A. In *WO 2008063912 A1* 2008.

## **Appendix One: SEC Plots Supporting Polymerization Studies Reported In Chapter Five**

### **A1.1 Chain extension of 4-carboxy-TIPNO-PSTY with styrene:**

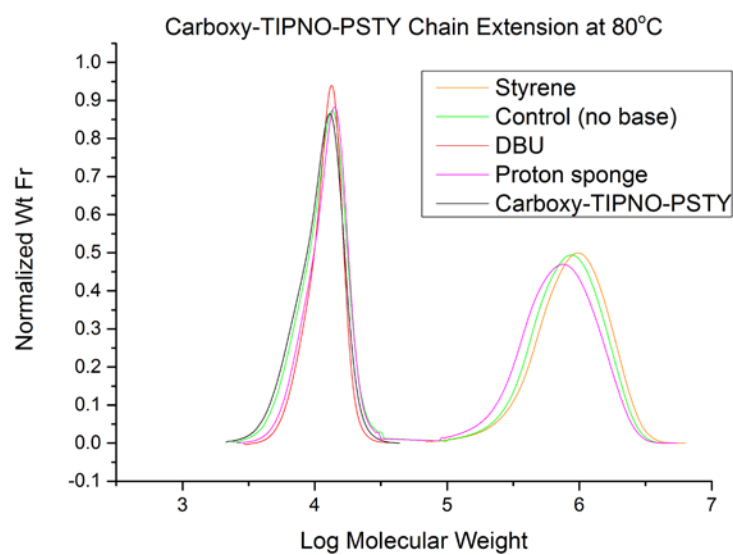


**Figure A1.1.1**

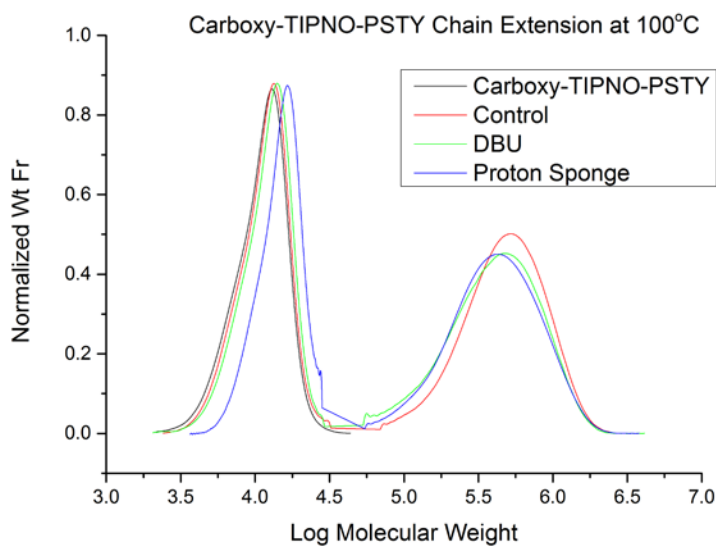


**Figure A1.1.2**

## A1.2 Effect of base on initiation

### A1.2.1 Polymerization of styrene with DBU:

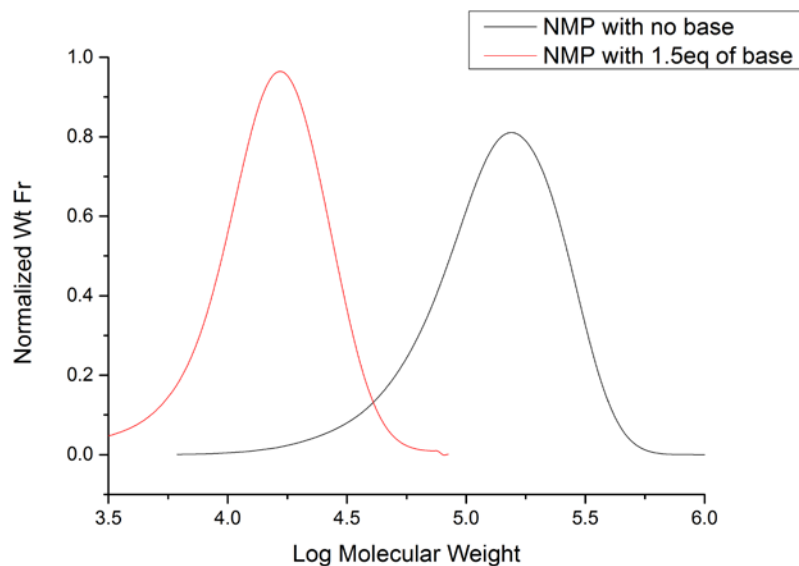


Figure A1.2.1.1

### A1.2.2 Polymerization of styrene with TEA and proton sponge:

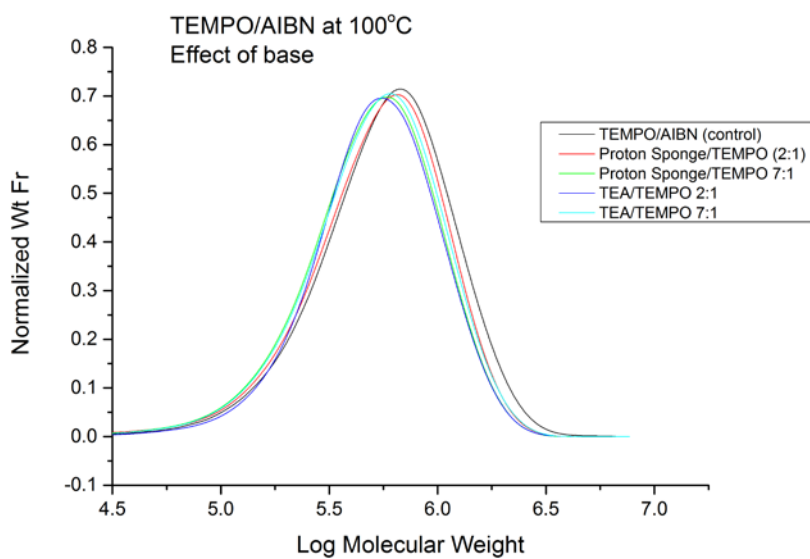


Figure A1.2.2.1

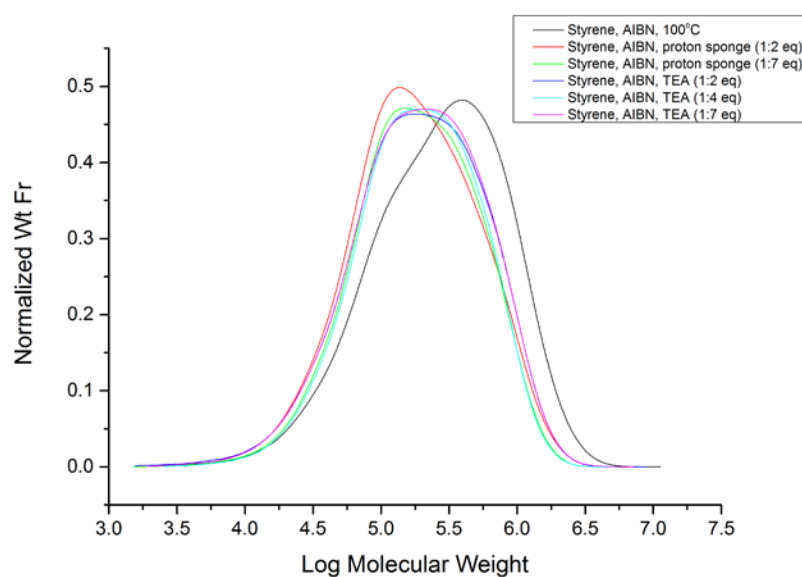


Figure A1.2.2.2

### A1.2.3 Test for cationic polymerization with ratio of benzoic acid to TEA and Proton Sponge:

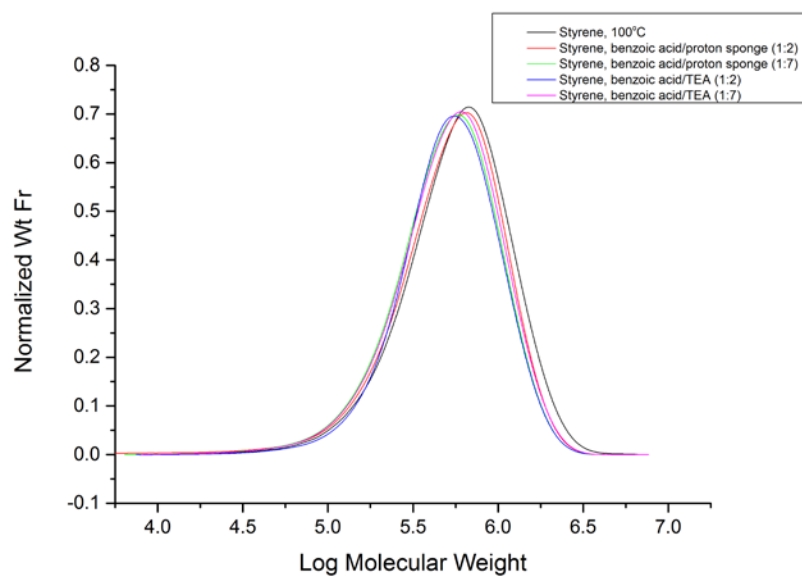
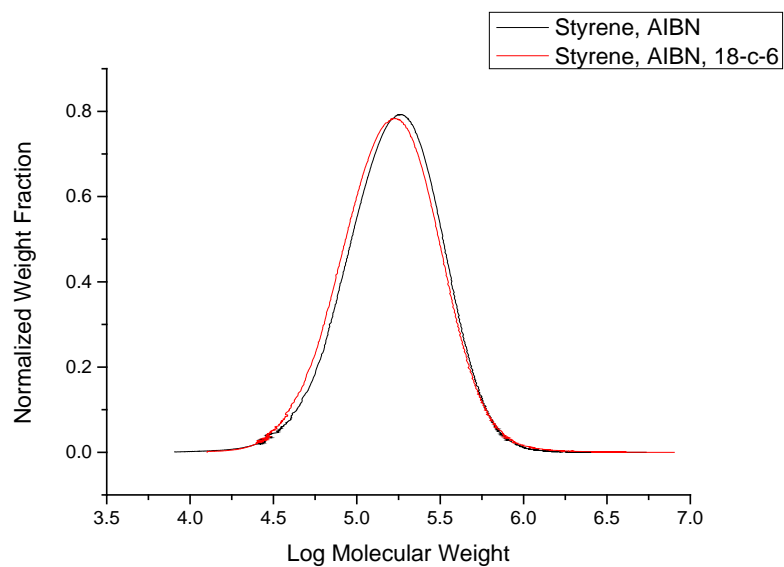
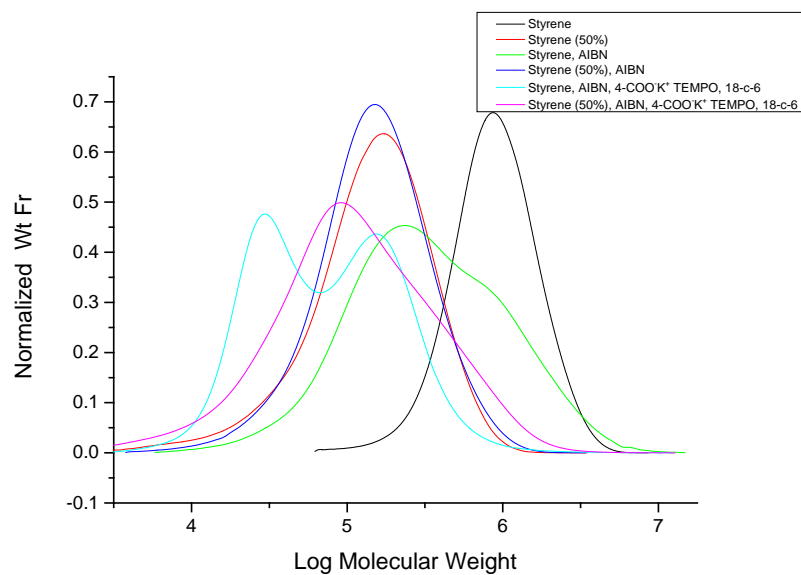
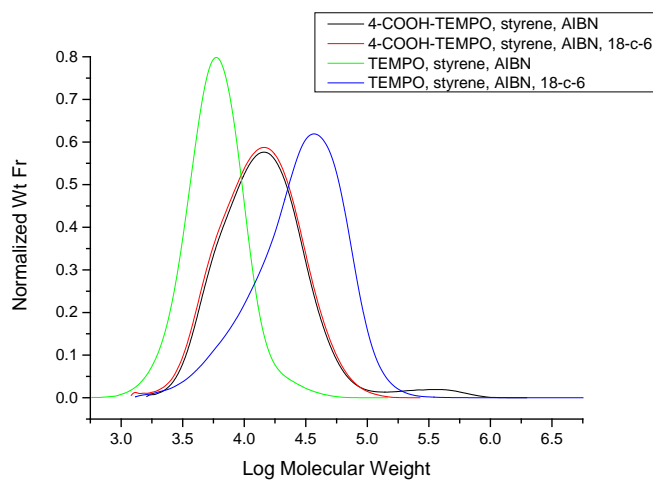
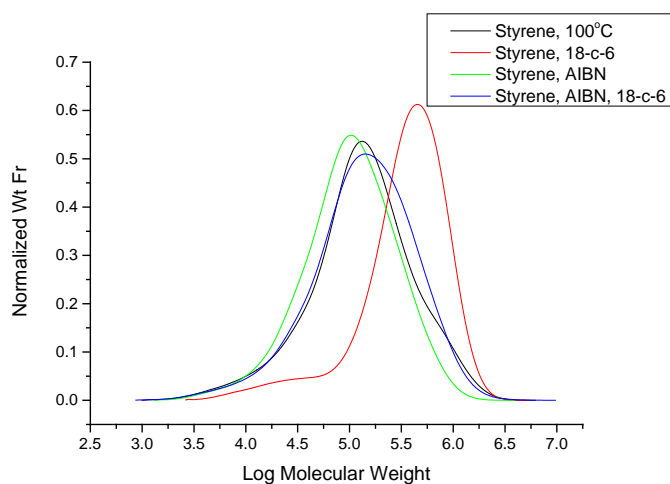


Figure A1.2.3.1

**A1.3 Control experiments at 60 °C****Figure A1.3.1****A1.4 Control experiments at 80 °C****Figure A1.4.1**



**A1.5 Control experiments at 100 °C****Figure A1.5.1****Figure A1.5.2**

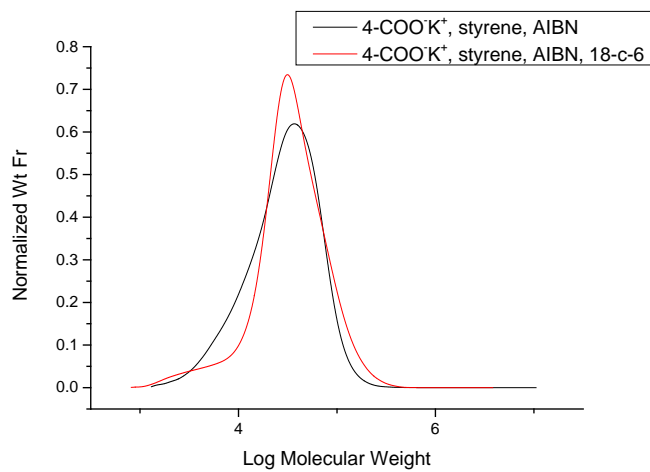


Figure A1.5.3

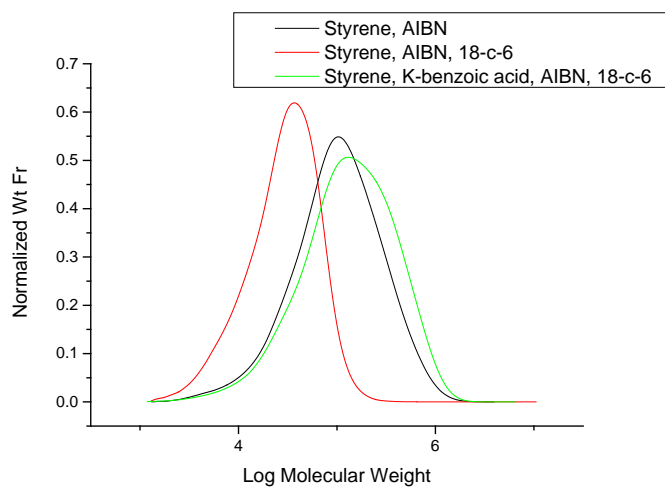


Figure A1.5.4

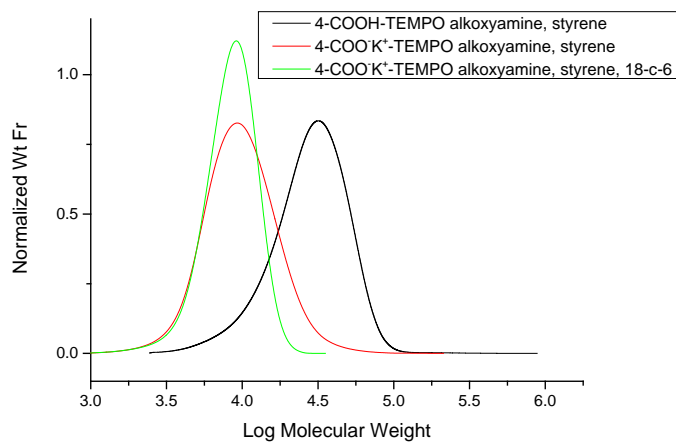
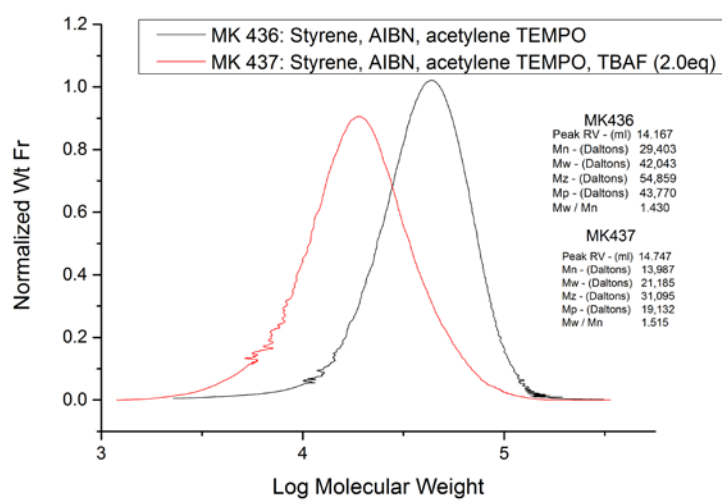


Figure A1.5.1

**A1.6 Acetylene switch – styrene polymerization:****Figure A1.6.1**

## Appendix Two: Calibration Curves and Kinetic Analysis for the Hydrogen Atom Transfer Experiment Reported in Chapter Six

### A2.1 Fluorescence Calibration Curves

Figure A2.1.1 PFN-H with 0.03 mM of 4-CT-H in dichloromethane at 25 °C:

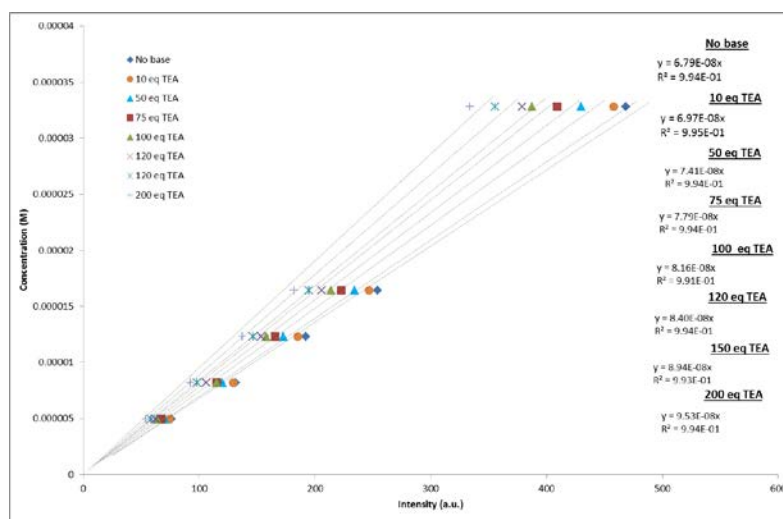
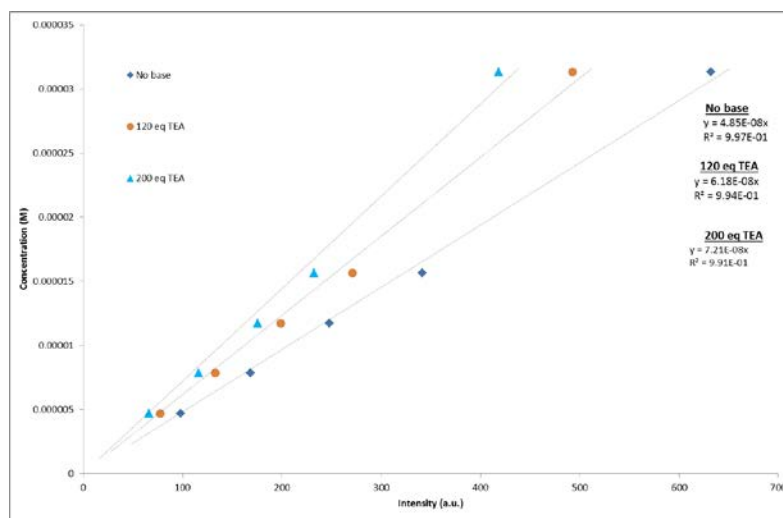
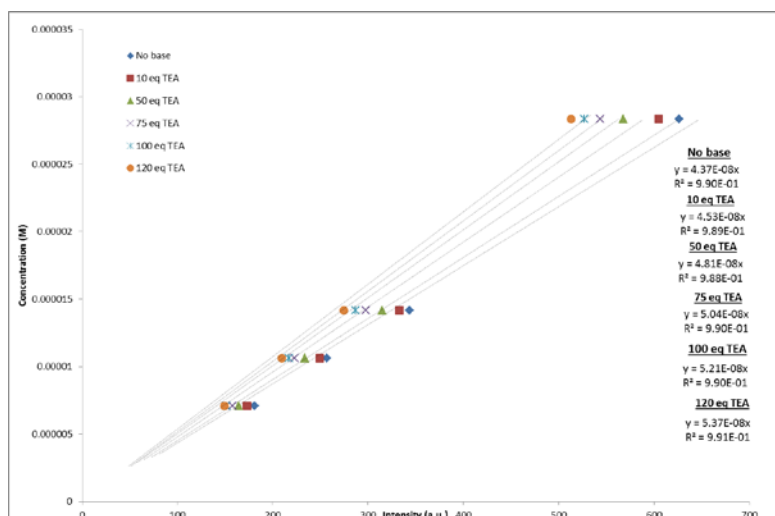
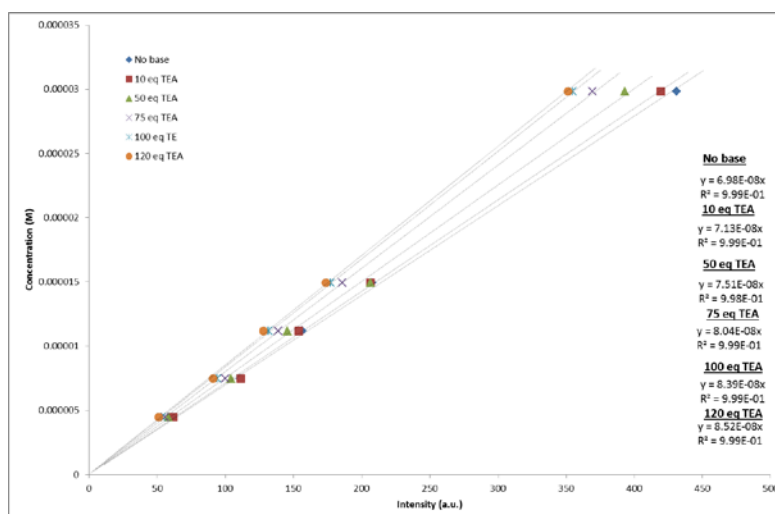


Figure A2.1.2 PFN-H with 0.03 mM of 4-CT-H in dichloromethane at 10 °C:

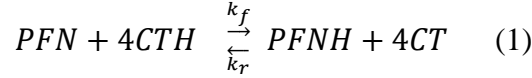


**Figure A2.1.3** PFN-H with 0.03 mM of 4-CT-H in acetonitrile:**Figure A2.1.4** PFN-H with 0.03 mM of TEMPO<sub>naph</sub>-H in dichloromethane:

Calibration of the response of intensity of the maximum fluorescence of PFN-H in all solvent solutions were done in the presence of 0.03 mM 4-CT-H. This concentration was chosen as this is the identical concentration of 4-CT-H during the exchange experiments. The intensity of the emission from the PFN-H fluorophore was measured with subsequent additions of a 10% solution of triethylamine in solvent to allow for the reduction in fluorescence with increasing pH in solution.

### A2.2 Second Order Kinetics in Equilibrium

The equilibrium exchange reaction can be depicted by the following equilibrium reaction scheme:



And therefore:

$$\frac{d[PFNH]}{dt} = k_f[PFN][4CTH] - k_r[PFNH][4CT] \quad (2)$$

If only PFN and 4-CT-H are present at the beginning of the reaction, then expressing this reaction in terms of the extent of reaction,  $x$ , gives us:

$$\frac{dx}{dt} = k_f([PFN]_0 - x)([4CTH]_0 - x) - k_r x^2 \quad (3)$$

By definition, at equilibrium:

$$K = \frac{k_f}{k_r} = \frac{x_e^2}{([PFN]_0 - x_e)([4CTH]_0)} \quad (4)$$

Substituting for  $k_r$  into equation (3) gives:

$$\frac{dx}{dt} = k_f([PFN]_0 - x)([4CTH]_0 - x) - k_f \frac{([PFN]_0 - x_e)([4CTH]_0)}{x_e^2} x^2 \quad (5)$$

Letting,  $[PFN]_0 = a$  and  $[4-CT-H]_0 = b$ , this can then be integrated by partial fractions to give:

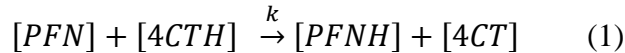
$$\ln \left\{ \frac{x[ab - (a+b)x_e] + ab x_e}{ab(x_e - x)} \right\} = k_f \frac{2ab - (a+b)x_e}{x_e} t \quad (6)$$

If  $[PFN]_0 = [4-CT-H]_0 = a$ ; then equation (6) simplifies to:

$$\ln \left\{ \frac{x[a - 2x_e] + a x_e}{a(x_e - x)} \right\} = k_f \frac{2a(a+b)x_e}{x_e} t \quad (7)$$

### A2.3 Second Order Kinetics Rate Constant

The reaction going to completion can be represented by the following reaction scheme:



In terms of extent of reaction,  $x$ , and initial concentrations of PFN and 4-CT-H, where  $[PFN]_0 = a$  and  $[4-CT-H]_0 = b$  we get:

$$\frac{dx}{dt} = k(a - x)(b - x) \quad (2)$$

The integrated form of this expression is given by:

$$\frac{1}{b-a} \ln \frac{a(b-x)}{b(a-x)} = kt \quad (3)$$

or

$$\frac{1}{a-b} \ln \frac{b(a-x)}{a(b-x)} = kt$$

Adapted From John W. Moore, Ralph G. Pearson, Kinetics and Mechanism, 3rd Edition, p 23, John Wiley & Sons, 1981 ISBN 0-471-03558-0

## A2.4 Kinetic Model Fitting Plots

### PFN/4-CT-H system in dichloromethane at 25 °C

Plots of  $\ln \left\{ \frac{x[ab-(a+b)x_e] + ab x_e}{ab(x_e-x)} \right\}$  versus time, slope =  $k_f \left( \frac{2ab-(a+b)x_e}{x_e} \right)$

**Figure A2.4.1** 0 eq TEA (no base)

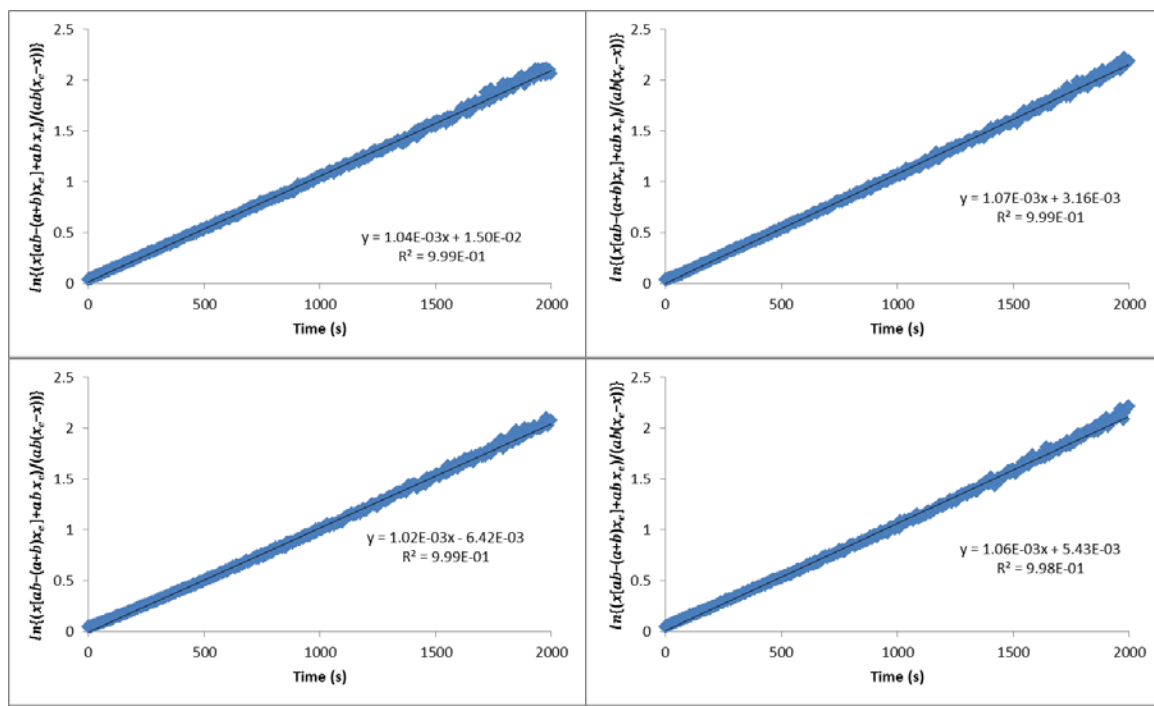


Figure A2.4.2 10 eq TEA

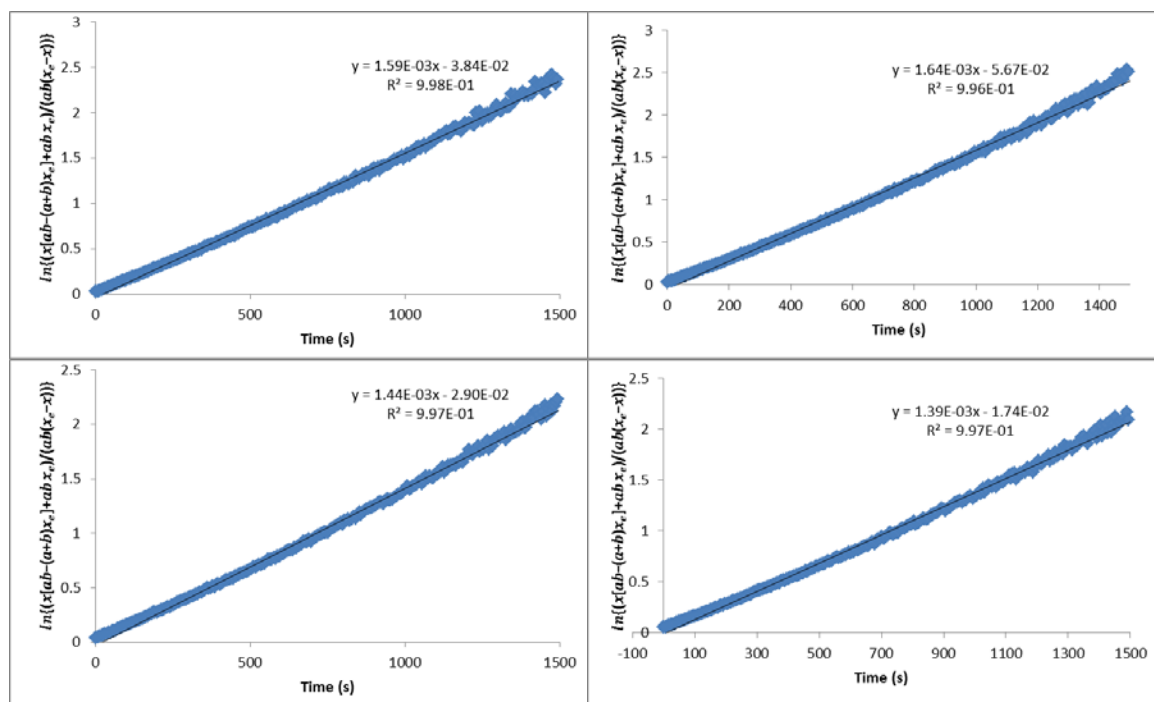


Figure A2.4.3 50 eq TEA

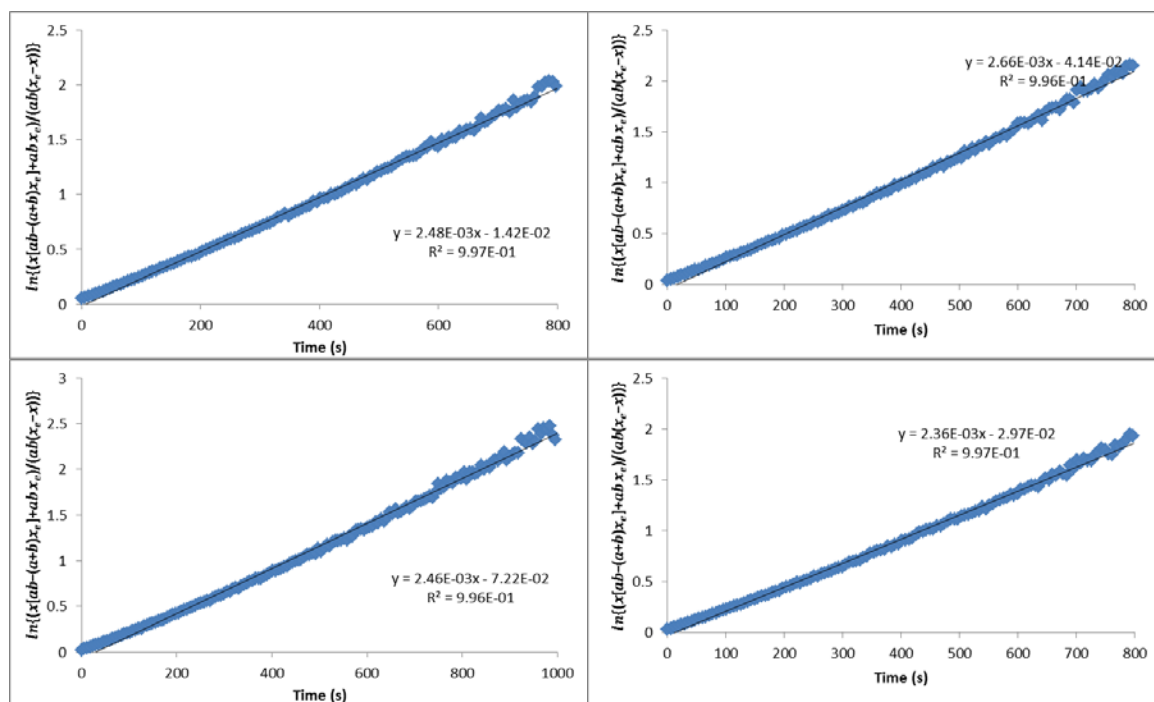




Figure A2.4.4 75 eq TEA

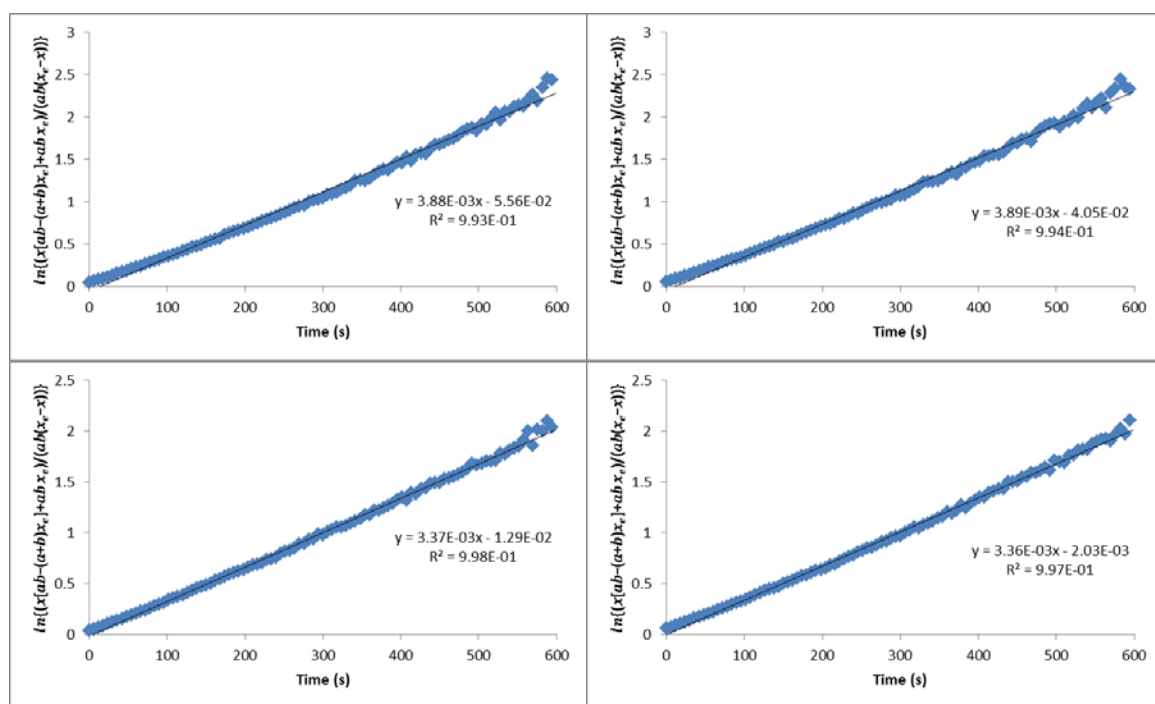


Figure A2.4.5 100 eq TEA

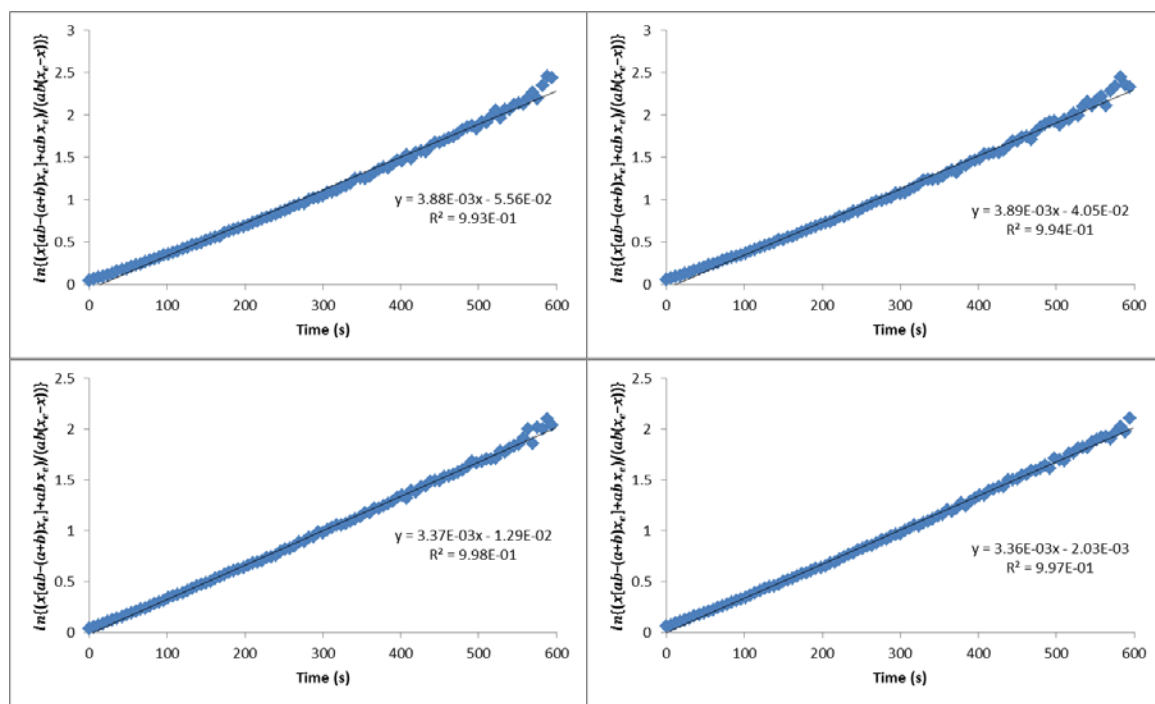


Figure A2.4.6 120 eq TEA

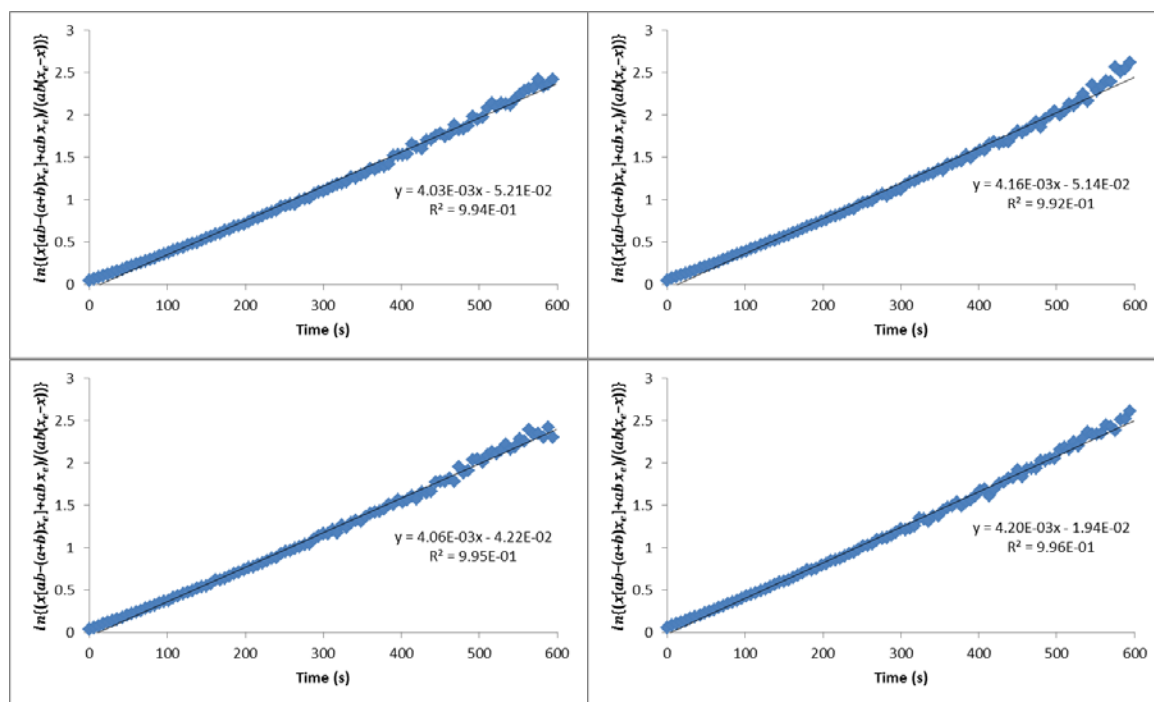


Figure A2.4.7 150 eq TEA

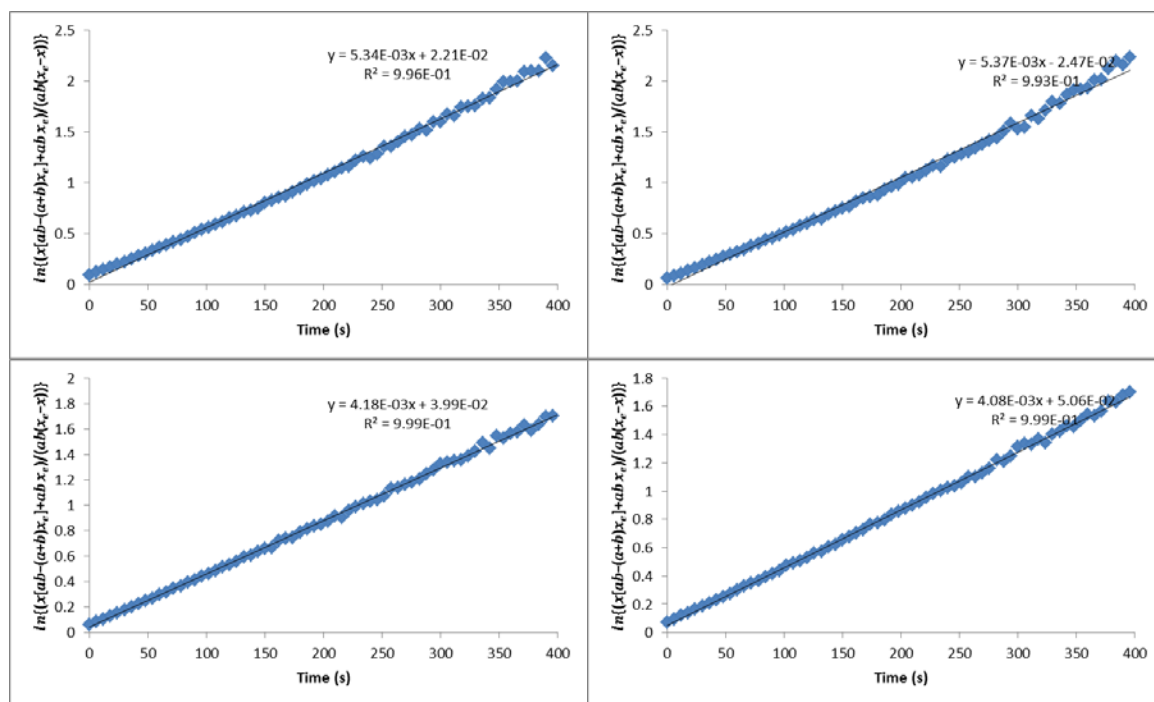
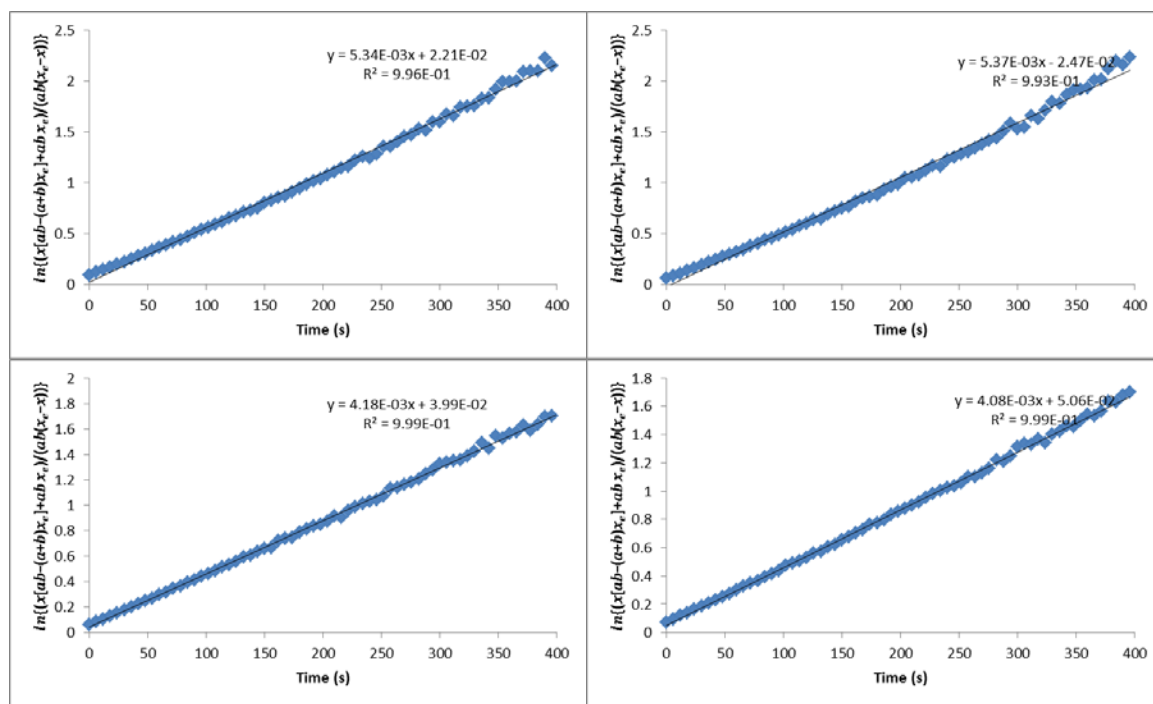


Figure A2.4.8 200 eq TEA



### A2.5 PFN/4-CT-H system in dichloromethane at 10 °C

Plots of  $\ln \left\{ \frac{x[ab-(a+b)x_e]+abx_e}{ab(x_e-x)} \right\}$  versus time, slope =  $k_f \left( \frac{2ab-(a+b)x_e}{x_e} \right)$

**Figure A2.5.1** 0 eq TEA (no base)

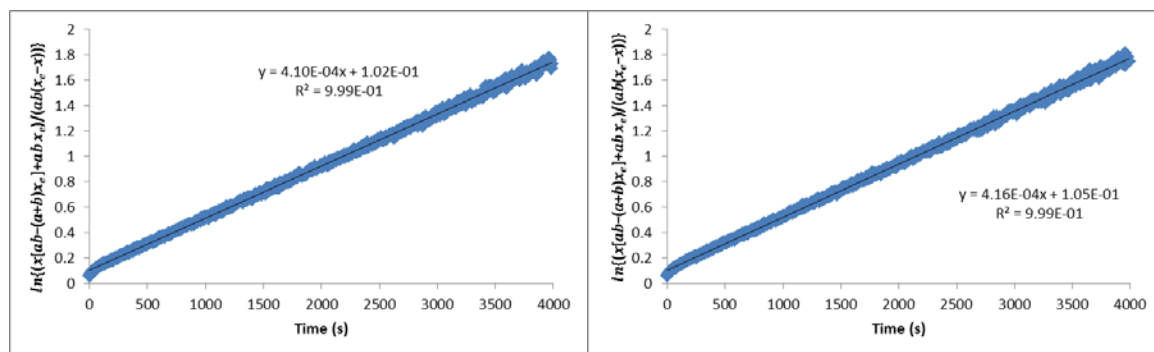
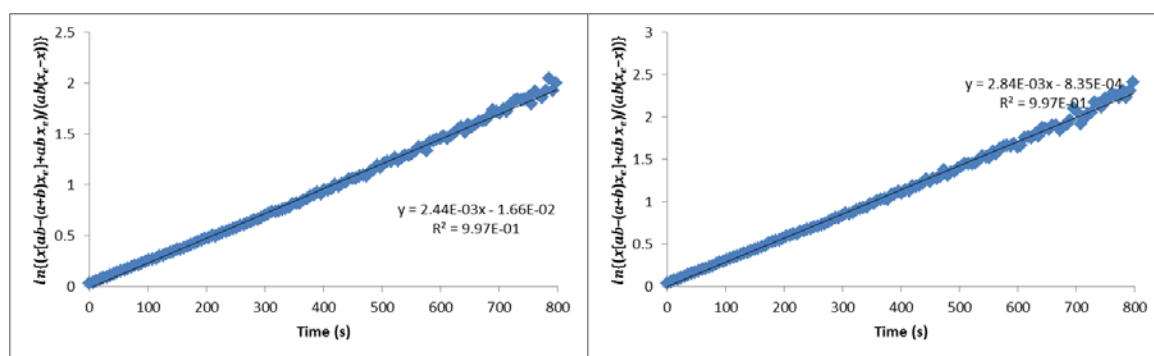


**Figure A2.5.2** 120 eq TEA



### A2.6 PFN/4-CT-H system in acetonitrile

Plots of  $\ln \left\{ \frac{x[ab-(a+b)x_e]+abx_e}{ab(x_e-x)} \right\}$  versus time; slope =  $k_f \left( \frac{2ab-(a+b)x_e}{x_e} \right)$

**Figure A2.6.1** 0 eq TEA (no base)

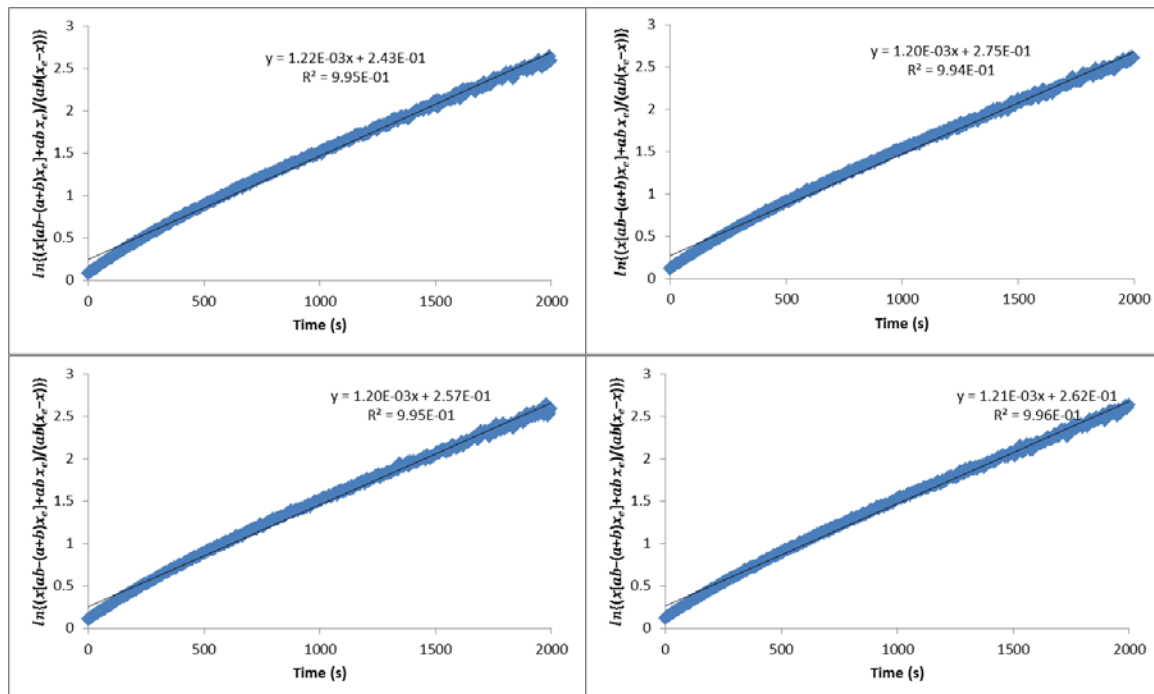


**Figure A2.6.2** 50 eq TEA

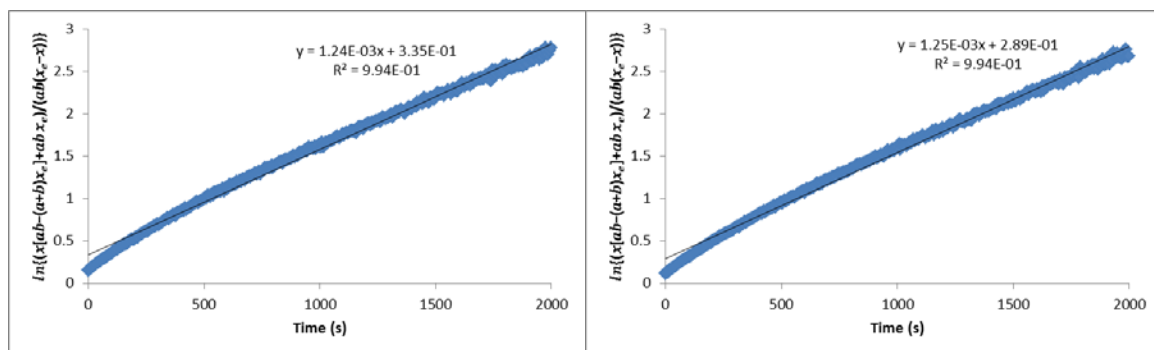


Figure A2.6.3 75 eq TEA

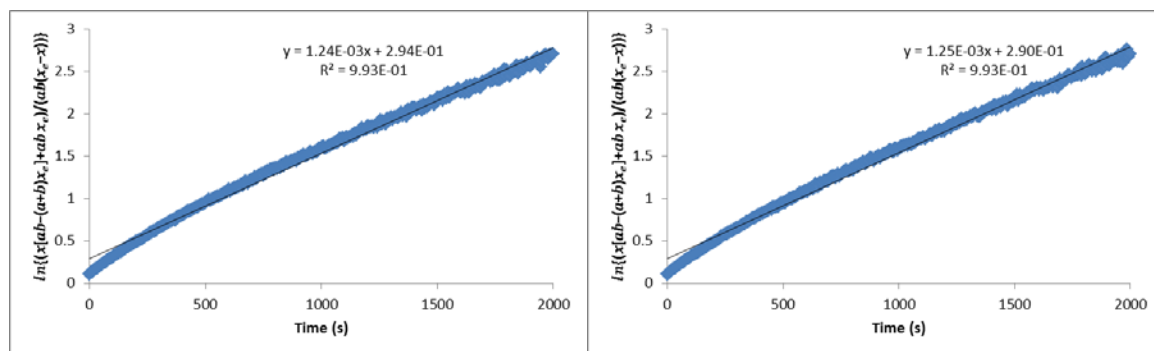
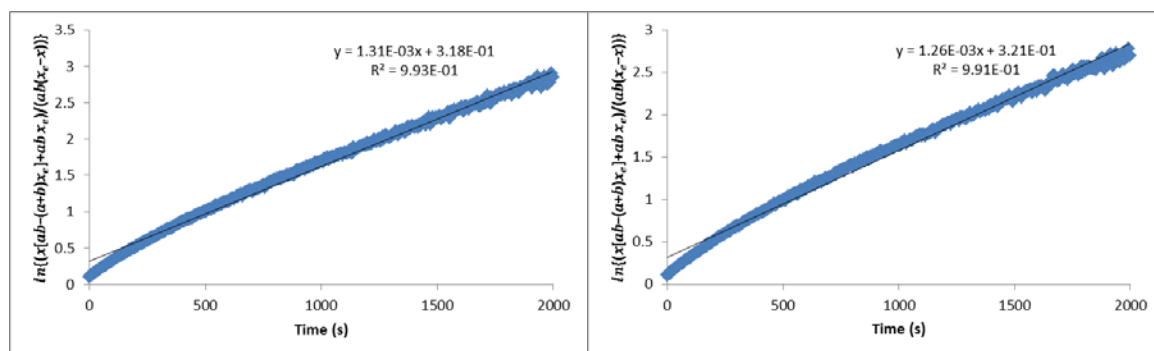


Figure A2.6.4 120 eq TEA



### A2.7 PFN/TEMPO<sub>n</sub>aph-H system in dichloromethane

Plots of  $\ln \left\{ \frac{x[ab-(a+b)x_e] + ab x_e}{ab(x_e-x)} \right\}$  versus time, slope =  $k_f \left( \frac{2ab-(a+b)x_e}{x_e} \right)$

Figure A2.7.1 0 eq TEA (no base)

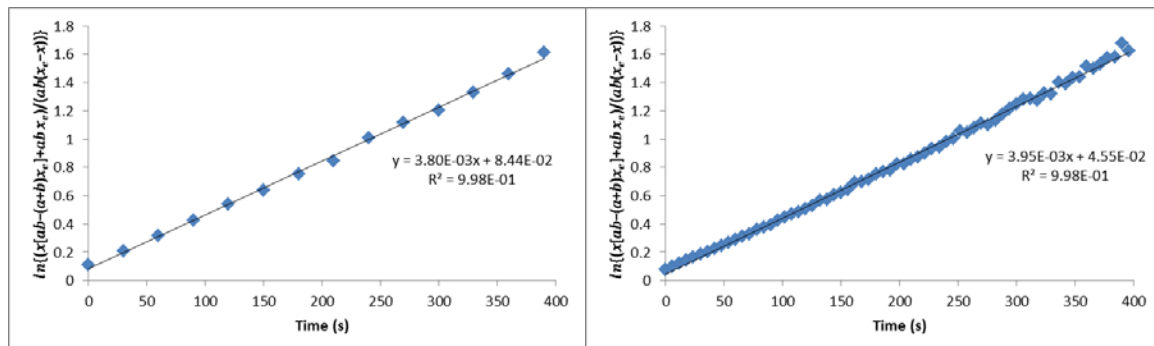


Figure A2.7.2 10 eq TEA

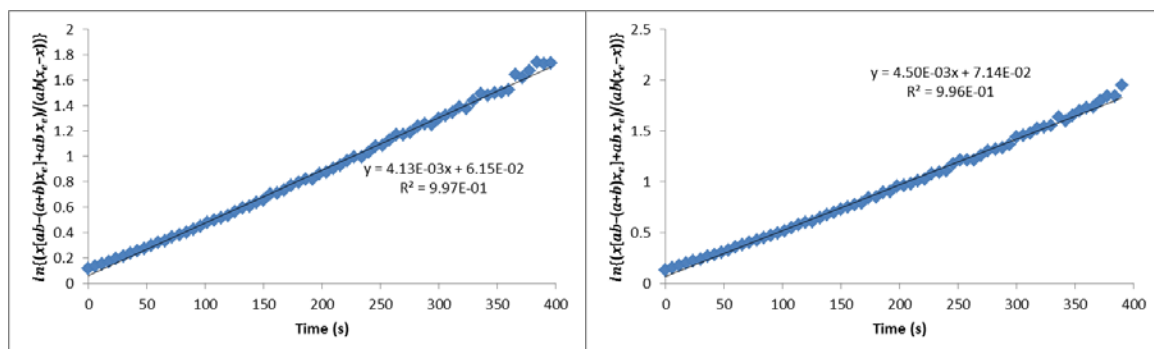


Figure A2.7.3 50 eq TEA

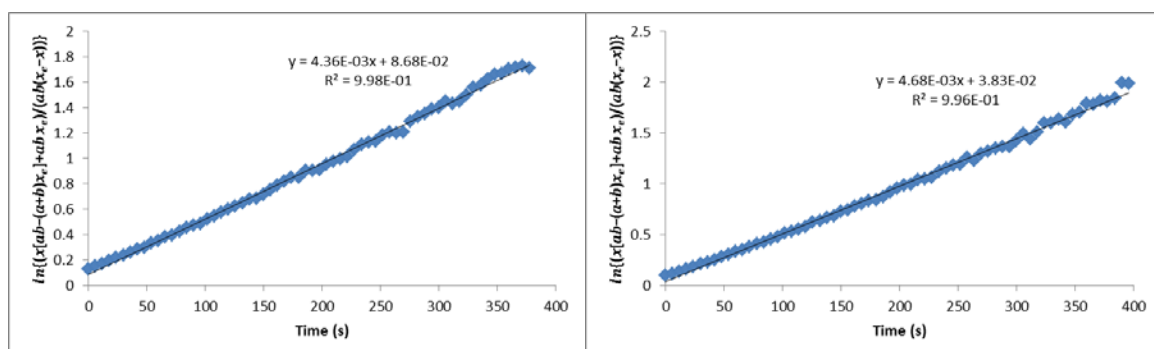


Figure A2.7.4 75 eq TEA

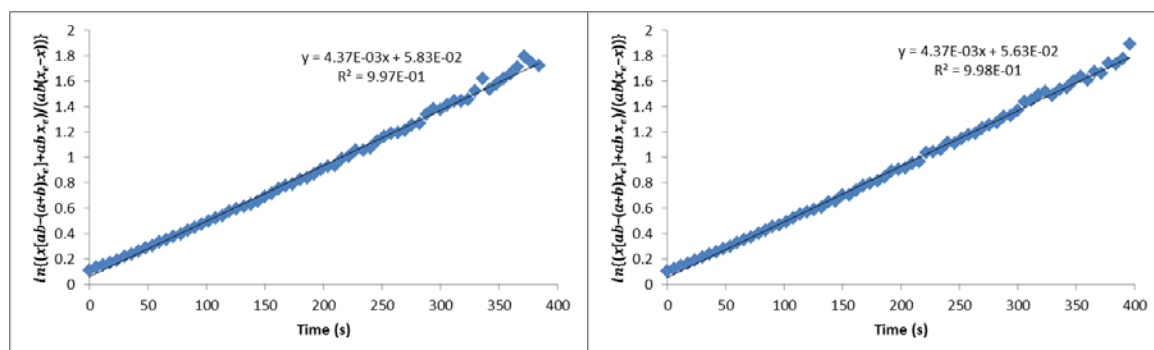


Figure A2.7.5 100 eq TEA

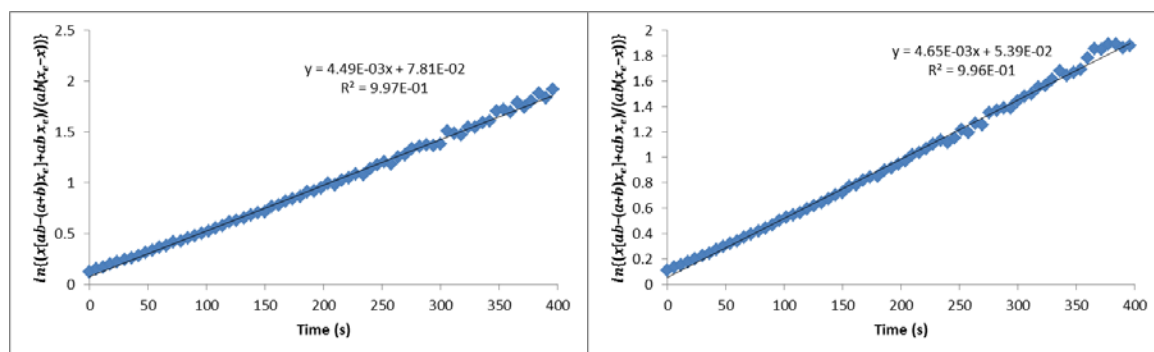
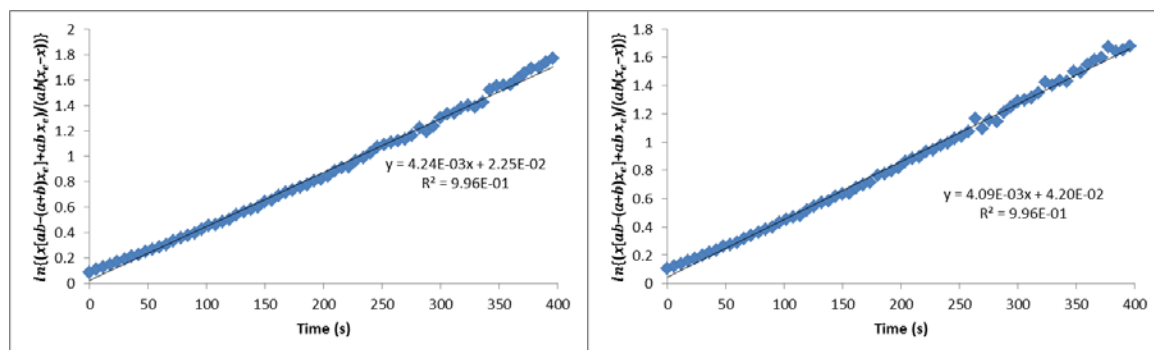


Figure A2.7.6 120 eq TEA





## A2.8 Kinetic and Thermodynamic Data

Table A2.8.1. Exchange Reaction of PFN and 4-CT-H in dichloromethane at 25°C

<i>Final Equilibrium concentrations (M)</i>							
Equivalents of TEA	[4-CT-H] M	[PFN] M	[4-CT] M	[PFN-H] M	K	$k_f$ (L.mol <sup>-1</sup> .s <sup>-1</sup> )	$k_r$ (L.mol <sup>-1</sup> .s <sup>-1</sup> )
0	2.52 x 10 <sup>-5</sup>	2.18 x 10 <sup>-5</sup>	9.58 x 10 <sup>-6</sup>	9.58 x 10 <sup>-6</sup>	0.17	6.3	37.8
0	2.52 x 10 <sup>-5</sup>	2.18 x 10 <sup>-5</sup>	9.58 x 10 <sup>-6</sup>	9.58 x 10 <sup>-6</sup>	0.17	6.5	39.2
0	2.54 x 10 <sup>-5</sup>	2.20 x 10 <sup>-5</sup>	9.39 x 10 <sup>-6</sup>	9.39 x 10 <sup>-6</sup>	0.16	6.2	39.6
0	2.53 x 10 <sup>-5</sup>	2.19 x 10 <sup>-5</sup>	9.51 x 10 <sup>-6</sup>	9.51 x 10 <sup>-6</sup>	0.16	6.5	40.0
10	1.70 x 10 <sup>-5</sup>	1.37 x 10 <sup>-5</sup>	1.78 x 10 <sup>-5</sup>	1.78 x 10 <sup>-5</sup>	1.36	25.3	18.7
10	1.74 x 10 <sup>-5</sup>	1.41 x 10 <sup>-5</sup>	1.73 x 10 <sup>-5</sup>	1.73 x 10 <sup>-5</sup>	1.23	23.3	19.0
10	1.59 x 10 <sup>-5</sup>	1.25 x 10 <sup>-5</sup>	1.89 x 10 <sup>-5</sup>	1.89 x 10 <sup>-5</sup>	1.79	32.1	18.0
10	1.62 x 10 <sup>-5</sup>	1.28 x 10 <sup>-5</sup>	1.86 x 10 <sup>-5</sup>	1.86 x 10 <sup>-5</sup>	1.67	32.0	19.1
10	1.50 x 10 <sup>-5</sup>	1.16 x 10 <sup>-5</sup>	1.96 x 10 <sup>-5</sup>	1.96 x 10 <sup>-5</sup>	2.20	41.4	18.8
50	1.32 x 10 <sup>-5</sup>	9.81 x 10 <sup>-6</sup>	2.15 x 10 <sup>-5</sup>	2.15 x 10 <sup>-5</sup>	3.59	70.3	19.6
50	1.31 x 10 <sup>-5</sup>	9.75 x 10 <sup>-6</sup>	2.16 x 10 <sup>-5</sup>	2.16 x 10 <sup>-5</sup>	3.66	66.3	18.1
50	1.23 x 10 <sup>-5</sup>	8.94 x 10 <sup>-6</sup>	2.24 x 10 <sup>-5</sup>	2.24 x 10 <sup>-5</sup>	4.57	79.9	17.5
50	1.28 x 10 <sup>-5</sup>	9.40 x 10 <sup>-6</sup>	2.20 x 10 <sup>-5</sup>	2.20 x 10 <sup>-5</sup>	4.02	80.4	20.0
75	1.25 x 10 <sup>-5</sup>	9.18 x 10 <sup>-6</sup>	2.21 x 10 <sup>-5</sup>	2.21 x 10 <sup>-5</sup>	4.27	94.7	22.2
75	1.25 x 10 <sup>-5</sup>	9.12 x 10 <sup>-6</sup>	2.22 x 10 <sup>-5</sup>	2.22 x 10 <sup>-5</sup>	4.34	94.3	21.7
75	1.18 x 10 <sup>-5</sup>	8.40 x 10 <sup>-6</sup>	2.29 x 10 <sup>-5</sup>	2.29 x 10 <sup>-5</sup>	5.32	110.5	20.8
75	1.20 x 10 <sup>-5</sup>	8.66 x 10 <sup>-6</sup>	2.27 x 10 <sup>-5</sup>	2.27 x 10 <sup>-5</sup>	4.94	120.7	24.4

<b>100</b>	$1.22 \times 10^{-5}$	$8.83 \times 10^{-6}$	$2.25 \times 10^{-5}$	$2.25 \times 10^{-5}$	4.69	110.1	23.5
<b>100</b>	$1.22 \times 10^{-5}$	$8.75 \times 10^{-6}$	$2.24 \times 10^{-5}$	$2.24 \times 10^{-5}$	4.70	110.1	23.4
<b>100</b>	$1.17 \times 10^{-5}$	$8.35 \times 10^{-6}$	$2.29 \times 10^{-5}$	$2.29 \times 10^{-5}$	5.39	135.9	25.2
<b>100</b>	$1.19 \times 10^{-5}$	$8.39 \times 10^{-6}$	$2.28 \times 10^{-5}$	$2.28 \times 10^{-5}$	5.20	134.0	25.8
<b>120</b>	$1.28 \times 10^{-5}$	$9.43 \times 10^{-6}$	$2.19 \times 10^{-5}$	$2.19 \times 10^{-5}$	3.65	121.3	33.2
<b>120</b>	$1.31 \times 10^{-5}$	$9.74 \times 10^{-6}$	$2.16 \times 10^{-5}$	$2.16 \times 10^{-5}$	3.97	122.2	30.8
<b>120</b>	$1.14 \times 10^{-5}$	$8.08 \times 10^{-6}$	$2.32 \times 10^{-5}$	$2.32 \times 10^{-5}$	5.36	145.2	27.1
<b>120</b>	$1.17 \times 10^{-5}$	$8.37 \times 10^{-6}$	$2.29 \times 10^{-5}$	$2.29 \times 10^{-5}$	5.83	146.7	25.2
<b>150</b>	$1.23 \times 10^{-5}$	$8.91 \times 10^{-6}$	$2.24 \times 10^{-5}$	$2.24 \times 10^{-5}$	4.58	133.6	29.2
<b>150</b>	$1.26 \times 10^{-5}$	$9.21 \times 10^{-6}$	$2.21 \times 10^{-5}$	$2.21 \times 10^{-5}$	4.21	128.7	30.6
<b>150</b>	$1.18 \times 10^{-5}$	$8.43 \times 10^{-6}$	$2.28 \times 10^{-5}$	$2.28 \times 10^{-5}$	5.25	165.0	31.4
<b>150</b>	$1.17 \times 10^{-5}$	$8.34 \times 10^{-6}$	$2.29 \times 10^{-5}$	$2.29 \times 10^{-5}$	5.39	168.6	31.3
<b>200</b>	$1.23 \times 10^{-5}$	$9.00 \times 10^{-6}$	$2.23 \times 10^{-5}$	$2.23 \times 10^{-5}$	4.47	133.5	29.9
<b>200</b>	$1.21 \times 10^{-5}$	$8.79 \times 10^{-6}$	$2.25 \times 10^{-5}$	$2.25 \times 10^{-5}$	4.73	134.1	28.3
<b>200</b>	$1.24 \times 10^{-5}$	$9.04 \times 10^{-6}$	$2.22 \times 10^{-5}$	$2.22 \times 10^{-5}$	4.41	169.4	38.4
<b>200</b>	$1.22 \times 10^{-5}$	$8.84 \times 10^{-6}$	$2.24 \times 10^{-5}$	$2.24 \times 10^{-5}$	4.67	175.3	37.6

*\*Number of equivalents of triethylamine relative to the concentration of 4-CT-H*

Table A2.8.2. Exchange Reaction of PFN and 4-CT-H in dichloromethane at 10°C

<i>Final Equilibrium concentrations (M)</i>							
Equivalents of TEA*	[4-CT-H] M	[PFN] M	[4-CT] M	[PFN-H] M	K	$k_f$ (L.mol <sup>-1</sup> .s <sup>-1</sup> )	$k_r$ (L.mol <sup>-1</sup> .s <sup>-1</sup> )
0	$2.97 \times 10^{-5}$	$2.34 \times 10^{-5}$	$5.05 \times 10^{-6}$	$5.05 \times 10^{-6}$	0.04	1.2	34.0
0	$2.92 \times 10^{-5}$	$2.29 \times 10^{-5}$	$5.58 \times 10^{-6}$	$5.58 \times 10^{-6}$	0.05	1.4	30.6
120	$1.21 \times 10^{-5}$	$5.81 \times 10^{-6}$	$2.25 \times 10^{-5}$	$2.25 \times 10^{-5}$	7.18	100.8	14.0
120	$1.23 \times 10^{-5}$	$5.95 \times 10^{-6}$	$2.23 \times 10^{-5}$	$2.23 \times 10^{-5}$	6.84	96.5	14.1
200	$1.14 \times 10^{-5}$	$5.07 \times 10^{-6}$	$2.31 \times 10^{-5}$	$2.31 \times 10^{-5}$	9.28	133.1	14.3
200	$1.15 \times 10^{-5}$	$5.15 \times 10^{-6}$	$2.30 \times 10^{-5}$	$2.30 \times 10^{-5}$	9.00	130.7	14.5

\*Number of equivalents of triethylamine relative to the concentration of 4-CT-H

Table A2.8.3. Exchange reaction of PFN and 4-CT-H in benzene

<i>Final Equilibrium Concentrations (M)</i>							
Equivalents of TEA*	[4-CT-H] M	[PFN] M	[4-CT] M	[PFN-H] M	K	$k_f$ (L.mol <sup>-1</sup> .s <sup>-1</sup> )	$k_r$ (L.mol <sup>-1</sup> .s <sup>-1</sup> )
0	6.07 x 10 <sup>-5</sup>	4.79 x 10 <sup>-5</sup>	8.92 x 10 <sup>-6</sup>	8.92 x 10 <sup>-6</sup>	0.027	4	155
0	6.01 x 10 <sup>-5</sup>	4.74 x 10 <sup>-5</sup>	9.49 x 10 <sup>-6</sup>	9.49 x 10 <sup>-6</sup>	0.032	5	163
10	5.67 x 10 <sup>-5</sup>	4.39 x 10 <sup>-5</sup>	1.29 x 10 <sup>-5</sup>	1.29 x 10 <sup>-5</sup>	0.067	9	133
10	5.70 x 10 <sup>-5</sup>	4.43 x 10 <sup>-5</sup>	1.26 x 10 <sup>-5</sup>	1.26 x 10 <sup>-5</sup>	0.063	9	140
50	5.28 x 10 <sup>-5</sup>	4.01 x 10 <sup>-5</sup>	1.68 x 10 <sup>-5</sup>	1.68 x 10 <sup>-5</sup>	0.133	17	126
50	5.22 x 10 <sup>-5</sup>	3.95 x 10 <sup>-5</sup>	1.74 x 10 <sup>-5</sup>	1.74 x 10 <sup>-5</sup>	0.146	19	131
75	5.01 x 10 <sup>-5</sup>	3.74 x 10 <sup>-5</sup>	1.95 x 10 <sup>-5</sup>	1.95 x 10 <sup>-5</sup>	0.202	27	134
75	4.99 x 10 <sup>-5</sup>	3.71 x 10 <sup>-5</sup>	1.97 x 10 <sup>-5</sup>	1.97 x 10 <sup>-5</sup>	0.211	27	130
100	4.85 x 10 <sup>-5</sup>	3.58 x 10 <sup>-5</sup>	2.11 x 10 <sup>-5</sup>	2.11 x 10 <sup>-5</sup>	0.256	35	136
100	4.82 x 10 <sup>-5</sup>	3.55 x 10 <sup>-5</sup>	2.14 x 10 <sup>-5</sup>	2.14 x 10 <sup>-5</sup>	0.267	36	133
120	4.67 x 10 <sup>-5</sup>	3.39 x 10 <sup>-5</sup>	2.29 x 10 <sup>-5</sup>	2.29 x 10 <sup>-5</sup>	0.331	39	119
120	3.47 x 10 <sup>-5</sup>	4.74 x 10 <sup>-5</sup>	2.22 x 10 <sup>-5</sup>	2.22 x 10 <sup>-5</sup>	0.299	41	138

\*Number of equivalents of triethylamine relative to the concentration of 4-CT-H

Table A2.8.4. Exchange Reaction of PFN and 4-CT-H in acetonitrile

<i>Final Equilibrium Concentrations (M)</i>							
Equivalents of TEA*	[PFN] M	[4-CT-H] M	[PFN-H] M	[4-CT] M	K	$k_f$ (L.mol <sup>-1</sup> .s <sup>-1</sup> )	$k_r$ (L.mol <sup>-1</sup> .s <sup>-1</sup> )
0	1.32 x 10 <sup>-5</sup>	1.32 x 10 <sup>-5</sup>	1.67 x 10 <sup>-5</sup>	1.67 x 10 <sup>-5</sup>	1.60	25.9	16.2
0	1.47 x 10 <sup>-5</sup>	1.47 x 10 <sup>-5</sup>	1.51 x 10 <sup>-5</sup>	1.51 x 10 <sup>-5</sup>	1.06	20.7	19.6
0	1.58 x 10 <sup>-5</sup>	1.58 x 10 <sup>-5</sup>	1.40 x 10 <sup>-5</sup>	1.40 x 10 <sup>-5</sup>	0.78	17.8	22.8
0	1.63 x 10 <sup>-5</sup>	1.63 x 10 <sup>-5</sup>	1.35 x 10 <sup>-5</sup>	1.35 x 10 <sup>-5</sup>	0.68	16.8	24.6
50	1.35 x 10 <sup>-5</sup>	1.35 x 10 <sup>-5</sup>	1.63 x 10 <sup>-5</sup>	1.63 x 10 <sup>-5</sup>	1.46	25.2	17.3
50	1.40 x 10 <sup>-5</sup>	1.40 x 10 <sup>-5</sup>	1.58 x 10 <sup>-5</sup>	1.58 x 10 <sup>-5</sup>	1.28	23.8	18.6
75	1.50 x 10 <sup>-5</sup>	1.49 x 10 <sup>-5</sup>	1.48 x 10 <sup>-5</sup>	1.48 x 10 <sup>-5</sup>	0.98	20.8	21.3
75	1.46 x 10 <sup>-5</sup>	1.46 x 10 <sup>-5</sup>	1.52 x 10 <sup>-5</sup>	1.52 x 10 <sup>-5</sup>	1.08	21.7	20.1
120	1.14 x 10 <sup>-5</sup>	1.14 x 10 <sup>-5</sup>	1.83 x 10 <sup>-5</sup>	1.83 x 10 <sup>-5</sup>	2.56	35.4	13.8
120	1.32 x 10 <sup>-5</sup>	1.32 x 10 <sup>-5</sup>	1.67 x 10 <sup>-5</sup>	1.67 x 10 <sup>-5</sup>	2.37	32.8	13.8

\*Number of equivalents of triethylamine relative to the concentration of 4-CT-H

Table A2.8.5. Exchange reaction of PFN and TEMPO<sub>naph</sub>-H in dichloromethane

<i>Final Equilibrium Concentrations (M)</i>							
Equivalents of TEA*	[TEMPO <sub>naph</sub> -H] M	[PFN] M	[TEMPO <sub>naph</sub> ] M	[PFN-H] M	K	$k_f$ (L.mol <sup>-1</sup> .s <sup>-1</sup> )	$k_r$ (L.mol <sup>-1</sup> .s <sup>-1</sup> )
<b>0</b>	8.29 x 10 <sup>-6</sup>	9.04 x 10 <sup>-6</sup>	2.24 x 10 <sup>-5</sup>	2.24 x 10 <sup>-5</sup>	6.68	158.14	23.66
<b>0</b>	8.91 x 10 <sup>-6</sup>	9.66 x 10 <sup>-6</sup>	2.18 x 10 <sup>-5</sup>	2.18 x 10 <sup>-5</sup>	5.50	149.17	27.11
<b>0</b>	9.08 x 10 <sup>-6</sup>	9.82 x 10 <sup>-6</sup>	2.16 x 10 <sup>-5</sup>	2.16 x 10 <sup>-5</sup>	5.23	166.80	31.88
<b>10</b>	7.19 x 10 <sup>-6</sup>	7.93 x 10 <sup>-6</sup>	2.35 x 10 <sup>-5</sup>	2.35 x 10 <sup>-5</sup>	9.68	206.76	21.37
<b>10</b>	7.68 x 10 <sup>-6</sup>	8.43 x 10 <sup>-6</sup>	2.30 x 10 <sup>-5</sup>	2.30 x 10 <sup>-5</sup>	8.16	206.86	25.36
<b>50</b>	7.99 x 10 <sup>-6</sup>	8.73 x 10 <sup>-6</sup>	2.27 x 10 <sup>-5</sup>	2.27 x 10 <sup>-5</sup>	7.38	190.65	25.83
<b>50</b>	8.50 x 10 <sup>-6</sup>	9.25 x 10 <sup>-6</sup>	2.22 x 10 <sup>-5</sup>	2.22 x 10 <sup>-5</sup>	6.25	188.28	30.14
<b>75</b>	7.82 x 10 <sup>-6</sup>	8.57 x 10 <sup>-6</sup>	2.29 x 10 <sup>-5</sup>	2.29 x 10 <sup>-5</sup>	7.80	196.38	25.19
<b>75</b>	8.21 x 10 <sup>-6</sup>	8.96 x 10 <sup>-6</sup>	2.25 x 10 <sup>-5</sup>	2.25 x 10 <sup>-5</sup>	6.87	184.32	26.85
<b>100</b>	8.47 x 10 <sup>-6</sup>	9.22 x 10 <sup>-6</sup>	2.22 x 10 <sup>-5</sup>	2.22 x 10 <sup>-5</sup>	6.32	181.64	28.76
<b>100</b>	8.75 x 10 <sup>-6</sup>	9.50 x 10 <sup>-6</sup>	2.19 x 10 <sup>-5</sup>	2.19 x 10 <sup>-5</sup>	5.78	180.02	31.13
<b>120</b>	6.73 x 10 <sup>-6</sup>	7.48 x 10 <sup>-6</sup>	2.39 x 10 <sup>-5</sup>	2.39 x 10 <sup>-5</sup>	11.40	230.40	20.20
<b>120</b>	6.78 x 10 <sup>-6</sup>	7.52 x 10 <sup>-6</sup>	2.39 x 10 <sup>-5</sup>	2.39 x 10 <sup>-5</sup>	11.20	220.29	19.66

\*Number of equivalents of triethylamine relative to the concentration of TEMPO<sub>naph</sub>-H

**Appendix Three: Single Crystal X-Ray Analysis Data for selected compounds reported in Parts One and Two**

**A3.1 Compound 1.95: ban1232**

**A3.2 Compound 2.14: ban1315**

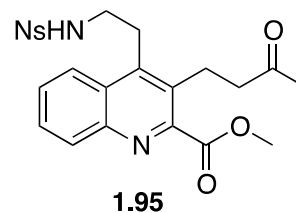
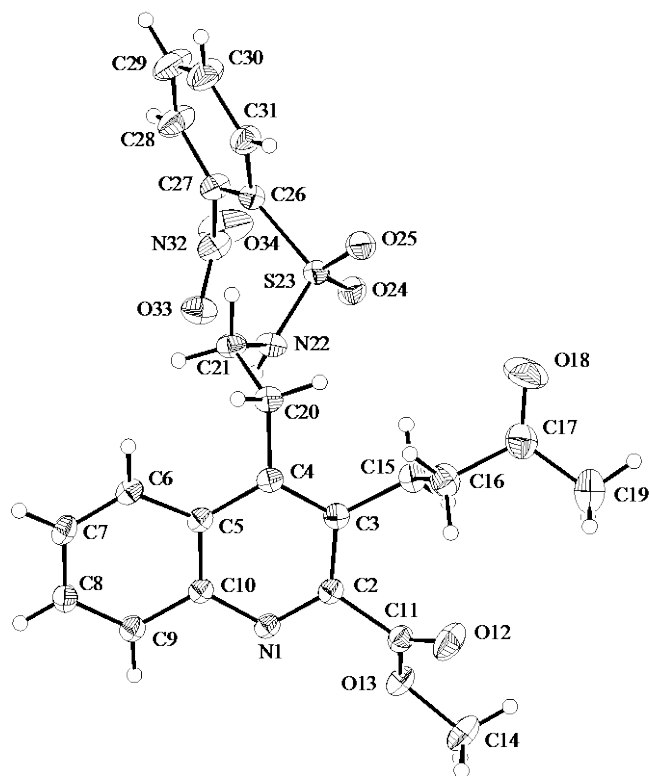
**A3.3 Compound 2.39: ban1436SN**

## Crystal structure of $C_{23}H_{23}N_3O_7S \cdot 0.5(CHCl_3)$ — ban1232

Marta Klinska, Martin G. Banwell and Anthony C. Willis\*

Research School of Chemistry, The Australian National University, Canberra, A. C. T. 0200, Australia

Correspondence email: willis@rsc.anu.edu.au



### Abstract

The crystal structure of  $C_{23}H_{23}N_3O_7S \cdot 0.5(CHCl_3)$  is reported.

### Comment

The crystallographic asymmetric unit consists of one  $C_{23}H_{23}N_3O_7S$  molecule and a chloroform molecule disordered about a crystallographic inversion symmetry operation.

### Experimental

The compound was prepared by MK and recrystallised from chloroform/pentane. The sample ID is MK1-90.

### Computing details

Data collection: *COLLECT* (Nonius, 2001).; cell refinement: *DENZO/SCALEPACK* (Otwinowski & Minor, 1997); data reduction: *DENZO/SCALEPACK* (Otwinowski & Minor, 1997); program(s) used to solve structure: *SIR92* (Altomare *et al.*, 1994); program(s) used to refine structure: *CRYSTALS* (Betteridge *et al.*, 2003); molecular graphics: *ORTEP-II* (Johnson 1976) in *TEXSAN* (MSC, 1992-1997); software used to prepare material for publication: *CRYSTALS* (Betteridge *et al.*, 2003).



**(ban1232)***Crystal data* $C_{23}H_{23}N_3O_7S \cdot 0.5(CHCl_3)$  $M_r = 545.21$ Triclinic,  $P\bar{1}$  $a = 7.9725 (2) \text{ \AA}$  $b = 12.8185 (4) \text{ \AA}$  $c = 12.8740 (4) \text{ \AA}$  $\alpha = 75.9818 (13)^\circ$  $\beta = 79.967 (2)^\circ$  $\gamma = 81.168 (2)^\circ$  $V = 1248.40 (6) \text{ \AA}^3$  $Z = 2$  $F(000) = 566.000$  $D_x = 1.450 \text{ Mg m}^{-3}$ Mo  $K\alpha$  radiation,  $\lambda = 0.71073 \text{ \AA}$ 

Cell parameters from 19075 reflections

 $\theta = 2.6\text{--}27.5^\circ$  $\mu = 0.34 \text{ mm}^{-1}$  $T = 200 \text{ K}$ 

Needle, White

 $0.43 \times 0.12 \times 0.07 \text{ mm}$ *Data collection*

Nonius KappaCCD

diffractometer

Graphite monochromator

 $\varphi$  and  $\omega$  scans with CCD

Absorption correction: Integration

via Gaussian method (Coppens, 1970) implemented in

maXus (2000)

 $T_{\min} = 0.955$ ,  $T_{\max} = 0.989$ 

25862 measured reflections

5730 independent reflections

4348 reflections with  $I > 2.0\sigma(I)$  $R_{\text{int}} = 0.036$  $\theta_{\max} = 27.5^\circ$ ,  $\theta_{\min} = 2.6^\circ$  $h = -9 \rightarrow 10$  $k = -16 \rightarrow 16$  $l = -16 \rightarrow 16$ *Refinement*Refinement on  $F^2$ 

Least-squares matrix: Full

 $R[F^2 > 2\sigma(F^2)] = 0.062$  $wR(F^2) = 0.177$  $S = 0.99$ 

5729 reflections

353 parameters

23 restraints

Primary atom site location: Structure-invariant direct methods

Hydrogen site location: Inferred from neighbouring sites

H atoms treated by a mixture of independent and constrained refinement

Method = Modified Sheldrick  $w = 1/[\sigma^2(F^2) + (0.09P)^2 + 1.37P]$ ,where  $P = (\max(F_o^2, 0) + 2F_c^2)/3$  $(\Delta/\sigma)_{\max} = 0.006$  $\Delta\rho_{\max} = 0.66 \text{ e \AA}^{-3}$  $\Delta\rho_{\min} = -0.71 \text{ e \AA}^{-3}$ *Special details*

*Refinement.* After location of the  $C_{23}H_{23}N_3O_7S$  molecule, a region of electron density was observed about (0,1/2,0). This was identified to be a chloroform molecule overlapping with its own inversion image. These atom sites were therefore assigned occupancies of 0.5.

Restraints were applied to distances, angles and displacement parameters for these sites. Peaks in a subsequent difference map suggested some disorder in the orientation of the acetyl group C17, O18, C19. Alternative sites O118 and C119 were introduced with fixed isotropic displacement parameters, while C17 was assumed to be common to both images. The relative occupancies were refined appropriately while distances and angles were restrained for the minor sites. The second image of the acetyl group is not well described and suggests that an alternative site for C17 could also perhaps be included in the model. As its occupancy would be only 0.14 and it would be very close to C17 anyway, it was decided not to pursue this further.

The H atoms of the  $C_{23}H_{23}N_3O_7S$  molecule (except those on C19/C119) were all located in a difference map, but those bonded to C were repositioned geometrically. They were initially refined with soft restraints on the bond lengths and angles to regularise their geometry (C—H in the range 0.93–0.98 Å, N—H = 0.87 Å) and with  $U_{\text{iso}}(\text{H})$  in the range 1.2–1.5 times  $U_{\text{eq}}$  of the parent atom, after which the positions were refined with riding constraints and the displacement parameters were held fixed. H221 on N22 was allowed to refine freely in the final refinement. H sites for C19 and C119 were simply included at calculated positions and ride on the atom to which they are bonded.

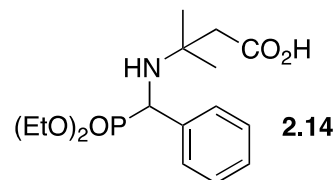
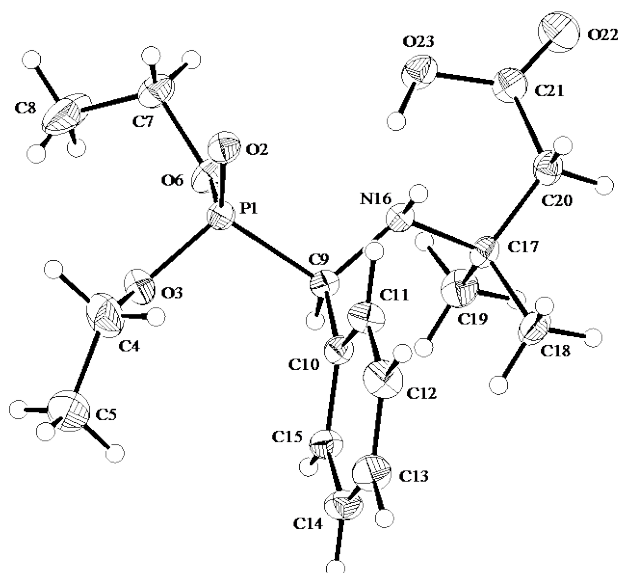
The peaks in the final difference map are located within disordered regions of the structure.

## Crystal structure of $C_{16}H_{26}NO_5P$ — ban1315

Marta Klinska, Martin G. Banwell and Anthony C. Willis\*

Research School of Chemistry, The Australian National University, Canberra, A. C. T. 0200, Australia

Correspondence email: willis@rsc.anu.edu.au



### Abstract

The crystal structure of  $C_{16}H_{26}NO_5P$  is reported.

### Comment

The crystallographic asymmetric unit consists of one molecule of  $C_{16}H_{26}NO_5P$ .

### Experimental

The compound was prepared by MK and recrystallised from dichloromethane/pentane. The sample ID is MK183B.

### Computing details

Data collection: *COLLECT* (Nonius, 2001).; cell refinement: *DENZO/SCALEPACK* (Otwinowski & Minor, 1997); data reduction: *DENZO/SCALEPACK* (Otwinowski & Minor, 1997); program(s) used to solve structure: *SIR92* (Altomare *et al.*, 1994); program(s) used to refine structure: *CRYSTALS* (Betteridge *et al.*, 2003); molecular graphics: *ORTEP-II* (Johnson 1976) in *TEXSAN* (MSC, 1992-1997); software used to prepare material for publication: *CRYSTALS* (Betteridge *et al.*, 2003).

### (ban1315)

#### Crystal data

$C_{16}H_{26}NO_5P$   
 $M_r = 343.36$

Monoclinic,  $P2_1/n$   
 $a = 9.5841(1) \text{ \AA}$

$b = 13.1656 (3) \text{ \AA}$   
 $c = 14.5838 (3) \text{ \AA}$   
 $\beta = 90.1015 (14)^\circ$   
 $V = 1840.19 (6) \text{ \AA}^3$   
 $Z = 4$   
 $F(000) = 736$   
 $D_x = 1.239 \text{ Mg m}^{-3}$

Mo  $K\alpha$  radiation,  $\lambda = 0.71073 \text{ \AA}$   
 Cell parameters from 20180 reflections  
 $\theta = 2.6\text{--}30^\circ$   
 $\mu = 0.17 \text{ mm}^{-1}$   
 $T = 200 \text{ K}$   
 Block, Colourless  
 $0.37 \times 0.36 \times 0.30 \text{ mm}$

#### Data collection

Nonius KappaCCD  
 diffractometer  
 Graphite monochromator  
 $\varphi$  and  $\omega$  scans with CCD  
 Absorption correction: Integration  
 via Gaussian method (Coppens, 1970) implemented in  
*maXus* (2000)  
 $T_{\min} = 0.939$ ,  $T_{\max} = 0.970$

31880 measured reflections  
 5389 independent reflections  
 4473 reflections with  $I > 2.0\sigma(I)$   
 $R_{\text{int}} = 0.030$   
 $\theta_{\max} = 30.0^\circ$ ,  $\theta_{\min} = 2.6^\circ$   
 $h = -13 \rightarrow 12$   
 $k = -18 \rightarrow 18$   
 $l = -20 \rightarrow 19$

#### Refinement

Refinement on  $F^2$   
 Least-squares matrix: Full  
 $R[F^2 > 2\sigma(F^2)] = 0.041$   
 $wR(F^2) = 0.112$   
 $S = 0.98$   
 5387 reflections  
 286 parameters  
 18 restraints

Primary atom site location: Structure-invariant direct  
 methods  
 Hydrogen site location: Difference Fourier map  
 Only H-atom coordinates refined  
 Method = Modified Sheldrick  $w = 1/[\sigma^2(F^2) + (0.06P)^2 + 0.64P]$ ,  
 where  $P = (\max(F_o^2, 0) + 2F_c^2)/3$   
 $(\Delta/\sigma)_{\max} = 0.006$   
 $\Delta\rho_{\max} = 0.32 \text{ e \AA}^{-3}$   
 $\Delta\rho_{\min} = -0.40 \text{ e \AA}^{-3}$

#### Special details

*Refinement.* Most of the H atoms were located in a difference electron density map, but those bonded to C were repositioned geometrically. H atoms were initially refined with soft restraints on the bond lengths and angles to regularise their geometry (C—H in the range 0.93–0.98 Å, N—H = 0.87 Å, O—H = 0.82 Å) and with  $U_{\text{iso}}(\text{H})$  in the range 1.2–1.5 times  $U_{\text{eq}}$  of the parent atom, after which the positions were refined freely and the displacement parameters were held fixed. Restraints were applied to distances and angles involving the H atoms of the methyl groups at C5 and C8.

Two inner reflections with poor agreement of  $F_o$  and  $F_c$  were removed from the refinement.

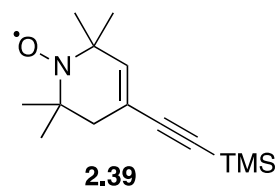
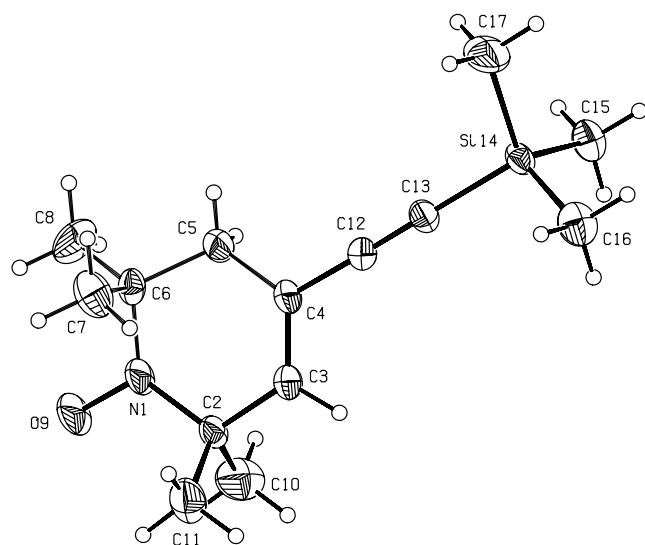
The largest peaks in the final difference map are located midway between bonded atoms or adjacent to C8. The latter might imply a small amount of disorder of that atom but this has not been pursued further as it is obviously of a very small degree.

## Crystal structure of $C_{14}H_{24}NOSi$ — ban1436SN

Marta Klinska, Martin G. Banwell and Anthony C. Willis\*

Research School of Chemistry, The Australian National University, Canberra, A. C. T. 0200, Australia

Correspondence email: willis@rsc.anu.edu.au



### Abstract

The crystal structure of  $C_{14}H_{24}NOSi$  is reported.

#### 1. Comment

The crystallographic asymmetric unit consists of one molecule of  $C_{14}H_{24}NOSi$ . There is disorder in the conformation of part of the molecule. The space group is noncentrosymmetric. The absolute structure was determined by refining the Flack parameter. (Flack, 1983) The space group is not enantiomorphic and the molecule has no chiral centres.

#### 2. Synthesis and crystallization

The compound was prepared by MK and recrystallized from hexane. The sample ID is MK421.

### Related literature

#### Computing details

Data collection: *CrysAlis PRO*, Agilent Technologies, Version 1.171.37.21t (release 24-10-2013 CrysAlis171 .NET) (compiled Oct 24 2013,16:12:21); cell refinement: *CrysAlis PRO*; data reduction: *CrysAlis PRO*; program(s) used to solve structure: Superflip (Palatinus & Chapuis, 2007); program(s) used to refine structure: *CRYSTALS* (Betteridge *et al.*, 2003); molecular graphics: *PLATON* (Spek, 2008); software used to prepare material for publication: *CRYSTALS* (Betteridge *et al.*, 2003).

**(ban1336SN)***Crystal data*

$C_{14}H_{24}NOSi$	$b = 12.8101 (1) \text{ \AA}$
$M_r = 250.44$	$c = 10.7452 (1) \text{ \AA}$
Monoclinic, $Pn$	$\beta = 99.3576 (8)^\circ$
Hall symbol: $P -2yac$	$V = 799.79 (2) \text{ \AA}^3$
$a = 5.8888 (1) \text{ \AA}$	$Z = 2$

$F(000) = 274.000$   
 $D_x = 1.040 \text{ Mg m}^{-3}$   
 Cu  $K\alpha$  radiation,  $\lambda = 1.54184 \text{ \AA}$   
 Cell parameters from 9262 reflections  
 $\theta = 5\text{--}72^\circ$

$\mu = 1.18 \text{ mm}^{-1}$   
 $T = 150 \text{ K}$   
 Plate, colourless  
 $0.37 \times 0.16 \times 0.03 \text{ mm}$

*Data collection*

SuperNova, Dual, Cu at zero, EosS2  
 diffractometer  
 Radiation source: Supernova (Cu) X-ray Source  
 Mirror monochromator  
 $\omega$  scans

Absorption correction: multi-scan  
*CrysAlis PRO*, Agilent Technologies, Version  
 1.171.37.21t (release 24-10-2013 CrysAlis171 .NET)  
 (compiled Oct 24 2013, 16:12:21) Empirical absorption  
 correction using spherical harmonics, implemented in  
 SCALE3 ABSPACK scaling algorithm.

$T_{\min} = 0.85$ ,  $T_{\max} = 0.97$   
 12214 measured reflections  
 2589 independent reflections  
 2549 reflections with  $I > 2.0\sigma(I)$   
 $R_{\text{int}} = 0.024$   
 $\theta_{\max} = 72.0^\circ$ ,  $\theta_{\min} = 3.5^\circ$   
 $h = -7 \rightarrow 7$   
 $k = -15 \rightarrow 15$   
 $l = -13 \rightarrow 10$

*Refinement*

Refinement on  $F^2$   
 Least-squares matrix: full  
 $R[F^2 > 2\sigma(F^2)] = 0.043$   
 $wR(F^2) = 0.107$   
 $S = 1.01$   
 2589 reflections  
 186 parameters  
 24 restraints  
 Primary atom site location: Other

Hydrogen site location: inferred from neighbouring  
 sites  
 H-atom parameters constrained  
 Method = Modified Sheldrick  $w = 1/[\sigma^2(F^2) +$   
 $(0.05P)^2 + 0.41P]$ ,  
 where  $P = (\max(F_o^2, 0) + 2F_c^2)/3$   
 $(\Delta/\sigma)_{\max} = 0.001$   
 $\Delta\rho_{\max} = 0.24 \text{ e \AA}^{-3}$   
 $\Delta\rho_{\min} = -0.21 \text{ e \AA}^{-3}$   
 Absolute structure: Flack (1983), 939 Friedel-pairs  
 Absolute structure parameter:  $-0.01 (4)$

*Special details**Refinement*

The initial solution showed a  $C_{14}H_{24}NOSi$  molecule with large displacement ellipsoids for C5, C7 and C8. The observed electron density was suggesting a superposition of two images of the molecule which differed only in their conformations at that part of the molecule. C5, C7 and C8 were therefore each split over two sites, and later C6 was split too. The relative occupancies of the sites were refined. Restraints were imposed so equivalent bond distances for the two images would tend to be similar. Restraints were also applied to displacement parameters of adjacent atom sites.

Hydrogen atoms were included at calculated positions ( $C-H = 0.95 \text{ \AA}$ ,  $U_{\text{iso}}(H) = 1.2 \times U_{\text{eq}}(\text{adjacent atom})$ ) and ride on the atom to which they are attached during refinement.

The final value of the Flack parameter is  $-0.01 (4)$  and the final value of the Hooft parameter is  $0.02 (1)$ .

The largest peaks in the final difference map are located within the disorder and near N1, O9 and C3, suggesting some disorder of these atoms too. As the electron density of these peaks was so low, no further modelling was attempted.

**References**

- Mackay, S., Gilmore, C. J., Edwards, C., Stewart, N. & Shankland, K. (2000). *maXus* Computer Program for the Solution and Refinement of Crystal Structures. Nonius, The Netherlands, MacScience, Japan & The University of Glasgow.
- Coppens, P. (1970). The Evaluation of Absorption and Extinction in Single-Crystal Structure Analysis. *Crystallographic Computing*. F. R. Ahmed, S. R. Hall and C. P. Huber, eds., Munksgaard. Copenhagen. pp 255-270.
- Altomare, A., Cascarano, G., Giacovazzo, G., Guagliardi, A., Burla, M. C., Polidori, G. & Camalli, M. (1994). *J. Appl. Cryst.* 27, 435.
- Betteridge, P. W., Carruthers, J. R., Cooper, R. I., Prout, K. & Watkin, D. J. (2003). *J. Appl. Cryst.* 36, 1487.
- Nonius (1997–2001). *COLLECT*. Nonius BV, Delft, The Netherlands.
- Otwinowski, Z. & Minor, W. (1997). *Methods in Enzymology*, Vol. 276, edited by C. W. Carter Jr & R. M. Sweet, pp. 307–326. New York: Academic Press.
- Molecular Structure Corporation. (1992–1997). *TEXSAN*. Single Crystal Structure Analysis Software. Version 1.8. MSC, 3200 Research Forest Drive, The Woodlands, TX 77381, USA.
- Johnson, C. K. (1976). *ORTEPII*, A Fortran Thermal-Ellipsoid Plot Program, Report ORNL-5138, Oak Ridge National Laboratory, Oak Ridge, Tennessee, USA.